UCLA

UCLA Electronic Theses and Dissertations

Title

Expanding the Tunable Nature of Redox-Active Dodecaborane Clusters

Permalink

https://escholarship.org/uc/item/2t08j799

Author

Wixtrom, Alex

Publication Date

2018

Peer reviewed|Thesis/dissertation

eScholarship.org Powered by the California Digital Library
University of California

UNIVERSITY OF CALIFORNIA
Los Angeles

Expanding the Tunable Nature of Redox-Active Dodecaborane Clusters

A dissertation submitted in partial satisfaction
of the requirements for the degree Doctor of Philosophy
in Chemistry

by

Alex Ian Wixtrom

2018

© Copyright by

Alex Ian Wixtrom

2018

ABSTRACT OF THE DISSERTATION

Expanding the Tunable Nature of Redox-Active Dodecaborane Clusters

by

Alex Ian Wixtrom

Doctor of Philosophy in Chemistry
University of California, Los Angeles, 2018
Professor Alexander Michael Spokoyny, Chair

This work describes synthetic investigations to rationally tune the redox properties of icosahedral dodecaborate clusters through perfunctionalization of all 12 boron vertices. Functionalization in this manner engenders redox activity of the boron cluster derivatives, with the ability to tune these redox properties as a function of the substituent(s) used. New methods were developed to rapidly produce perfunctionalized boron clusters under ambient conditions, enabling the accelerated preparation of additional cluster derivatives. Several clusters featuring higher redox potentials than any cluster derivatives to date were reported, extending the tunable range of clusters of the type $B_{12}(OR)_{12}$ to over 1 V for the same redox event. Further modification of the cluster through vertex-differentiation by incorporating a single NO_2 group created a new class of $B_{12}(OR)_{11}NO_2$ clusters. These vertex differentiated clusters featured redox potentials ~ 0.5 V higher than their $B_{12}(OR)_{12}$ analogues, demonstrating a further expansion of the tunable redox properties of perfunctionalized boron clusters. After thorough demonstration of the high degree of redox tunability possible with

perfunctionalized boron clusters, their extremely stable nature was shown *via* bulk electrochemical cycling using flow cell battery testing. The $B_{12}(OR)_{12}$ derivatives tested in a symmetric cell exhibit no observable degradation even after 1000+ hours and ~500 cycles, and a proof-of-concept all-boron cluster flow cell battery prototype device showed stable cycling for over a week. In summary, new methods to decorate dodecaborate clusters with a diverse array of functional groups were reported, along with new insights on the significantly expanded available redox potential window for these molecules.

The dissertation of Alex Ian Wixtrom is approved.

Richard B. Kaner

Joseph Ambrose Loo

Dante A. Simonetti

Alexander Michael Spokoyny, Committee Chair

University of California, Los Angeles

2018

To my wife and my parents, for their encouragement and support,
and for always inspiring me to work hard in pursuit of my goals.

Table of Contents

List of Figures ix

List of Tables xi

Vita xiii

Chapter 1: Introduction to Boron Cluster Chemistry 1

Chapter 2: Rapid Synthesis of Redox-Active Dodecaborane $B_{12}(OR)_{12}$ Clusters Under Ambient Conditions 5

- Introduction 6
- Results and Discussion 8
- Conclusions 21
- Acknowledgements 22
- Supporting Information 23
  - Experimental Section 23
  - General considerations 23
  - Materials 23
  - Instruments 23
  - X-ray data collection and processing parameters 24
  - Cyclic voltammetry and IRSEC 24
  - Microwave Synthesis 25
  - Dicesium dodecahydroxy-closo-dodecaborate Cs_2[1] 26
  - General ether alkylation/benzylation of TBA_2[1] to $B_{12}(OR)_{12}$ microwave procedure 28
  - Dodeca(benzyloxy)-*hypercloso*-dodecaborane [2] 30
  - Dodeca(allyloxy)-*hypercloso*-dodecaborane [3] 31
  - Dodeca(ethoxy)-*hypercloso*-dodecaborane [4] 31
  - Dodeca(hexoxy)-*hypercloso*-dodecaborane [5] 32
  - Dodeca(6-hexeneoxy)-*hypercloso*-dodecaborane [6] 33
  - Dodeca(11-undeceneoxy)-*hypercloso*-dodecaborane [7] 33
  - Dodeca(ethylbutyratoxy)-*hypercloso*-dodecaborane [8] 34
  - Dodeca(4-methylbenzyloxy)-*hypercloso*-dodecaborane [9] 35
  - Dodeca(4-bromobenzyloxy)-*hypercloso*-dodecaborane [10] 36
  - Dodeca(4-trifluoromethylbenzyloxy)-*hypercloso*-dodecaborane [11] 37
  - Dodeca(4-nitrobenzyloxy)-*hypocloso*-dodecaborane $[12]^{1-}$ 38
  - Dodeca(3,5-bis(trifluoromethyl)$_2$benzyloxy)-*hypocloso*-dodecaborane $[13]^{1-}$ 39
  - Benzyloxy undeca(ethoxy)-*hypercloso*-dodecaborane [14] 40

Chapter 3: Tuning the Electrochemical Potential of Perfunctionalized Dodecaborate Clusters Through Vertex Differentiation 42

Introduction 43
Results and Discussion 44
Conclusions 51
Acknowledgements 51
Supporting Information 53
  Experimental Section 53
  General considerations 53
  Materials 53
  Instrumentation 54
  X-ray data collection and processing parameters 54
  Cyclic voltammetry 55
  Microwave synthesis 55
  Synthesis of [1] 56
  Synthesis of [2a] 56
  Synthesis of [2b] 57
  Synthesis of [2c] 58
  Synthesis of [2c]-ME 60
  Synthesis of [3], $[3]^{1-}$, and $[3]^{2-}$ 61

Chapter 4: Perfunctionalized Dodecaborate Clusters as Stable Metal-Free Active Materials for Charge Storage 64
Introduction 65
Results and Discussion 68
Conclusion 75
Associated Content 76
Supporting Information 76
Author Information 76
Acknowledgements 76
Supporting Information 78
  Experimental Section 78
  General considerations 78
  Materials 78
  Instrumentation 79
  Microwave synthesis 79
  Synthesis of $[N^{n}Bu_4]_2B_{12}(OH)_{12}$ 80
  Synthesis of $[1]^{2-}$ & $[1]^{1-}$ 80
  Synthesis of $[2]^{0}$ 82
  Cyclic Voltammetry and Randles-Sevcik Analysis 83

Flow Battery Methods and Discussion 85
Post-Flow Cell Analysis of $[1]^{2-}$ & $[1]^{1-}$ 87

Chapter 5: Conclusions 89

Appendices (Supplemental Spectra & Data) 90
Supplemental spectra & data for Chapter 2 90
Supplemental spectra & data for Chapter 3 186
Supplemental spectra & data for Chapter 4 210

References 225

List of Figures

Figure 1. Synthetic route to produce functionalized ether-linked derivatives of the *hypercloso* boron clusters (2-14) via microwave-assisted synthesis. Precursor synthesis of $[1]^{2-}$ was adapted from previously described methods (see SI for details).[31,42,43] 8

Figure 2. Synthesis of **2** from TBA_2**[1]** using microwave-based method along with two previously reported methods indicating dramatic reduction in reaction time without compromising the isolated yield of $\mathbf{[2]^0}$.[31] 9

Figure 4. (a) Redox potential of $[B_{12}(OR)_{12}]^{2-/1-}$ and (b) $[B_{12}(OR)_{12}]^{1-/0}$ substituted with various benzyl substituents plotted vs Hammett constants.[3,45] Previously characterized[40] (black) and new (red) $[B_{12}(OR)_{12}]^0$ clusters are shown. 13

Figure 5. (a) Reversible redox activity of **13**; (b) Cyclic voltammogram (CV) demonstrating two independent, one-electron oxidation/reduction waves between 2-/1-, and 1-/0 states (1 mM **13** with 0.1 M $TBAPF_6$ in CH_2Cl_2; glassy carbon working electrode, Pt wire counter electrode, Ag/AgCl pseudoreference electrode behind a CoralPor tip; referenced to an internal ferrocene standard); (c) Infrared spectroelectrochemical (IRSEC)[48,49] analysis of 0/1-/2- states of **13**; (d) ^{19}F NMR spectra of $\mathbf{[13]^{1-}}$ and $\mathbf{[13]^{2-}}$ with EPR of $\mathbf{[13]^{1-}}$ (inset); (e) UV-Vis spectra of $\mathbf{[13]^{1-}}$ and $\mathbf{[13]^{2-}}$. 15

Figure 6. (A-B) Solid state X-ray structures for $\mathbf{[13]^{1-}}$ and $\mathbf{[11]^0}$ shown with 50% thermal ellipsoid probabilities for the boron atoms (hydrogen atoms omitted for clarity). B atoms are blue, O – red, C – black, and F – green. Selected bond lengths and angles of the boron cores (substituents omitted for clarity) for $\mathbf{[11]^0}$ and $\mathbf{[13]^{1-}}$ are shown on the bottom. Overlay of the two cores ($\mathbf{[13]^{1-}}$ in blue, $\mathbf{[11]^0}$ in red) is depicted in the middle. 17

Figure 7. (a) Boron XPS spectra for $TBA_2\mathbf{[1]^{2-}}$, TBA$\mathbf{[12]^{1-}}$, and $\mathbf{[11]^0}$ showing an increase in B–B bond energy with increasing oxidation state; (b) Boron XPS spectra for $TBA_2\mathbf{[13]^{2-}}$ and TBA$\mathbf{[13]^{1-}}$ indicating the higher B-B bond energies of the $\mathbf{[13]^{2-}}$ and $\mathbf{[13]^{1-}}$ anions compared to the other substituted clusters. 19

Figure 8. One-pot synthesis of vertex-differentiated *hypercloso* cluster $[\mathbf{14}]^0$ from a 60:1:1 molar mixture of benzyl bromide:bromoethane:TBA_2[**1**]. Isolated yield of $\mathbf{[14]^0}$ was 18% (compound $\mathbf{[4]^0}$ was also formed as an additional product of the reaction). ^{11}B NMR spectra indicates loss of the icosahedral symmetry due to vertex differentiation, ^1H NMR integrations show 24H (CH_2) and 36H (CH_3) for the 11 ethyl groups and 2H (CH_2) and 5H (Ph) for the single benzyl moiety. 20

Figure 9. (a) Synthetic route to produce **[1]** from $Cs_2[B_{12}H_{12}]^{2-}$. (b) Microwave synthesis of the $B_{12}(OR)_{11}NO_2$ cluster **[2]** studied in this work, showing all three oxidation states of **[2]** isolated (neutral $\mathbf{[2a]^0}$, radical $\mathbf{[2b]^{1-}}$, and the dianionic $\mathbf{[2c]^{2-}}$). 45

Figure 10. (a) ^{11}B and ^{19}F NMR spectra of all redox states of **[2]** with EPR (inset, g = 2.00674) and photo of **[2b]**$^{\mathbf{1-}}$ in MeCN; (b) UV-vis spectra of **[2a]**$^{\mathbf{0}}$ and **[2b]**$^{\mathbf{1-}}$ (50 mM) and **[2c]**$^{\mathbf{2-}}$ (100 mM) in CH_2Cl_2; (c) XPS spectra for all redox states of **[2]** showing increasing B-B binding energy as redox state increases. 47

Figure 11. (a) Single crystal X-ray structure of **[2b]**$^{1-}$ (hydrogens and $[N^{n}Bu_4]^+$ counter ion omitted for clarity); (b) Overlay of **[2b]**$^{1-}$ and **[3]**$^{1-}$; (c) Single crystal X-ray structure of **[3]**$^{1-}$ (hydrogens and $[N^{n}Bu_4]^+$ counter ion omitted for clarity); (d) Cyclic voltammogram for **[2b]**$^{1-}$ and **[3]** in acetonitrile with glassy carbon working electrode, Pt wire counter electrode, and Ag/AgCl reference electrode (in sat. KCl) internally referenced to the Fc/Fc$^+$ couple. 49

Figure 12. (a) Scheme showing the S_NAr reaction between **[2c]**$^{\mathbf{2-}}$ and mercaptoethanol; (b) ^{19}F NMR spectrum of the starting material **[2c]**$^{\mathbf{2-}}$; (c) ^{19}F NMR spectrum of the reaction product showing full conversion to **[2c]-ME** based upon the disappearance of the *para*-fluorine signal. 50

Figure 13. "Anatomy of a boron cluster" illustrating reversible redox activity tunable via substituents, the robust nature of the cluster core stabilized by strong B—O bonds, and the highly delocalized electron density in 3D around the entire cage. 67

Figure 14. Cyclic voltammograms of $\mathbf{1}^{2-/1-}$ (top, red), $\mathbf{2}^{0/1-}$ (middle, black), and a mixture of the two clusters (bottom, blue) at 1 mM in 0.5 M $TBAPF_6$ in MeCN at a scan rate of 10 mV s^{-1}, referenced to ferrocene/ferrocenium at 0 V. 69

Figure 15. Symmetric flow cell cycling results. a) Symmetric flow cell setup. b) Charge and discharge capacity plotted (left) as a function of cycle number in along with coulombic efficiency (right). Arrowheads (colors match c) indicate cycles for which the voltage profile is shown in (c). c) Charge and discharge voltage profiles are shown for select cycles. d) Detailed view of coulombic efficiency as a function of cycle number. Gray dashed lines in (b) and (d) indicate interruptions of the experiment due to intentional electrolyte rebalancing (424 h) and a building power outage (632 h). 70

Figure 16. Full cell cycling results. a) Flow cell setup for cycling at 5 mA cm^{-2} showing premixed redox-active electrolytes. b) Voltage profiles for selected cycles. c) Capacity and d) efficiency as a function of cycle number 73

Figure S1. Background cyclic voltammograms of 0.5 M $TBAPF_6$ in MeCN taken at a scan rate of 10 mV s^{-1}. 84

Figure S2. Cyclic voltammograms as a function of scan rate for **1** (a) and **2** (c), and the corresponding Randles-Sevcik peak-current analysis for **1** (b) and **2** (d). All of the experiments were conducted with 1 mM active material in 0.5 M $TBAPF_6$ in MeCN. 85

Figure S3. Symmetric cell EIS at 50% state-of-charge. 87

Figure S4. Full cell EIS at 0% state-of-charge. 87

List of Tables

Table 1. Crystal data and structure refinement for $[2b]^{1-}$ 63

Table 2. Measured redox potentials, peak separations, peak-current ratios, and diffusion coefficients for $1^{2-/1-}$ and $2^{0/1-}$. 70

Acknowledgements

I would like to thank the members of my thesis committee, my colleagues in the Spokoyny lab, and Dr. Alexander Spokoyny for providing an intellectually stimulating research environment.

Vita

Education

- Master of Science, Chemistry—Jan 2016; University of California, Los Angeles, CA
- Master of Science, Environmental Science—Dec 2012; Christopher Newport University, VA
- Bachelor of Science, Chemistry—Apr 2011; Christopher Newport University, VA

Research Experience

Ph.D. and M.S. Research, University of California, Los Angeles, Dept. of Chemistry & Biochemistry, 2013–Present

- Developed rapid microwave-based synthetic route to produce perfunctionalized icosahedral boron clusters under ambient conditions up to 500x faster than prior methods
- Synthesized and characterized 30+ cluster derivatives featuring tailored photophysical properties

M.S. Thesis Research, Christopher Newport University, Dept. of Molecular Biology & Chemistry, 2011–2012

- Optimized 100% acid-free electrochemical polishing for the Thomas Jefferson National Accelerator Facility
- Designed and taught a green chemistry lab experiment published in the Journal of Chemical Education

Chemistry Intern, Thomas Jefferson National Accelerator Facility, 2011

- Developed alternative to eliminate use of 100+ L of H_2SO_4 and HF acids for SRF cavity preparation
- Investigated electrochemical deposition of 100% recycled niobium as thin films on copper substrates

Chemistry Research Assistant, Christopher Newport University, BCES Dept., 2009–2011

- Prepared samples and conducted analysis for diverse projects focused on catalysis and green chemistry

Independent Research, Christopher Newport University/Thomas Jefferson National Accelerator Facility, 2009–2011

- Developed mechanochemical syntheses for different polymorphs of porphyrin-based metal complexes

Honors

- Seaborg Symposium Poster Award—November 2017
- Dissertation Year Fellowship from UCLA—October 2017
- Travel grant from the Electrochemical Society for the 222nd National Meeting—October 2012
- 1st Place — Bridging Research Communities Poster Competition, Carnegie Mellon University—October 2010

Presentations

- 254th American Chemical Society National Meeting Oral Presentation—Washington, DC, August 2017
- Seaborg Symposium Research Poster Presentation—Los Angeles, CA, November 2016
- 251st American Chemical Society National Meeting Poster Presentation—San Diego, CA, March 2016
- Seaborg Symposium Research Poster Presentation—Los Angeles, CA, October 2015
- 14th Annual Sigma Xi Tidewater Region Student Poster Presentation—Newport News, VA, November 2012
- 222nd Meeting of the Electrochemical Society Oral and Poster Presentations—Honolulu, HI, October 2012
- 220th Meeting of the Electrochemical Society Poster Presentation—Boston, MA, October 2011
- Poster Competition Bridging Research Communities—Carnegie Mellon University, October 2010
- 12th Annual Sigma Xi Tidewater Region Student Poster Presentation— Newport News, VA, November 2010

Publications

1. Wixtrom, A. I.; Barton, J. L.; Kowalski, J. A.; Brushett, F. R.; Spokoyny, A. M. Perfunctionalized Dodecaborate Clusters as Stable Metal-Free Active Materials for Charge Storage. **2018**, *in preparation*.
2. Wixtrom, A. I.; Parvez, Z. A.; Savage, M. D.; Qian, E. A.; Jung, D.; Khan, S. I.; Rheingold, A. L.; Spokoyny, A. M. Tuning the Electrochemical Potential of Perfunctionalized Dodecaborate Clusters through Vertex Differentiation. *Chem. Commun.* **2018**, *54* (46), 5867–5870
3. Axtell, J. C.; Saleh, L. M. A.; Qian, E. A.; Wixtrom, A. I.; Spokoyny, A. M. Synthesis and Applications of Perfunctionalized Boron Clusters. *Inorg. Chem.* **2018**, *57* (5), 2333–2350
4. Kirlikovali, K. O.; Cho, E.; Downard, T. J.; Grigoryan, L.; Han, Z.; Hong, S.; Jung, D.; Quintana, J. C.; Reynoso, V.; Ro, S.; Shen, Y.; Swartz, K.; Ter Sahakyan, E.; Wixtrom, A. I.; Yoshida, B.; Rheingold, A. L.; Spokoyny, A. M. Buchwald–Hartwig Amination Using Pd(I) Dimer Precatalysts Supported by Biaryl Phosphine Ligands. *Dalt. Trans.* **2018**, *47* (11), 3684–3688
5. Jung, D.; Saleh, L. M. A.; Berkson, Z. J.; El-Kady, M. F.; Hwang, J. Y.; Mohamed, N.; Wixtrom, A. I.; Titarenko, E.; Shao, Y.; McCarthy, K.; Guo, J.; Martini, I. B.; Kraemer, S.; Wegener, E. C.; Saint-Cricq, P.; Ruehle, B.; Langeslay, R. R.; Delferro, M.; Brosmer, J. L.; Hendon, C. H.; Gallagher-Jones, M.; Rodriguez, J.; Chapman, K. W.; Miller, J. T.; Duan, X.; Kaner, R. B.; Zink, J. I.; Chmelka, B. F.; Spokoyny, A. M. A Molecular Cross-Linking Approach for Hybrid Metal Oxides. *Nat. Mater.* **2018**, *17* (4), 341–348
6. Abdel-Fattah, T. M.; Wixtrom, A.; Arias, L.; Zhang, K.; Baumgart, H. Quantitative Analysis of X-Ray Fluorescence Absorption and Emission for Thickness Determination of ALD-Grown Metal and Oxide Nanoscaled Films. *J. Nanosci. Nanotechnol.* **2017**, *17* (8), 5745–5750
7. Qian, E. A.; Wixtrom, A. I.; Axtell, J. C.; Saebi, A.; Jung, D.; Rehak, P.; Han, Y.; Moully, E. H.; Mosallaei, D.; Chow, S.; Messina, M. S.; Wang, J. Y.; Royappa, A. T.; Rheingold, A. L.; Maynard, H. D.; Král, P.; Spokoyny, A. M. Atomically Precise Organomimetic Cluster Nanomolecules Assembled via Perfluoroaryl-Thiol SNAr Chemistry. *Nat. Chem.* **2017**, *9* (4), 333–340
8. Wixtrom, A. I.; Shao, Y.; Jung, D.; Machan, C. W.; Kevork, S. N.; Qian, E. A.; Axtell, J. C.; Khan, S. I.; Kubiak, C. P.; Spokoyny, A. M. Rapid Synthesis of Redox-Active Dodecaborane $B_{12}(OR)_{12}$ Clusters under Ambient Conditions. *Inorg. Chem. Front.* **2016**, *3* (5), 711–717
9. Messina, M. S.; Axtell, J. C.; Wang, Y.; Chong, P.; Wixtrom, A. I.; Kirlikovali, K. O.; Upton, B. M.; Hunter, B. M.; Shafaat, O. S.; Khan, S. I.; Winkler, J. R.; Gray, H. B.; Alexandrova, A. N.; Maynard, H. D.; Spokoyny, A. M. Visible-Light-Induced Olefin Activation Using 3D Aromatic Boron-Rich Cluster Photooxidants. *J. Am. Chem. Soc.* **2016**, *138* (22), 6952–6955
10. Abdel-Fattah, T. M.; Wixtrom, A.; Zhang, K.; Cao, W.; Baumgart, H. Catalytic Reduction of 4-Nitrophenol Using Gold Nanoparticles Supported on Carbon Nanotubes. *ECS J. Solid State Sci. Technol.* **2014**, *3* (4), M18–M20
11. Lapidus, S. H.; Naik, A.; Wixtrom, A.; Massa, N. E.; Ta Phuoc, V.; del Campo, L.; Lebègue, S.; Ángyán, J. G.; Abdel-Fattah, T.; Pagola, S. The Black Polymorph of TTF-CA: TTF Polymorphism and Solvent Effects in Mechanochemical and Vapor Digestion Syntheses, FT-IR, Crystal Packing, and Electronic Structure. *Cryst. Growth Des.* **2014**, *14* (1), 91–100
12. Wixtrom, A.; Buhler, J.; Abdel-Fattah, T. Mechanochemical Synthesis of Two Polymorphs of the Tetrathiafulvalene-Chloranil Charge Transfer Salt: An Experiment for Organic Chemistry. *J. Chem. Educ.* **2014**, *91* (8), 1232–1235
13. Abdel-Fattah, T. M.; Wixtrom, A.; Zhang, K.; Cao, W.; Baumgart, H. Highly Uniform Self-Assembled Gold Nanoparticles over High Surface Area ZnO Nanorods as Catalysts. *ECS J. Solid State Sci. Technol.* **2014**, *3* (10), M61–M64
14. Wixtrom, A. I.; Buhler, J. E.; Reece, C. E.; Abdel-Fattah, T. M. Electrochemical Polishing Applications and EIS of a Vitamin B4-Based Ionic Liquid. *J. Electrochem. Soc.* **2013**, *160* (3), E22–E26
15. Wixtrom, A. I.; Buhler, J. E.; Reece, C. E.; Abdel-Fattah, T. M. Reclamation of Niobium Compounds from Ionic Liquid Electrochemical Polishing of Superconducting Radio Frequency Cavities. *J. Environ. Chem. Eng.* **2013**, *1*, 18–22
16. Damiano, B. T.; Shenenberger, A.; Wixtrom, A. I.; Abdel-Fattah, T. M. Electrochemical Deposition of Cobalt onto the Surface of Copper Using a Choline Chloride-Based Ionic Liquid. *ECS Trans.* **2013**, *50* (11), 277–281.
17. Wixtrom, A. I.; Buhler, J.; Reece, C. E.; Abdel-Fattah, T. M. Electrochemical Deposition of Niobium onto the Surface of Copper Using a Novel Choline Chloride-Based Ionic Liquid. *ECS Trans.* **2012**, 50.
18. Wixtrom, A. I.; Buhler, J.; Reece, C. E.; Abdel-Fattah, T. M. Electrochemical Polishing Applications and EIS of a Novel Choline Chloride-based Ionic Liquid. *ECS Trans.* **2012**, 50.

Chapter 1: Introduction to Boron Cluster Chemistry

The first simple borane compounds were discovered in 1912 by Alfred Stock,[1–3] and were initially regarded as exotic species lacking practical value outside of academic curiosity. Additionally, their inherent pyrophoric properties complicated their synthesis and characterization. However, in the 1940's, a new wave of interest in boron compounds emerged, initiated by the hypothesis that pentaborane, B_5H_9, and decaborane, $B_{10}H_{14}$, would prove to function as enhanced rocket fuels compared to traditional hydrocarbons.[2,3] Since B-H bond energy is higher than the C-H bond energy found in hydrocarbon fuels, it was predicted that the boron-based fuels could serve as better propellants. Efforts to produce suitable high-energy fuels stalled when it was discovered that borates formed from the combustion of borane materials clog the jet engines they were intended to power,[3,4] though the interest brought about by these fuel application studies initiated the so-called "renaissance era" of boron chemistry. One of the most important concepts that shaped our modern understanding of borane chemistry was the notion of three-center two-electron bonding in boron compounds.[5] Lipscomb predicted the existence of an icosahedral boron hydride ($B_{12}H_{12}$) in 1954, which Longuet-Higgins and Roberts treated to a theoretical molecular orbital-based approach in 1955, and they reached the conclusion that it would likely only be stable as a dianion.[5,6] The first experimental evidence of the predicted *closo*-$[B_{12}H_{12}]^{2-}$ was observed by Shapiro and Williams in 1959,[7] followed shortly by the successful isolation (albeit in a relatively low yield) of the triethylammonium salt of *closo*-$[B_{12}H_{12}]^{2-}$ in 1960 by Hawthorne and co-workers.[8]

After the discovery of this new three-dimensional boron hydride, the "renaissance era" in the field of boron cluster chemistry flourished for several decades, led by the pioneering work of

Hawthorne, Knoth, Muetterties, and several other practicioners.[2,9–22] During the course of their studies, the synthesis of *closo*-$[B_{12}H_{12}]^{2-}$ was improved to allow for significantly larger scale production with much higher yields (>90%).[2] Perhaps the most important discovery in the history of boron clusters is that they can undergo facile functionalization chemistry reminiscent of classical organic molecules such as benzene, thus enabling the development of functionalized boron clusters.[3,23,24] For years the prevailing (and largely incorrect) viewpoint of boron hydride compounds was that they were exotic and highly unstable species, and they would rapidly degrade when exposed to heat, acids, or bases. Efforts to utilize boron hydrides as rocket fuels were stymied by the unavoidable borane combustion products degrading jet engine performance.[3,4] With the advent of the *closo*-$[B_{12}H_{12}]^{2-}$ cluster, now possible to readily synthesize at large scales with high yields, studies of the icosahedral cluster revealed their remarkable stability. Several different salts of *closo*-$[B_{12}H_{12}]^{2-}$ were subjected to harsh conditions including heating to 95 °C in strongly acidic (3 N HCl) and basic (3 N NaOH) media with no observable degradation, and even heating the cluster to 810 °C failed to result in degradation.[21]

The surprisingly exceptional thermal stability of *closo*-$[B_{12}H_{12}]^{2-}$ and remarkable resistance to extremely harsh conditions, combined with the demonstrated potential for facile functionalization of the cluster inspired several research groups to study new derivatives of this fascinating molecule. Knoth and co-workers were the first to report persubstitution (where all 12 vertices of the icosahedron were functionalized) of *closo*-$[B_{12}H_{12}]^{2-}$ with halogens, isolating *closo*-$[B_{12}F_{12}]^{2-}$, *closo*-$[B_{12}Cl_{12}]^{2-}$, *closo*-$[B_{12}Br_{12}]^{2-}$ and *closo*-$[B_{12}I_{12}]^{2-}$ clusters.[12,25] After successful perfunctionalization of $[B_{12}H_{12}]^{2-}$ with halogens was demonstrated, additional derivatives were developed featuring methyl and hydroxy groups.[26–30] Of these newer derivatives, *closo*-

$[B_{12}(OH)_{12}]^{2-}$ is of particular interest as it possesses the ability to be further functionalized *via* formation of ether, ester, carbonate, and carbamate linkages.[29,31–33]

Another unique feature found in these clusters is three-dimensional delocalization of the electron density across the entire icosahedral cage, which allows perfunctionalized boron clusters to access electronic states that do not conform to Wade's rules.[34] Despite the accurate prediction that the parent dodecaborate cluster *closo*-$[B_{12}H_{12}]^{2-}$ could only exist as a dianion,[6] perfunctionalization with halogens, methyl, and hydroxy groups led others to investigate the possibility of two additional oxidation states: a stable radical *hypocloso*-$[B_{12}R_{12}]^{1-}$ and neutral *hypercloso*-$[B_{12}R_{12}]^{0}$. Attempts to oxidize the parent *closo*-$[B_{12}H_{12}]^{2-}$ cluster resulted in irreversible degradation *via* formation of a B–B linked dimer,[13] yet several perfunctionalized cluster derivatives were found to exhibit reversible redox behavior.[35] In 1985, the first evidence of a single electron oxidation of *closo*-$[B_{12}X_{12}]^{2-}$ resulting in formation of a *hypocloso*-$[B_{12}X_{12}]^{1-}$ radical was reported by Rupich,[36] the identity of which was later confirmed by Weber and co-workers as *hypocloso*-$[B_{12}Cl_{12}]^{1-}$.[37] The perhydroxylated and permethylated radicals *hypocloso*-$[B_{12}(OH)_{12}]^{1-}$ and *hypocloso*-$[B_{12}Me_{12}]^{1-}$ were also successfully synthesized,[38,39] indicating these cluster radicals are both stable and isolable species. The neutral clusters *hypercloso*-$[B_{12}Cl_{12}]^{0}$ and *hypercloso*-$[B_{12}(OCH_2Ph)_{12}]^{0}$ were also isolated, confirming the stability of the neutral oxidation state for these clusters.[37,40]

More thorough investigation of the redox properties of dodecaborate clusters was performed by Hawthorne and co-workers focusing on the perbenzylated species $[B_{12}(OCH_2Ph)_{12}]$, which was isolated in all three possible oxidation states.[40] Full spectroscopic characterization of dianionic *closo*-$[B_{12}(OCH_2Ph)_{12}]^{2-}$, radical *hypocloso*-$[B_{12}(OCH_2Ph)_{12}]^{1-}$, and neutral *hypercloso*-$[B_{12}(OCH_2Ph)_{12}]^{0}$) was reported in this study along with single crystal X-ray structures for all three species.[40] These three oxidation states were accessible *via* two sequential, quasi-reversible one-electron oxidation reactions of the parent dianion.[40] In a later study, the redox activity of multiple benzyl and alkyl functionalized $B_{12}(OR)_{12}$ clusters was evaluated electrochemically, all of which were found to exhibit similarly reversible redox behavior.[31] One of the more interesting observations from these cluster redox studies was that the redox potential of $B_{12}(OR)_{12}$ species is rationally tunable as a function of the O-bound substituent, reminiscent of the tunable nature of metal-based redox-active inorganic complexes.[31,35,41] While this intriguing feature certainly warranted further study of the degree of tunability possible with $B_{12}(OR)_{12}$ clusters, all reported synthetic routes to perfunctionalize *closo*-$[B_{12}(OH)_{12}]^{2-}$ to date required extremely long reaction duration (days to weeks) or highly specialized high-pressure equipment. Additionally, all synthetic routes reported had strict inert atmospheric requirements, further complicating the production of new derivatives.[29,31,40] A need exists for a more robust and flexible synthetic method that would allow development of perfunctionalized $B_{12}(OR)_{12}$ clusters under more favorable conditions, with a significantly reduced reaction duration. This would allow for a much more rapid exploration of novel cluster derivatives, with the ability to design cluster species with specific desired properties for a plethora of applications ranging from photocatalysis to energy storage.

Chapter 2: Rapid Synthesis of Redox-Active Dodecaborane $B_{12}(OR)_{12}$ Clusters Under Ambient Conditions

Alex I. Wixtrom,[a] Yanwu Shao,[a] Dahee Jung,[a] Charles W. Machan,[b] Shaunt N. Kevork,[a] Elaine A. Qian,[a] Jonathan C. Axtell,[a] Saeed I. Khan,[a] Clifford P. Kubiak[b] and Alexander M. Spokoyny[a]*

[a]*Department of Chemistry and Biochemistry, University of California, Los Angeles*
607 Charles E. Young Drive East, Los Angeles, California 90095-1569
[b]*Department of Chemistry and Biochemistry, University of California, San Diego, 9500 Gilman Drive, La Jolla, California 92093-0358*

* Corresponding author. E-mail: spokoyny@chem.ucla.edu

We have developed a fast and efficient route to obtain perfunctionalized ether-linked alkyl and benzyl derivatives of the *closo*-$[B_{12}(OH)_{12}]^{2-}$ icosahedral dodecaborate cluster via microwave-assisted synthesis. These icosahedral boron clusters exhibit three-dimensional delocalization of the cage-bonding electrons, tunable photophysical properties, and a high degree of stability in air in both solid and solution states. A series of *closo*-$[B_{12}(OR)_{12}]^{2-}$, *hypocloso*-$[B_{12}(OR)_{12}]^{1-}$ and *hypercloso*-$[B_{12}(OR)_{12}]^{0}$ clusters have been prepared with reaction times ranging from hours to several minutes. This method is superior to previously reported protocols since it dramatically decreases the reaction times required and eliminates the need for inert atmosphere conditions. The generality of the new microwave-based method has been further demonstrated through the synthesis of several new derivatives, which feature redox potentials up to 0.6 V more positive than previously known $B_{12}(OR)_{12}$ cluster compounds. We further show how this method can be applied to a one-pot synthesis of hybrid, vertex-differentiated species $B_{12}(OR)_{11}(OR')$ that was formerly accessible only via multi-step reaction sequence.

Introduction

The existence of an icosahedral dodecaborate $[B_{12}H_{12}]$ cluster was first predicted by Lipscomb and co-workers in 1954.[5] In a subsequent theoretical molecular orbital-based approach published in 1955[6], Longuet-Higgins and Roberts predicted that such a cluster would only be stable as dianionic $[B_{12}H_{12}]^{2-}$. A 1959 study by Shapiro and Williams[7] suggested the possible formation of a $[B_{12}H_{12}]^{2-}$ icosahedron, and in 1960 this cluster was first successfully isolated and characterized as a triethylammonium salt by Pitochelli and Hawthorne, albeit in a relatively low yield.[8] Subsequent pioneering studies by Hawthorne, Knoth, Muetterties, and others initiated a new era in the field of boron cluster chemistry.[2,9–22] Specifically, these groups have shown that $[B_{12}H_{12}]^{2-}$ can be prepared on a large scale in a high yield (>90%)[2] and undergo facile functionalization chemistry that parallels some properties of classical organic molecules (*e.g.* benzene).[3,23,24] This was an exciting discovery, since previously many boron hydride clusters were perceived as highly unstable species prone to fast degradation by heat, acids, and bases. Conversely, $[B_{12}H_{12}]^{2-}$ salts were shown to be stable in acids and bases, and were thermally stable as high as 810 °C with no observable decomposition.[21] Knoth and co-workers were the first to demonstrate the persubstitution of $[B_{12}H_{12}]^{2-}$, producing halogenated $[B_{12}F_{12}]^{2-}$, $[B_{12}Cl_{12}]^{2-}$, $[B_{12}Br_{12}]^{2-}$ and $[B_{12}I_{12}]^{2-}$ derivatives.[12,25] In the past two decades, persubstitution of $[B_{12}H_{12}]^{2-}$ was improved with new synthetic methods and extended towards other functional groups including $[B_{12}Me_{12}]^{2-}$ and $[B_{12}(OH)_{12}]^{2-}$.[26–30] Among the perfunctionalized derivatives synthesized, *closo*-$[B_{12}(OH)_{12}]^{2-}$ is particularly appealing, as it is capable of undergoing further functionalization by forming ether, ester, carbonate, and carbamate linkages.[29,31–33]

While controlled oxidation of the parent $[B_{12}H_{12}]^{2-}$ anion leads to an irreversible cluster degradation forming a B–B linked dimer,[13] several perfunctionalized variants have been previously observed to undergo reversible redox behavior.[35] For example, Rupich reported that $[B_{12}X_{12}]^{2-}$ could undergo a single electron oxidation to form a stable radical $[B_{12}X_{12}]^{1-}$,[36] which was recently isolated and structurally confirmed as the oxidized radical $[B_{12}Cl_{12}]^{1-}$ species by Weber and co-workers.[37] Hawthorne and co-workers reported that the perfunctionalized $B_{12}(OCH_2Ph)_{12}$ cluster can exist in three distinct redox states accessible via two sequential and quasi-reversible one-electron oxidation reactions of the parent dianionic *closo* species.[40] The same group later showed that other benzyl and alkyl functionalized $B_{12}(OR)_{12}$ clusters can be synthesized, and all of these species exhibit similarly reversible redox behavior.[31] Schleid and co-workers subsequently showed that the parent $[B_{12}(OH)_{12}]^{2-}$ cluster can undergo a one-electron oxidation to form a stable radical $[B_{12}(OH)_{12}]^{1-}$ species.[38] Interestingly, the redox potential of the ether-linked $B_{12}(OR)_{12}$ species can be rationally tuned as a function of the O-bound substituent, reminiscent of many metal-based redox-active inorganic complexes.[31,35,41] Unfortunately, all of the reported synthetic routes towards $B_{12}(OR)_{12}$ clusters currently require either extremely long reaction times (weeks) or highly specialized high-pressure equipment. Furthermore, in all cases strict inert atmospheric conditions are also required for their synthesis.[29,31,40]

Herein we report a rapid, scalable, and robust synthetic route to a wide range of perfunctionalized $B_{12}(OR)_{12}$ cluster derivatives utilizing a bench-top microwave reactor. This technology has emerged over the past several decades and has been successfully employed in a large number of synthetic schemes[42] which necessitate the reaction heating above the boiling point of the solvent. Our work shows that the microwave-based method enables synthesis of perfunctionalized ether-linked boron clusters within minutes and does not require the use of inert atmosphere and rigorously dried solvents. We further show the synthetic utility of our method in the preparation of previously unknown $B_{12}(OR)_{12}$ derivatives featuring highly oxidizing redox potentials as well as vertex-differentiated molecular architectures. Synthesized cluster species were all isolated and characterized using solution-based NMR and IR spectroscopic tools and mass spectrometry. Electron delocalization of the radical state in these species was further evaluated by electron paramagnetic resonance (EPR) spectroscopy and elucidated by X-ray photoelectron spectroscopy (XPS).

Results and Discussion

The tetrabutylammonium (TBA) salt of *closo*-$[B_{12}(OH)_{12}]^{-2}$ (TBA$_2$**[1]**) was chosen for use with our microwave synthesis due to its enhanced solubility in organic solvents compared to alkali metal salts of **1** (Figure 1).[31] The synthesis of TBA$_2$**[1]** was adapted from previously reported protocols by Hawthorne and co-workers (see SI for details).[31,43,44]

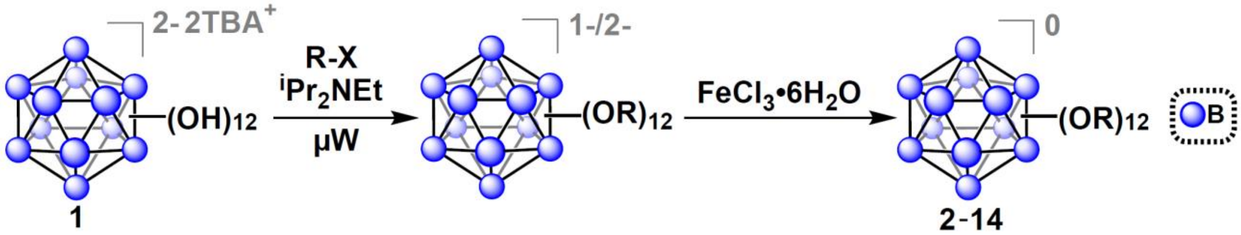

Figure 1. Synthetic route to produce functionalized ether-linked derivatives of the *hypercloso* boron clusters (2-14) via microwave-assisted synthesis. Precursor synthesis of $[1]^{2-}$ was adapted from previously described methods (see SI for details).[31,43,44]

Oxygen-free, anhydrous conditions (oven-dried glassware, dried and distilled solvents, nitrogen atmosphere) were initially employed for microwave-assisted syntheses of alkyl- and benzyl-functionalized *closo*-$[B_{12}(OH)_{12}]^{2-}$ **[1]** ether-linked derivatives, due to previously described high-pressure and reflux-based methods necessitating stringent air and moisture free conditions.

To our surprise, we discovered that microwave reactions utilizing previously reported conditions (benzyl bromide and TBA$_2$[**1**] in the presence of *N*,*N*-diisopropylethylamine (DIEA, Hünig's base) in acetonitrile) are driven at a much higher rate, resulting in quantitative formation of a mixture of charged 1-/2- TBA salts of **2** within 15 minutes at 140 °C, as indicated by *in situ* ^{11}B NMR spectroscopy. Specifically, no parent ^{11}B NMR resonance at δ –18 corresponding to the $[B_{12}(OH)_{12}]^{2-}$ starting material is observed, and a singlet at δ –16 can be seen instead. Concomitant presence of **[2]$^{1-}$** radical species in the product mixture can be deduced from the diagnostic pink color of the solution and its measured signature EPR signal (G-factor = 2.008121). Oxidation of the reaction mixture using $FeCl_3{\cdot}6H_2O$ in 90/10 ethanol/acetonitrile followed by column chromatography on silica gel produces the pure neutral cluster **[2]^0** in 63% yield (Figure 2). Oxidation can be conveniently monitored by ^{11}B NMR, where the fully oxidized cluster **[2]^0** exhibits a downfield resonance shift at δ 41.8. Overall, this represents a significant reduction in reaction duration from the originally reported 6 days and 4 hours required for reflux and high-pressure reactor methods, respectively, while retaining similar yield.[31]

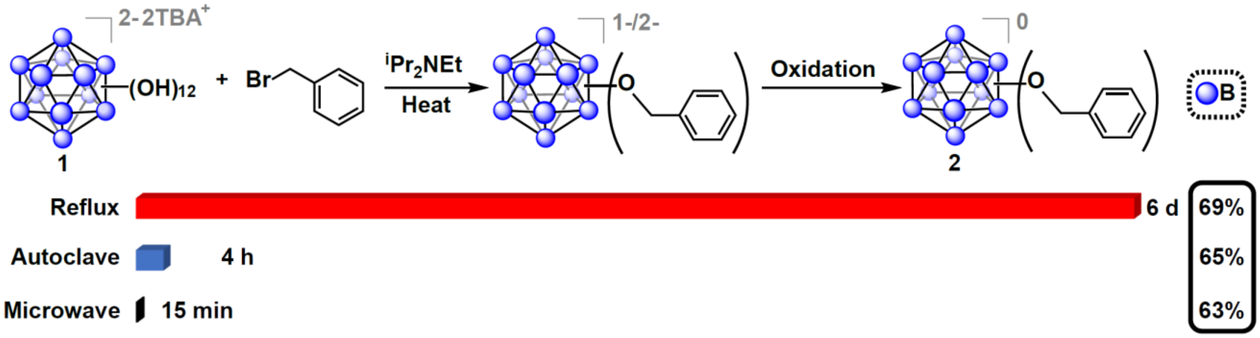

Figure 2. Synthesis of **2** from TBA$_2$**[1]** using microwave-based method along with two previously reported methods indicating dramatic reduction in reaction time without compromising the isolated yield of **[2]^0**.[31]

Encouraged by these results, we then optimized the microwave reaction times with allyl bromide and bromoethane reagents independently, and in both cases observed that complete substitution can be accomplished within 15 - 30 minutes at 140 °C. These compounds were isolated in their fully oxidized neutral form in a similar fashion to **[2]^0**, (compounds **[3]^0** and **[4]^0,** respectively; Figure 3). Notably, previously reported high-pressure reactor synthesis of these species required 3 and 12 hours, respectively, for alkylation to occur at all twelve vertices, suggesting that the microwave-based method can be generally applied to several classes of ether-linked $B_{12}(OR)_{12}$ clusters and is potentially superior to the previously developed methods.[31]

The relatively short perfunctionalization reaction times made possible by this new microwave technique prompted us to investigate whether it would be possible to utilize ambient synthetic conditions. Specifically, we hypothesized that the fast rate of product formation would outcompete the rate of degradation stemming from the presence of adventitious air and moisture during the synthesis. We therefore tested the synthesis of **2** using as-received non-dried acetonitrile (see SI) with the reagents added to a reaction vessel open to air. The open-air synthesis of **2** proceeded with full conversion in 15 minutes as indicated by ^{11}B NMR spectroscopy on the crude mixture. Following the normal work-up procedure (see SI), **[2]^0** was isolated in a 63% yield, suggesting that rigorous exclusion of air and moisture is not necessary for this transformation. This open-air synthesis method was successfully used for all subsequent ether-based cluster syntheses reported in this work. We decided to further explore the scope of this transformation by using longer-chain alkyl substituents. Hexyl chain substitution required increased reaction times compared to the shorter ethyl substituent, yet persubstitution was still achieved within two hours, as opposed to 8 hours when using a high-pressure reactor[31] (isolated as **[5]^0**, Figure 3). This increased reaction time likely stems from the increase in the length and size of the alkyl reagent affecting the kinetics of the reaction.[45,46] To further probe the limits of the microwave-based method we tested hexene- and undecene-based electrophiles, and even with the requisite increase in reaction time to 7 and 8 hours respectively, persubstitution proceeded to full conversion. Neutral **[6]^0** and **[7]^0** were isolated in 43% and 28% yields, respectively, after oxidation and normal purification procedures (Figure 3). These derivatives have not been synthesized prior to this report, and their preparation illustrates how one can dramatically increase the size of these ether-based dodecaborate clusters via a direct linkage of large substituents featuring terminal olefins onto $[B_{12}(OH)_{12}]^{2-}$.

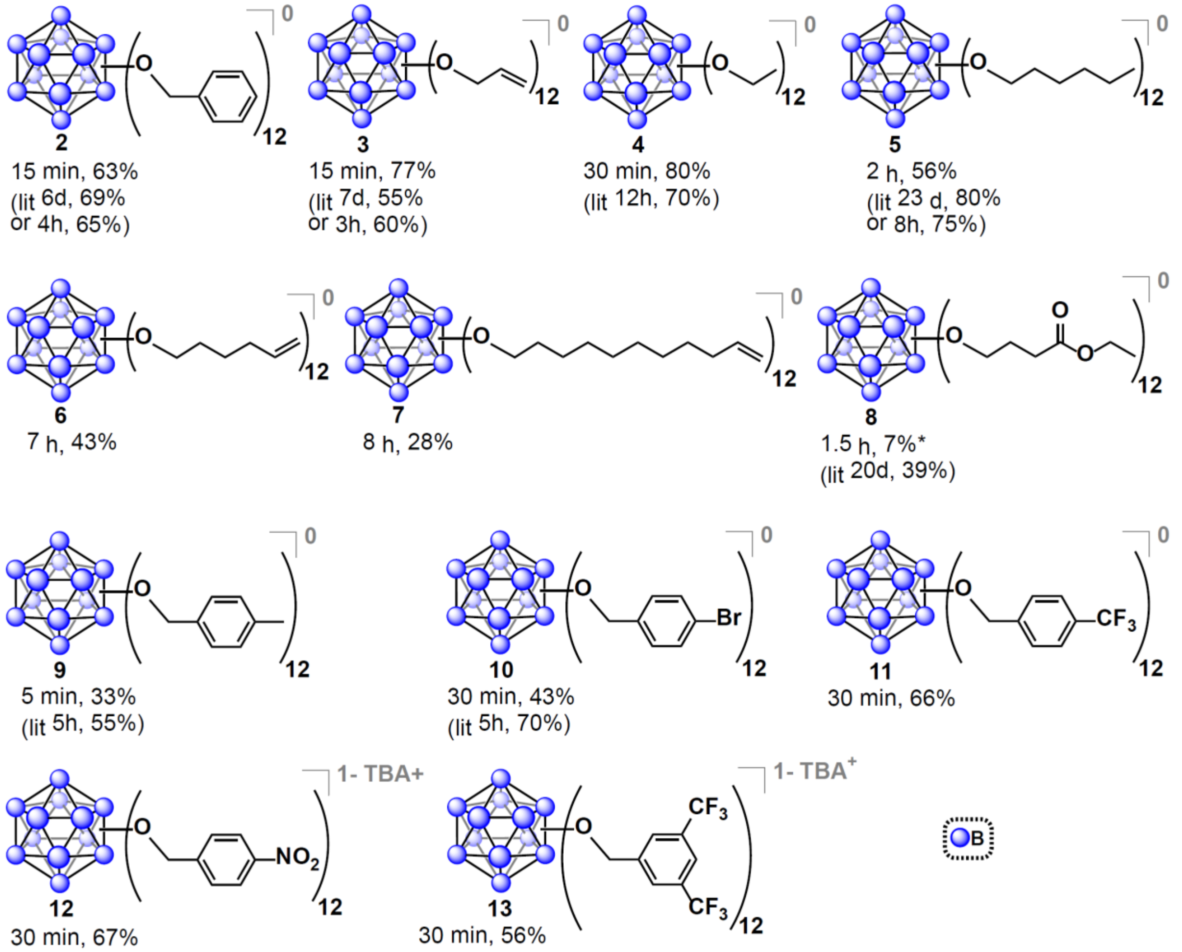
0
O
12
2
15 min, 63%
(lit 6d, 69%
or 4h, 65%)
0
O
12
3
15 min, 77%
(lit 7d, 55%
or 3h, 60%)
0
O
12
4
30 min, 80%
(lit 12h, 70%)
0
O
12
5
2 h, 56%
(lit 23 d, 80%
or 8h, 75%)
0
O
12
6
7 h, 43%
0
O
12
7
8 h, 28%
0
O
O
O
12
8
1.5 h, 7%*
(lit 20d, 39%)
0
O
12
9
5 min, 33%
(lit 5h, 55%)
0
O
Br
12
10
30 min, 43%
(lit 5h, 70%)
0
O
CF3
12
11
30 min, 66%
1- TBA+
O
NO2
12
12
30 min, 67%
1- TBA+
O
CF3
CF3
12
13
30 min, 56%
B

Figure 3. Synthesized $B_{12}(OR)_{12}$ clusters *via* microwave-based method. Yields are reported for the species isolated in a designated oxidation state as an average of two independent trials. For previously synthesized species, reported yield is given for comparison.[31] *Additional 8% of 1-/2- non-oxidized species collected.

Based on the success of the long-chain olefin-containing moieties, we investigated the compatibility of this system with less stable reagents by using ethyl 4-bromobutyrate with TBA_2[**1**]. Perfunctionalization with ethyl butyrate has been challenging using prior synthetic methods, requiring multiple-step sequential additions of the alkyl halide and Hünig's base for 20 days while being handled under inert atmosphere conditions.[47] However, utilizing microwave-assisted synthesis, the same product (Figure 3, **[8]$^{\mathbf{0}}$**) was obtained via a single 1.5 hour reaction, followed by oxidation with $FeCl_3 \cdot 6H_2O$ overnight and purification with column chromatography on Sephadex™ and silica gel.

Benzyl-substituted ether-based clusters can feature a high degree of electrochemical tunability as a function of the substituents attached to the aromatic ring.[41] Our method allows for the efficient synthesis of clusters containing both electron-rich (**9**) and electron-withdrawing (**10**) benzyl derivatives in yields matching previous methods but with significantly reduced reaction times (Figure 3). We were further intrigued by the possibility of extending the accessible electrochemical window for this class of compounds by utilizing benzyl halide precursors containing highly electron-withdrawing substituents. The perfunctionalized cluster featuring a trifluoromethyl (CF_3) group attached to the *para* position of the benzyl moiety was prepared using our method in 30 minutes, and following oxidation the isolated neutral compound **[11]$^{\mathbf{0}}$** was obtained in 66% yield (Figure 3). The oxidation potential of [**11**]$^{\mathbf{1-}}$/[**11**]$^{\mathbf{0-}}$ ($E_{1/2}$ = 0.56 V vs Fc/Fc^+) measured by cyclic voltammetry (CV) is particularly notable since it is higher than any reported $B_{12}(OR)_{12}$ cluster to date (previously 0.09 V vs Fc/Fc^+).[41] Plotting the Hammett constants of various benzyl substituents[46] versus the redox potentials of [$B_{12}(OR)_{12}$] clusters perfunctionalized with these groups[41] (Figure 4) indicates the oxidation potential of these clusters can be rationally extended beyond the previously reported electrochemical window.

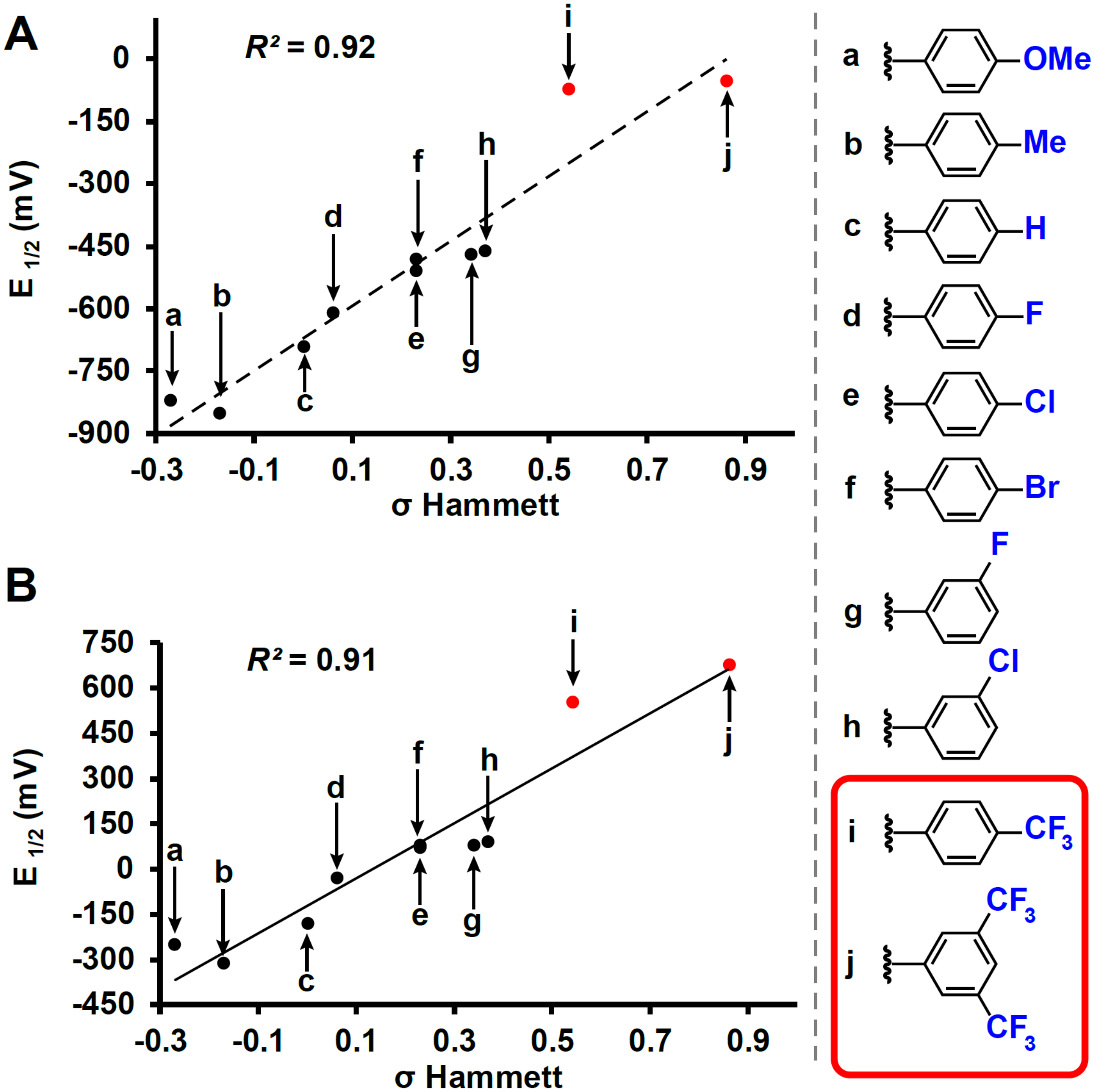

Figure 4. (a) Redox potential of $[B_{12}(OR)_{12}]^{2-/1-}$ and (b) $[B_{12}(OR)_{12}]^{1-/0}$ substituted with various benzyl substituents plotted vs Hammett constants.[3,46] Previously characterized[41] (black) and new (red) $[B_{12}(OR)_{12}]^{0}$ clusters are shown.

For example, according to the trend suggested by this Hammett plot, a *para*-nitrobenzyl-substituted cluster should exhibit a higher 1-/0 oxidation potential than **11** (Figure 3 and Figure 4).[46] The perfunctionalized cluster **12** featuring *para*-nitro (NO_2) substituent attached to the benzyl was successfully synthesized using our method in 30 minutes, however, oxidation of the reaction mixture containing [**12**]$^{\mathbf{2-/1-}}$ with $FeCl_3{\cdot}6H_2O$ did not produce any *hypercloso*-neutral species **[12]**$^{\mathbf{0}}$. Instead, the radical cluster species **[12]**$^{\mathbf{1-}}$ was isolated as the only product in 67% yield (Figure 3). This is not surprising, given the predicted oxidation potential for the [**12**]$^{\mathbf{1-}}$/**[12]**$^{\mathbf{0}}$ redox couple is more positive than the oxidizing strength of $FeCl_3{\cdot}6H_2O$.[48] Attempts to use stronger chemical oxidants (e.g. ceric ammonium nitrate) resulted in cluster degradation. Furthermore, insufficient solubility of **[12]**$^{\mathbf{1-}}$ as a TBA salt precluded us from obtaining CV measurements for this derivative. Nevertheless, convinced we could expand the electrochemical window for $B_{12}(OR)_{12}$ species featuring benzyl-based substituents, we turned our attention to a potentially more soluble compound containing a 3,5-*bis*(trifluoromethyl)benzyl group instead.

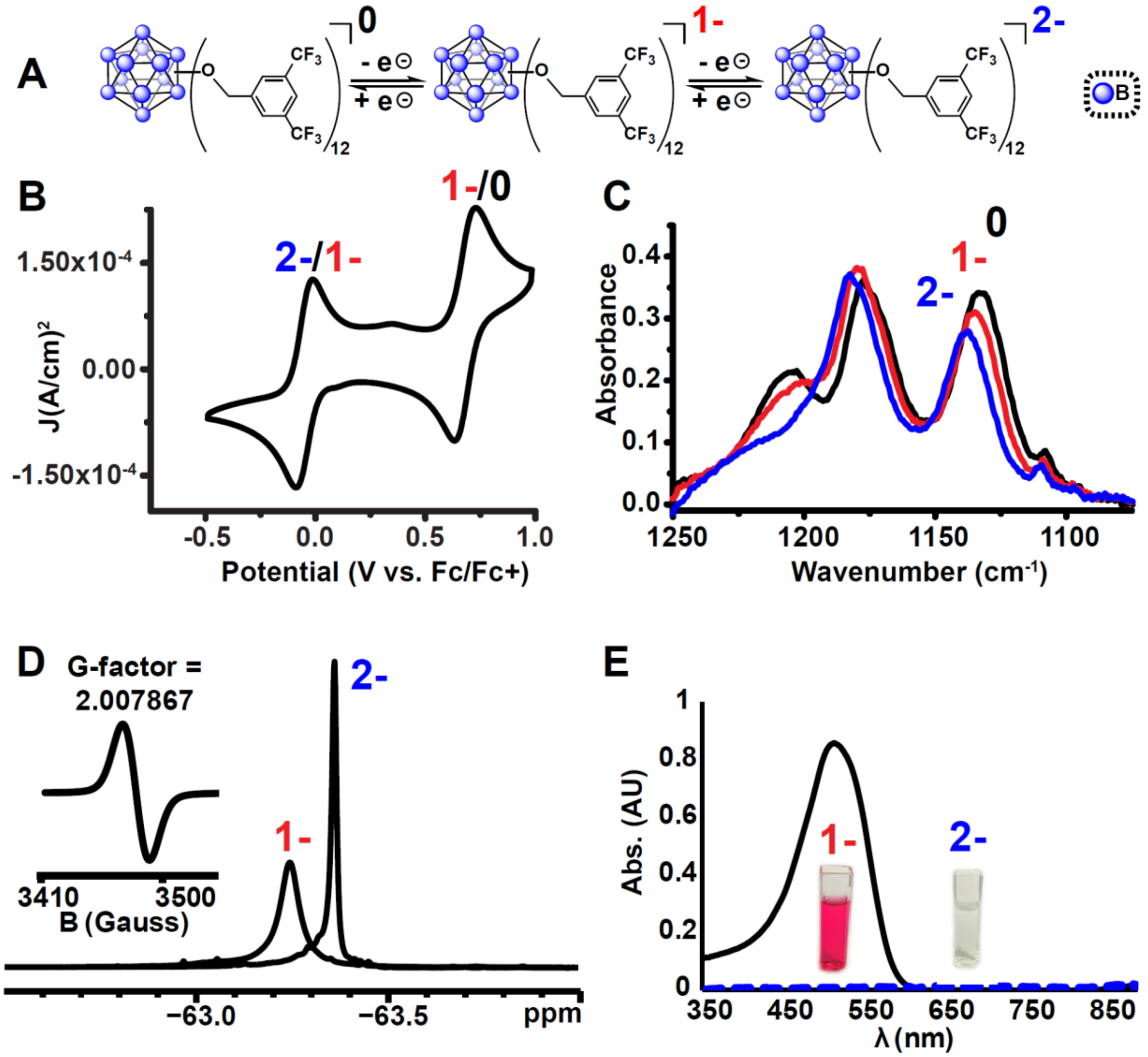

Figure 5. (a) Reversible redox activity of **13**; (b) Cyclic voltammogram (CV) demonstrating two independent, one-electron oxidation/reduction waves between 2-/1-, and 1-/0 states (1 mM **13** with 0.1 M TBAPF$_6$ in CH$_2$Cl$_2$; glassy carbon working electrode, Pt wire counter electrode, Ag/AgCl pseudoreference electrode behind a CoralPor tip; referenced to an internal ferrocene standard); (c) Infrared spectroelectrochemical (IRSEC)[49,50] analysis of 0/1-/2- states of **13**; (d) ^{19}F NMR spectra of **[13]**$^{1-}$ and **[13]**$^{2-}$ with EPR of **[13]**$^{1-}$ (inset); (e) UV-Vis spectra of **[13]**$^{1-}$ and **[13]**$^{2-}$.

Using the microwave method described above, cluster **13** was synthesized in 30 minutes. Interestingly, unlike all of the synthesized clusters reported thus far, the post-microwave reaction mixture was colorless, which is a characteristic feature of the pure dianionic state **[13]**$^{2-}$ for these clusters. The lack of color persisted even after column chromatography purification on silica gel in air. The identity of the pure isolated TBA salt of **[13]**$^{2-}$ (73% yield) was validated by full spectroscopic characterization and mass spectrometry (see SI). Oxidation of **[13]**$^{2-}$ with $FeCl_3{\cdot}6H_2O$ did not produce the neutral cluster, rather the pure **[13]**$^{1-}$ radical species was isolated in 78% yield, resulting in 56% net yield for **[13]**$^{1-}$ species starting from TBA_2[**1**]. Use of stronger chemical oxidants such as ceric ammonium nitrate (CAN) degraded the boron cage, producing a diagnostic ^{11}B NMR resonance at δ 20 characteristic of borates.[51] Nevertheless, we were able to observe neutral cluster **[13]**^{0} electrochemically via infrared spectroelectrochemistry (IR-SEC) and cyclic voltammetry (CV) in CH_2Cl_2 (Figure 5, B, C). CVs of **[13]**$^{1-}$ as the TBA salt in CH_2Cl_2 showed two quasi-reversible redox features at -0.05 V and 0.68 V vs Fc/Fc^+, corresponding to the 2-/1- and 1-/0 transitions, respectively. IR-SEC experiments where the applied potential was increased to more positive potentials incrementally on the TBA salt of **[13]**$^{2-}$ showed subtle changes in the IR stretching modes for all three oxidation states of [**13**] around 1130-1140 cm^{-1} and 1200-1220 cm^{-1}. The shift in these IR bands assigned to the B–O bond[52] to higher wavenumbers from **[13]**$^{2-}$/**[13]**$^{1-}$/**[13]**^{0} is consistent with those observed in the same region for the analogous *para*-CF_3 compound **[11]**^{0} which can be isolated in its neutral form via direct synthesis (see SI). The high oxidation potential for the **[13]**$^{1-}$/**[13]**^{0} redox couple observed from cyclic voltammetry ($E_{1/2}$ = 0.70 V vs Fc/Fc^+) is notable since it is the highest observed 1-/0 oxidation potential for the $B_{12}(OR)_{12}$ class of clusters reported to date[41] and is ~130 mV higher that the *para*-CF_3 benzyl cluster **11**. ^{19}F NMR spectroscopy provides another diagnostic handle on the oxidation state of this compound (Figure 5, D). ^{11}B NMR spectra for these clusters typically show a singlet around δ -14 to -16 for the 2- state, though the 1- state is silent due to the presence of the paramagnetic radical (confirmed by EPR, Figure 5D (inset)). However, with ^{19}F NMR spectroscopy, a shift from a singlet resonance in **[13]**$^{2-}$ at δ -63.36 to a broad singlet at δ -63.24 for

[13]$^{1-}$ was observed. This broadening is consistent with the paramagnetic nature of **[13]**$^{1-}$**,** where F atoms are located far enough from the unpaired electron-carrying B_{12}-based cluster core to be resolved by ^{19}F NMR spectroscopy.

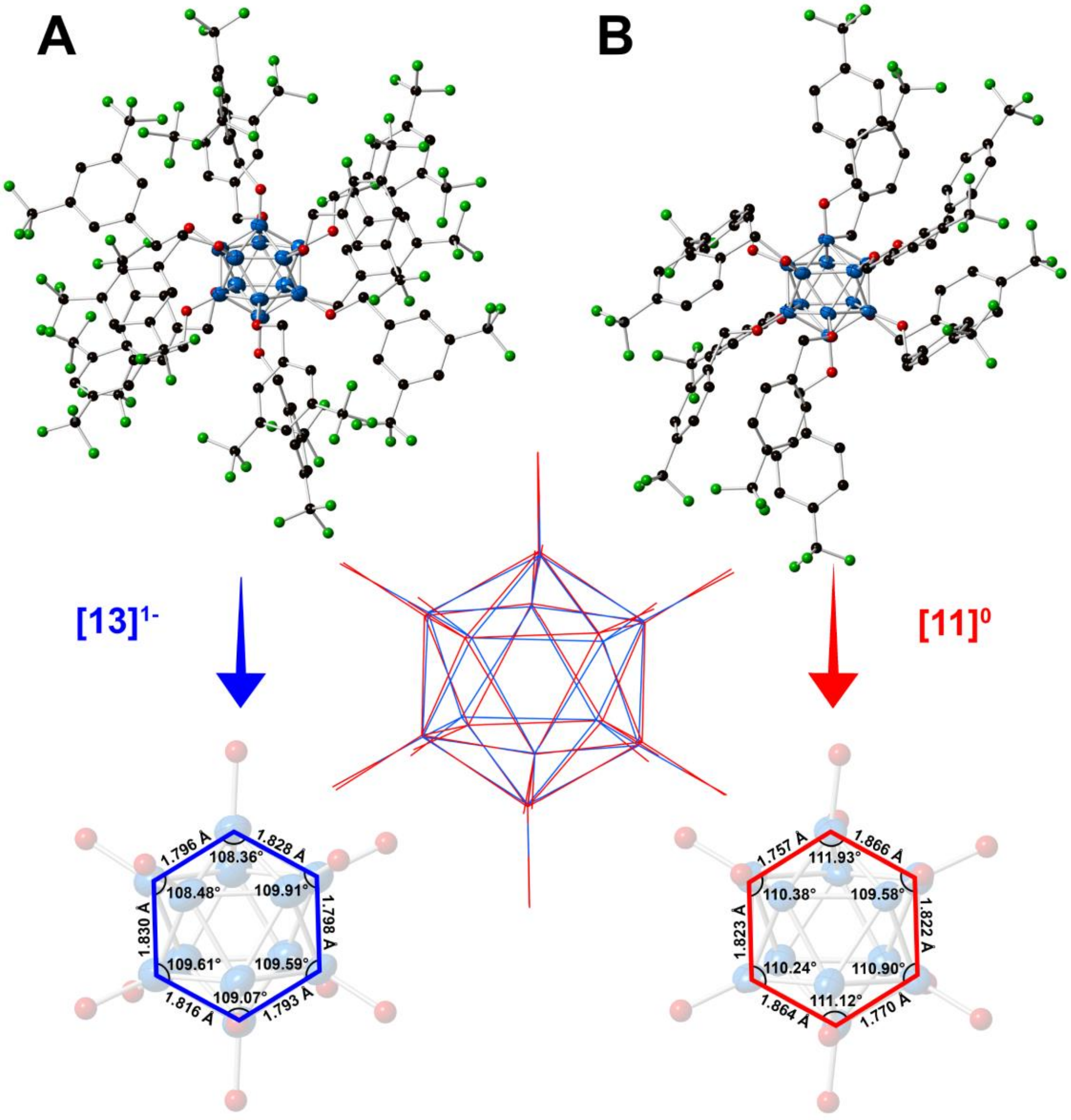
A
B
[13]1-
[11]0
1.796 Å
108.36°
1.828 Å
108.48°
109.91°
1.830 Å
1.798 Å
109.61°
109.59°
109.07°
1.816 Å
1.793 Å
1.757 Å
111.93°
1.866 Å
110.38°
109.58°
1.823 Å
1.822 Å
110.24°
110.90°
111.12°
1.864 Å
1.770 Å

Figure 6. (A-B) Solid state X-ray structures for **[13]**$^{1-}$ and **[11]**^{0} shown with 50% thermal ellipsoid probabilities for the boron atoms (hydrogen atoms omitted for clarity). B atoms are blue, O – red, C – black, and F – green. Selected bond lengths and angles of the boron cores (substituents omitted for clarity) for **[11]**^{0} and **[13]**$^{1-}$ are shown on the bottom. Overlay of the two cores (**[13]**$^{1-}$ in blue, **[11]**^{0} in red) is depicted in the middle.

The structural parameters of the boron clusters featuring persubstituted vertices can exhibit significant distortions in the solid state as a function of the substituent and the redox state as determined by X-ray crystallographic studies. Specifically, **[2]**$^{2-}$ exhibits nearly identical B–B bond distances (1.781(4) – 1.824(4) Å) and angles (B–B–B 107.798°<a<109.229°) as expected for a perfect icosahedron, yet as the cluster is oxidized to the electron-deficient **[2]**$^{1-}$ the structure expands and distorts slightly, with further distortion observed in the neutral state.[40] Additionally, the B–O bond lengths decrease as the cluster is oxidized from **[2]**$^{2-}$**,** which contains the longest average B–O distances, to the neutral **[2]**^{0} state with the shortest B–O distances.[40] This observed trend of B–B bond lengthening, B–O bond contraction, and B–B–B angle distortion within the core as a function of cluster oxidation state is supported qualitatively by the crystal structures for neutral **[11]**^{0} and radical **[13]**$^{1-}$ (Figure 6), which show comparable changes to those observed between **[2]**$^{1-}$ and **[2]**^{0}. Selected bond lengths and angles for **[11]**^{0} and **[13]**$^{1-}$ are shown in Figure 6.

X-ray photoelectron spectroscopy (XPS) has been widely used to study oxidation states in inorganic compounds.[53–56] We therefore decided to utilize this technique to further elucidate the oxidation state and effect of functionalization for these boron clusters. Boron XPS spectra for several representative clusters synthesized in our study (Figure 7) indicate a clear trend observed in the shift of B–B bond peak energies depending on the redox state of the functionalized cluster. The observed geometric distortion of these boron cluster icosahedra with oxidation from 2- to 1- and further to neutral species results in an increased B–B binding energy (Figure 7A). The nature of the substituents also produces a clear trend in these measurements, as compound **13** also exhibits an increase in B–B binding energy as the cluster increases in oxidation state from **[13]**$^{2-}$ to **[13]**$^{1-}$ (Figure 7B), yet both are higher in energy than that of neutral cluster **[11]**^{0}. However, despite the change in oxidation potential and binding energy observed from the XPS data from substituent effects, the nature of the electron radical delocalization throughout the boron-based core remains consistent. A single, broad symmetric EPR signal centered between 3450 and 3500 Gauss was observed for all cluster species isolated in the radical form with *g* values ranging between 2.0079 and 2.0081 depending on the substituent (see SI). Due to the 3D delocalization of the single electron across the 12 boron nuclei comprising the cluster, there exist a large number of possible hyperfine couplings.[36] Overlap of these hyperfine couplings ultimately gives rise to the single broad line observed in the EPR spectra.

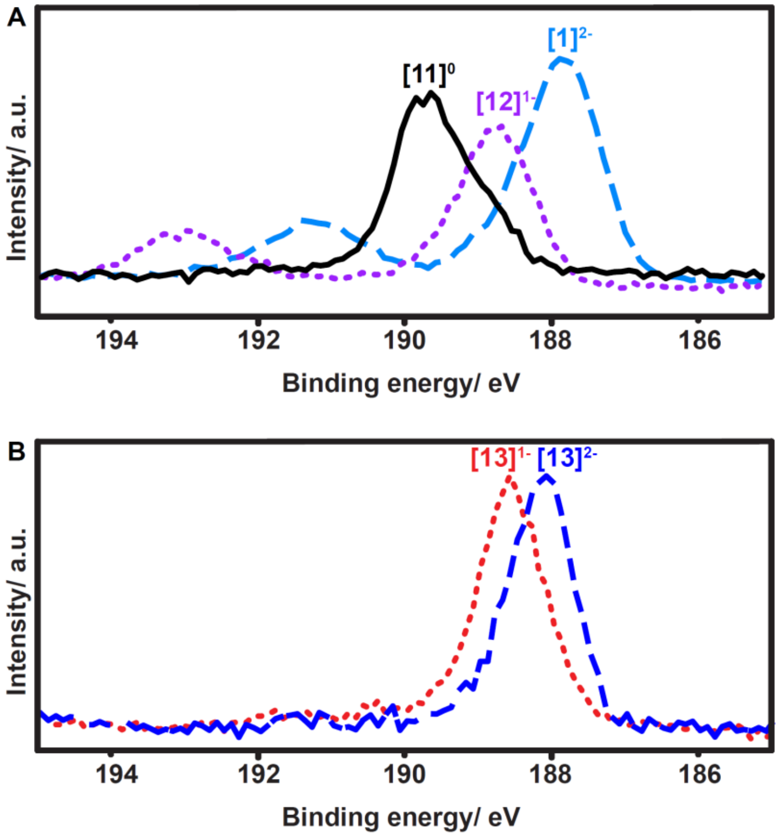

Figure 7. (a) Boron XPS spectra for TBA$_2$**[1]**$^{2-}$, TBA**[12]**$^{1-}$, and **[11]**^{0} showing an increase in B–B bond energy with increasing oxidation state; (b) Boron XPS spectra for TBA$_2$**[13]**$^{2-}$ and TBA**[13]**$^{1-}$ indicating the higher B-B bond energies of the **[13]**$^{2-}$ and **[13]**$^{1-}$ anions compared to the other substituted clusters.

In addition to previously mentioned benefits such as shortened reaction durations and the lack of stringent requirements for inert reaction conditions, microwave-assisted synthesis allows for one-pot, single-step reactions that would otherwise require more elaborate protocols. Monosubstitution of a benzyl ligand followed by persubstitution of the remaining eleven vertices has previously required a lengthy process involving multi-step syntheses,[57] whereas we demonstrate a one-pot approach enabled by our microwave-based method. For example, mixed-substituent $B_{12}(OEt)_{11}(OBn)$ cluster (**14**, Figure 8) can be formed in a single step simply by adding a stoichiometric amount of the desired reagents into a single reaction vessel.

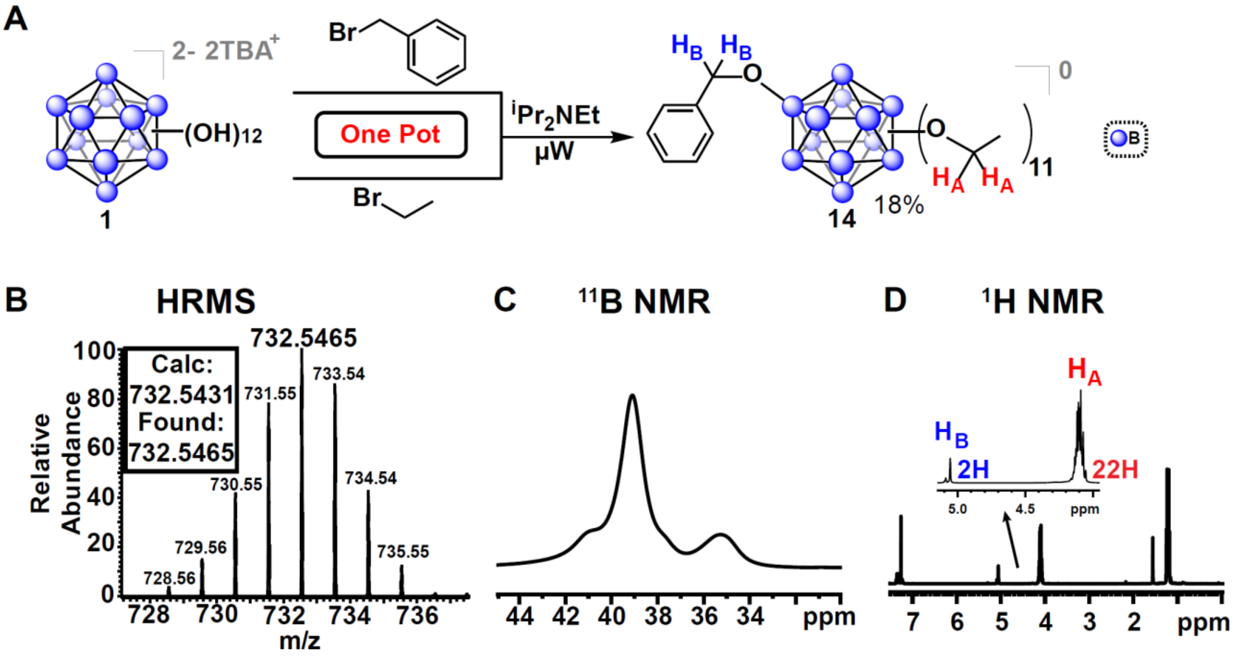

Figure 8. One-pot synthesis of vertex-differentiated *hypercloso* cluster **[14]**^{0} from a 60:1:1 molar mixture of benzyl bromide:bromoethane:TBA$_2$[**1**]. Isolated yield of **[14]^0** was 18% (compound **[4]^0** was also formed as an additional product of the reaction). ^{11}B NMR spectra indicates loss of the icosahedral symmetry due to vertex differentiation, ^{1}H NMR integrations show 24H (CH_2) and 36H (CH_3) for the 11 ethyl groups and 2H (CH_2) and 5H (Ph) for the single benzyl moiety.

This reaction was completed in 30 minutes, producing three distinct species as a mixture which were oxidized with $FeCl_3 \cdot 6H_2O$ as previously described and subsequently isolated via column chromatography on silica: the perfunctionalized ethyl cluster **[4]$^{\mathbf{0}}$**, a small amount (<5%) of di-substituted $[B_{12}(OEt)_{10}(OBn)_2]^0$ clusters, and the desired **[14]$^{\mathbf{0}}$** in 18% yield. This method represents a significantly faster route to produce this class of $[B_{12}(OR)_{11}(OR')]$ mixed-substituent clusters.

Conclusions

A rapid microwave-assisted synthetic route to perfunctionalized ether-linked $B_{12}(OR)_{12}$ clusters is disclosed and the robust nature of the technique demonstrated by the synthesis and characterization of multiple derivatives of **1**. For previously synthesized compounds, reaction duration was significantly reduced and prior requirements for oxygen-free and anhydrous reaction conditions were eliminated. Our method also allows for a unique one-pot synthesis of mixed-substituent clusters with good selectivity under the same open-air conditions. The cluster species described here maintain the attractive properties of earlier derivatives, behaving as redox-active cores which show delocalization of electrons throughout the entire 3D boron cage, while the new functional groups provide a significant expansion to the available tuneable redox potential window for this class of clusters.

Acknowledgements

We gratefully acknowledge Department of Chemistry and Biochemistry at UCLA for start-up funds. Portions of this material are based upon work supported by the National Science Foundation (CHE-1048804). E.A.Q. acknowledges USPHS of the National Institute of Heath for the predoctoral training fellowship under the National Research Service Award (T32GM008496). C.W.M. and C.P.K. acknowledge support for this work from the AFOSR through a Basic Research Initiative (BRI) grant (FA9550-12-1-0414). We would like to thank Kent Kirlikovali for assisting with EPR sample preparation. We thank Dr Liban Saleh for commenting on the manuscript.

Supporting Information

Experimental Section

General considerations. Initial microwave synthesis reactions were carried out under an inert atmosphere of nitrogen using standard glovebox techniques. All post-microwave work-up and characterization was performed under ambient conditions. All reactions designated as "open-air" were carried out and worked up under ambient conditions. The "ambient conditions" for this manuscript refer to room temperature (20 - 25 °C) and uncontrolled laboratory air.

Materials. Deuterated solvents were purchased from Cambridge Isotope Laboratories and used as received. MilliQ water described in this manuscript refers to purified potable water with a resistivity at 25 °C of ≤18.2 MΩ·cm. $[NEt_3H]_2[B_{12}H_{12}]$ was purchased from Boron Specialties (USA). Ethanol (200 proof) was purchased from Decon Labs and used as received. $FeCl_3 \cdot 6H_2O$ (≥97%), $CsOH \cdot 1H_2O$ (≥99.5%), H_2O_2 (30% in H_2O), $[N^nBu_4]OH$ (40% in H_2O), bromoethane (≥99%), 6-bromo-1-hexane (98%) allyl bromide (99%), 4-nitrobenzyl bromide (99%), acetonitrile (≥99.9%), CH_2Cl_2 (≥99.5%), ethyl acetate (≥99.5%), hexanes (≥98.5%), methanol (≥99.8%), *N,N*-diisopropylethylamine (≥99%), and tetrabutylammonium hexafluorophosphate (≥99.0%, electrochemical grade and 98%, recrystallized from ethanol and dried under vacuum at 90 °C) were purchased from Sigma-Aldrich. Benzyl bromide (99%) and ethyl 4-bromobutyrate (98%) were purchased from Alfa Aesar, and 4-methylbenzyl bromide (98%) was purchased from Acros. 6-bromo-1-hexene (98%), undec-10-enyl bromide (95%), 4-trifluoromethylbenzyl bromide (99%), and 3,5-bis$(CF_3)_2$-benzyl bromide (97%) were purchased from Oakwood. All reagents were used as received unless otherwise indicated.

Instruments. Bruker AV400 and AV500 spectrometers were used to obtain ^{11}B, $^{13}C\{^1H\}$, ^1H, and ^{19}F NMR spectra and Bruker Topspin software was used to process the NMR data. $^{13}C\{^1H\}$ and

^1H NMR spectra were referenced to residual solvent resonances in deuterated solvents (due to high humidity H_2O resonances are often present). ^{11}B and ^{19}F NMR spectra were referenced to $BF_3 \cdot Et_2O$ and $CFCl_3$ standards, respectively. A Bruker EMX EPR spectrometer was used to acquire EPR spectra, with all spectra collected in CH_2Cl_2 at ambient temperature. Mass spectrometry data was acquired using a Thermo Scientific^{TM} Q-Exactive^{TM} Plus instrument with a quadrupole mass filter and Orbitrap mass analyzer (compounds 2-13), and a Thermo Instruments Exactive Plus with IonSense ID-CUBE DART source instrument for compound 14. IR spectroscopy was acquired on solid samples using a PerkinElmer Spectrum Two FT-IR spectrometer equipped with a diamond universal ATR probe. X-ray photoelectron spectroscopy (XPS) data was acquired using an AXIS Ultra DLD instrument (Kratos Analytical Inc., Chestnut Ridge, NY, USA) with a monochromatic Al Kα X-ray source (10 mA for survey and high-resolution scans). A 300 x 700 nm oval spot size and ultrahigh vacuum (10^{-9} Torr) were used, with 160 eV pass energy for survey spectra and 20 eV for high-resolution spectra of B 1s using a 200 ms dwell time and 20 scans. All XPS peaks were externally referenced to the C 1s signal at 284.6 eV. The experimental setup and design of the infrared-spectroelectrochemistry (IR-SEC) cell has been published previously.[49,50]

X-ray data collection and processing parameters. For [**11**] and [**13**]$^{1-}$, a single crystal was mounted on a nylon loop using perfluoropolyether oil and cooled rapidly to 100 K with a stream of cold dinitrogen. Diffraction data were measured using a Bruker APEX-II CCD diffractometer using Mo-K_α radiation. The cell refinement and data reduction were carried out using Bruker SAINT and the structure was solved with SHELXS-97. All subsequent crystallographic calculations were performed using SHELXL-2013.

Cyclic voltammetry and IRSEC. Cyclic voltammetry was performed on [**11**] and [**14**] using a CH Instruments CHI630D potentiostat with a glassy carbon disc working electrode, platinum wire counter electrode, and Ag/Ag^+ wire pseudoreference. All experiments were conducted in 0.1M $[N^nBu_4]PF_6/CH_2Cl_2$ with 0.5 mM analyte concentrations (11.2 mg in 10 mL for [**11**] and 3.7 mg in 10 mL for [**14**]). The CH_2Cl_2 was dried in house with a custom drying system running through two alumina columns prior to use. The solution was degassed by bubbling Ar, and the cyclic voltammetry was performed under Ar gas. For [**11**], a scan rate of 0.1 mV/s was used with Fc/Fc^+ as an external standard. For [**14**], a scan rate of 0.5 mV/s was used with Fc/Fc^+ as an internal standard.

IRSEC and cyclic voltammetry for [**13**] were performed using a Pine Instrument Company model AFCBP1 bipotentiostat and BAS Epsilon potentiostat, respectively. For IR-SEC, as the potential was scanned, thin-layer bulk electrolysis was monitored by Fourier-Transform Reflectance IR off the electrode surface. All experiments were conducted in 0.1 M $[N^nBu_4]PF_6/CH_2Cl_2$ solutions with analyte concentrations of ~5 mM (13.9 mg in 1 mL) prepared under a nitrogen atmosphere. The IR-SEC cell used a glassy carbon working electrode, Pt wire counter electrode, and Ag wire pseudoreference electrode. The anionic $[N^nBu_4]_2[$**13**$]^{2-}$ was used for IRSEC, starting at resting potential and increasing to more oxidizing potentials stepwise.

Microwave Synthesis. Microwave reactions were performed using a CEM Discover SP microwave synthesis reactor. Except where noted otherwise, all reactions were performed in glass 10 mL microwave reactor vials purchased from CEM with silicone/PTFE caps. Flea micro PTFE-coated stir bars were used in the vials with magnetic stirring set to high and 15 seconds of premixing prior to the temperature ramping. All microwave reactions were carried out at 140 °C with the pressure release limit set to 250 psi (no reactions exceeded this limit to trigger venting) and the maximum wattage set to 250W (the power applied was dynamically controlled by the microwave instrument and did not exceed this limit for any reactions). Column chromatography was performed using 2.0 - 2.25 cm inner diameter glass fritted chromatography columns with 20-30 cm of slurry-packed silica gel to ensure full separation of reagents and products. Unfiltered pressurized air was used to assist column chromatography.

Dicesium dodecahydroxy-closo-dodecaborate Cs_2[1]

$CsOH \cdot H_2O$ (14.00 g, 83.4 mmol) was dissolved in methanol (130 mL) in a 300 mL glass round bottom flask. $[NEt_3H]_2[B_{12}H_{12}]$ (13.3758 g, 38.9 mmol) was added along with a PTFE-coated stir bar, and the reaction was left to stir vigorously for 18 h at ambient temperature. The cloudy suspension was then filtered through a 60 mL fritted glass funnel and washed with methanol (3 x 20 mL). The resulting white solid was dried on the frit for 1.5 h then left under high vacuum for 12 h and complete conversion to $Cs_2[\textit{closo}\text{-}B_{12}H_{12}]$ was confirmed by the absence of amine resonances in the ^1H NMR spectrum. Alternatively, commercially-obtained $Cs_2[B_{12}H_{12}]$ (98%, Strem) can be utilized for hydroxylation.

Note: The perhydroxylation procedure described herein should always be undertaken with caution and careful planning in order to ensure the $Cs_2[B_{12}H_{12}]$ reagent is pure and contains no organic contaminants. Blast shielding to contain any possible explosions should be utilized. Under no circumstances should the hydrogen peroxide used in the reaction come into contact with any organic material or solvents due to the possibility of an explosion. Synthesis of $Cs_2[B_{12}(OH)_{12}]$ and the ion exchange to produce $[N^nBu_4]_2[B_{12}(OH)_{12}]$ have been described elsewhere,[43,44] but will be reported here for convenience. $Cs_2[B_{12}H_{12}]$ (15.0 g, 36.8 mmol) was added to a glass three-necked round bottom flask with a water-cooled condensing coil in the top slot. The rear neck outlet contained a stopcock for venting pressure, and the front outlet was sealed with a glass stopper and secured with a plastic Keck clip. The apparatus was suspended in a silicone oil bath on a hot plate and secured, with a blast shield in front as a precaution against any potential explosion. The oil bath was heated to 95 °C, and a 50 mm oval PTFE stir bar was added to the flask, and the reaction was initiated with the addition of H_2O_2 (50 mL, 30% in H_2O). The flask was stoppered and the mixture allowed to stir at that temperature for 2 h. After 2 h, additional H_2O_2 (12 mL) was added, with the flask being vented, the glass stopper removed, and upon completion of addition, re-stoppering the flask. This addition of H_2O_2 was repeated every 2 h until a total volume of 60 mL was added to the reaction mixture. Upon completion of the addition, the oil bath temperature was increased to 105 °C, and additional H_2O_2 aliquots (10-15 mL) were added every 2 - 3 days, cooling the solution in the flask by raising it out of the oil bath and leaving it to cool for 20 – 30 minutes prior to each addition. After 14 days, the progress of the reaction was assessed *via* ^{11}B NMR, with reaction completion indicated by the appearance of a broad resonance at -18.0 ppm corresponding to $Cs_2[B_{12}(OH)_{12}]$ and the disappearance of the resonance at -16 ppm corresponding to unreacted $Cs_2[B_{12}H_{12}]$. Once the reaction is complete (as assessed by ^{11}B NMR), the mixture was cooled to 2 – 8 °C and cold MilliQ water was used to transfer the solution and solid product to a 150 mL glass fritted filter funnel. The crude product was washed with additional MilliQ water prior to drying on the filter frit under water-aspirator vacuum for 6 – 12 hours. Yield: 18.8 g (85 %).

From this point, N^nBu_4 will be referred to as TBA. For the cation exchange, Dowex 50X8 (100-200 mesh, hydrogen form, Sigma-Aldrich) was washed with MilliQ water in a 500 mL glass beaker until neutral (decanting and discarding the wash fractions), and [TBA]OH (40% in H_2O) was added in 10 mL increments until basic with magnetic stirring using a 50 mm PTFE coated standard stir bar. After 30 minutes, the pH was assessed again, and if no longer basic, additional [TBA]OH was added to restore basicity and left to stir overnight covered with a watch glass. The resin was slurry-packed into a 5 x 30 cm column wrapped with heating tape (controller set to hold temperature at 50 °C), and washed with MilliQ water until neutral. $Cs_2[B_{12}(OH)_{12}]$ (5.996 g, 10.0 mmol) was dissolved in boiling water (600 mL), cooled to 50 °C and slowly added to column. The product was washed with an additional 750 mL of 50 °C water, and the product was concentrated *in vacuo* and lyophilized to produce pure TBA$_2$[**1**]. Yield: 6.90 g (85 %). TBA$_2$[**1**] is a white solid. ^{1}H NMR (500 MHz, CDCl$_3$): δ 4.66 (s, 12H, OH), 3.08 (m, 8H, N-CH$_2$), 1.54 (m, 8H, N-CH$_2$CH$_2$), 1.25 (m, 8H, N-(CH$_2$)$_2$CH$_2$), 0.84 (m, 12H, N-(CH$_2$)$_3$CH$_3$). ^{11}B{^{1}H} NMR (128 MHz, D$_2$O): δ -17.9. *Note: TBA$_2$[**1**] is air-stable, but hygroscopic. Store under inert atmosphere or in a sealed desiccator to prevent excess absorption of water over extended periods of time under storage.*

General ether alkylation/benzylation of TBA$_2$[1] to B$_{12}$(OR)$_{12}$ microwave procedure Reactions were performed using TBA$_2$[**1**] which was weighed and placed into a 10 mL glass microwave vial and transferred out of a nitrogen-filled glovebox, being opened to the air prior to synthesis. The acetonitrile solvent, base, and alkyl reagents were all used under ambient temperature and pressure conditions with no additional purification or drying. *Note: the initial inert-atmosphere trials mentioned in the main text for **2**, **3**, and **4** were prepared inside a nitrogen-filled glovebox using rigorously anhydrous solvent. Once the PTFE/silicone cap was placed on the microwave vial it was transferred out of the glovebox and the reactions were performed identically to the open-air reactions.* TBA$_2$[**1**] (50.0 mg, 0.061 mmol) was transferred to a 10 mL glass microwave vial containing a flea micro stir bar and dissolved in acetonitrile (1 mL). *N,N*-diisopropylethylamine (Hünig's base, 0.2 mL, 1.15 mmol) and alkyl halide (7.6 mmol) were added, and a PTFE/silicone cap was placed on the microwave vial. The mixture was heated to 140 °C with stirring in the microwave for 5 min to 8 hrs (depending upon the alkyl halide), with the progress of the reaction monitored *via* ^{11}B NMR spectroscopy. Multiple resonances between -14 and -16 ppm are first observed, indicating partial substitution of the 12 vertices. The reaction has reached completion when these resonances coalesce to a broad singlet resonance between -14 and -16 ppm corresponding to the fully substituted $[B_{12}(OR)_{12}]^{2-}$ species. The color of the reaction mixture is typically a faint yellow initially, with the completed reaction mixture changing to a pink/purple, faint pink, or deep red/orange color indicative of the 1- species. Upon completion of the reaction, excess acetonitrile and base were removed *via* rotary evaporation. With the exception of **3**, **4**, **6,** and **14** the remaining reaction mixture containing product and unreacted alkyl halide were separated *via* column chromatography with silica gel. The unreacted alkyl halide (clear and colorless or slightly yellow/orange, UV active) was eluted first, followed by the elution of the remaining pink/purple product mixture consisting of 1-/2- species (note that the 2- species is colorless). The excess solvent was removed *via* a rotary evaporator, and the remaining 1-/2- product mixture was dissolved in a 90/5/5 ethanol/acetonitrile/MilliQ H_2O or 90/10 ethanol/acetonitrile mixture and transferred to a 50 mL round bottom flask. $FeCl_3{\cdot}6H_2O$ (0.3 g, 1.11 mmol) was added to the dissolved mixture, and subsequently stirred vigorously for 12-24 h at ambient temperature. The solvent was removed from the resulting dark orange/brown mixture *via* rotary evaporation, and the neutral [*hypercloso*-$B_{12}(OR)_{12}]^0$ or radical TBA[*hypocloso*-$B_{12}(OR)_{12}]^{1-}$ product was separated from the $FeCl_3{\cdot}6H_2O$ *via* column chromatography with silica gel. A dark orange, yellow-orange, or red-orange band consisting of neutral [*hypercloso*-$B_{12}(OR)_{12}]^0$ was eluted with CH_2Cl_2, with a pink/purple band containing charged 1-/2- species eluting next if any product was not fully oxidized. The red or orange fraction containing the desired neutral closomer was dried with rotary evaporation followed by high vacuum, and the above procedure for oxidation could be repeated on the remaining 1-/2- mixture to obtain additional neutral product if any non-fully oxidized product remains. *Note: if the final oxidized product* *appears to have any impurities (via ^1H NMR spectroscopy), eluting the product through an additional silica plug or short column with 1:1 CH_2Cl_2/hexanes should remove any contaminants.*

Dodeca(benzyloxy)-*hypercloso*-dodecaborane [2]

TBA$_2$[**1**] (50.0 mg, 0.061 mmol) was added to a 10 mL glass microwave vial and transferred out of a nitrogen filled glovebox, opened to the air, and dissolved in 1 mL acetonitrile. *N*,*N*-diisopropylethylamine (0.2 mL, 1.15 mmol) and benzyl bromide (1.74 mL, 14.7 mmol) were added along with a flea micro stir bar, the vial was sealed with a PTFE/silicone cap, and the mixture was heated at 140 °C with stirring in the microwave for 15 min. The volatiles were removed *via* rotary evaporation, and the excess reagent was eluted through a slurry-packed silica gel column with 65/35 hexanes/ethyl acetate, and the pink/purple product mixture was eluted with CH_2Cl_2. The CH_2Cl_2 was removed *via* rotary evaporation, the remaining charged 1-/2- product mixture was dissolved in 5 mL 90/5/5 ethanol/acetonitrile/H_2O, $FeCl_3 \cdot 6H_2O$ (0.3 g, 1.11 mmol) was added and the mixture was left to stir for 12-24 h. Following oxidation, the solvent mixture was removed *via* rotary evaporation, and an orange band containing the neutral product was separated from the $FeCl_3 \cdot 6H_2O$ through a slurry-packed silica gel column with CH_2Cl_2. The CH_2Cl_2 was removed *via* rotary evaporation and the final neutral product **2** was dried under high vacuum to obtain an isolated yield of 54.3 mg (63%). Compound **2** is a dark orange solid. ^1H NMR (500 MHz, $CDCl_3$): δ 7.08 - 7.19 (m, 60H, C_6H_5), 5.25 (s, 24H, O-$\underline{CH_2}$). $^{13}C\{^1H\}$ NMR (125 MHz, $CDCl_3$): δ 140.8, 128.4, 127.3, 73.4. $^{11}B\{^1H\}$ NMR (128 MHz, $CDCl_3$): δ 41.8. HRMS (Orbitrap): *m/z* calculated for $C_{84}H_{84}B_{12}O_{12}$ (M^-), 1414.7152 Da; found, 1414.7183 Da.

Dodeca(allyloxy)-*hypercloso*-dodecaborane [3]

Note: this reaction should be performed with minimal exposure to light. TBA$_2$[**1**] (100.0 mg, 0.122 mmol) was added to a 10 mL glass microwave vial and transferred out of a nitrogen filled glovebox, opened to the air, and dissolved in 2 mL acetonitrile. *N,N*-diisopropylethylamine (0.4 mL, 2.30 mmol) and allyl bromide (1.28 mL, 14.68 mmol) were added along with a flea micro stir bar, the vial was sealed with a PTFE/silicone cap, and the mixture was heated at 140 °C with stirring in the microwave for 15 min. The volatiles and excess reagent were removed *via* rotary evaporation and the purple 1-/2- product mixture was dissolved in 5 mL 90/10 ethanol/acetonitrile, $FeCl_3{\cdot}6H_2O$ (0.3 g, 1.11 mmol) was added and the mixture was left to stir for 12-24 h (wrapped in foil to avoid excessive light exposure). Following oxidation, the solvent mixture was removed *via* rotary evaporation, and a yellow band containing the neutral product was separated from the $FeCl_3{\cdot}6H_2O$ through a slurry-packed silica gel column with CH_2Cl_2. The CH_2Cl_2 was removed *via* rotary evaporation and the final neutral product **3** was dried under high vacuum to obtain an isolated yield of 76.8 mg (77%). Compound **3** is a dark yellow-orange viscous oil. ^{1}H NMR (500 MHz, $CDCl_3$): δ 5.91 – 5.99 (m, 12H, CH), 5.21 (dq, 12H, CH), 5.05 (dq, 12H, CH), 4.62 (m, 24H, O-$\underline{CH_2}$). ^{13}C{^{1}H} NMR (125 MHz, $CDCl_3$): δ 136.9, 114.2, 71.6. ^{11}B{^{1}H} NMR (128 MHz, $CDCl_3$): δ 41.1. HRMS (Orbitrap): *m/z* calculated for $C_{36}H_{60}B_{12}O_{12}$ (M^-), 814.5274 Da; found, 814.5333 Da. *Note: Compound **3** should be stored at -20 °C or used immediately.*

Dodeca(ethoxy)-*hypercloso*-dodecaborane [4]

TBA$_2$[**1**] (50.0 mg, 0.061 mmol) was added to a 10 mL glass microwave vial and transferred out of a nitrogen filled glovebox, opened to the air, and dissolved in 1 mL acetonitrile. *N,N*-diisopropylethylamine (0.2 mL, 1.15 mmol) and bromoethane (1.65 mL, 22.1 mmol) were added along with a flea micro stir bar, the vial was sealed with a PTFE/silicone cap, and the mixture was heated at 140 °C with stirring in the microwave for 30 min. The volatiles and excess reagent were removed *via* rotary evaporation, the remaining charged 1-/2- product mixture was dissolved in 4 mL 90/5/5 ethanol/acetonitrile/H_2O, $FeCl_3{\cdot}6H_2O$ (0.3 g, 1.11 mmol) was added and the mixture was left to stir for 12-24 h. Following oxidation, the solvent mixture was removed *via* rotary evaporation, and an orange band containing the neutral product was separated from the $FeCl_3{\cdot}6H_2O$ through a slurry-packed silica gel column with CH_2Cl_2. The CH_2Cl_2 was removed *via* rotary evaporation and the final neutral product **4** was dried under high vacuum to obtain an isolated yield of 32.7 mg (80%). Compound **4** is a dark orange solid. ^{1}H NMR (500 MHz, $CDCl_3$): δ 4.09 (q, 24H, O-$\underline{CH_2}$), 1.24 (t, 36H, CH_3). $^{13}C\{^1H\}$ NMR (125 MHz, $CDCl_3$): δ 66.8, 17.8. $^{11}B\{^1H\}$ NMR (128 MHz, $CDCl_3$): δ 37.7. HRMS (Orbitrap): *m/z* calculated for $C_{24}H_{60}B_{12}O_{12}$ (M^-), 670.5274 Da; found, 670.5278 Da.

Dodeca(hexoxy)-*hypercloso*-dodecaborane [5]

TBA$_2$[**1**] (99.0 mg, 0.121 mmol) was added to a 10 mL glass microwave vial and transferred out of a nitrogen filled glovebox, opened to the air, and dissolved in 2 mL acetonitrile. *N,N*-diisopropylethylamine (0.4 mL, 2.30 mmol) and 6-bromo-1-hexane (2.85 mL, 20.3 mmol) were added along with a stir bar, the vial was sealed with a PTFE/silicone cap, and the mixture was heated at 140 °C with stirring in the microwave for 2 h. The volatiles were removed *via* rotary evaporation at 65 °C, the remaining charged 1-/2- product mixture was dissolved in 5 mL 90/5/5 ethanol/acetonitrile/H_2O, $FeCl_3{\cdot}6H_2O$ (0.3 g, 1.11 mmol) was added and the mixture was left to stir for 12-24 h. Following oxidation, the solvent mixture was removed *via* rotary evaporation, and an orange band containing the neutral product was separated from the $FeCl_3{\cdot}6H_2O$ through a slurry-packed silica gel column with CH_2Cl_2. The CH_2Cl_2 was removed *via* rotary evaporation and the final neutral product **5** was dried under high vacuum to obtain an isolated yield of 91.4 mg (56%). Compound **5** is a dark yellow-orange oil. ^{1}H NMR (400 MHz, $CDCl_3$): δ 4.02 (t, 24H, O-

$\underline{CH_2}$), 1.54 (m, 24H, $CH_2\underline{CH_2}(CH_2)_3CH_3$), 1.31, (m, 72H, $CH_2CH_2\underline{(CH_2)_3}CH_3$), 0.89 (m, 36H, CH_3). $^{13}C\{^1H\}$ NMR (125 MHz, $CDCl_3$): δ 70.2, 32.2, 31.8, 25.9, 22.8, 14.1. $^{11}B\{^1H\}$ NMR (128 MHz, $CDCl_3$): δ 42.0. HRMS (Orbitrap): *m/z* calculated for $C_{72}H_{156}B_{12}O_{12}$ (M^-), 1343.2786 Da; found, 1343.2838 Da.

Dodeca(6-hexeneoxy)-*hypercloso*-dodecaborane [6]

Note: this reaction should be performed with minimal exposure to light. TBA_2[**1**] 50.0 mg (0.061 mmol) was added to a 10 mL glass microwave vial and transferred out of a nitrogen filled glovebox, opened to the air, and dissolved in 1 mL acetonitrile. *N,N*-diisopropylethylamine (0.2 mL, 1.15 mmol) and 6-bromo-1-hexene (0.59 mL, 4.41 mmol) were added along with a stir bar, the vial was sealed with a PTFE/silicone cap, and the mixture was heated at 140 °C with stirring in the microwave for 7 h. The volatiles and excess reagent were removed *via* rotary evaporation, and the remaining charged 1-/2- product mixture was dissolved in 5 mL 90/10 ethanol/acetonitrile, $FeCl_3 \cdot 6H_2O$ (0.3 g, 1.11 mmol) was added and the mixture was left to stir for 12-24 h. Following oxidation, the solvent mixture was removed *via* rotary evaporation, and an orange band containing the neutral product was separated from the $FeCl_3 \cdot 6H_2O$ through a slurry-packed silica gel column with CH_2Cl_2. The CH_2Cl_2 was removed *via* rotary evaporation and the final neutral product **6** was dried under high vacuum to obtain an isolated yield of 35.0 mg (43%). Compound **6** is a dark yellow-orange oil. ^1H NMR (400 MHz, $CDCl_3$): δ 5.79 (m, 12H, CH), 4.95 (m, 24H, $\underline{CH_2}CH$), 4.02 (t, 24H, O-$\underline{CH_2}$), 2.05 (q, 24H, $(CH_2)_3\underline{CH_2}CH_2CH$), 1.56 (m, 24H, $CH_2\underline{CH_2}(CH_2)_3CH$), 1.43 (m, 24H, $(CH_2)_2\underline{CH_2}(CH_2)_2CH$). $^{13}C\{^1H\}$ NMR (125 MHz, $CDCl_3$): δ 139.1, 114.2, 70.1, 33.6, 31.7, 25.5. $^{11}B\{^1H\}$ NMR (128 MHz, $CDCl_3$): δ 41.6. HRMS (Orbitrap): *m/z* calculated for $C_{72}H_{132}B_{12}O_{12}$ (M^-), 1319.0908 Da; found, 1319.1003 Da.

Dodeca(11-undeceneoxy)-*hypercloso*-dodecaborane [7]

Note: this reaction should be performed with minimal exposure to light. TBA$_2$[**1**] (50.0 mg, 0.061 mmol) was added to a 10 mL glass microwave vial and transferred out of a nitrogen filled glovebox, opened to the air, and dissolved in 1 mL acetonitrile. *N,N*-diisopropylethylamine (0.2 mL, 1.15 mmol) and undec-10-enyl bromide (1.54 mL, 7.33 mmol) were added along with a stir bar, the vial was sealed with a PTFE/silicone cap, and the mixture was reacted at 140 °C with stirring in the microwave for 8 h. The volatiles were removed *via* rotary evaporation, the excess reagent was eluted through a slurry-packed silica gel column with hexanes, and the product mixture yellow-orange and red-orange fractions were eluted with CH$_2$Cl$_2$ followed by a pink fraction with ethyl acetate. The CH$_2$Cl$_2$/ethyl acetate was removed *via* rotary evaporation, the remaining charged 1-/2- product mixture was dissolved in 9 mL 49/49/2 ethanol/CH$_2$Cl$_2$/acetonitrile, FeCl$_3$·6H$_2$O (0.5 g, 1.85 mmol) was added and the mixture was left to stir for 12-24 h. Following oxidation, the solvent mixture was removed *via* rotary evaporation, and a dark brown/black band containing the neutral product was separated from the FeCl$_3$·6H$_2$O through a slurry-packed silica gel column with CH$_2$Cl$_2$. The CH$_2$Cl$_2$ was removed *via* rotary evaporation and the final neutral product **7** was dried under high vacuum to obtain an isolated yield of 37.1 mg (28%). Compound **7** is a dark, brown/black oil. ^{1}H NMR (400 MHz, CD$_2$Cl$_2$): δ 5.81 (m, 12H, CH), 4.98 (m, 12H, *trans*-C$\underline{\text{H}}_2$CH), 4.91 (m, 12H, *cis*-C$\underline{\text{H}}_2$CH), 4.01 (t, 24H, O-$\underline{\text{CH}_2}$), 2.03 (m, 24H, O-CH$_2\underline{\text{CH}_2}$), 1.54 (m, 24H, O-(CH$_2$)$_2\underline{\text{CH}_2}$), 1.32 (m, 144H, O-(CH$_2$)$_3\underline{(\text{CH}_2)_6}CH_2$CH. ^{13}C{^{1}H} NMR (125 MHz, CD$_2$Cl$_2$): δ 139.3, 113.8, 70.4, 33.9, 32.3, 29.9, 29.7, 29.6, 29.3, 29.1, 26.2. ^{11}B{^{1}H} NMR (128 MHz, CD$_2$Cl$_2$): δ 41.5. *m/z* calculated for C$_{132}$H$_{252}$B$_{12}$O$_{12}$ (M$^-$), 2161.0332 Da; due to solubility issues, the molecule was incompatible with our M.S. instrument.

Dodeca(ethylbutyratoxy)-*hypercloso*-dodecaborane [8]

TBA_2[**1**] (100.0 mg, 0.122 mmol) was added to a 10 mL glass microwave vial and transferred out of a nitrogen filled glovebox, opened to the air, and dissolved in 2 mL acetonitrile. *N*,*N*-diisopropylethylamine (0.4 mL, 2.30 mmol) and ethyl 4-bromobutyrate (1.08 mL, 7.55 mmol) were added along with a stir bar, the vial was sealed with a PTFE/silicone cap, and the mixture was heated at 140 °C with stirring in the microwave for 1.5 h. The volatiles were removed *via* rotary evaporation, and the reaction mixture was eluted through Sephadex LH-20 size exclusion column with methanol, with the pink fraction containing the desired 1-/2- product collected. The methanol was removed *via* rotary evaporation, and the charged 1-/2- product mixture was oxidized by eluting through a slurry-packed silica gel column with 90/10 CH_2Cl_2/ethanol, collecting the orange fraction. Following oxidation, the solvent mixture was removed *via* rotary evaporation, and the product was purified by eluting through a short (15 cm) silica gel column slurry-packed with 1:1 hexanes/ethyl ether, with ~50 mL 1:1 hexanes/ethyl ether followed by ~50 mL ethyl ether eluting an orange band. The volatiles were removed *via* rotary evaporation, and the final neutral product **8** was dried under high vacuum to obtain an isolated yield of 14.0 mg (7%). *Note: ~8% additional 1-/2- product was collected from the first silica column, and by repeating the oxidation step with the charged 1-/2- mixture additional* **8** can be isolated. Compound **8** is an orange solid. ^1H NMR (500 MHz, $CDCl_3$): δ 4.11 (q, 24H, O-$\underline{CH_2}$), 4.03 (t, 24H, COO$\underline{CH_2}$), 2.34 (t, 24H, $\underline{CH_2}$COO), 1.87 (m, 24H, O-$CH_2\underline{CH_2}$), 1.24 (t, 36H, CH_3). $^{13}C\{^1H\}$ NMR (125 MHz, $CDCl_3$): δ, 173.3, 69.7, 60.3, 30.9, 27.4, 14.2. $^{11}B\{^1H\}$ NMR (128 MHz, $CDCl_3$): δ 41.9. HRMS (Orbitrap): *m/z* calculated for $C_{72}H_{132}B_{12}O_{36}$ (M^-), 1702.9688 Da; found, 1702.9714 Da.

Dodeca(4-methylbenzyloxy)-*hypercloso*-dodecaborane [9]

TBA_2[**1**] (48.0 mg, 0.059 mmol) was added to a 10 mL glass microwave vial and transferred out of a nitrogen filled glovebox, opened to the air, and dissolved in 1 mL acetonitrile. *N*,*N*-

diisopropylethylamine (0.2 mL, 1.15 mmol) and 4-methylbenzyl bromide (1.362 g, 7.36 mmol) were added along with a stir bar, the vial was sealed with a PTFE/silicone cap, and the mixture was heated at 140 °C with stirring in the microwave for 5 min. The volatiles were removed *via* rotary evaporation, and the excess reagent was eluted through a slurry-packed silica gel column with 90/10 hexanes/ethyl acetate, and the pink/purple product mixture was eluted with acetonitrile. The volatiles were removed *via* rotary evaporation, the remaining charged 1-/2- product mixture was dissolved in 5 mL 90/10 ethanol/acetonitrile, $FeCl_3 \cdot 6H_2O$ (0.3 g, 1.11 mmol) was added and the mixture was left to stir for 12-24 h. Following oxidation, the solvent mixture was removed *via* rotary evaporation, and a dark orange band containing the neutral product was separated from the $FeCl_3 \cdot 6H_2O$ through a slurry-packed silica gel column with CH_2Cl_2. The CH_2Cl_2 was removed via rotary evaporation and the final neutral product **9** was dried under high vacuum to obtain an isolated yield of 30.9 mg (33%). Compound **9** is a brown/orange viscous oil. ^1H NMR (400 MHz, $CDCl_3$): δ 6.98 (m, 48H, C_6H_4), 5.17 (s, 24H, CH_2), 2.31 (s, 36H, CH_3). $^{13}C\{^1H\}$ NMR (125 MHz, $CDCl_3$): δ 137.9, 136.4, 128. 7, 127.3, 72.8, 21.2. $^{11}B\{^1H\}$ NMR (128 MHz, $CDCl_3$): δ 41.6. HRMS (Orbitrap): *m/z* calculated for $C_{96}H_{108}B_{12}O_{12}$ (M^-), 1582.9030 Da; found, 1582.9058 Da.

Dodeca(4-bromobenzyloxy)-*hypercloso*-dodecaborane [10]

TBA_2[**1**] (50.0 mg, 0.061 mmol) was added to a 10 mL glass microwave vial and transferred out of a nitrogen filled glovebox, opened to the air, and dissolved in 1 mL acetonitrile. *N*,*N*-diisopropylethylamine (0.2 mL, 1.15 mmol) and 4-bromobenzyl bromide (1.358 g, 7.36 mmol) were added along with a stir bar, the vial was sealed with a PTFE/silicone cap, and the mixture was heated at 140 °C with stirring in the microwave for 30 min. The volatiles were removed *via* rotary evaporation, and the excess reagent was eluted through a slurry-packed silica gel column with hexanes, and the red-pink product mixture was eluted with CH_2Cl_2 followed by ethyl acetate.

The volatiles were removed *via* rotary evaporation, the remaining charged 1-/2- product mixture was dissolved in 5 mL 90/10 ethanol/acetonitrile, $FeCl_3{\cdot}6H_2O$ (0.3 g, 1.11 mmol) was added and the mixture was left to stir for 12-24 h. Following oxidation, the solvent mixture was removed *via* rotary evaporation, and a dark orange band containing the neutral product was separated from the $FeCl_3{\cdot}6H_2O$ through a slurry-packed silica gel column with CH_2Cl_2. The CH_2Cl_2 was removed via rotary evaporation and the final neutral product **10** was dried under high vacuum to obtain an isolated yield of 62.5 mg (43%). Compound **10** is a dark-orange solid. ^{1}H NMR (400 MHz, $CDCl_3$): δ 7.33 (d, 24H, *m*-$C_6\underline{H}_4$), 6.86 (d, 24H, *o*-$C_6\underline{H}_4$), 5.07 (s, 24H, O-$\underline{CH_2}$). ^{13}C{^{1}H} NMR (125 MHz, $CDCl_3$): δ, 138.5, 131.6, 128.5, 121.6, 72.6. ^{11}B{^{1}H} NMR (128 MHz, $CDCl_3$): δ 41.4. HRMS (Orbitrap): *m/z* calculated for $C_{84}H_{72}B_{12}Br_{12}O_{12}$ (M^-), 2361.6291 Da; found, 2361.6311 Da.

Dodeca(4-trifluoromethylbenzyloxy)-*hypercloso*-dodecaborane [11]

TBA_2[**1**] (50.0 mg, 0.061 mmol) was added to a 10 mL glass microwave vial and transferred out of a nitrogen filled glovebox, opened to the air, and dissolved in 1 mL acetonitrile. *N*,*N*-diisopropylethylamine (0.2 mL, 1.15 mmol) and 4-trifluoromethylbenzyl bromide (1.765 g, 7.5 mmol) were added along with a stir bar, the vial was sealed with a PTFE/silicone cap, and the mixture was reacted at 140 °C with stirring in the microwave for 30 min. The volatiles were removed *via* rotary evaporation, and the excess reagent was eluted through a slurry-packed silica gel column with hexanes, and the pink/purple product mixture was eluted with acetonitrile. The acetonitrile was removed *via* rotary evaporation, the remaining charged 1-/2- product mixture was dissolved in 5 mL of 90/10 ethanol/acetonitrile, $FeCl_3{\cdot}6H_2O$ (0.4 g, 1.48 mmol) was added and the mixture was left to stir for 12-24 h. Following oxidation, the solvent mixture was removed *via* rotary evaporation, and an orange band containing the neutral product was separated from the

$FeCl_3 \cdot 6H_2O$ through a slurry-packed silica gel column with CH_2Cl_2. The CH_2Cl_2 was removed *via* rotary evaporation and the final neutral product **11** was dried under high vacuum to obtain an isolated yield of 89.6 mg (66%). Compound **11** is a red-orange solid. ^{1}H NMR (500 MHz, $CDCl_3$): δ 7.38 - 7.48 (m, 24H, *m*-$C_6\underline{H}_4$), 7.06 - 7.15 (m, 24H, *o*-$C_6\underline{H}_4$), 5.27 (s, 24H, O-$\underline{CH_2}$). ^{13}C{^{1}H} NMR (125 MHz, $CDCl_3$): δ 143.0, 130.6, 126.6, 125.7, 125.0, 122.8, 72.9. ^{11}B{^{1}H} NMR (128 MHz, $CDCl_3$): δ 41.8. ^{19}F NMR (376 MHz, $CDCl_3$): δ -62.76 (s, 36F). HRMS (Orbitrap): *m/z* calculated for $C_{96}H_{72}B_{12}F_{36}O_{12}$ (M^-), 2231.5672 Da; found, 2231.5637 Da. Crystallized from $CDCl_3$ and pentane at room temperature for 1 week to obtain a single crystal for X-ray diffraction analysis.

Dodeca(4-nitrobenzyloxy)-*hypocloso*-dodecaborane $[\mathbf{12}]^{1-}$

TBA$_2$[**1**] (50.0 mg, 0.061 mmol) was added to a 10 mL glass microwave vial and transferred out of a nitrogen filled glovebox, opened to the air, and dissolved in 1 mL acetonitrile. *N*,*N*-diisopropylethylamine (0.2 mL, 1.15 mmol) and 4-nitrobenzyl bromide (1.585 g, 7.34 mmol) were added along with a stir bar, the vial was sealed with a PTFE/silicone cap, and the mixture was heated at 140 °C with stirring in the microwave for 30 min. The volatiles were removed *via* rotary evaporation, and the excess reagent was eluted through a slurry-packed silica gel column with 50/50 hexanes/CH_2Cl_2, and the orange product mixture was eluted with acetonitrile. The volatiles were removed *via* rotary evaporation, the remaining charged 1-/2- product mixture was dissolved in 5 mL 90/10 ethanol/acetonitrile, $FeCl_3 \cdot 6H_2O$ (0.3 g, 1.11 mmol) was added and the mixture was left to stir for 12-24 h. Following oxidation, the solvent mixture was removed *via* rotary evaporation, and the product mixture was washed with 150 – 200 mL ethanol in a glass fritted 30 mL filter funnel to remove the remaining $FeCl_3 \cdot 6H_2O$. The remaining orange radical 1- product TBA$[\mathbf{12}]^{1-}$ was removed from the funnel and dried under high vacuum to obtain an isolated yield of 89.0 mg (66%). Compound TBA[**12**]$^{1-}$ is an orange solid. ^{1}H NMR (400 MHz, $CDCl_3$): δ 8.49 - 7.41 (m, 48H, C_6H_4). *Note: The* CH_2 *signal is masked and all other peaks are quite broad due to the paramagnetic radical state of the molecule.* ^{13}C{^{1}H} NMR (125 MHz, $CDCl_3$): δ 191.26, 147.47, 140.59, 130.55, 124.24. *Note: The* CH_2 *signal is masked and all other peaks are quite broad due to the paramagnetic radical state of the molecule.* No resonances are visible by ^{11}B NMR due to paramagnetic broadening (a trace resonance at 20.4 ppm is indicative of borates, which result from decomposition). HRMS (Orbitrap): *m/z* calculated for $C_{84}H_{72}B_{12}N_{12}O_{36}$ (M^-), 1954.5361 Da; found, 1954.5363 Da.

Dodeca(3,5-bis(trifluoromethyl)$_2$benzyloxy)-*hypocloso*-dodecaborane [13]$^{1-}$

TBA_2[**1**] (99.0 mg, 0.121 mmol) was added to a 10 mL glass microwave vial and transferred out of a nitrogen filled glovebox, opened to the air, and dissolved in 2 mL acetonitrile. *N*,*N*-diisopropylethylamine (0.4 mL, 2.30 mmol) and 3,5-bis(trifluoromethyl)benzyl bromide (2.68 mL, 14.6 mmol) were added along with a stir bar, the vial was sealed with a PTFE/silicone cap, and the mixture was heated at 140 °C with stirring in the microwave for 30 min. The volatiles were removed *via* rotary evaporation, and the excess reagent was eluted through a slurry-packed silica gel column with 65/35 hexanes/ethyl acetate, and the colorless/very light pink product mixture was eluted with CH_2Cl_2. After removal of the CH_2Cl_2 *via* rotary evaporation, compound TBA_2[**13**]$^{2-}$, a clear, colorless solid, was dried under high vacuum to obtain an isolated yield of 313.6 mg (73%). After spectroscopic characterization, the dianionic TBA_2[**13**]$^{2-}$ was dissolved in 5 mL 90/10 ethanol/acetonitrile, 0.3 g (1.11 mmol) $FeCl_3{\cdot}6H_2O$ was added and the mixture was left to stir for 12-24 h. Following oxidation, the solvent mixture was removed *via* rotary evaporation, and a red-purple band containing [**13**]$^{1-}$ was separated from the $FeCl_3{\cdot}6H_2O$ through a slurry-packed silica gel column with CH_2Cl_2. The CH_2Cl_2 was removed *via* rotary evaporation and the final isolated radical [**13**]$^{1-}$ was dried under high vacuum to obtain an isolated yield of 226.4 mg (56%). Compound [**13**]$^{1-}$ is a red-purple solid. ^{1}H NMR (500 MHz, $CDCl_3$): δ 7.40 – 8.74 (m, 36H, C_6H_3), 3.13 (m, 8H, N-$\underline{CH_2}$), 1.65 (m, 8H, N-$CH_2\underline{CH_2}$), 1.47 (m, 8H, N-$(CH_2)_2\underline{CH_2}$), 1.05 (m, 12H, N-$(CH_2)_3\underline{CH_3}$). *Note: The CH_2 signal for the cluster is masked and all other peaks are quite broad due to the paramagnetic radical state of the molecule.* ^{13}C{^{1}H} NMR (125 MHz, $CDCl_3$): δ 189.0, 132.7, 132.5, 129.4, 124.6, 122.5, 121.0, 68.0, 59.2, 59.2, 59.1, 30.9, 25.6, 23.8, 19.7, 19.7, 13.4. No resonances are visible by ^{11}B NMR, due to paramagnetic broadening. ^{19}F NMR (376 MHz, $CDCl_3$): δ -63.22 (s, 72F). HRMS (Orbitrap): *m/z* calculated for $C_{108}H_{60}B_{12}F_{72}O_{12}$ (M^-), 3047.4158 Da; found, 1523.7080 (z=2) Da. Crystallized from $CDCl_3$ and pentane at room temperature for 1 week to obtain a single crystal for X-ray diffraction analysis.

Benzyloxy undeca(ethoxy)-*hypercloso*-dodecaborane [14]

TBA_2[**1**] (100.0 mg, 0.122 mmol) was added to a 10 mL glass microwave vial and transferred out of a nitrogen filled glovebox, opened to the air, and dissolved in 2 mL acetonitrile. *N,N*-diisopropylethylamine (0.4 mL, 2.30 mmol), benzyl bromide (0.0204 g, 0.119 mmol) and bromoethane (0.8055g, 7.39 mmol) were added along with a stir bar, the vial was sealed with a PTFE/silicone cap, and the mixture was heated at 140 °C with stirring in the microwave for 30 min. The volatiles and excess bromoethane were removed *via* rotary evaporation, the remaining charged 1-/2- product mixture was dissolved in 5 mL 90/10 ethanol/acetonitrile, $FeCl_3 \cdot 6H_2O$ (0.3 g, 1.11 mmol) was added and the mixture was left to stir for 12-24 h. Following oxidation, the solvent mixture was removed *via* rotary evaporation, and the product mixture was separated from the $FeCl_3 \cdot 6H_2O$ with CH_2Cl_2. The CH_2Cl_2 was removed *via* rotary evaporation, and the product mixture was loaded onto a long (30 – 35 cm) silica gel column slurry-packed with 80/20 CH_2Cl_2/hexanes, and the products were separated by eluting fractions with 80/20 CH_2Cl_2/hexanes.

The first orange band eluted contained randomly di-substituted benzyl$_2$ethyl$_{10}$ species, followed by an orange band with the neutral closomer **14**, with extra **4** in a third yellow-orange band eluting last. *Note: The fractions overlap, and due to the similar colors of the different products, thin layer chromatography (TLC) with 80/20 CH_2Cl_2/hexanes was performed on the fractions near the band edges to determine which fractions contained a mixture of products.* The fractions containing only a single species according to TLC that eluted after the di-substituted product and prior to the pure **4** bands were combined. The volatiles were removed *via* rotary evaporation, and the final neutral product **14** was dried under high vacuum to obtain an isolated yield of 15.7 mg (18%). Compound **14** is a yellow-orange solid. ^{1}H NMR (400 MHz, $CDCl_3$): δ 7.30 (m, 5H, C_6H_5), 5.07 (m, 2H, $\underline{CH_2}C_6H_5$), 4.10 (m, 22H, $\underline{CH_2}CH_3$), 1.22 (m, 33H, $CH_2\underline{CH_3}$).^{13}C{^{1}H} NMR (125 MHz, $CDCl_3$): δ 141.2, 128.0, 126.6, 71.6, 66.8, 17.7. ^{11}B NMR (128 MHz, $CDCl_3$): δ 39.0, 35.2. HRMS (DART): *m/z* calculated for $C_{29}H_{62}B_{12}O_{12}$ (M^-), 732.5431 Da; found, 732.5464 Da.

Chapter 3: Tuning the Electrochemical Potential of Perfunctionalized Dodecaborate Clusters Through Vertex Differentiation

Alex I. Wixtrom, [a] Zeeshan Parvez, [a] Miles A. Savage, [a] Elaine A. Qian, [a,b,c] Dahee Jung, [a,b] Saeed I. Khan,[a] Arnold L. Rheingold,[d] and Alexander M. Spokoyny [a,b]*

[a]*Department of Chemistry and Biochemistry, University of California, Los Angeles, 607 Charles E. Young Drive East, Los Angeles, CA 90095, United States*
[b]*California NanoSystems Institute (CNSI), University of California, Los Angeles, 570 Westwood Plaza, Los Angeles, CA 90095, United States*
[c]*Department of Bioengineering, University of California, Los Angeles, 420 Westwood Plaza, Los Angeles, CA 90095, United States*
[d]*Department of Chemistry and Biochemistry, University of California, San Diego, La Jolla, California 92093, USA*

* Corresponding author. E-mail: spokoyny@chem.ucla.edu

We report a new class of redox-active vertex-differentiated dodecaborate clusters featuring pentafluoroaryl groups. These [$B_{12}(OR)_{11}NO_2$] clusters share several unique photophysical properties with their [$B_{12}(OR)_{12}$] analogues, while exhibiting significantly higher (+0.5 V) redox potentials. This work describes the synthesis, characterization, and isolation of [$B_{12}(O\text{-}CH_2C_6F_5)_{11}NO_2$] clusters in all 3 oxidation states (dianion, radical, and neutral). Reactivity to post-functionalization with thiol species via S_NAr on the pentafluoroaryl groups is also demonstrated.

Introduction

The dodecaborate cluster *closo*-$[B_{12}H_{12}]^{2-}$ is a unique three-dimensional molecule which can be functionalized in a manner reminiscent of classical organic aromatic compounds (*e.g.* benzene). [2,3,23,24] Three-dimensional aromaticity in this icosahedral cluster is manifested in its exceptional thermal and chemical stability.[21] The *closo*-$[B_{12}H_{12}]^{2-}$ cluster has been previously subjected to various homoperfunctionalization strategies leading to molecules decorated with a diverse array of functional groups including halogens,[12,25,28] ethers, esters, carbonates, and carbamates.[29,31–33,58,59] While the parent *closo*-$[B_{12}H_{12}]^{2-}$ cluster does not undergo a reversible electrochemical transformation, homoperfunctionalization *via* substitution of all 12 B-H vertices can engender reversible redox behavior for some of the aforementioned derivatives.[41,58–65] This redox activity can provide access to isolable compounds in *hypo*- and *hypercloso*- forms. These additional redox states are accessed *via* sequential one-electron oxidation of the parent dianionic *closo*-$[B_{12}X_{12}]^{2-}$ species to form stable radical *hypocloso*-$[B_{12}X_{12}]^{1-}$ molecules, followed by the consecutive one–electron oxidation allowing isolation of neutral *hypercloso*-$[B_{12}X_{12}]$ clusters. Importantly, the redox potential of the 2-/1- and 1-/0 transitions for these clusters can be tuned as a function of the substituent by well over 1 V for the same redox event.[41,58,59] Among the redox active B_{12}-based clusters, homoperfunctionalized $[B_{12}(OR)_{12}]^{2-/1-/0}$ compounds represent, perhaps, the most modular class of redox active species, for which the electrochemical potential window was previously shown to be tunable in the range between -1.1 – +0.67 V *vs.* Fc/Fc^{+}.[58] This tunability is achieved by rationally changing an organic substituent (R) attached to the cluster *via* ether linkage. However, it remains unclear whether highly reversible redox behavior is inherent to only $B_{12}(OR)_{12}$ species and whether electronic perturbations on the cluster core with mixed substituents other than the alkoxy group can produce molecules with similar properties.[66–77] Here we present a new approach to further tune the redox properties of the perfunctionalized B_{12}-based clusters by substituting one of the OR moieties with an NO_2 group, thus introducing an additional structural handle *via* heterofunctionalization. As a result, a new class of $[B_{12}(OR)_{11}NO_2]^{2-/1-/0}$ clusters can be isolated which feature pronouncedly different electrochemical properties when compared to those of their $[B_{12}(OR)_{12}]$ analogues.

Results and Discussion

Commercially available $Cs_2[B_{12}H_{12}]$ undergoes selective monoamination in 60% yield on a decagram scale.[66] This compound can be safely subjected to the perhydroxylation conditions using 30% H_2O_2 (*safety note* – see SI) as was previously reported by Hawthorne and co-workers[66] (Figure 9, **[1]**). Based on this protocol, one can isolate $[B_{12}(OH)_{11}(NO_2)]^{2-}$ as a tetrabutylammonium (TBA) salt **[1]** on a multigram scale in 70% yield (see SI). Compound **[1]** is highly soluble in polar organic solvents, which allowed us to subject this compound perbenzylation conditions similar to those developed for the perfunctionalization of *closo*-$[B_{12}(OH)_{12}]^{2-}$.[58] The reaction of **[1]** with pentafluorobenzyl bromide dissolved in acetonitrile (MeCN) in the presence of an amine base under microwave conditions at 140 ºC resulted in a nearly quantitative conversion of the parent cluster molecule as judged by the ^{11}B NMR spectroscopy and mass spectrometry taken *in situ* after 1 hour.

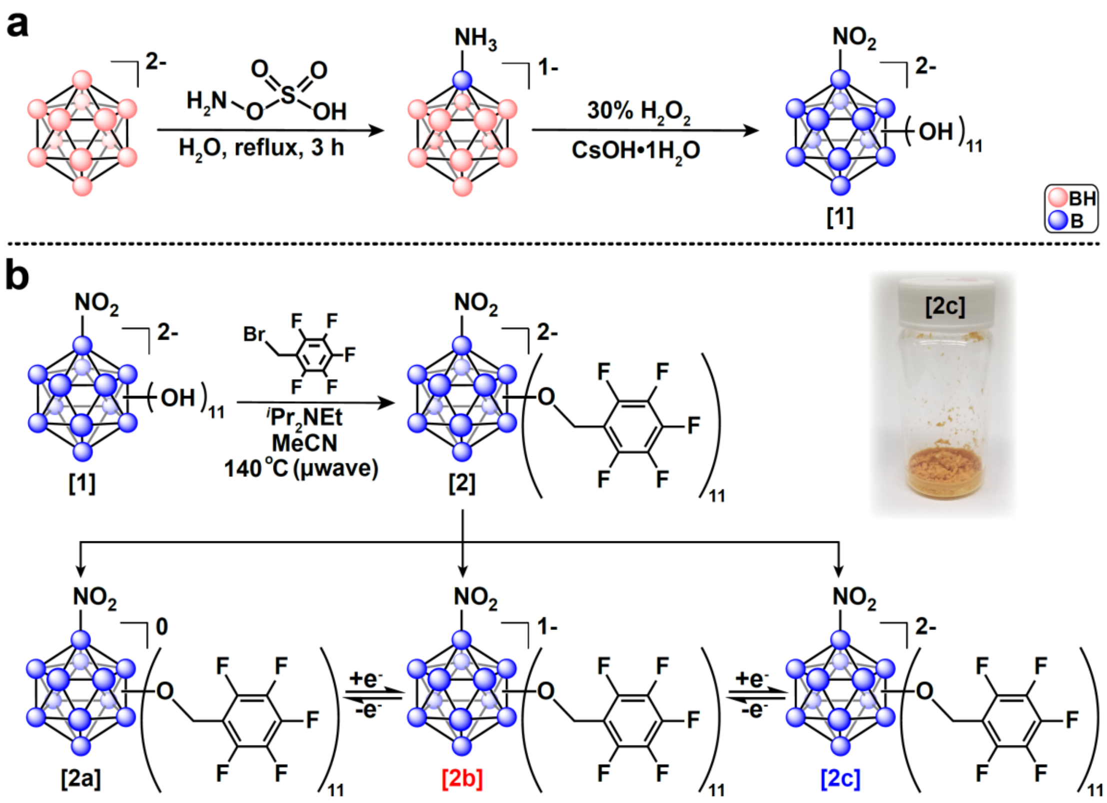
a
2-
$H_2N-O-SO_2-OH$
H_2O, reflux, 3 h
NH_3
1-
30% H_2O_2
$CsOH•1H_2O$
NO_2
2-
$(OH)_{11}$
[1]
BH
B
b
NO_2
2-
$(OH)_{11}$
[1]
Br
F
$^i Pr_2NEt$
MeCN
140 °C (μwave)
[2]
O
11
[2c]
0
1-
+e⁻
-e⁻
[2a]
[2b]
[2c]

Figure 9. (a) Synthetic route to produce **[1]** from $Cs_2[B_{12}H_{12}]^{2-}$. (b) Microwave synthesis of the $B_{12}(OR)_{11}NO_2$ cluster **[2]** studied in this work, showing all three oxidation states of **[2]** isolated (neutral $\mathbf{[2a]^0}$, radical $\mathbf{[2b]^{1-}}$, and the dianionic $\mathbf{[2c]^{2-}}$).

The desired product **[2c]** was isolated via purification on a silica gel column followed by ion exchange to the Na^+ salt using a cation-exchange resin (see SI). The identity of Na_2**[2c]** was confirmed by ^{11}B, ^{19}F, and ^1H NMR spectroscopy, mass spectrometry, and elemental analysis. Performing the same synthesis followed by oxidation of the unpurified crude $\mathbf{[2c]}^{2-}$ obtained directly from the microwave reaction with $FeCl_3•6H_2O$ in 9:1 [v/v] mixture of ethanol:MeCN yielded a dark purple solution. This mixture was subjected to silica gel column chromatography resulting in the isolation of analytically pure *hypocloso* species $\mathbf{[2b]^{1-}}$ as a TBA salt (see SI for characterization). In contrast, when $\mathbf{[2c]}^{2-}$ was exposed to $NOBF_4$, a stronger oxidant, in dry MeCN, neutral $\mathbf{[2a]^0}$ formed and was subsequently isolated.

All three species exhibit distinctive splitting patterns in both their ^{11}B and ^{19}F NMR spectra arising from the unique symmetry of the molecule. Unlike homoperfunctionalized $[B_{12}(OR)_{12}]$ species, which possesses a nearly perfect icosahedral structure (hence appearing as a singlet in ^{11}B NMR spectrum), the introduction of the nitro (NO_2) group in **[2]** breaks the symmetry of the cluster. The ^{11}B NMR spectra obtained confirm the asymmetry of the molecule, with both **[2c]**$^{2-}$ and **[2a]**^{0} exhibiting four distinct signals with relative integrations of 1:5:5:1 (Figure 10a). The ^{11}B NMR of the radical **[2b]**$^{1-}$ shows no visible signals consistent with the paramagnetic nature of the cluster in this oxidation state and is further corroborated by EPR spectroscopy (Figure 10a, inset). Specifically, the broad singlet in the EPR spectrum of **[2b]**$^{1-}$ showcases a highly delocalized doublet state, where an electron is shared by all twelve boron atoms in the cluster. This feature as well as the *g*-factor observed in the EPR spectrum of **[2b]**$^{1-}$ are similar to other $[B_{12}(OR)_{12}]^{1-}$ species (Figure 10).

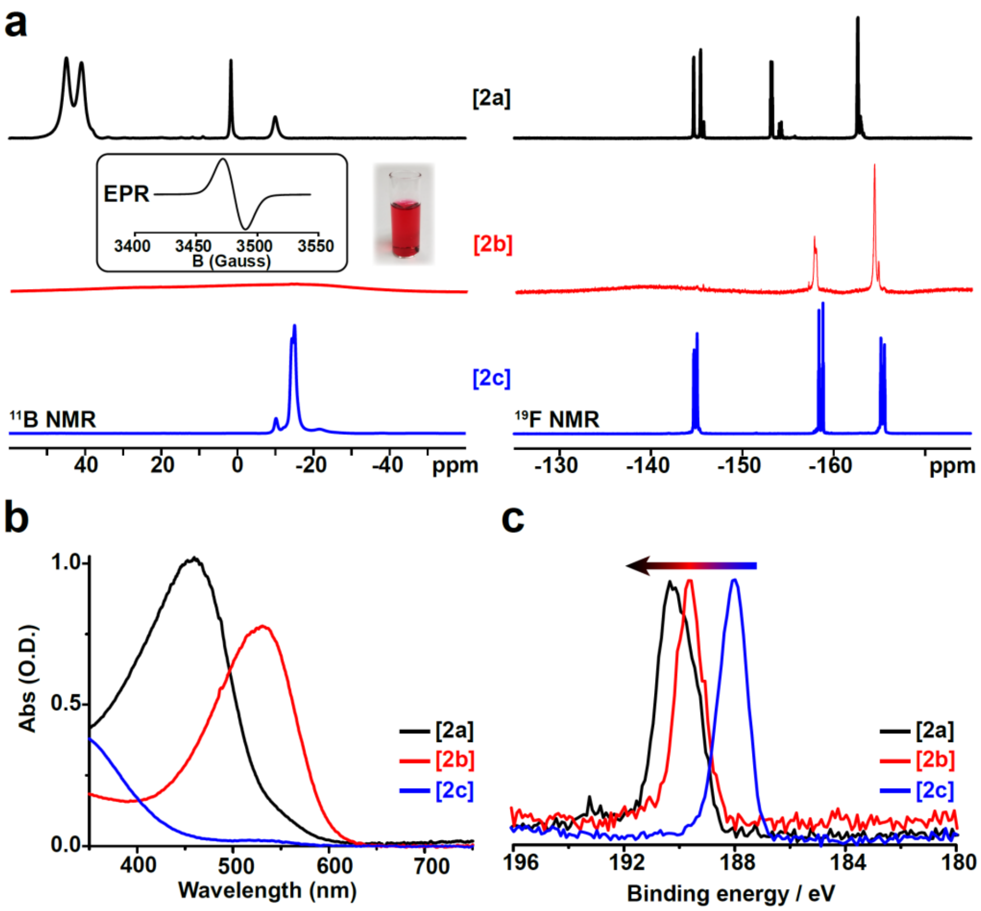

Figure 10. (a) ^{11}B and ^{19}F NMR spectra of all redox states of **[2]** with EPR (inset, g = 2.00674) and photo of **[2b]**$^{1-}$ in MeCN; (b) UV-vis spectra of **[2a]**^{0} and **[2b]**$^{1-}$ (50 mM) and **[2c]**$^{2-}$ (100 mM) in CH_2Cl_2; (c) XPS spectra for all redox states of **[2]** showing increasing B-B binding energy as redox state increases.

An unexpected but very interesting phenomenon is observed in the ^{19}F NMR spectra of **[2]** series. Normally, the spectra for all previously reported $[B_{12}(OR)_{12}]$ species containing fluorine atoms in the close vicinity from the boron cluster core show a single signal for each set of equivalent atoms.[11,18,19] However, **[2c]**$^{2-}$ exhibits three distinct (though partially overlapping) fluorine signals for each of the equivalent pentafluoroaryl fluorine atoms, which show the same 1:5:5 relative integrations stemming from the symmetry of the boron cluster core. The *ortho*-fluorine signal for **[2b]**$^{1-}$ is difficult to observe due to the significant paramagnetic broadening that normally affects the atoms closest to the paramagnetic center (boron cluster core). Since the *meta*- and *para*-fluorine atoms are located further away from the paramagnetic cluster in **[2b]**$^{1-}$, their ^{19}F signals could be resolved and also exhibit a 1:5:5 relative pattern similar to the one observed in **[2c]**$^{2-}$ (Figure 10a). Likewise, a 1:5:5 pattern can be well resolved for the diamagnetic **[2a]**^{0} species. Furthermore, the two methylene proton resonances (1:10 integration) can be resolved in the ^{1}H NMR spectrum of **[2a]**^{0} consistent with the introduction of asymmetry by the NO_2 group.

Consistent with the $[B_{12}(OR)_{12}]^{2-}$ clusters synthesized to date, pure dianionic **[2c]**$^{2-}$ cluster is essentially colourless and shows little visible absorption in its UV-vis spectrum. There is a small absorbance in the UV-vis spectrum of **[2c]**$^{2-}$around 350 – 400 nm stemming from the presence of the NO_2 group, while the UV-vis spectrum for **[3]**$^{2-}$ ($[B_{12}(OR)_{12}]$ when R = $CH_2C_6F_5$) shows negligible absorption across the entire visible region (See SI). On the other hand, the radical **[2b]**$^{1-}$ exhibits a deep pink/purple color when dissolved in CH_2Cl_2, and the neutral species **[2a]**^{0} appears as a bright red-orange when dissolved in the same solvent (Figure 10b). These light absorption properties are similar to those of homoperfunctionalized $[B_{12}(OR)_{12}]$ clusters in the corresponding oxidation states. X-ray photoelectron spectroscopy analysis of **[2]** series also reveals a similar trend to that observed with $[B_{12}(OR)_{12}]$ clusters, where the B-B binding energy increases with higher oxidation states sequentially from **[2c]**$^{2-}$ to **[2b]**$^{1-}$ and **[2a]**^{0} (Figure 10c).

A single crystal suitable for X-ray diffraction analysis was obtained for the radical $[N^{n}Bu_4]$**[2b]** from a chloroform/pentane solution of **[2b]**$^{1-}$, and the crystal structure (Figure 11a) shows a structural similarity to that of the radical **[3]**$^{1-}$ (Figure 11c, see SI). Overlaying the two structures (Figure 11b) effectively illustrates these similarities, with only the rotation of a few pentafluorobenzyl rings nearest the NO_2 group differing significantly, while the core bonding metrics (B-B and B-O bond lengths and angles) remain indistinguishable within the margin of error produced by the experiment. Despite the remarkably clear effects visible in the ^{19}F NMR spectra of the asymmetry introduced into the molecule by the lone NO_2 group in solution, the two different clusters retain very similar structures in the solid-state. This structural similarity, especially in the radical state, is consistent with the EPR evidence that the environment of the unpaired electron in **[2b]**$^{1-}$ is largely unchanged from **[3]**$^{1-}$.

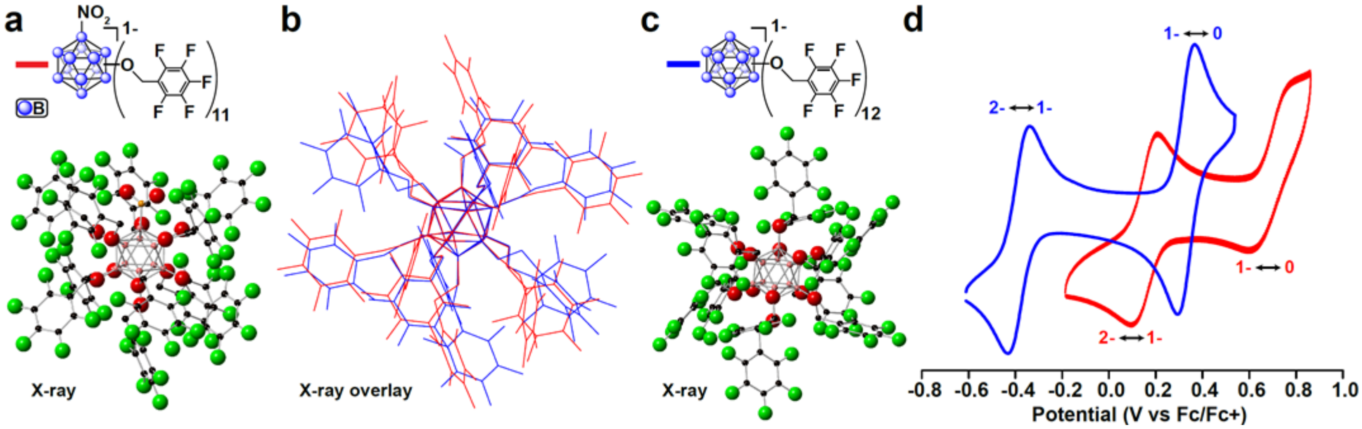

Figure 11. (a) Single crystal X-ray structure of **[2b]**$^{1-}$ (hydrogens and $[N^nBu_4]^+$ counter ion omitted for clarity); (b) Overlay of **[2b]**$^{1-}$ and **[3]**$^{1-}$; (c) Single crystal X-ray structure of **[3]**$^{1-}$ (hydrogens and $[N^nBu_4]^+$ counter ion omitted for clarity); (d) Cyclic voltammogram for **[2b]**$^{1-}$ and **[3]** in acetonitrile with glassy carbon working electrode, Pt wire counter electrode, and Ag/AgCl reference electrode (in sat. KCl) internally referenced to the Fc/Fc$^+$ couple.

Despite all these similarities, perhaps the most striking difference between the two species is the exceptional increase in redox potential of **[2]** compared to that of **[3]**. The significant difference between the redox potential of **[2]** and **[3]** of over +0.5 V for the same redox couple (Figure 11b) is remarkable given the aforementioned similarities between most of the photophysical properties discussed. For the 2-/1- redox event, **[3]** displays a reversible wave with an $E_{1/2}$ of -0.38 V vs Fc/Fc$^+$, while the same couple for **[2c]**$^{2-}$/**[2b]**$^{1-}$ has an $E_{1/2}$ of +0.15 V (Figure 11 d). The increase in the 1-/0 redox couple is less extreme, but still significant, going from an $E_{1/2}$ of +0.33 V for **[3]**$^{1-}$/**[3]**^{0} up to an $E_{1/2}$ of 0.69 V (vs Fc/Fc$^+$) for **[2b]**$^{1-}$/**[2a]**^{0}. The substitution of a single boron vertex with a NO_2 group instead of an ether moiety therefore provides a dramatic shift in the electrochemical potential in this class of clusters.

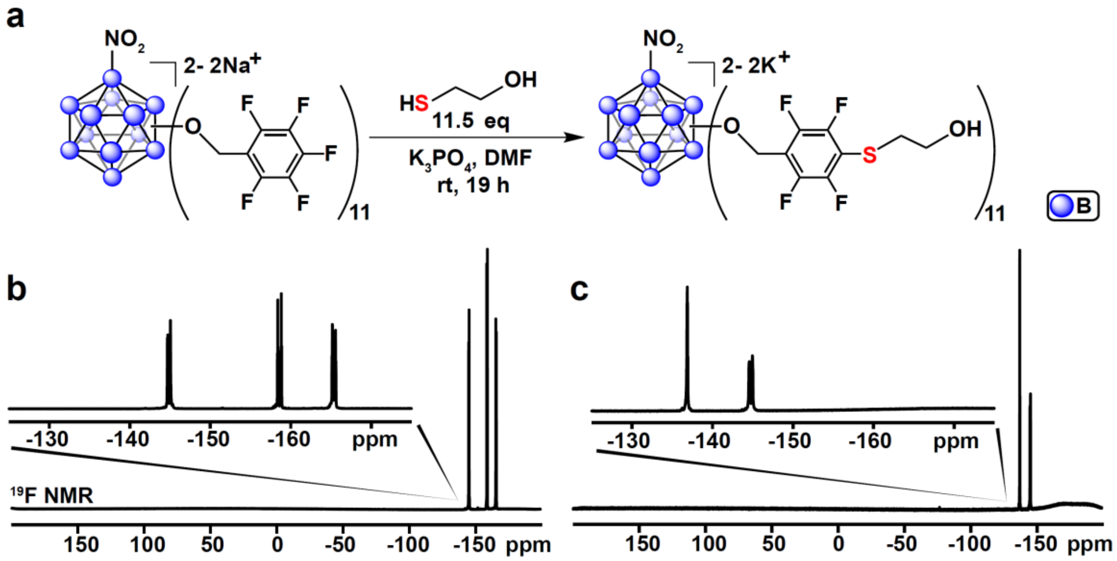

Figure 12. (a) Scheme showing the S_NAr reaction between **[2c]$^{2-}$** and mercaptoethanol; (b) ^{19}F NMR spectrum of the starting material **[2c]$^{2-}$**; (c) ^{19}F NMR spectrum of the reaction product showing full conversion to **[2c]-ME** based upon the disappearance of the *para*-fluorine signal.

Consistent with the reactivity previously observed for **[3]**,[64] **[2]** undergoes a facile S_NAr reaction with thiols enabling dense functionalization of this class of three-dimensional scaffolds (Figure 12). Under similar conditions to those described for **[3]** previously,[64] full substitution of the *para*-fluorines on **[2c]$^{2-}$** with mercaptoethanol was achieved using only 1.05 equiv. of the thiol per pentafluoroaryl group at room temperature within 19 hours (Figure 12). The quantitative conversion observed under these mild conditions to form **[2c]-ME** indicates that the introduction of the nitro group does not interfere with the S_NAr chemistry and **[2]** is potentially well-suited for building atomically precise hybrid nanomolecule assemblies.[64]

Conclusions

In summary, a new class of perfunctionalized, vertex-differentiated boron clusters was developed and fully characterized. While several routes exist to achieve vertex-differentiated perfunctionalization with other boron cluster molecules with inherent asymmetry such as monocarborane,[67–69,71,78] significantly fewer synthetic pathways have been developed to form vertex-differentiated perfunctionalized dodecaborate clusters.[20,26] These NO_2-substituted dodecaborate clusters feature higher redox potentials while retaining key beneficial traits found in their perfunctionalized $[B_{12}(OR)_{12}]$ analogues, including three distinct accessible redox states. The readily-accessible isolable radical cluster also represents a new addition to the boron-centered radical molecules.[79–85] The pentafluoroaryl groups decorating the cluster were demonstrated to be amenable to facile post-functionalization with thiol-containing groups *via* S_NAr chemistry, thus enabling the possibility of orthogonal substitution without affecting the B-NO_2 vertex. Overall, this chemistry provides another unique entry towards robust and redox-active 3D aromatic building blocks for potentially designing new photoredox reagents[65] and hybrid materials.[86]

Acknowledgements

A.M.S. acknowledges the University of California, Los Angeles (UCLA) Department of Chemistry and Biochemistry for start-up funds, 3M for a Non-Tenured Faculty Award, the Alfred P. Sloan Foundation for a research fellowship in chemistry and the NIGMS for the Maximizing Investigators Research Award (MIRA, R35GM124746). The authors thank the MRI program of the National Science Foundation (NSF grant no. 1532232 and no. 1625776). E.A.Q. thanks the US Public Health Service of the National Institutes of Health (NIH) for the Predoctoral Training Fellowship through the UCLA Chemistry-Biology Interface Training Program under the National

Research Service Award (T32GM008496). We thank UCLA Molecular Instrumentation Center for mass spectrometry and NMR spectroscopy (NIH grant 1S10OD016387-01).

Supporting Information

Experimental Section

General considerations

Microwave synthesis reactions and all post-microwave work-up and characterization was performed under ambient conditions. The "ambient conditions" for this manuscript refer to room temperature (20 - 25 °C) and uncontrolled laboratory air. The oxidation of **[2c]** to form **[2a]** and the synthesis of **[2c]-ME** describe the use of a nitrogen-filled glovebox for several steps, all other reactions were performed open to air.

Materials

Deuterated solvents were purchased from Cambridge Isotope Laboratories and used as received. MilliQ water described in this manuscript refers to purified potable water with a resistivity at 25 °C of ≤18.2 MΩ·cm. $[NEt_3H]_2[B_{12}H_{12}]$ was purchased from Boron Specialties (USA). Ethanol (200 proof) was purchased from Decon Labs and used as received. Dowex 50W X8 (100-200 mesh, hydrogen form), dimethylformamide (anhydrous, 99.8%), $FeCl_3 \cdot 6H_2O$ (≥97%), $CsOH \cdot 1H_2O$ (≥99.5%), hydrogen peroxide (30% in H_2O), $[N^nBu_4]OH$ (40% in H_2O), bromoethane (≥99%), acetonitrile (≥99.9%), dichloromethane (≥99.5%), ethyl acetate (≥99.5%), hexanes (≥98.5%), methanol (≥99.8%), 2-mercaptoethanol (≥99%), potassium phosphate tribasic (≥98%), and *N*,*N*-diisopropylethylamine (≥99%) were purchased from Sigma-Aldrich. Tetrabutylammonium hexafluorophosphate (≥98%, recrystallized from ethanol and dried under vacuum at 90 °C), nitrosonium tetrafluoroborate (95%), hydroxylamine-O-sulfonic acid (97%), and 2,3,4,5,6 pentaflurobenzyl bromide (98%) were purchased from Oakwood. NaOH (Certified ACS, 99.2%) was purchased from Fisher. Sodium borohydride (98%) was purchased from Strem. All reagents were used as received unless otherwise indicated.

Instrumentation

A Bruker AV400 spectrometer was used to obtain ^{11}B, ^{1}H, and ^{19}F NMR spectra and Bruker Topspin software was used to process the NMR data. ^{1}H NMR spectra were referenced to residual solvent resonances in deuterated solvents. ^{11}B and ^{19}F NMR spectra were referenced to $BF_3{\cdot}Et_2O$.

A Bruker EMX EPR spectrometer was used to acquire EPR spectra, with all spectra collected in CH_2Cl_2 at ambient temperature.

Mass spectrometry data was acquired using a Thermo Scientific^{TM} Q-Exactive^{TM} Plus instrument with a quadrupole mass filter and Orbitrap mass analyzer.

UV-vis analysis was performed on an Ocean Optics Flame Spectrometer with an Ocean Optics DH-2000-S-DUV-TTL light source and a quartz cuvette.

IR spectroscopy was acquired on solid samples using a PerkinElmer Spectrum One FT-IR spectrometer equipped with a diamond universal ATR probe.

X-ray photoelectron spectroscopy (XPS) data was acquired using an AXIS Ultra DLD instrument (Kratos Analytical Inc., Chestnut Ridge, NY, USA) with a monochromatic Al Kα X-ray source (10 mA for survey and high-resolution scans). A 300 x 700 nm oval spot size and ultrahigh vacuum (10^{-9} Torr) were used, with 160 eV pass energy for survey spectra and 20 eV for high-resolution spectra of B 1s using a 200 ms dwell time and 20 scans. All XPS peaks were externally referenced to the C 1s signal at 284.6 eV.

Elemental analyses were performed by Atlantic Microlab, Inc. (Norcross, GA).

X-ray data collection and processing parameters

For [**2b**] and **[3]**$^{1-}$, a single crystal was mounted on a nylon loop using perfluoropolyether oil and cooled rapidly to 100 K with a stream of cold dinitrogen. Diffraction data were measured using a

Bruker APEX-II CCD diffractometer using Mo-K_α radiation. The cell refinement and data reduction were carried out using Bruker SAINT and the structure was solved with SHELXT. All subsequent crystallographic calculations were performed using SHELXT. Olex2 software was used to export the report for **[3]**$^{1-}$.[87]

Cyclic voltammetry

Cyclic voltammetry was performed on [**2b**] using a CH Instruments CHI630D potentiostat with a glassy carbon disc working electrode, platinum wire counter electrode, and Ag/AgCl (in saturated KCl solution) reference electrode. The experiment was conducted in 0.1M $[N^nBu_4]PF_6/CH_3CN$ with 1 mM analyte concentration. The CH_3CN was dried in house with a custom drying system running through two alumina columns prior to use. The solution was degassed by bubbling N_2, and the cyclic voltammetry was performed under N_2 gas. For [**2b**] a scan rate of 100 mV/s was used with Fc/Fc^+ as an internal standard.

Microwave synthesis

Microwave reactions were performed using a CEM Discover SP microwave synthesis reactor. Except where noted otherwise, all reactions were performed in glass 10 mL microwave reactor vials purchased from the vendor. Reaction vials were sealed with silicone/PTFE caps. Flea micro PTFE-coated stir bars were used in the vials with magnetic stirring set to high and 15 seconds of premixing prior to the temperature ramping. All microwave reactions were carried out at 140 °C with the pressure release limit set to 250 psi (no reactions exceeded this limit to trigger venting) and the maximum wattage set to 250W (the power applied was dynamically controlled by the microwave instrument and did not exceed this limit for any reactions). Column chromatography was performed using 2.0 - 2.25 cm inner diameter glass fritted chromatography columns with 20-

30 cm of slurry-packed silica gel to ensure full separation of reagents and products. Unfiltered pressurized air was used to assist column chromatography.

Synthesis of [1]

Synthesis of $[N^nBu_4]_2B_{12}(OH)_{11}(NO_2)$ (**[1]**) was performed starting with $Cs_2[B_{12}H_{12}]$ (ion exchanged from $[NEt_3H]_2[B_{12}H_{12}]$ using $CsOH{\cdot}1H_2O$) according to a reported procedure.[66] *Note: the hydroxylation procedure should always be undertaken with caution and careful planning to ensure the $Cs_2[B_{12}H_{12}]$ reagent is pure and contains no organic contaminants. Blast shielding to contain any possible explosions should be utilized. Under no circumstances should the hydrogen peroxide used in the reaction come into contact with any organic material or solvents due to possibility of an explosion.*

Synthesis of [2a]

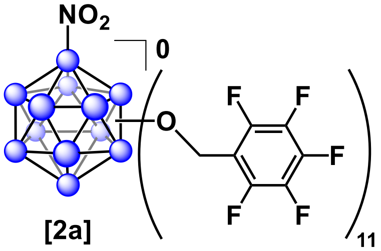

[2a]

$[N^nBu_4]_2B_{12}(OH)_{11}(NO_2)$ (100 mg, 0.12 mmol) was added to a 10 mL glass microwave vial and dissolved in 1 mL of acetonitrile. *N,N*-diisopropylethylamine (0.47 mL, 2.7 mmol) and 1-(bromomethyl)-2,3,4,5,6-pentafluorobenzene (2.00 mL, 13.2 mmol) were added along with a flea micro stir bar, the vial was sealed with a PTFE/silicone cap, and the mixture was heated at 140 °C with stirring in the microwave for 1 hour. The excess acetonitrile was evaporated by rotary evaporation and the excess reagents were removed through a slurry-packed silica gel column with 35/65 [v/v] ethyl acetate/hexane, followed by acetone (~20 mL) to elute the yellow-orange product band. The acetone was removed by rotary evaporation, the residue was dried under high vacuum and transferred into the glovebox. 75 mg (0.64 mmol) nitrosonium tetrafluoroborate ($NOBF_4$) was added, 2 mL of acetonitrile was added, and the solution was left to stir at room temperature for ~16 hours. The solution was transferred out of the glovebox, cooled to -15 °C for 1 hour, filtered using a glass fritted funnel, and the orange solid was carefully washed with ~1 mL of cold (-15 °C) acetonitrile 3 times, then dried on the frit for 5 min. The solid product was transferred to a glass vial and dried under high vacuum to obtain 113 mg (41%) of pure, isolated product. Compound [**2a**]^0 is an orange solid. ^{1}H NMR (400 MHz, CD_2Cl_2): δ 5.36 – 5.06 (m, 11H, O-C$\underline{H_2}$-C_6F_5). ^{11}B NMR (128 MHz, CD_2Cl_2): δ 45.22 – 41.32 (m, 10B, $\underline{B}$-OR), 1.99 (s, 1B, $\underline{B}$-NO_2), -9.58 (s, 1B, $\underline{B}$-OR). ^{19}F NMR (376 MHz, CD_2Cl_2): δ -144.34 – -145.48 (m, 22F, *ortho*-$C_6\underline{F_5}$), -152.78 – -154.05 (m, 11F, *para*-$C_6\underline{F_5}$), -162.26 – -162.75 (m, 22F, *meta*-$C_6\underline{F_5}$). HRMS: *m/z* calculated for $C_{77}H_{22}B_{12}F_{55}NO_{13}$ (M^{2-}), 1172.5665 Da; found, 1172.5735 (z = 2) Da. Calc. for $C_{77}H_{22}B_{12}F_{55}NO_{13}$: C, 39.46; H, 0.95; N, 0.60. Found: C, 39.64; H, 0.90; N, 0.62.

Synthesis of [2b]

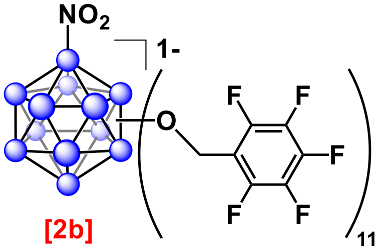

[2b]

$[N^nBu_4]_2B_{12}(OH)_{11}(NO_2)$ (100 mg, 0.12 mmol) was added to a 10 mL glass microwave vial and dissolved in 1 mL of acetonitrile. *N,N*-diisopropylethylamine (0.47 mL, 2.7 mmol) and 1-(bromomethyl)-2,3,4,5,6-pentafluorobenzene (2.00 mL, 13.2 mmol) were added along with a flea micro stir bar, the vial was sealed with a PTFE/silicone cap, and the mixture was heated at 140 °C with stirring in the microwave for 1 hour. The excess acetonitrile was evaporated by rotary evaporation and the excess reagents were removed through a slurry-packed silica gel column with 35/65 [v/v] ethyl acetate/hexane, followed by acetone (~20 mL) to elute the yellow-orange product band. The acetone was removed by rotary evaporation, and the residue was dissolved in 5 mL of 9:1 [v/v] ethanol/acetonitrile. 0.3 g (1.11 mmol) iron chloride hexahydrate was added, and the solution was left to stir at room temperature for ~48 hours. The volatiles were removed *via* rotary evaporation followed by high vacuum for 5 minutes, and the residue was dissolved in dichloromethane and loaded onto a slurry-packed silica gel column. The product was eluted with dichloromethane and the dark purple band was collected. The dichloromethane was removed *via* rotary evaporation, and the solid product was dried under high vacuum to obtain 107 mg (35%) isolated product. Compound [N^{n}Bu$_4$][**2b**] is a purple solid. ^{1}H NMR (400 MHz, CD_3CN): δ 3.11 – 3.04 (m, 8H, [N^{n}Bu$_4$]), 1.65 – 1.55 (m, 8H, [N^{n}Bu$_4$]), 1.40 – 1.30 (m, 8H, [N^{n}Bu$_4$]), 0.97 (t, 12H, [N^{n}Bu$_4$]). *Note: the methylene peak is not visible in ^{1}H NMR due to paramagnetic broadening.* ^{11}B NMR (128 MHz, CD_3CN): No visible signals due to paramagnetic broadening. ^{19}F NMR (376 MHz, CD_3CN): δ -140.13 (br s, *ortho*-$C_6\underline{F_5}$), -157.27 – -158.18 (m, *para*-$C_6\underline{F_5}$), -163.74 – -165.03 (m, *meta*-$C_6\underline{F_5}$). *Note: the ortho fluorine signal is extremely broad from the proximity to the paramagnetic core.* HRMS: *m/z* calculated for $C_{77}H_{22}B_{12}F_{55}NO_{13}$ (M^{2-}), 1172.5665 Da; found, 1172.5724 (z = 2) Da. Calc. for $C_{93}H_{58}B_{12}F_{55}N_2O_{13}$: C, 43.19; H, 2.26; N, 1.08. Found: C, 43.39; H, 2.21; N, 1.06. Crystallized from $CHCl_3$ and pentane at room temperature for 3 days to obtain a single crystal for X-ray diffraction analysis.

Synthesis of [2c]

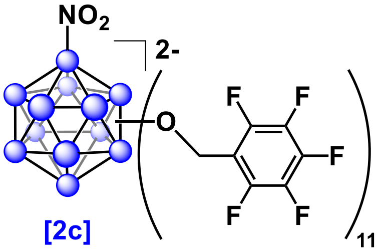

[2c]

150 mg scale: $[N^nBu_4]_2B_{12}(OH)_{11}(NO_2)$ (150 mg, 0.18 mmol) was added to a 10 mL glass microwave vial and dissolved in 3 mL of acetonitrile. *N*,*N*-diisopropylethylamine (0.71 mL, 4.1 mmol) and 1-(bromomethyl)-2,3,4,5,6-pentafluorobenzene (2.93 mL, 19.4 mmol) were added along with a flea micro stir bar, the vial was sealed with a PTFE/silicone cap, and the mixture was heated at 140 °C with stirring in the microwave for 1 hour. The excess acetonitrile was evaporated by rotary evaporation and the excess reagents were removed through a slurry-packed silica gel column with 35/65 [v/v] ethyl acetate/hexane, followed by acetone to elute the yellow-orange product band. The acetone was removed by rotary evaporation, and the residue was dissolved in 5 mL of acetonitrile. This solution was added to 100 mL of 1:1 [v/v] acetonitrile/water and ion exchanged using Dowex 50W X8 cation exchange resin loaded with Na^+ by eluting the solution through a 1.5 x 40 cm column slurry-packed with ~30 cm of Dowex resin (solution-swelled volume) and washing with an additional 100 mL of 1:1 [v/v] acetonitrile/water. The methanol and water were removed *via* rotary evaporation followed by high vacuum overnight to obtain 308 mg (71%) isolated product. Compound Na_2[**2c**] is a dark yellow solid.

300 mg scale: $[N^nBu_4]_2B_{12}(OH)_{11}(NO_2)$ (300 mg, 0.36 mmol) was added to a 35 mL glass microwave vial and dissolved in 6 mL of acetonitrile. *N*,*N*-diisopropylethylamine (1.42 mL, 8.2 mmol) and 1-(bromomethyl)-2,3,4,5,6-pentafluorobenzene (5.86 mL, 38.8 mmol) were added along with a flea micro stir bar, the vial was sealed with a PTFE/silicone cap, and the mixture was heated at 140 °C with stirring in the microwave for 1 hour. The excess acetonitrile was evaporated by rotary evaporation and the excess reagents were removed through a slurry-packed silica gel column with 35/65 [v/v] ethyl acetate/hexane, followed by acetone to elute the yellow-orange product band. The acetone was removed by rotary evaporation, and the residue was dissolved in 5 mL of acetonitrile. This solution was added to 200 mL of 1:1 [v/v] acetonitrile/water and ion exchanged using Dowex 50W X8 cation exchange resin loaded with Na^+ by eluting the solution through a 6 x 30 cm column slurry-packed with ~25 cm of Dowex resin (solution-swelled volume) and washing with an additional 250 mL of 1:1 [v/v] acetonitrile/water. *Note: if residual [N^nBu_4]$^+$ remains after the ion exchange, repeating the exchange procedure using freshly Na^+-loaded Dowex with the partially-exchanged product will remove any traces of [N^nBu_4]$^+$.* The methanol and water were removed *via* rotary evaporation followed by high vacuum overnight to obtain 610 mg (70%) isolated product. Compound Na_2[**2c**] is a dark yellow solid. ^{1}H NMR (400 MHz, CD_3CN): δ 5.54 – 5.21 (m, 22H, methylene). ^{11}B NMR (128 MHz, CD_3CN): δ -10.16 (s, 1B, $\underline{B}$-NO_2), -11.87 – -18.32 (m, 10B, $\underline{B}$-OR), -21.53 (br s, 1B, $\underline{B}$-OR). ^{19}F NMR (376 MHz, CD_3CN): δ -144.39 (m, 22F, *ortho*-$C_6\underline{F_5}$), -157.85 – -158.97 (m, 11F, *para*-$C_6\underline{F_5}$), -164.86 – -165.77 (m, 22F, *meta*-$C_6\underline{F_5}$). HRMS: *m/z* calculated for $C_{77}H_{22}B_{12}F_{55}NO_{13}$ (M^{2-}), 1172.5665 Da; found, 1172.5734 (z = 2) Da. Calc. for $C_{77}H_{22}B_{12}F_{55}NNa_2O_{13}$: C, 38.70; H, 0.93; N, 0.59. Found: C, 38.67; H, 1.06; N, 1.45.

Synthesis of [2c]-ME

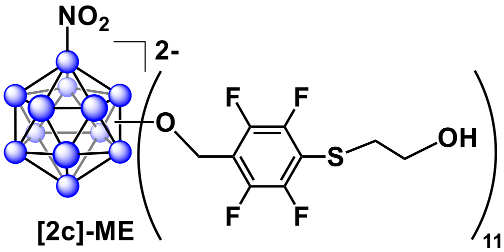

[2c]-ME

[2c] (7.5 mg, 0.0031 mmol) and K_3PO_4 (22.3 mg, 0.105 mmol) were added along with a flea micro stir bar to a 4-mL glass vial, which was then sealed with a PTFE/silicone cap under ambient conditions. The vial was then purged and backfilled with N_2 three times before being transferred into the glovebox. In the glovebox, the vial was opened and 150 µL anhydrous DMF was added, followed by 2-mercaptoethanol (2.54 µL, 0.036 mmol). The vial was sealed again and set to stir at 400 rpm for 22 hours. The vial was transferred out of the glovebox, and its contents were transferred into an NMR tube for *in situ* ^{19}F NMR spectroscopy to ensure nearly quantitative conversion and *in situ* ^{11}B NMR spectroscopy to ensure structural integrity of the cluster. The crude mixture was filtered through a 0.45 µm pore size syringe filter unit, then transferred into a 15-mL conical centrifuge tube and lyophilized for solvent removal. The dried sample was redissolved in MeOD and subjected to characterization *via* ^{1}H, ^{11}B, and ^{19}F NMR spectroscopy. Compound K_2[**2c**] is a dark yellow solid. ^{1}H NMR (400 MHz, CD_3OD): δ 5.58 – 5.35 (m, 22H, methylene), 3.70 – 3.58 (m, 22H, S-$CH_2C\underline{H_2}$-OH), 3.05 – 2.96 (m, 22H, S-$C\underline{H_2}CH_2$-OH). ^{11}B NMR (128 MHz, CD_3OD): δ -9.61 (br s, 1B, $\underline{B}$-NO_2), -14.71 (br s, 11B, $\underline{B}$-OR). ^{19}F NMR (376 MHz, CD_3OD): δ -136.40 – -137.35 (m, 22F, *ortho*-$C_6\underline{F_5}$), -143.99 – -145.38 (m, 22F, *meta*-$C_6\underline{F_5}$). HRMS: *m/z* calculated for $C_{77}H_{22}B_{12}F_{55}NO_{13}$ (M^{2-}), 1491.6089 Da; found, 1491.6154 (z = 2) Da.

Synthesis of [3], [3]$^{1-}$, and [3]$^{2-}$

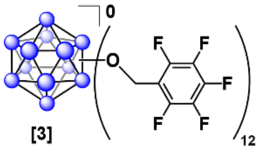

[3]

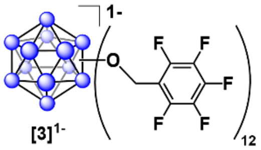

[3]$^{1-}$

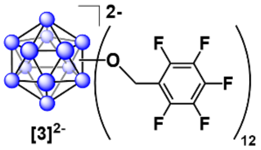

[3]$^{2-}$

Synthesis of **[3]** was performed according to a previously reported procedure.[65] *Note: the procedure below was not optimized, and was only suitable to produce enough of the radical salt to crystallize for X-ray diffraction analysis for comparison with **[2b]***. **[3]**$^{1-}$ was synthesized by performing an extraction with 25 mL dichloromethane and a solution of 0.65 g disodium EDTA in 150 mL MilliQ H_2O in lieu of the reported post-oxidation column chromatography with dichloromethane, vigorously stirring and shaking the mixture before draining off the organic layer and drying with sodium sulfate. The volatiles were removed *via* rotary evaporation, the residue was re-dissolved in dichloromethane and eluted through a plug of silica, and the dichloromethane was removed *via* rotary evaporation followed by high vacuum. The purple solid residue was taken up in chloroform and pentane was layered on top, resulting in formation of single crystals suitable for X-ray analysis after 5 days at room temperature. The UV-vis analysis of **[3]**$^{2-}$ was performed on a small sample of **[3]**^{0} (2.3 mg, 0.9 μmol) reduced with $NaBH_4$ (2.0 mg, 53 mmol) in 9:1 [v/v] ethanol/acetonitrile by shaking for 5 min at room temperature.

Table 1. Crystal data and structure refinement for [**2b**]$^{1-}$

Identification code	**[2b]**$^{1-}$	
Empirical formula	C93 H58 B12 F55 N2 O13	
Formula weight	2586.13	
Temperature	100.0 K	
Wavelength	0.71073 Å	
Crystal system	Triclinic	
Space group	P-1	
Unit cell dimensions	a = 14.1250(3) Å	α= 110.4400(10)°.
	b = 27.2616(5) Å	β= 91.6990(10)°.
	c = 29.4644(6) Å	γ = 97.1390(10)°.
Volume	10516.5(4) Å^3	
Z	4	
Density (calculated)	1.633 Mg/m^3	
Absorption coefficient	0.170 mm^{-1}	
F(000)	5156	
Crystal size	0.32 x 0.28 x 0.2 mm^3	
Theta range for data collection	1.273 to 25.292°.	
Index ranges	-16<=h<=16, -32<=k<=32, -30<=l<=35	
Reflections collected	79433	
Independent reflections	38080 [R(int) = 0.0454]	
Completeness to theta = 25.242°	99.9 %	
Absorption correction	Semi-empirical from equivalents	
Max. and min. transmission	0.6462 and 0.6188	
Refinement method	Full-matrix least-squares on F^2	
Data / restraints / parameters	38080 / 3236 / 3184	
Goodness-of-fit on F^2	1.033	
Final R indices [I>2sigma(I)]	R1 = 0.0857, wR2 = 0.2226	
R indices (all data)	R1 = 0.1376, wR2 = 0.2595	
Largest diff. peak and hole	1.257 and -0.520 e.Å^{-3}	
SQUEEZE	Found 129e/uc. Calc'ed for 2 $CHCl_3$, 116e/uc	

Chapter 4: Perfunctionalized Dodecaborate Clusters as Stable Metal-Free Active Materials for Charge Storage

Alex I. Wixtrom,[⊥,∥] John L. Barton,[†,‡,∥] Jeffrey A. Kowalski,[†,‡,∥] Fikile R. Brushett,[*,†,‡] Alexander M. Spokoyny.[*,⊥,§]

† Joint Center for Energy Storage Research, Argonne National Laboratory, 9700 South Class Ave, Bldg. 200, Argonne, Illinois, USA
‡ Department of Chemical Engineering, Massachusetts Institute of Technology, 77 Massachusetts Ave, Cambridge, Massachusetts 02139, USA
⊥Department of Chemistry and Biochemistry, University of California, Los Angeles, 607 Charles E. Young Drive East, Los Angeles, California 90095-1569, USA
§California NanoSystems Institute, University of California, Los Angeles, 570 Westwood Plaza, Los Angeles, California 90095-1569, USA

We report a class of perfunctionalized dodecaborate clusters that exhibit high stability towards high concentration electrochemical cycling. These boron clusters afford several degrees of freedom in material design to tailor properties including solubility and redox potential. The exceptional stability of these clusters was demonstrated using a symmetric flow cell setup for electrochemical cycling between two oxidation states for 45 days, with post-run analysis showing negligible decomposition of the active species (<0.1%). To further probe the limits of this system, a prototype flow device with two different boron cluster materials was used to determine that the two cluster species were stable in the presence of each other. This work effectively illustrates the potential of bespoke boron clusters as stable materials for electrochemical cycling applications.

Introduction

The ability to reversibly shuttle electrons over a range of timescales is a ubiquitous feature found in both natural and synthetic molecules containing metals, and is essential for energy conversion and storage applications.[88–97] Energy storage systems often utilize redox active metal cations as stable salts or coordination complexes, though inherent limitations hinder the degree to which solubility and redox potential of these species can be modified.[98] Metal-free species also undergo well-defined redox processes, with several organic systems featuring highly tunable electrochemical and physical properties, though decomposition due to inherent reactivity of radical intermediates formed during single electron shuttling is a common pitfall.[99,100] To mitigate this undesired reactivity, systems have been designed to delocalize radical density throughout neighboring bonds and/or sterically protect the site of the unpaired electron, which can lead to a dramatic improvement in the electrochemical cycling of these compounds.[98,99,101]

Perfunctionalized dodecaborate clusters ($B_{12}(OR)_{12}$) are a promising new class of redox materials, which have been demonstrated to exhibit highly reversible redox activity when decorated by different substituents (Figure 13).[41,102] Many of these boron clusters are extremely robust molecules, exhibiting remarkable thermal stability (up to 500 °C with no degradation) and resistance to strong acids and bases.[21] Over a dozen $B_{12}(OR)_{12}$ clusters have been synthesized and electrochemically characterized by cyclic voltammetry (CV), exhibiting a wide range of electrochemical properties for the same redox transitions, reversibly accessible *via* sequential one-electron oxidation or reduction.[41,102] In addition, the solubility and size of functionalized boron clusters can be modified to incorporate specific properties tailored for desired applications.[59,65,102,103] Multiple tunable parameters, combined with the exceptional stability of the cluster core allows for a broad design space with several degrees of freedom. Extending beyond voltammetric studies and ex-situ evaluation of stability, this work seeks to demonstrate the viability of these boron clusters in complex electrolyte environments found in modern and emerging electrochemical systems. In this work, we demonstrate that these $B_{12}(OR)_{12}$ compounds can be electrochemically charged and discharged multiple times over 1000 hours without any apparent chemical degradation (see SI). Utilizing these attractive electrochemical properties, we have furthermore assembled a proof-of-concept redox flow battery device, where performance of this metal-free cluster system was further tested.

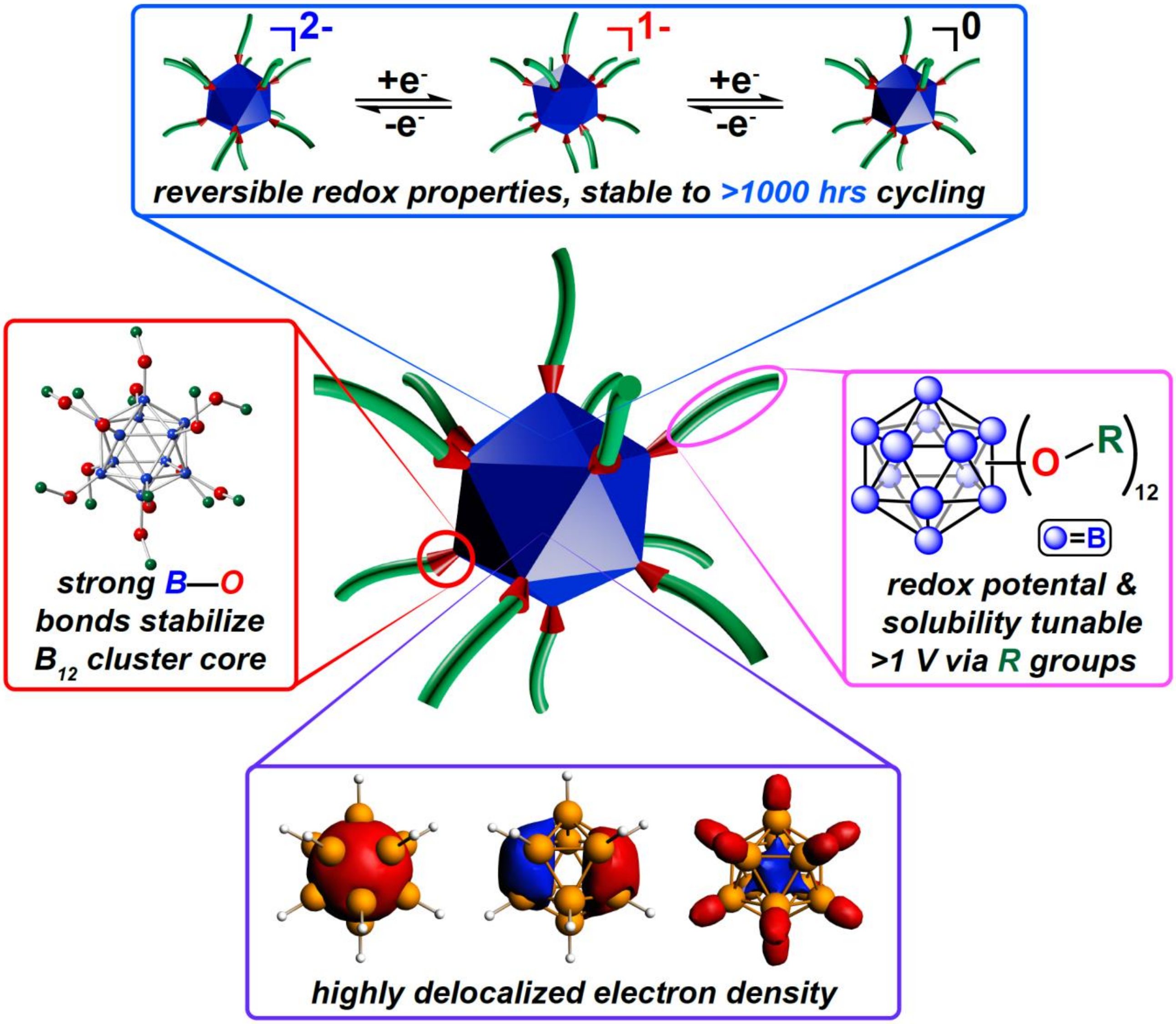
2-
+e-
-e-
1-
+e-
-e-
0
reversible redox properties, stable to >1000 hrs cycling
strong B—O bonds stabilize B_{12} cluster core
O
R
12
=B
redox potential & solubility tunable >1 V via R groups
highly delocalized electron density

Figure 13. "Anatomy of a boron cluster" illustrating reversible redox activity tunable via substituents, the robust nature of the cluster core stabilized by strong B—O bonds, and the highly delocalized electron density in 3D around the entire cage.

An improved method to synthesize $B_{12}(OR)_{12}$ clusters was recently reported, allowing full substitution of all 12 vertices of $[B_{12}(OH)_{12}]^{2-}$ with alkyl or benzyl functional groups *via* microwave-assisted synthesis.[102] Importantly, we and others have previously demonstrated that this class of molecules can undergo reversible redox reactions using cyclic voltammetry (CV) and the electrode potential at which these redox events occur can be tuned as a function of the R group.[41,102] While voltammetric analysis of these compounds can be useful for initial analysis of redox processes, during these tests the materials are only charged for short durations, with only a small fraction of the active material charged at any given time. In order to better evaluate and understand the stability of this system to electrochemical cycling associated with bulk charge storage, we decided to test these molecules further under controlled conditions that more closely mimic energy storage applications. We started by identifying two model $B_{12}(OR)_{12}$ cluster systems with high (**1**) and low (**2**) redox potentials relative to each other. The high-potential cluster **1** features 12 benzyl substituents with perfluorinated alkyl groups, which, due to their inherent inductive electron-withdrawing nature, increase redox potential for the 2-/1- redox couple.[102] For a cluster system exhibiting redox properties at lower potential, we designed **2**, which contains 12 inductively electron-donating alkyl groups with terminating OMe moieties that improve solubility in polar solvents. Both species have a solubility >0.1 M in acetonitrile.

Results and Discussion

As an initial test for benchmarking stability, cyclic voltammetry (CV) on a glassy carbon electrode was conducted to provide information about the redox potential (average of the anodic and cathodic peak potentials), chemical reversibility (peak current ratio), electrochemical reversibility / kinetics (anodic and cathodic peak potential separation), and the diffusion coefficient. All CV measurements were performed in 0.5 M tetrabutylammonium hexafluorophosphate ($TBAPF_6$) in acetonitrile (MeCN) (background scan Figure S1) with a gold counter electrode, and a fritted Ag/Ag^+ reference electrode. The reference electrode was calibrated to the ferrocene/ferrocenium (Fc/Fc^+) redox couple before every measurement taken. Figure 14 shows the cyclic voltammograms for accessing the first oxidation of **1**, the first reduction of **2**, and the mixture of the two compounds to ensure that no deleterious interactions occur.

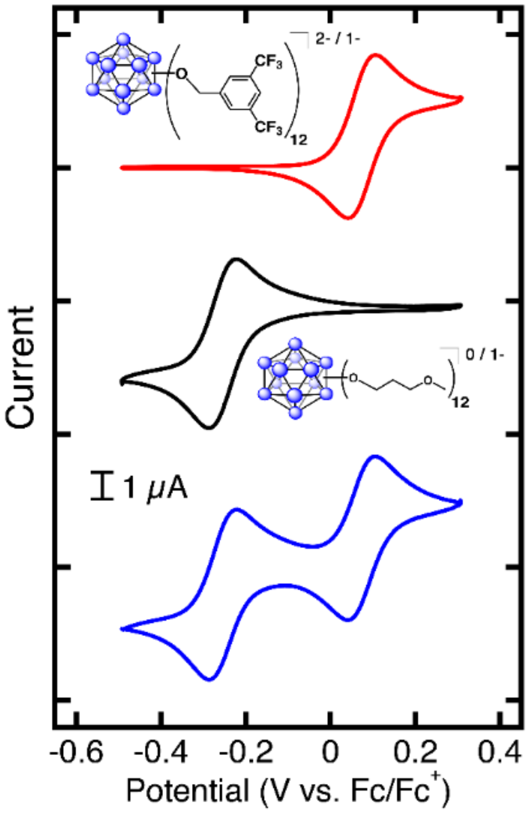

Figure 14. Cyclic voltammograms of **1**$^{2-/1-}$ (top, red), **2**$^{0/1-}$ (middle, black), and a mixture of the two clusters (bottom, blue) at 1 mM in 0.5 M $TBAPF_6$ in MeCN at a scan rate of 10 mV s^{-1}, referenced to ferrocene/ferrocenium at 0 V.

The first oxidation of **1** and the first reduction of **2** occur at 0.074 V vs. Fc/Fc^+ and -0.256 V vs. Fc/Fc^+, respectively. Both materials show excellent chemical reversibility on the CV timescale (~seconds-minutes) as evidenced by a peak current ratio close to one across all scan rates (**1**: 0.97 ± 0.01, **2**: 1.00 ± 0.02). Additionally, both redox couples show electrochemical reversibility because they both have a peak separation of 61 ± 1 mV (Nernstian is 60 mV at ambient glovebox temperature), which is invariant of scan rate. Lastly, the diffusion coefficients of the starting materials were calculated using Randles-Sevcik analysis (Figure S2) with scan rates of 10, 20, 30, 40, 50, 60, 75, and 100 mV s^{-1}, and were determined to be 3.3×10^{-6} cm^2 s^{-1}. While these

Table 2. Measured redox potentials, peak separations, peak-current ratios, and diffusion coefficients for $\mathbf{1}^{2-/1-}$ and $\mathbf{2}^{0/1-}$. All cyclic voltammetry was performed at 1 mM active material concentration. The peak separations and peak-current ratios were calculated at a scan rate of 10 mV s^{-1} in 0.5 M TBAPF$_6$ in MeCN. All measurements were performed in triplicate.

	Potential (V vs. Fc/Fc$^+$)	Peak Separation (mV)	Peak Current Ratio ($i_{p,red}/i_{p,ox}$)	Diffusion Coefficient ($\times 10^{-6}$ cm^2 s^{-1})
$\mathbf{1}^{2-}$	0.074 ± 0.001	61 ± 1	0.97 ± 0.01	3.3 ± 0.1
$\mathbf{2}^{0}$	-0.256 ± 0.001	61 ± 1	1.00 ± 0.02	3.3 ± 0.1

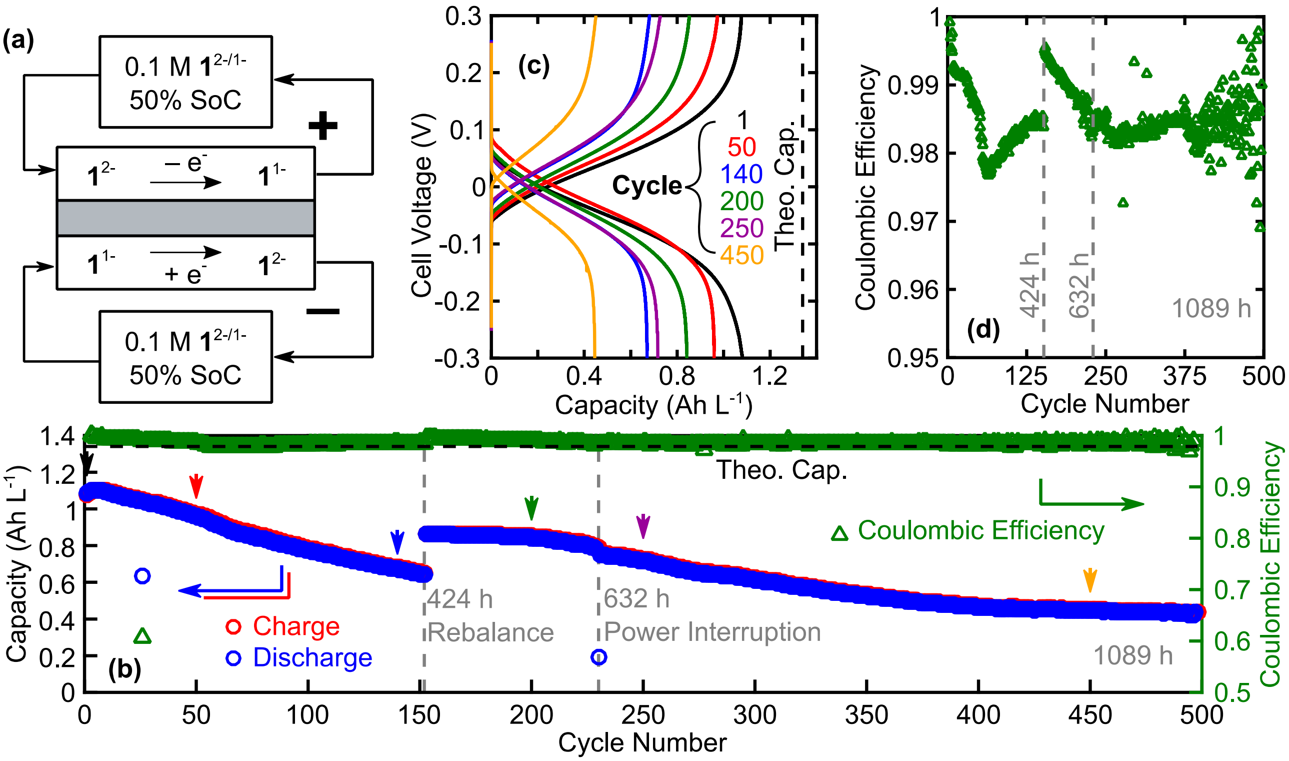

Figure 15. Symmetric flow cell cycling results. a) Symmetric flow cell setup. b) Charge and discharge capacity plotted (left) as a function of cycle number in along with coulombic efficiency (right). Arrowheads (colors match c) indicate cycles for which the voltage profile is shown in (c). c) Charge and discharge voltage profiles are shown for select cycles. d) Detailed view of coulombic efficiency as a function of cycle number. Gray dashed lines in (b) and (d) indicate interruptions of the experiment due to intentional electrolyte rebalancing (424 h) and a building power outage (632 h).

values are about an order of magnitude lower than the small organic molecules reported in similar electrolyte solutions, as expected based on the Stokes-Einstein relation (diffusivity is inversely proportionally to the molecular radius) and borate cluster size, the diffusion coefficients are still sufficiently large to support a range of electrochemical applications.[95,104] Table 2 summarizes the properties obtained from the electrochemical techniques. Clusters **1** and **2** appear to be non-interacting on the CV timescale because the voltammogram with both materials present is a superposition of the two independent scans with no changes in original peak shape, height, or position, and no new peaks appearing as a function of cycling.

The symmetric flow cell allows for cycling of both the reduced and oxidized species in the cluster redox pairs to determine the active species stability without the convoluting effects of side products generated at the counter electrode or the mass transport enforced concentration limitations which are both associated with conventional bulk electrolysis apparatus.[105–107] We ran a symmetric flow cell with **1**, and the results are shown in Figure 15. Figure 15a shows the cell setup, initial active species distribution within the reservoirs, and primary redox reactions occurring during a charging step. During a discharge step, these reactions occur in reverse. All flow cell experiments used a 2.55 cm^2 cell [96,108] with interdigitated flow fields, 2 layers of SGL 29AA carbon paper electrodes, a flowrate of 10 mL min^{-1}, and a Daramic 175 separator. Each reservoir initially contained 10 mL of 0.05 M $\mathbf{1}^{2-}$ / 0.05 M $\mathbf{1}^{1-}$ / 0.5 M $TBAPF_6$ in MeCN. Although it is generally desirable to test at higher active species concentrations (> 0.1 M), to both reduce mass transport resistance and explore more practical electrolyte formulation, given the challenges associated with materials synthesis at this scale, we sought to first demonstrate behavior a lower concentration. Consequently, we have used a low current density of 5 mA cm^{-2}, to mitigate the effect of mass transfer limitations on the accessed capacity. Detailed experimental conditions and impedance spectra are included in the SI (Figure S3). Figure 15b shows capacity and coulombic efficiency as a function of cycle number and illustrates the low fade rate due to the high level of material stability. The cell retained high (> 96%) coulombic efficiency and 40% of the initial cell capacity after 1089 h (45 days) of cycling, which exceeds the duration of many of the published nonaqueous RFB stability studies.[109–112] We suspect that some of the late-stage attributes of cell fade, specifically the decrease in accessed capacity and unstable coulombic efficiency, are due to a combination of imperfect sealing within our system and pressure driven crossover. Although compression fittings and expanded PTFE gaskets are used for sealing purposes, we inevitably lose some redox active electrolyte. A slow rate of evaporation may also bias these material losses towards volatile components, specifically the solvent, which will slowly increase the solution viscosity and can promote slow leaks (observed), via an increased system pressure, within our cell over time. Dashed gray vertical lines indicate experimental interruptions. The cycling was stopped briefly to rebalance the electrolyte reservoirs at 424 h as the reservoir levels were visibly mismatched (ca. 5 mL vs. 15 mL). A second (unintentional) interruption occurred at 632 h when the building lost power. Voltage profiles from select cycles, as indicated by arrowheads, are shown in Figure 15c, illustrating the appreciable fraction of the theoretical capacity that is repeatedly accessible for select cycles over all uninterrupted segments of the experiment. Note that at least one cycle is shown from each uninterrupted segment of the cycling protocol. The third cycle shown, cycle 200, takes place after the electrolyte rebalancing at 424 h, and the increase in capacity (30%) from cycle 140 is indicative of a crossover imbalance within our experimental setup. We attribute the limited approach to theoretical capacity (80% for cycle 1) to the mass-transfer limitations at extreme states of charge which are exacerbated by the relatively low total concentration (0.1 M). Figure 15d shows the coulombic efficiency as a function of cycle number over 498 cycles in detail. For the entire experiment the coulombic efficiency remained high (> 96%), indicating good material stability.

Given the demonstrated material stability, electrochemical activity, and design variability of perfunctionalized dodecaborate clusters, we sought to evaluate their use in a full redox flow battery (RFB). RFBs utilize flowable, redox-active electrolytes, which are pumped through an electrochemical reactor to store and release energy as redox-active components are oxidized or reduced.[113] Economic viability of RFB systems are particularly sensitive to active species material properties,[114] such as solubility and redox potential, thus, it seems appropriate for a tunable molecular framework.

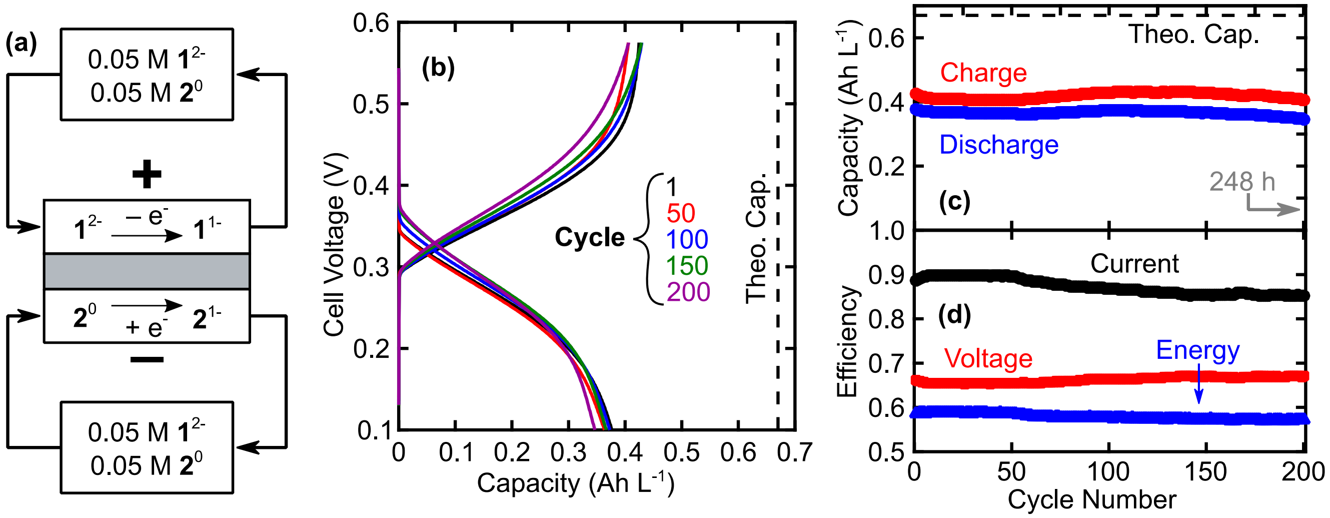

Figure 16. Full cell cycling results. a) Flow cell setup for cycling at 5 mA cm^{-2} showing premixed redox-active electrolytes. b) Voltage profiles for selected cycles. c) Capacity and d) efficiency as a function of cycle number

Figure 16 shows the full cell results where we cycle $\mathbf{2}^{0/1-}$ (low potential) vs. $\mathbf{1}^{2-/1-}$ (high potential) at 5 mA cm^{-2}. Both reservoirs initially contained 10 mL of 0.05 M $\mathbf{2}^{0}$ / 0.05 M $\mathbf{1}^{2-}$ / 0.5 M $TBAPF_6$ in MeCN. Utilizing the two materials together leads to a cell voltage of 0.33 V. Indeed, this is lower than desirable for a RFB, but full cell cycling can highlight the stability of the highly tunable borate clusters.[102] Specifically, this pairing of borate clusters was selected for this experiment based on preliminary assessment of stability, solubility, and synthesis simplicity in spite of the low average discharge voltage, 0.258 V. The cell configuration, which used pre-mixed electrolytes, similar to an Fe-Cr RFB to mitigate crossover-driven capacity fade, is shown in Figure 16a[113,115]. Detailed experimental conditions and impedance spectra are included in the SI (Figure S4). Figure 16b shows the charge and discharge profiles for cycles 1, 50, 100, 150, and 200, spanning 248 h of experiment time. Figure 16c shows the capacity as a function of cycle number, which remains relatively stable and has a mean value of 0.366 Ah L^{-1} (55% of theoretical) based on discharge. Energy, current, and voltage efficiencies are shown in Figure 16d. The low average voltage efficiency, 66%, can be largely attributed to the low cell voltage, as well as significant contributions from ohmic and mass-transfer overpotentials as we are operating at a low concentration of active species. Specifically, the voltage losses within the cell are not atypically large as compared to prior nonaqueous flow battery literature[111,116,117]; however, they constitute a larger fraction of the total cell voltage, thus significantly impacting the voltaic efficiency. The ohmic resistance, as determined through a high-frequency electrochemical impedance scan, was 3.6 Ω cm^2, and contributes 23% of the voltage losses (i.e., 8% of the average charging voltage). The combination of stable capacity along with moderate average coulombic efficiency, 87%, suggests that the cell experiences significant non-destructive, parasitic charge-transfer pathways, presumably crossover coupled to self-discharge. These system losses may be largely improved through ongoing membrane research for RFBs [104,118,119]. In particular, these clusters may in fact be large enough[103] (ca. 2-3 nm) to appreciably reduce crossover rates with size-selective separators when compared with smaller redox-active organic molecules (ca. 0.6 nm), and possibly avoid functionalized membranes, which has significant implications in terms of system cost and research timeline [119–122].

Conclusion

In conclusion, we have demonstrated the design versatility and some electrochemical properties of perfunctionalized dodecaborate clusters. This broad class of materials offers numerous material design pathways through the tailoring of the cluster decoration for improvements in solubility, redox potential, and stability. This work expands upon the repertoire of cluster-based materials amenable to electrochemical cycling,[123–128] with symmetric flow cell cycling of $\mathbf{1}^{2-/1-}$ validating the exceptional stability of this material as it is cycled between 2 oxidation states for 45 days. Full flow cell cycling illustrates stability of $\mathbf{1}^{2-/1-}$ and $\mathbf{2}^{0/1-}$ in the presence of each other and the viability of these clusters as RFB active materials. The most promising pathway for improvement of cell performance is through development of a higher voltage redox pair, which would greatly reduce the relative contributions of these losses. Although this preliminary flow cell demonstration has relatively non-competitive performance attributes, we have briefly discussed several pathways towards its improvement. Specifically, our future work will look to improve the system performance in terms of cell voltage and capacity through the modification of dodecaborate cluster functionalization and cell design characteristics, such as separator selection.

Associated Content

Supporting Information

NMR spectra, elemental analysis, and mass spectra of the dodecaborate clusters along with additional flow cell and bulk electrolysis data is provided.

Author Information

Corresponding Authors

*brushett@mit.edu

*spokoyny@chem.ucla.edu

Author Contributions

‖ A.I.W, J.L.B, and J.A.K contributed equally.

Notes

The authors declare no competing financial interests.

Acknowledgements

J. L. B., J. A. K., and F. R. B. gratefully acknowledge support from the Joint Center for Energy Storage Research, an Energy Innovation Hub funded by the U.S. Department of Energy, Office of Science, Basic Energy Sciences. J. L. B. acknowledges additional funding from the ExxonMobil-MIT Energy Fellowship (2017-2018). A. M. S. acknowledges the University of California, Los Angeles (UCLA) Department of Chemistry and Biochemistry for start-up funds, 3M for a Non-Tenured Faculty Award, the Alfred P. Sloan Foundation for a research fellowship in chemistry and the NIGMS for the Maximizing Investigators Research Award (MIRA, R35GM124746). The authors thank the MRI program of the National Science Foundation (NSF grant no. 1532232 and 1625776). We thank UCLA Molecular Instrumentation Center for mass spectrometry and NMR spectroscopy (NIH grant 1S10OD016387-01).

Supporting Information

Experimental Section

General considerations

Microwave synthesis reactions and all post-microwave work-up and characterization was performed under ambient conditions. The “ambient conditions” for this manuscript refer to room temperature (20 - 25 °C) and uncontrolled laboratory air.

Materials

Deuterated solvents were purchased from Cambridge Isotope Laboratories and used as received. MilliQ water described in this manuscript refers to purified potable water with a resistivity at 25 °C of $\leq$ 18.2 MΩ·cm. $[NEt_3H]_2[B_{12}H_{12}]$ was purchased from Boron Specialties (USA). Ethanol (200 proof) was purchased from Decon Labs and used as received. Dowex 50W X8 (100-200 mesh, hydrogen form), $FeCl_3 \cdot 6H_2O$ ($\geq$ 97%), $CsOH \cdot 1H_2O$ ($\geq$ 99.5%), $[N^nBu_4]OH$ (40% in H_2O), acetonitrile ($\geq$ 99.99%), dichloromethane ($\geq$ 99.5%), ethyl acetate ($\geq$ 99.5%), hexanes ($\geq$ 98.5%), triethylamine ($\geq$ 99%), and *N,N*-diisopropylethylamine ($\geq$ 99%) were purchased from Sigma-Aldrich. 3,5-Bis(trifluoromethyl)benzyl bromide (97%) and 1-bromo-3-methoxypropane (98%) were purchased from Oakwood. NaOH (Certified ACS, 99.2%) and hydrogen peroxide (30% in H_2O) were purchased from Fisher. For electrolyte preparation, acetonitrile (MeCN, 99.9%, Extra Dry AcroSeal®) was purchased from Acros Organics, and tetraethylammonium tetrafluoroborate (TEABF4, 99.9%) was purchased from BASF. All electrolyte solutions were prepared in an Ar-filled (Airgas, 99.999%) glovebox at room temperature in volumetric flasks. All reagents were used as received unless otherwise indicated.

Instrumentation

A Bruker AV400 spectrometer was used to obtain ^{11}B, ^{1}H, and ^{19}F NMR spectra and Bruker Topspin software was used to process the NMR data. ^{1}H NMR spectra were referenced to residual solvent resonances in deuterated solvents (δ 7.26 for $CDCl_3$). ^{11}B and ^{19}F NMR spectra were referenced to $BF_3{\cdot}Et_2O$ (δ 0.00 and δ -153.38 for ^{11}B and ^{19}F, respectively).

Mass spectrometry data was acquired using a Thermo Scientific™ Q-Exactive™ Plus instrument with a quadrupole mass filter and Orbitrap mass analyzer.

Elemental analyses were performed by Atlantic Microlab, Inc. (Norcross, GA).

Microwave synthesis

Microwave reactions were performed using a CEM Discover SP microwave synthesis reactor. Except where noted otherwise, all reactions were performed in glass microwave reactor vials purchased from the vendor. Reaction vials were sealed with silicone/PTFE caps, or using the 80 mL vessel pressure regulator accessory cap. Small (1 cm long) egg-shaped PTFE-coated stir bars were used in the vials with magnetic stirring set to high and 15 seconds of premixing prior to the temperature ramping. All microwave reactions were carried out at 140 °C with the pressure release limit set to 250 psi (no reactions exceeded this limit to trigger venting) and the maximum wattage set to 250 W (the power applied was dynamically controlled by the microwave instrument and did not exceed this limit for any reactions). Column chromatography was performed using 4 cm inner diameter glass fritted chromatography columns with 20-30 cm of slurry-packed silica gel to ensure full separation of reagents and products. Unfiltered pressurized air was used to assist column chromatography.

Synthesis of $[N^nBu_4]_2B_{12}(OH)_{12}$

Synthesis of $[N^nBu_4]_2B_{12}(OH)_{12}$ was performed starting with $Cs_2[B_{12}H_{12}]$ (ion exchanged from $[NEt_3H]_2[B_{12}H_{12}]$ using $CsOH{\cdot}1H_2O$) according to a reported procedure.[66] *Note: the hydroxylation procedure should always be undertaken with caution and careful planning to ensure the* $Cs_2[B_{12}H_{12}]$ *reagent is pure and contains no organic contaminants. Blast shielding to contain any possible explosions should be utilized. Under no circumstances should the hydrogen peroxide used in the reaction come into contact with any organic material or solvents due to possibility of an explosion.*

Synthesis of $[\mathbf{1}]^{2-}$ & $[\mathbf{1}]^{1-}$

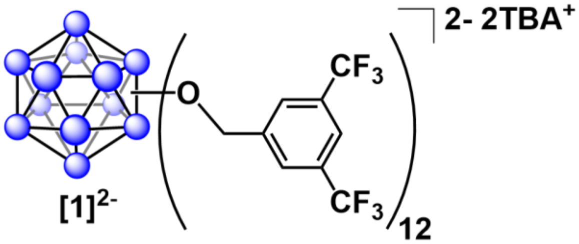

$[\mathbf{1}]^{2-}$

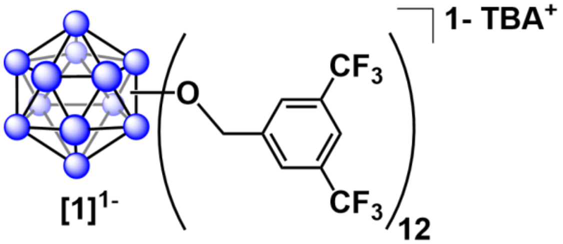

$[\mathbf{1}]^{1-}$

Clusters $[\mathbf{1}]^{2-}$ and $[\mathbf{1}]^{1-}$ were synthesized using an adapted method from a previous report.[102]

$[\mathbf{1}]^{2-}$: $[N^nBu_4]_2B_{12}(OH)_{12}$ (2.0 g, 2.4 mmol) was added to an 80 mL glass microwave vial and dissolved in 15 mL of acetonitrile. *N*,*N*-diisopropylethylamine (8.0 mL, 45.9 mmol) and 3,5-bis(trifluoromethyl)benzyl bromide (8.0 mL, 43.6 mmol) were added along with a stir bar, the vial was sealed with an 80 mL vessel pressure regulator accessory cap, and the mixture was heated at 140 °C with stirring in the microwave for 1.5 hours. The excess acetonitrile was evaporated by rotary evaporation in a round bottom flask, and the residue was loaded onto a slurry-packed silica gel column (pre-flushed with 30 mL triethylamine dissolved in 140 mL 35/65 [v/v] ethyl acetate/hexane) using 35/65 [v/v] ethyl acetate/hexane and ~3-4 mL acetone (to rinse the sides of the round bottom flask). The remaining 3,5-bis(trifluoromethyl)benzyl bromide reagent was eluted through the silica column using 35/65 [v/v] ethyl acetate/hexane, followed by acetone to elute the light-yellow product band (near solvent front). The acetone was removed by rotary evaporation and transferred to a 20 mL glass vial, and the oily substance was dried under high vacuum at 60 °C for 2 hours to obtain 8.04 g (93.6%) of pure, isolated product. Compound [**1**]$^{2-}$ is a very light yellow solid ^{1}H NMR (400 MHz, $CDCl_3$): δ 7.73 (br s, 24H, *ortho*-$C_6\underline{H_3}$), 7.50 (br s, 12H, *para*-C_6H_3), 5.55 (br s, O-$C\underline{H_2}$), 3.06 – 2.96 (m, 16H, N-$C\underline{H_2}$), 1.60 – 1.47 (m, 16H, N-$CH_2C\underline{H_2}$), 1.41 – 1.27 (m, 16H, N-$(CH_2)_2C\underline{H_2}$), 0.94 (t, 24H, N-$(CH_2)_3C\underline{H_3}$). $^{11}B\{^{1}H\}$ NMR (128 MHz, $CDCl_3$): δ -15.43 (br s, 12B). ^{19}F NMR (376 MHz, $CDCl_3$): δ -63.50 (s, 72F). HRMS (Orbitrap): *m/z* calculated for $C_{108}H_{60}B_{12}F_{72}O_{12}$ (M^{2-}), 1523.7079 Da; found, 1523.7042 (z=2) Da. Calc. for $C_{140}H_{132}B_{12}F_{72}N_2O_{12}$: C, 47.61; H, 3.77. Found: C, 47.17; H, 3.76.

[**1**]$^{1-}$: $[N^{n}Bu_4]_2B_{12}(OH)_{12}$ (2.0 g, 2.4 mmol) was added to an 80 mL glass microwave vial and dissolved in 15 mL of acetonitrile. *N*,*N*-diisopropylethylamine (8.0 mL, 45.9 mmol) and 3,5-bis(trifluoromethyl)benzyl bromide (8.0 mL, 43.6 mmol) were added along with a stir bar, the vial was sealed with an 80 mL vessel pressure regulator accessory cap, and the mixture was heated at 140 °C with stirring in the microwave for 1.5 hours. The excess acetonitrile was evaporated by rotary evaporation in a round bottom flask, and the residue was loaded onto a slurry-packed silica gel column using 35/65 [v/v] ethyl acetate/hexane and ~1-2 mL acetonitrile (to rinse the sides of the round bottom flask). The remaining 3,5-bis(trifluoromethyl)benzyl bromide reagent was eluted through the silica column using 35/65 [v/v] ethyl acetate/hexane, followed by acetone to elute the slightly pink/light-yellow product band (near solvent front). The acetone was removed by rotary evaporation and the residue was dissolved in 21 mL 9:1 [v/v] ethanol/acetonitrile, 1.67 g $FeCl_3{\cdot}6H_2O$ was added, and the mixture was left to stir at room temperature overnight. The volatiles were removed *via* rotary evaporation, and the residue was dissolved in dichloromethane

and filtered through a 1 cm thick silica plug in a wide glass fritted funnel (8.5 cm inner diameter) to remove most of the iron. The filtrate was concentrated *via* rotary evaporation, then eluted through a silica gel column with dichloromethane, collecting the purple band containing the product. The dichloromethane was removed *via* rotary evaporation, and the solids were transferred to a 20 mL glass vial and dried under high vacuum overnight to obtain 5.80 g (72.5%) of pure, isolated product. Compound [**1**]$^{1-}$ is a red-purple solid. ^{1}H NMR (400 MHz, $CDCl_3$): δ 8.45 – 7.41 (br m, 36H, $C_6\underline{H_3}$), 3.19 – 3.07 (m, 8H, N-C$\underline{H_2}$), 1.72 – 1.63 (m, 8H, N-$CH_2C\underline{H_2}$), 1.53 – 1.42 (m, 8H, N-$(CH_2)_2C\underline{H_2}$), 1.05 (t, 12H, N-$(CH_2)_3C\underline{H_3}$). *Note: The CH_2 signal for the cluster is masked and all other peaks are quite broad due to the paramagnetic radical state of the molecule.* No resonances are visible by ^{11}B NMR, due to paramagnetic broadening. ^{19}F NMR (376 MHz, $CDCl_3$): δ -63.45 (s, 72F). HRMS (Orbitrap): *m/z* calculated for $C_{108}H_{60}B_{12}F_{72}O_{12}$ (M^{2-}), 1523.7079 Da; found, 1523.7059 (z = 2) Da. Calc. for $C_{124}H_{96}B_{12}F_{72}NO_{12}$: C, 45.27; H, 2.94. Found: C, 45.26; H, 3.06.

Synthesis of [2]^0

$[N^nBu_4]_2B_{12}(OH)_{12}$ (0.5 g, 0.61 mmol) was added to an 35 mL glass microwave vial and dissolved in 10 mL of acetonitrile. *N*,*N*-diisopropylethylamine (2.0 mL, 11.5 mmol) and 1-bromo-3-methoxypropane (8.2 mL, 73.4 mmol) were added along with a stir bar, the vial was sealed with a silicone/PTFE cap, and the mixture was heated at 140 °C with stirring in the microwave for 2 hours. The excess acetonitrile was evaporated by rotary evaporation in a round bottom flask, and the residue was loaded onto a slurry-packed silica gel column using 35/65 [v/v] ethyl acetate/hexane. The remaining 1-bromo-3-methoxypropane reagent was eluted through the silica column using 35/65 [v/v] ethyl acetate/hexane, followed by 3:1 [v/v] hexane/acetone to elute the product, initially a pink band which turns orange as it oxidizes along the length of the column.

After elution of the orange neutral product band, the remaining pink 1-/2- cluster was eluted with acetone. For the pink fraction, the acetone was removed by rotary evaporation and eluted through a second slurry-packed silica gel column using the same 3:1 [v/v] hexane/acetone solution. The orange product was collected and combined with the first orange fraction, the acetone was removed by rotary evaporation, the product was transferred to a 20 mL glass vial, and the oily substance was dried under high vacuum overnight to obtain 231 mg (31.5%) of pure, isolated product. Compound [**2**]^0 is a dark brown oil. ^{1}H NMR (400 MHz, $CDCl_3$): δ 4.10 (t, 24H, B-O-C$\underline{H_2}$), 3.44 (t, 24H, C$\underline{H_2}$-OCH_3), 3.31 (s, 36H, CH_2-OC$\underline{H_3}$), 1.83 (quin, 24H, O-CH_2-C$\underline{H_2}$-CH_2-O). ^{11}B{^{1}H} NMR (128 MHz, $CDCl_3$): δ 41.60 (br s, 12B). HRMS (Orbitrap): *m/z* calculated for $C_{48}H_{108}B_{12}O_{24}$ (M^-), 1198.8420 Da; found, 1198.8425 Da. Calc. for $C_{48}H_{108}B_{12}O_{24}$: C, 48.08; H, 9.08. Found: C, 48.65; H, 9.19.

Cyclic Voltammetry and Randles-Sevcik Analysis

All preparation and cyclic voltammetry (CV) measurements were performed in an argon-filled glovebox (MBraun Labsaster, O_2 < 1 ppm, H_2O < 5 ppm) at ca. 26 °C. The electrolyte used was 0.5 M $TBAPF_6$ in MeCN (**figure S1**). Solutions were prepared in a volumetric flask in order to account for the volume change from the high concentration of supporting salt. CV was performed in a 3-electrode cell with a 3 mm diameter glassy carbon disk working electrode (CH Instruments), a gold coil counter electrode (CH Instruments), and a fritted Ag/Ag+ reference electrode (fill solution: 0.05 M $AgBF_4$, 0.5 M $TEAPF_6$, propylene carbonate). Before every CV, the working electrode was polished on a MicroCloth pad with an aqueous slurry of 0.05 μm alumina powder (Buehler Ltd.), rinsed with deionized water (Millipore), and dried with lens paper (VWR). In order to reference to ferrocene, before every CV measurement, an additional CV was taken in the electrolyte with ferrocene as the active material. All CV data was collected on a VSP-300 potentiostat (Bio-Logic), and a 100% automated *i*R compensation was applied. The average resistance measured was about 20 Ω, leading to a total voltage compensation of about 0.3 mV for the highest currents. CV measurements were taken at scan rates of 10, 20, 30, 40, 50, 75, and 100 mV s^{-1} and were used to calculate the redox potential, peak separation, peak current ratio, and diffusion coefficient. The redox potential was calculated by taking the average of the potentials corresponding to the anodic and cathodic peak currents, while the peak separation was calculated by taking the difference between these two potentials. The peak current ratio was calculated by taking the ratio of the background corrected peak current for the anodic and cathodic peak.

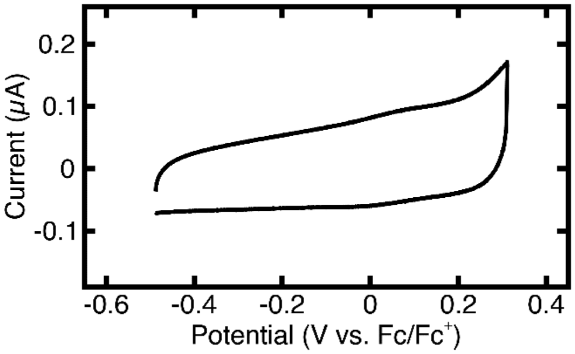

Figure S1. Background cyclic voltammograms of 0.5 M $TBAPF_6$ in MeCN taken at a scan rate of 10 mV s^{-1}.

In order to calculate the diffusion coefficient, the Randles-Sevcik relationship (**figure S2**) was used for all of the scan rates:

$$i_p = 0.4463nFAC\left(\frac{nFD}{RT}\nu\right)^{0.5}$$

where i_p is the peak current (A), n is the number of electrons transferred ($n = 1$), F is Faraday's constant (96485 C (mol $e^-)^{-1}$), A is the electrode area (0.0707 cm^2), C is the bulk concentration (1 × 10^{-6} mol/cm^3), R is the universal gas constant (8.314 J mol^{-1} K^{-1}), T is the temperature (299.15

K), D is the diffusion coefficient (cm^2 s^{-1}) and v is the scan rate (V s^{-1}). Again the peak current was determined from the peak current from the voltammograms and subtracting an extrapolated background current.

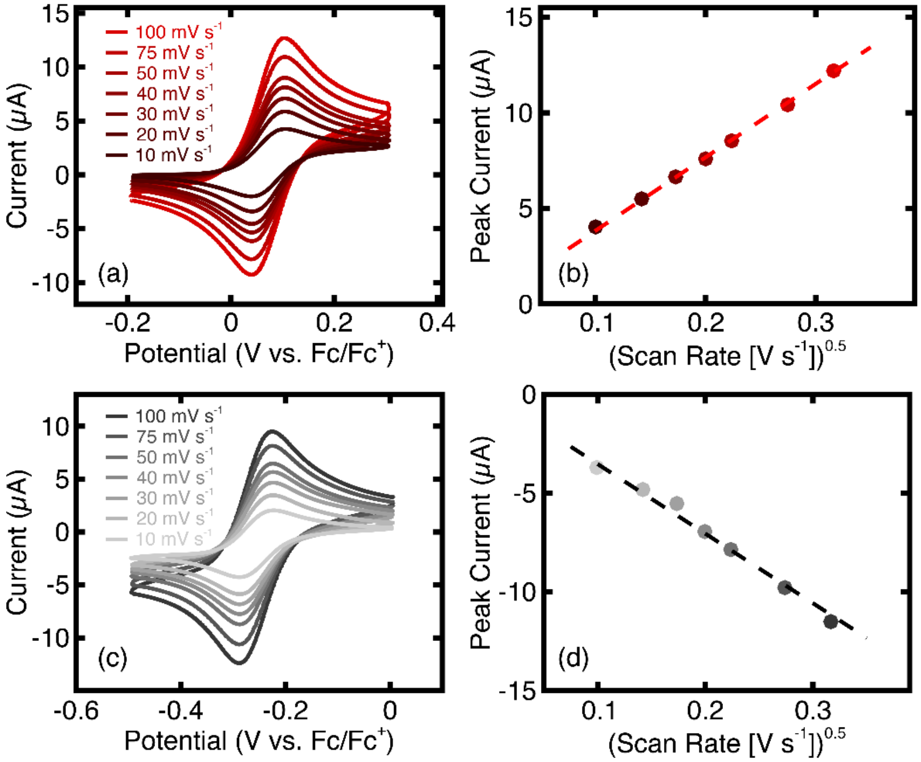

Figure S2. Cyclic voltammograms as a function of scan rate for **1** (a) and **2** (c), and the corresponding Randles-Sevcik peak-current analysis for **1** (b) and **2** (d). All of the experiments were conducted with 1 mM active material in 0.5 M TBAPF$_6$ in MeCN.

Flow Battery Methods and Discussion

Flow cell measurements employed a research-scale, 2.55 cm^2 flow cell described in past work[95,129]. Flow fields were machined from impermeable graphite (Tokai G347B, MWI, Inc.) in-house and the engineering drawings are published in past work[96]. Sigracet® SGL 29AA carbon paper electrodes (190 ± 30 μm) were purchased from the Fuel Cell Store and used as received. Both the symmetric and full cells were tested with a flowrate of 10 mL/min, a Daramic 175 porous separator, 2 layers of Gore® expanded polytetrafluoroethylene (ca. 250 μm thick) gaskets, and 2 layers of carbon paper per side. A Cole-Parmer Masterflex® pump drive with an Easy-Load® II pump head was used to control the flowrate. Perfluoroalkoxy reservoirs (10 mL) were purchased from Savillex, and the volumetric capacities presented within this work only accounted for the total volume of electrolyte within the system (20 mL). For the symmetric flow cell, each 10 mL reservoir contained 0.05 M $\mathbf{1}^{1-}$ / 0.05 M $\mathbf{1}^{2-}$ / 0.5 M $TBAPF_6$ in MeCN initially. For the full cell, each 10 mL reservoir contained of 0.05 M $\mathbf{2}^{0}$ / 0.05 M $\mathbf{1}^{2-}$ / 0.5 M $TBAPF_6$ in MeCN. Premixing was employed to mitigate confounding effects of rapid crossover due to the use of Daramic 175, a nonselective porous separator.

All flow cell experiments were controlled with a Bio-Logic VMP3 potentiostat. After setting up the initial cell and turning the pump on, the cell was allowed to sit for 30 min prior to electrochemical measurements. We then cell was then subjected to electrochemical impedance spectroscopy (EIS), followed by galvanostatic cycling with potential limitations (GCPL). EIS measurements were taken with frequencies ranging from 200 kHz to 10 mHz with 6 points per decade, 5 measures per frequency, and an absolute (sine) amplitude of 10 mV. The EIS is shown in **figures S3** and **S4** for the symmetric and full cell, respectively. GCPL was performed at 5 mA cm^{-2}, without any constant potential holds. Voltage limitations were set as -0.3 V – 0.3 V and 0.10 V – 0.58 V for the symmetric and full cells respectively.

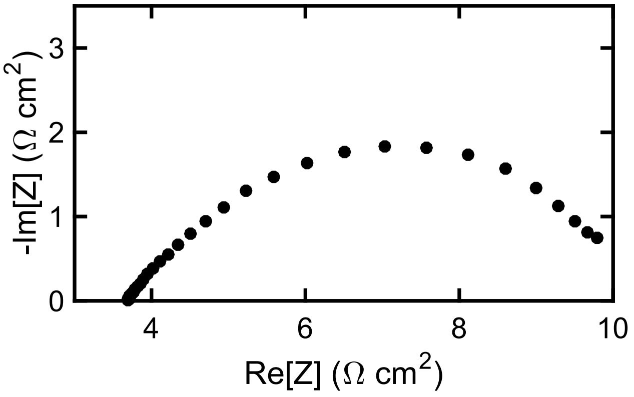

Figure S3. Symmetric cell EIS at 50% state-of-charge.

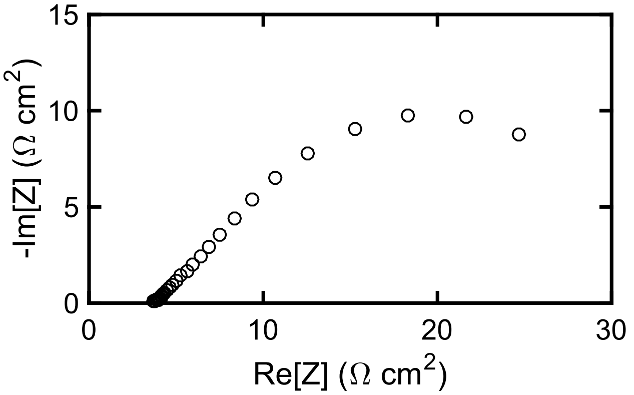

Figure S4. Full cell EIS at 0% state-of-charge.

Post-Flow Cell Analysis of [1]$^{2-}$ & [1]$^{1-}$

After the symmetric flow cell cycling of [**1**]$^{2-}$ & [**1**]$^{1-}$, the solution containing the two materials and the electrolyte (TBA-PF$_6$) was recollected and the solvent was removed *via* rotary evaporation. The mixture was analyzed by ^{11}B{^{1}H}, ^{19}F, and ^{1}H NMR spectroscopy for evidence of any chemical degradation (easily identified by the presence of any borate decomposition products with characteristic resonances around δ 20.0 or 0.0 in the ^{11}B{^{1}H} NMR). There were no decomposition products visible in any of the NMR spectra, only resonances matching both the 2-

and 1- oxidation states of [**1**] along with the presence of TBA-PF_6. The only non-cluster signal visible in the $^{11}B\{^1H\}$ NMR integrates to below 0.1%, indicating no chemical decomposition of the boron cage.

Chapter 5: Conclusions

In conclusion, new methods were developed to rapidly synthesize perfunctionalized dodecaborate clusters, thus enabling fine control of desired redox potential and other photophysical properties for novel cluster species. A new microwave-based method for synthesizing perfunctionalized $B_{12}(OR)_{12}$ dodecaborate clusters under ambient conditions was demonstrated. This method significantly reduced reaction times compared to previously reported protocols while completely eliminating the need for handling reactions in inert atmosphere. This method enabled rapid synthesis of 20+ known and novel cluster derivatives, including multiple $B_{12}(OR)_{12}$ species featuring higher redox potentials than any reported clusters of this type. The robust nature of the microwave-assisted synthesis method also allowed the formation of hybrid vertex-differentiated $B_{12}(OR)_{11}(OR^{'})$ clusters *via* a one-pot, single-step reaction, previously inaccessible except through lengthy multi-step protocols. A new class of vertex-differentiated $B_{12}(OR)_{11}(NO_2)$ clusters was also developed using the same microwave-based methods, which exhibited redox properties ~ 0.5 V higher than their $B_{12}(OR)_{12}$ analogues, further extending the tunable redox window for perfunctionalized boron clusters. Lastly, the extreme electrochemical stability of these clusters was demonstrated by bulk cycling in a flow cell apparatus. $B_{12}(OR)_{12}$ clusters in symmetric flow cell exhibited no decomposition even after 1000+ hours and ~500 cycles, and a prototype all-boron cluster flow battery device exhibited stable cycling for more than a week. In summary, the new methods developed allow targeted rapid synthesis of boron clusters with specific photophysical and redox properties, enabling significantly accelerated investigation of new research directions.

Appendices (Supplemental Spectra & Data)

Supplemental spectra & data for Chapter 2

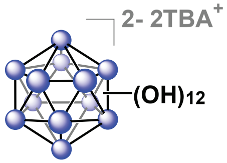

$^{11}B\ \{^{1}H\}$ NMR

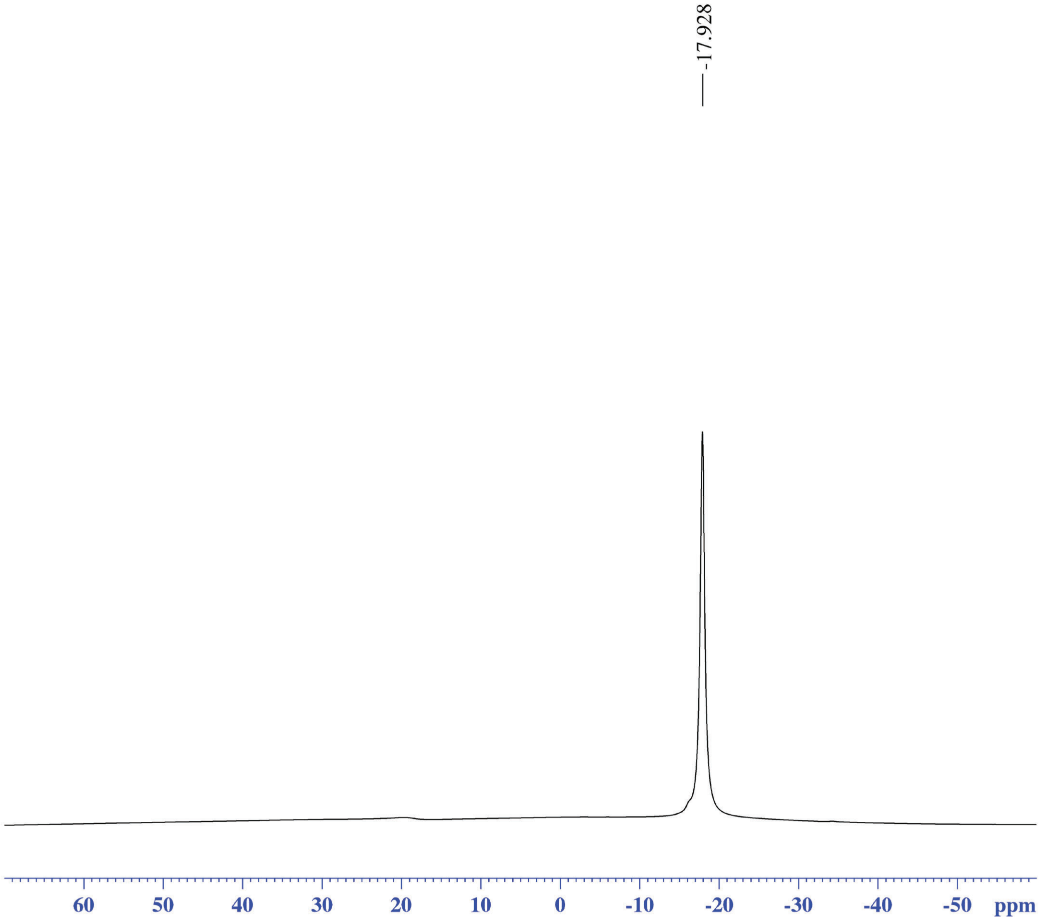

```
Current Data Parameters
NAME     Apr27-2015-spokoyny
EXPNO              31
PROCNO              1

F2 - Acquisition Parameters
Date_        20150427
Time            17.32
INSTRUM         av400
PROBHD   5 mm PABBO BB/
PULPROG       zgdc.js
TD               5096
SOLVENT           D2O
NS               1024
DS                  0
SWH        51020.406 Hz
FIDRES     10.011854 Hz
AQ         0.0499408 sec
RG             189.85
DW              9.800 usec
DE               6.50 usec
TE              300.0 K
D1         0.00000400 sec
D11        0.03000000 sec
TD0                 1

======== CHANNEL f1 ========
SFO1      128.3776052 MHz
NUC1             11B
P1             10.00 usec
PLW1     52.00000000 W

======== CHANNEL f2 ========
SFO2      400.1324008 MHz
NUC2              1H
CPDPRG[2       waltz16
PCPD2          90.00 usec
PLW2     13.00000000 W
PLW12     0.36111000 W

F2 - Processing parameters
SI             32768
SF        128.3776050 MHz
WDW               EM
SSB     0
LB             50.00 Hz
GB      0
PC              1.40
```

^{1}H NMR

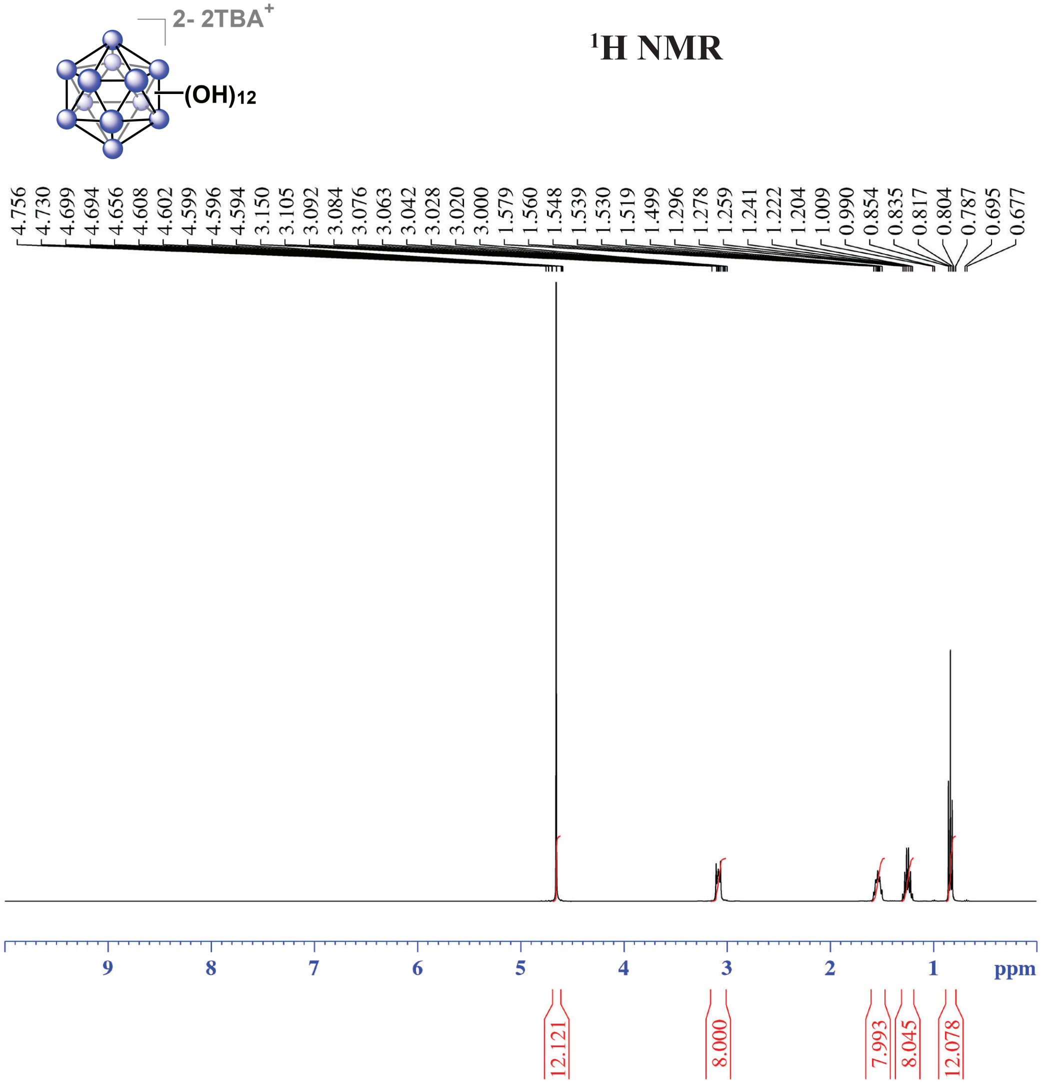

```
Current Data Parameters
NAME     Apr27-2015-spokoyny
EXPNO              30
PROCNO              1

F2 - Acquisition Parameters
Date_        20150427
Time            17.29
INSTRUM         av400
PROBHD   5 mm PABBO BB/
PULPROG          zg30
TD              52882
SOLVENT           D2O
NS                  8
DS                  0
SWH          8012.820 Hz
FIDRES       0.151523 Hz
AQ          3.2998369 sec
RG             155.85
DW             62.400 usec
DE               6.50 usec
TE              299.7 K
D1         2.00000000 sec
TD0                 1

======== CHANNEL f1 ========
SFO1      400.1324008 MHz
NUC1               1H
P1              15.00 usec
PLW1      13.00000000 W

F2 - Processing parameters
SI              65536
SF        400.1300184 MHz
WDW                EM
SSB     0
LB               0.30 Hz
GB      0
PC               1.00
```

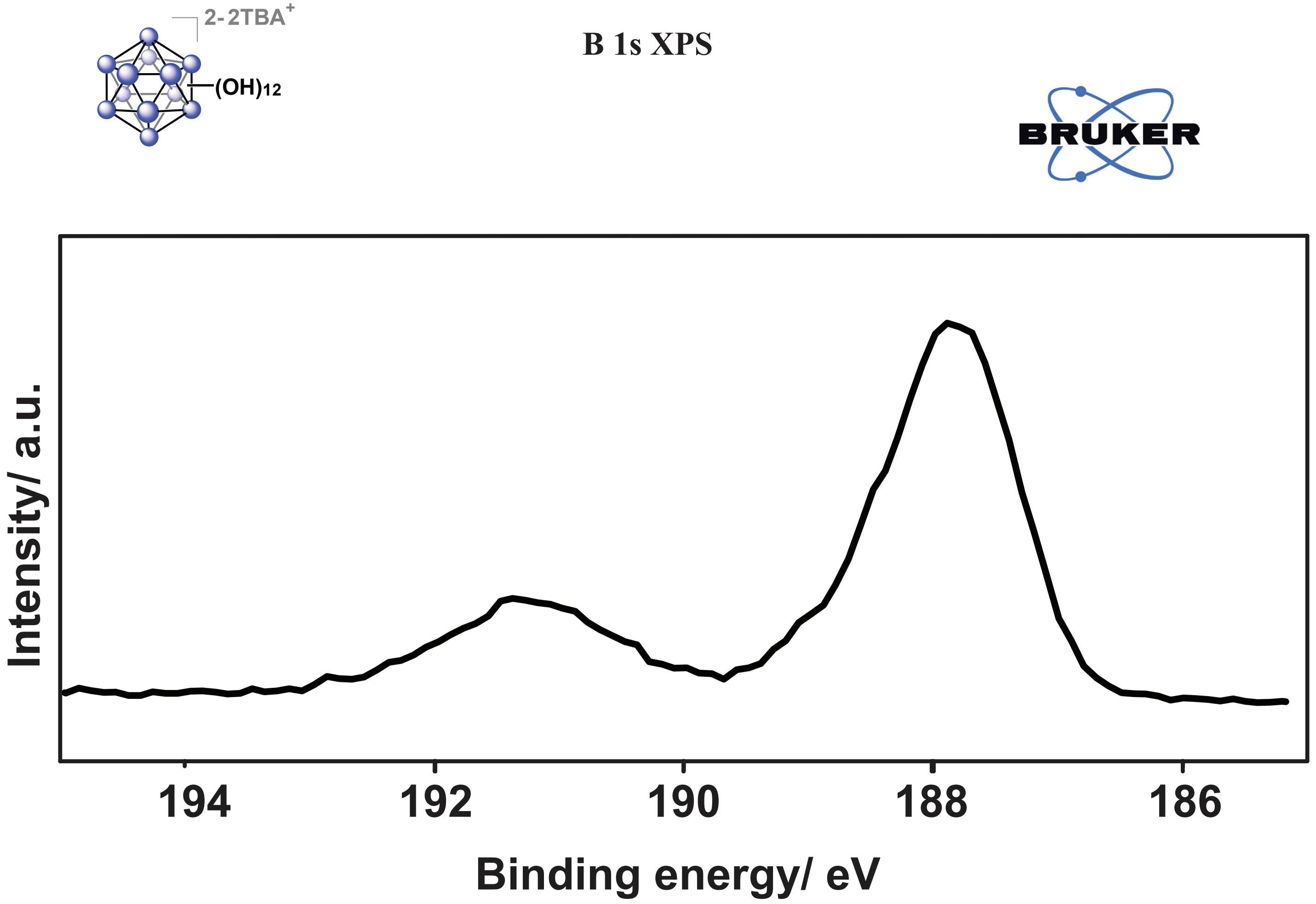2-2TBA+
(OH)12
B 1s XPS
BRUKER
Intensity/ a.u.
194
192
190
188
186
Binding energy/ eV

^{11}B {^{1}H} NMR

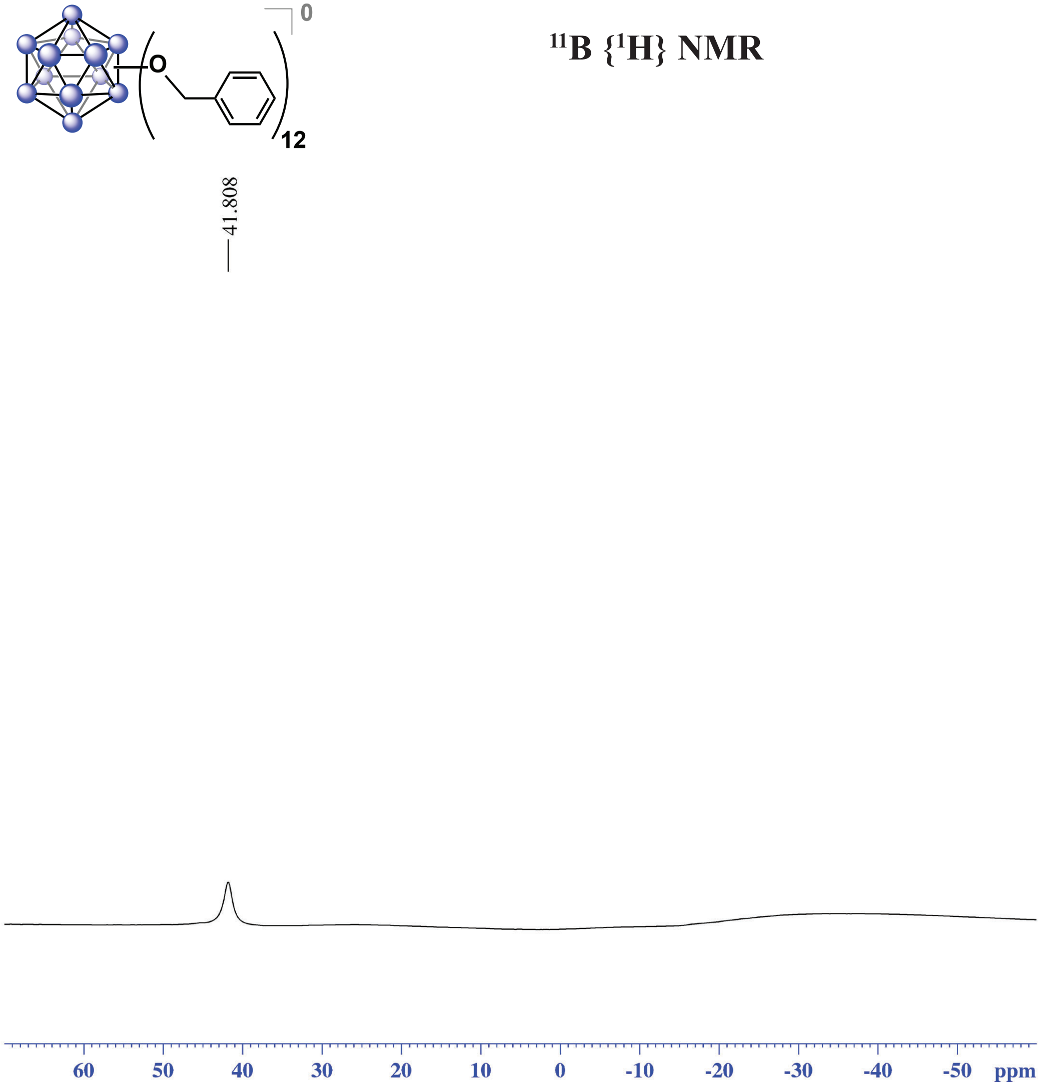

Current Data Parameters
NAME B12(O-Bn)12
EXPNO 40
PROCNO 1

F2 - Acquisition Parameters
Date_ 20150410
Time 16.58
INSTRUM av400
PROBHD 5 mm PABBO BB/
PULPROG zgdc.js
TD 5096
SOLVENT CDCl3
NS 1024
DS 0
SWH 51020.406 Hz
FIDRES 10.011854 Hz
AQ 0.0499408 sec
RG 189.85
DW 9.800 usec
DE 6.50 usec
TE 299.1 K
D1 0.00000400 sec
D11 0.03000000 sec
TD0 1

======== CHANNEL f1 ========
SFO1 128.3776052 MHz
NUC1 11B
P1 10.00 usec
PLW1 52.00000000 W

======== CHANNEL f2 ========
SFO2 400.1324008 MHz
NUC2 1H
CPDPRG[2 waltz16
PCPD2 90.00 usec
PLW2 13.00000000 W
PLW12 0.36111000 W

F2 - Processing parameters
SI 32768
SF 128.3776050 MHz
WDW EM
SSB 0
LB 50.00 Hz
GB 0
PC 1.40

^{13}C NMR

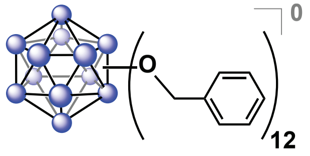

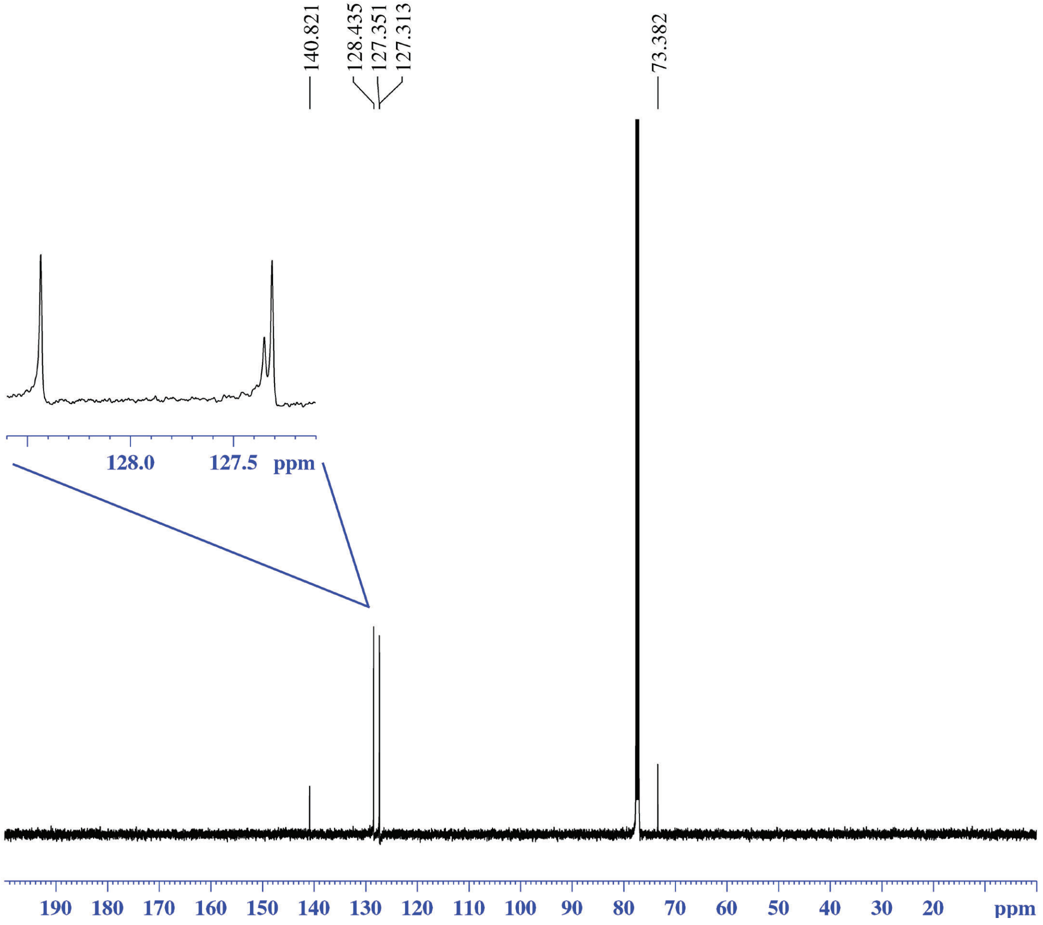

```
Current Data Parameters
NAME        B12(O-Bn)12
EXPNO              100
PROCNO               1

F2 - Acquisition Parameters
Date_        20150407
Time             0.07
INSTRUM          av500
PROBHD   5 mm DCH 13C-1
PULPROG        zgpg30
TD             65536
SOLVENT      CH3OH+D2O
NS                64
DS                 2
SWH         31250.000 Hz
FIDRES       0.476837 Hz
AQ          1.0485760 sec
RG             204.54
DW             16.000 usec
DE              18.00 usec
TE              298.0 K
D1         2.00000000 sec
D11        0.03000000 sec
TD0                 1

======== CHANNEL f1 ========
SFO1       125.7722511 MHz
NUC1              13C
P1               9.63 usec
PLW1      23.00000000 W

======== CHANNEL f2 ========
SFO2       500.1330008 MHz
NUC2               1H
CPDPRG[2        waltz16
PCPD2           80.00 usec
PLW2      13.50000000 W
PLW12      0.21094000 W
PLW13      0.13500001 W

F2 - Processing parameters
SI             131072
SF        125.7574315 MHz
WDW                EM
SSB     0
LB               1.00 Hz
GB      0
PC               1.40
```

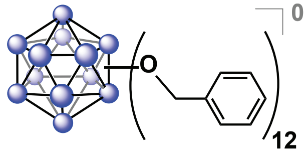

^{1}H NMR

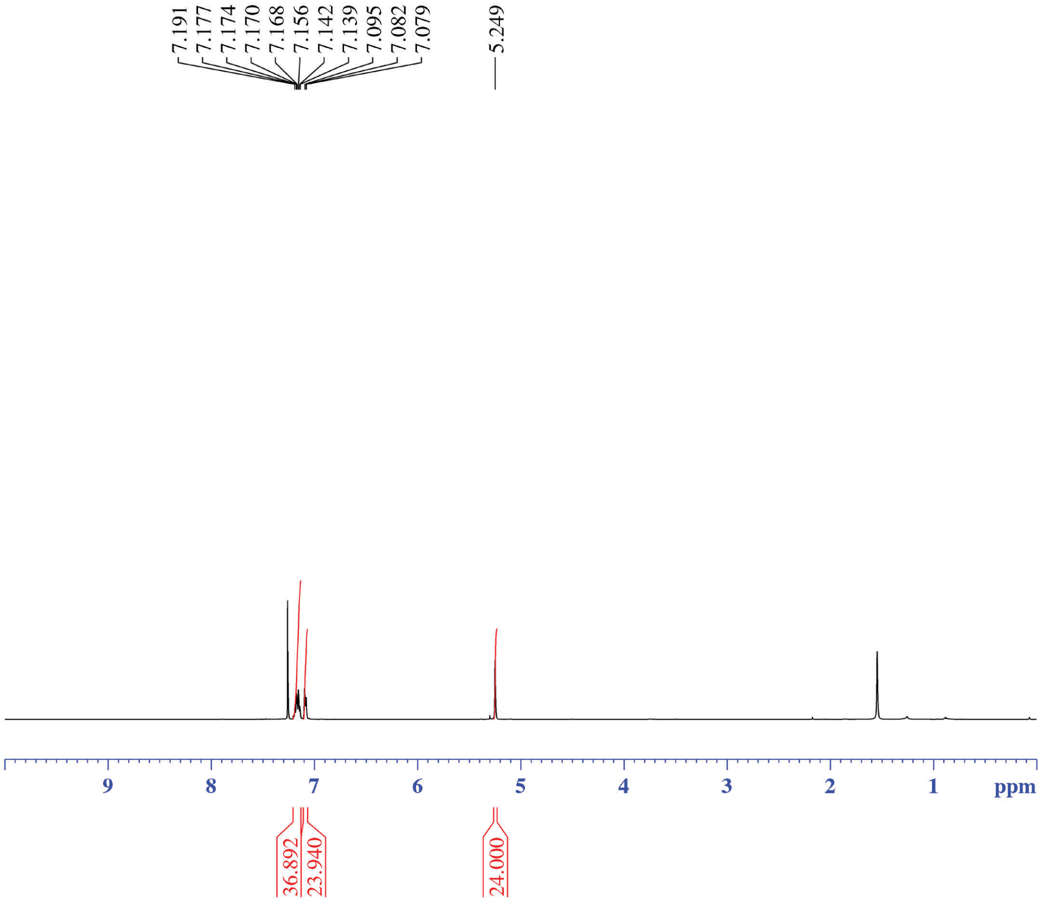

Current Data Parameters
NAME B12(O-Bn)12
EXPNO 101
PROCNO 1

F2 - Acquisition Parameters
Date_ 20150407
Time 0.09
INSTRUM av500
PROBHD 5 mm DCH 13C-1
PULPROG zg30
TD 65536
SOLVENT CH3OH+D2O
NS 8
DS 0
SWH 10000.000 Hz
FIDRES 0.152588 Hz
AQ 3.2767999 sec
RG 63.27
DW 50.000 usec
DE 10.00 usec
TE 298.0 K
D1 2.00000000 sec
TD0 1

======== CHANNEL f1 ========
SFO1 500.1330008 MHz
NUC1 1H
P1 10.00 usec
PLW1 13.50000000 W

F2 - Processing parameters
SI 65536
SF 500.1287429 MHz
WDW EM
SSB 0
LB 0.30 Hz
GB 0
PC 1.00

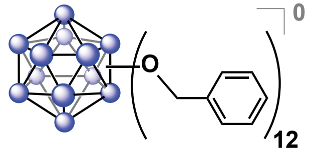

Q Exactive
High-Res Mass Spec

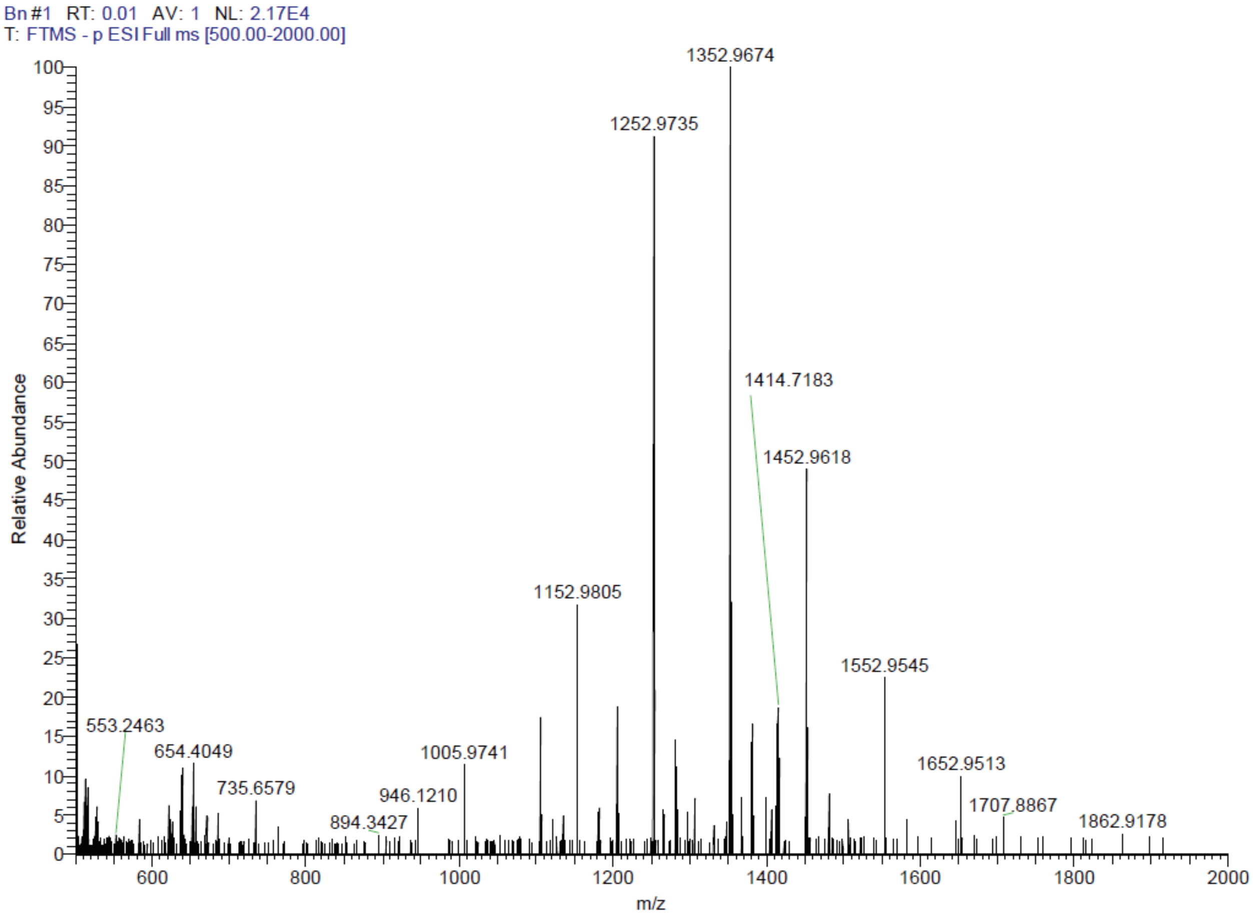

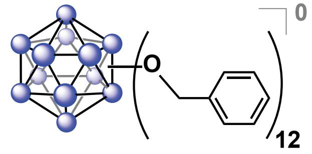

Q Exactive
High-Res Mass Spec

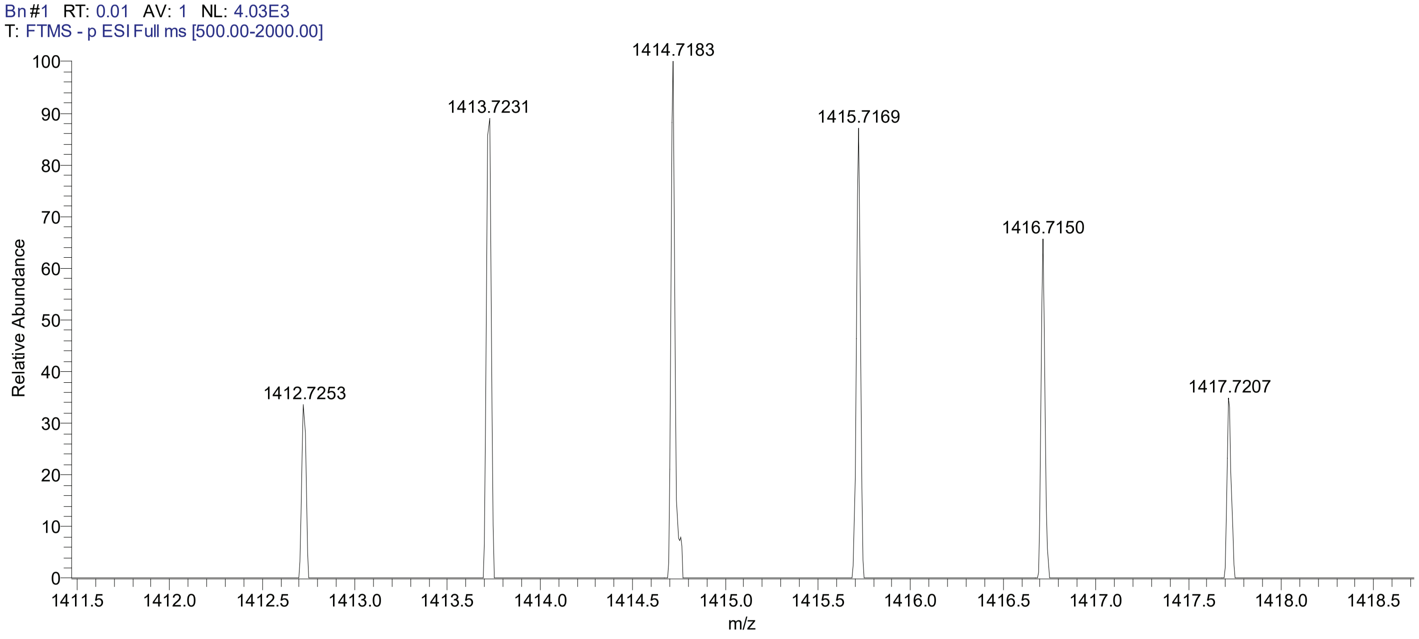

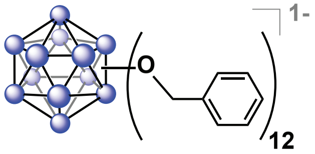

EPR

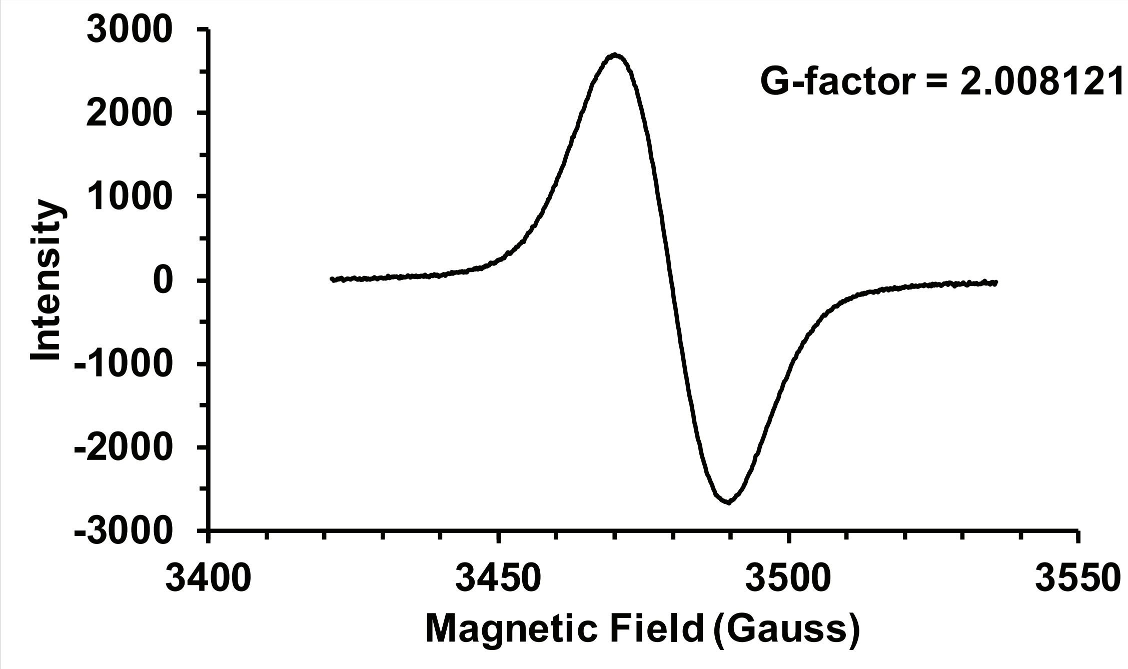

DOS	Format
ANZ	1024
MIN	-2666.883789
MAX	2704.116211
JSS	0
GST	3421.274884
GSI	114.543004
JUN	G
JON	Bruker BioSpin GmbH
JDA	11/9/2015
JTM	14:44
JRE	c:\programfiles\bruker-emx\syscal\st0103.cal
JEX	field-sweep
JSD	1
HCF	3478.546386
HSW	114.543004
EMF	0
RCT	20.48
RTC	20.48
RRG	8.93E+03
RMA	4
MF	9.776766
MP	6.38E-01
MPD	25

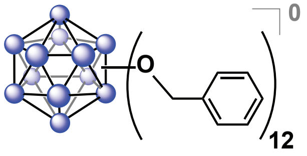

B 1s XPS

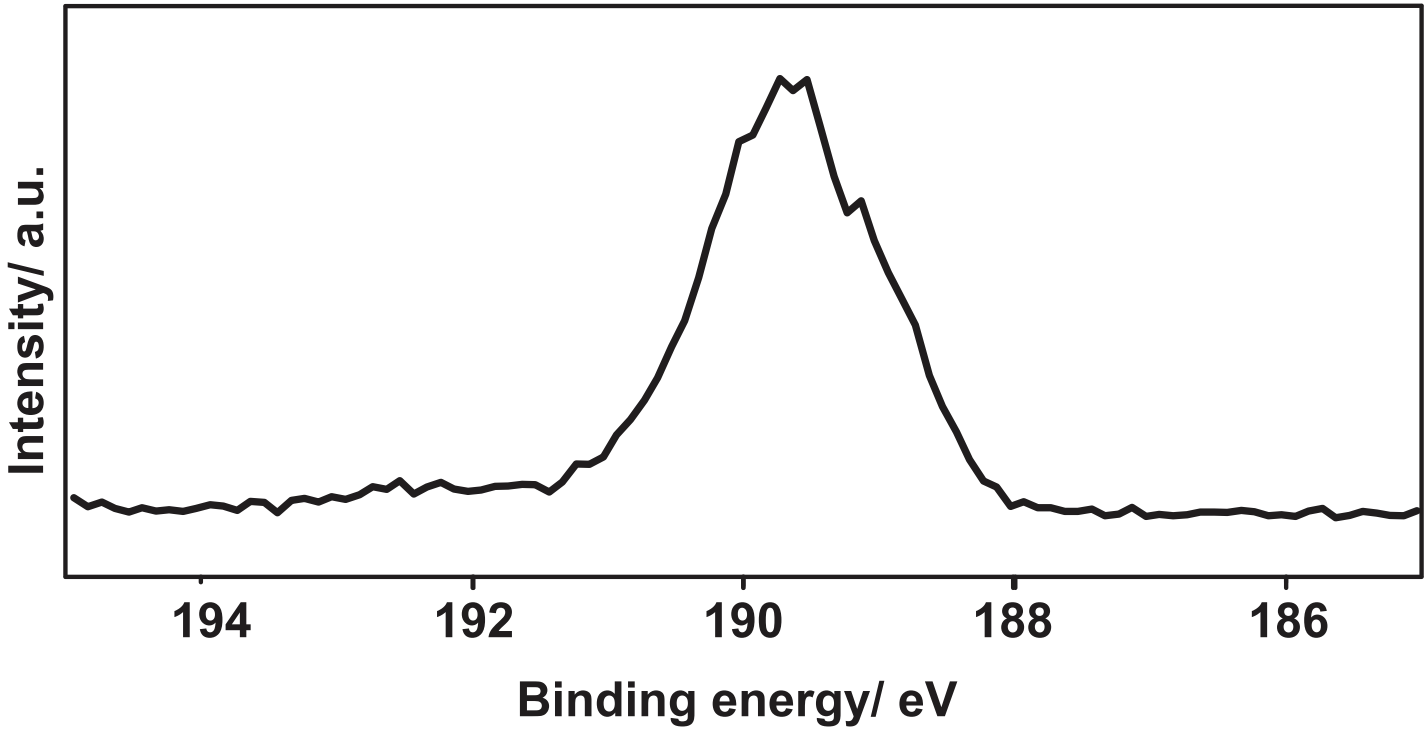

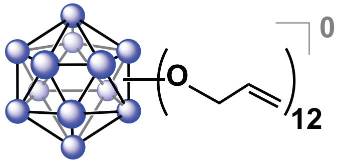

$^{11}B\ \{^{1}H\}$ NMR

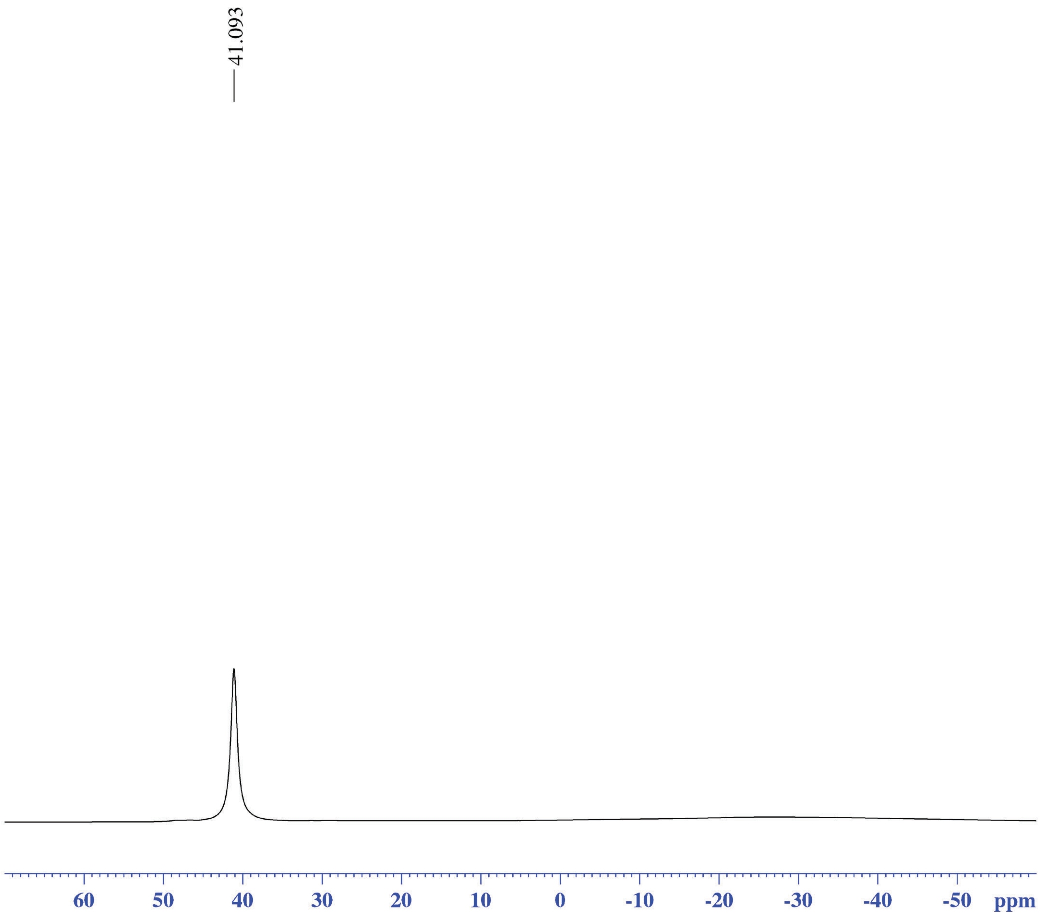

```
Current Data Parameters
NAME     B12(O-Allyl)12
EXPNO              130
PROCNO               1

F2 - Acquisition Parameters
Date_         20150221
Time             17.36
INSTRUM          av400
PROBHD   5 mm PABBO BB/
PULPROG        zgdc.js
TD                5096
SOLVENT          CDCl3
NS                1024
DS                   0
SWH       51020.406 Hz
FIDRES    10.011854 Hz
AQ       0.0499408 sec
RG              189.85
DW           9.800 usec
DE            6.50 usec
TE             299.0 K
D1       0.00000400 sec
D11      0.03000000 sec
TD0                  1

======== CHANNEL f1 ========
SFO1      128.3776052 MHz
NUC1                 11B
P1             10.00 usec
PLW1       52.00000000 W

======== CHANNEL f2 ========
SFO2      400.1324008 MHz
NUC2                  1H
CPDPRG[2         waltz16
PCPD2          90.00 usec
PLW2       13.00000000 W
PLW12       0.36111000 W

F2 - Processing parameters
SI               32768
SF       128.3776050 MHz
WDW                 EM
SSB     0
LB            50.00 Hz
GB      0
PC                1.40
```

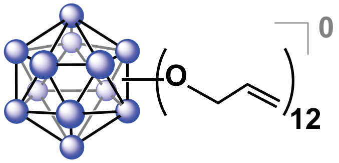

^{13}C NMR

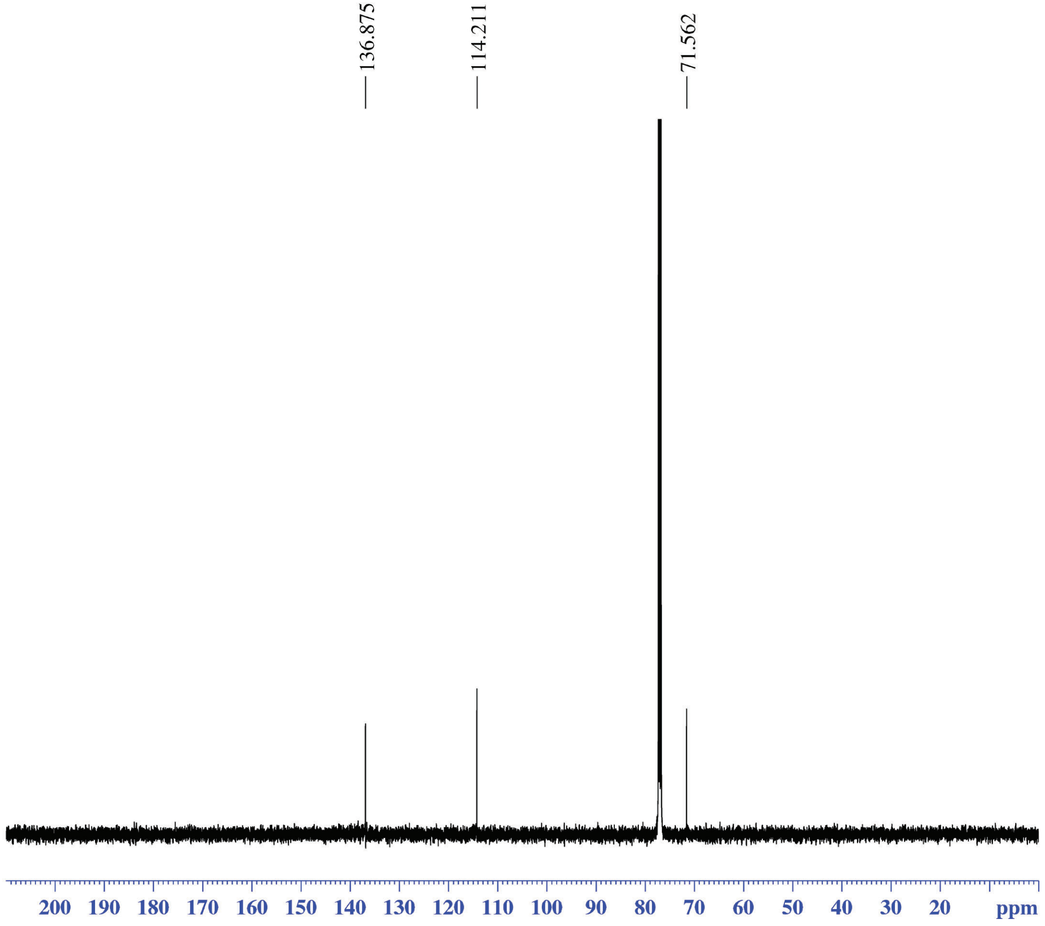

```
Current Data Parameters
NAME     B12(O-Allyl)12
EXPNO              80
PROCNO              1

F2 - Acquisition Parameters
Date_        20150406
Time            23.59
INSTRUM         av500
PROBHD   5 mm DCH 13C-1
PULPROG        zgpg30
TD              65536
SOLVENT         CDCl3
NS                 64
DS                  2
SWH        31250.000 Hz
FIDRES      0.476837 Hz
AQ         1.0485760 sec
RG             204.54
DW             16.000 usec
DE              18.00 usec
TE              298.0 K
D1         2.00000000 sec
D11        0.03000000 sec
TD0                 1

======== CHANNEL f1 ========
SFO1     125.7722511 MHz
NUC1              13C
P1               9.63 usec
PLW1      23.00000000 W

======== CHANNEL f2 ========
SFO2     500.1330008 MHz
NUC2               1H
CPDPRG[2         waltz16
PCPD2           80.00 usec
PLW2      13.50000000 W
PLW12      0.21094000 W
PLW13      0.13500001 W

F2 - Processing parameters
SI             131072
SF       125.7577890 MHz
WDW                EM
SSB     0
LB               1.00 Hz
GB      0
PC               1.40
```

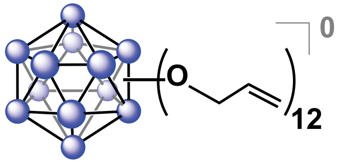

^{1}H NMR

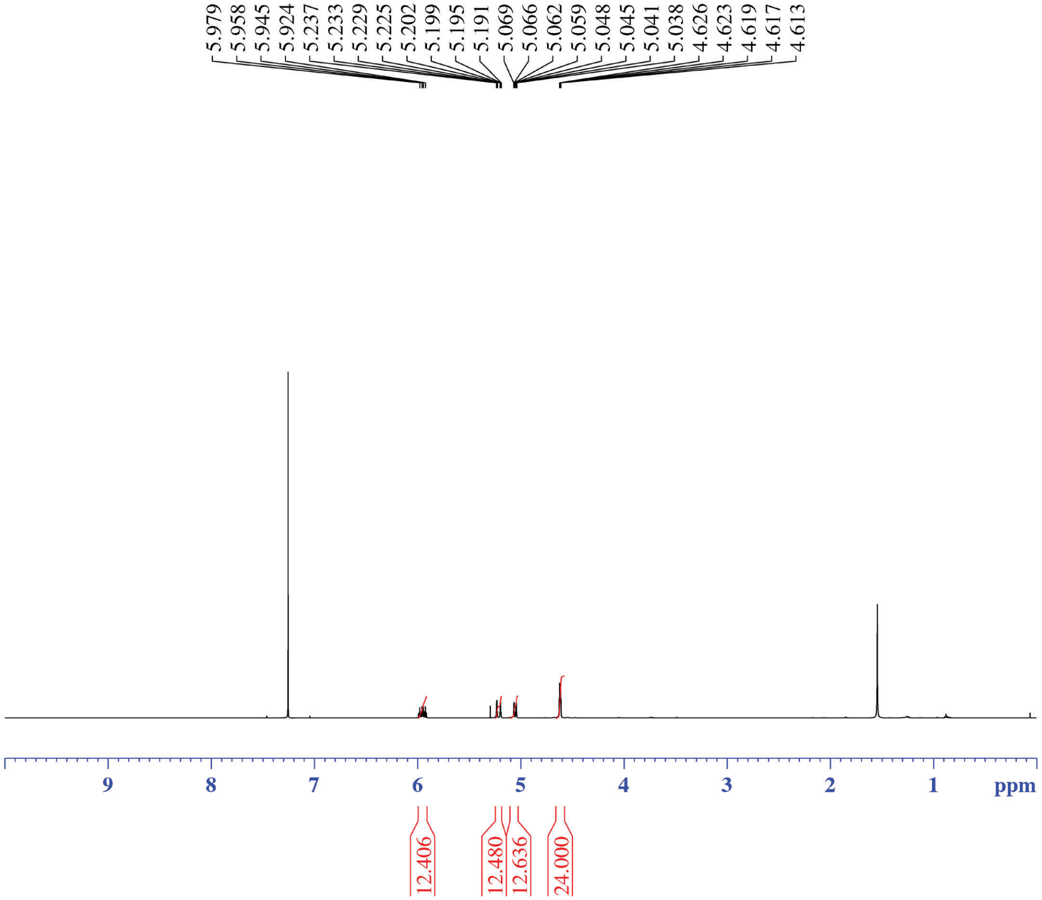

```
Current Data Parameters
NAME     B12(O-Allyl)12
EXPNO              81
PROCNO              1

F2 - Acquisition Parameters
Date_        20150407
Time             0.01
INSTRUM         av500
PROBHD   5 mm DCH 13C-1
PULPROG          zg30
TD              65536
SOLVENT         CDCl3
NS                  8
DS                  0
SWH        10000.000 Hz
FIDRES      0.152588 Hz
AQ         3.2767999 sec
RG              63.27
DW             50.000 usec
DE              10.00 usec
TE              298.0 K
D1       2.00000000 sec
TD0                 1

======== CHANNEL f1 ========
SFO1      500.1330008 MHz
NUC1               1H
P1              10.00 usec
PLW1      13.50000000 W

F2 - Processing parameters
SI              65536
SF        500.1300146 MHz
WDW                EM
SSB     0
LB               0.30 Hz
GB      0
PC               1.00
```

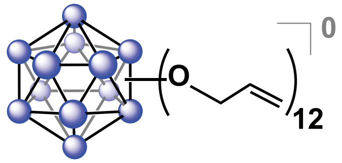

Q Exactive
High-Res Mass Spec

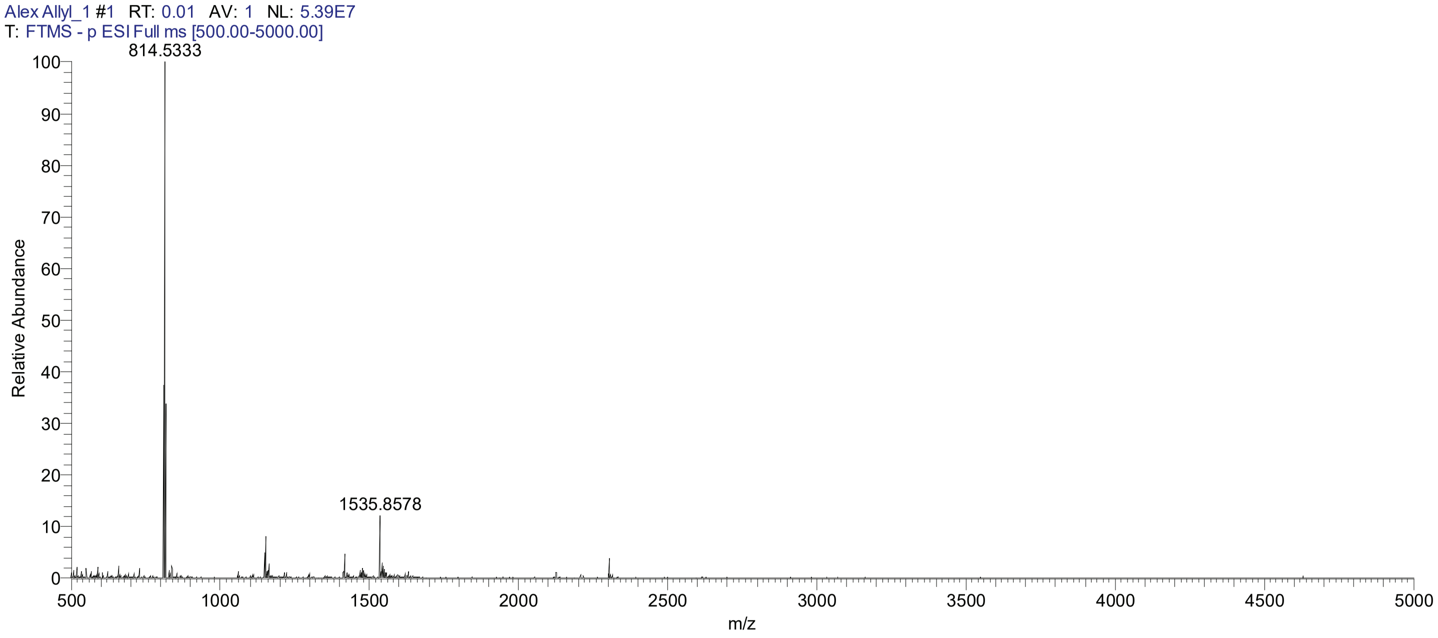

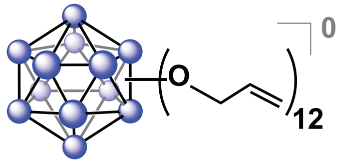

Q Exactive
High-Res Mass Spec

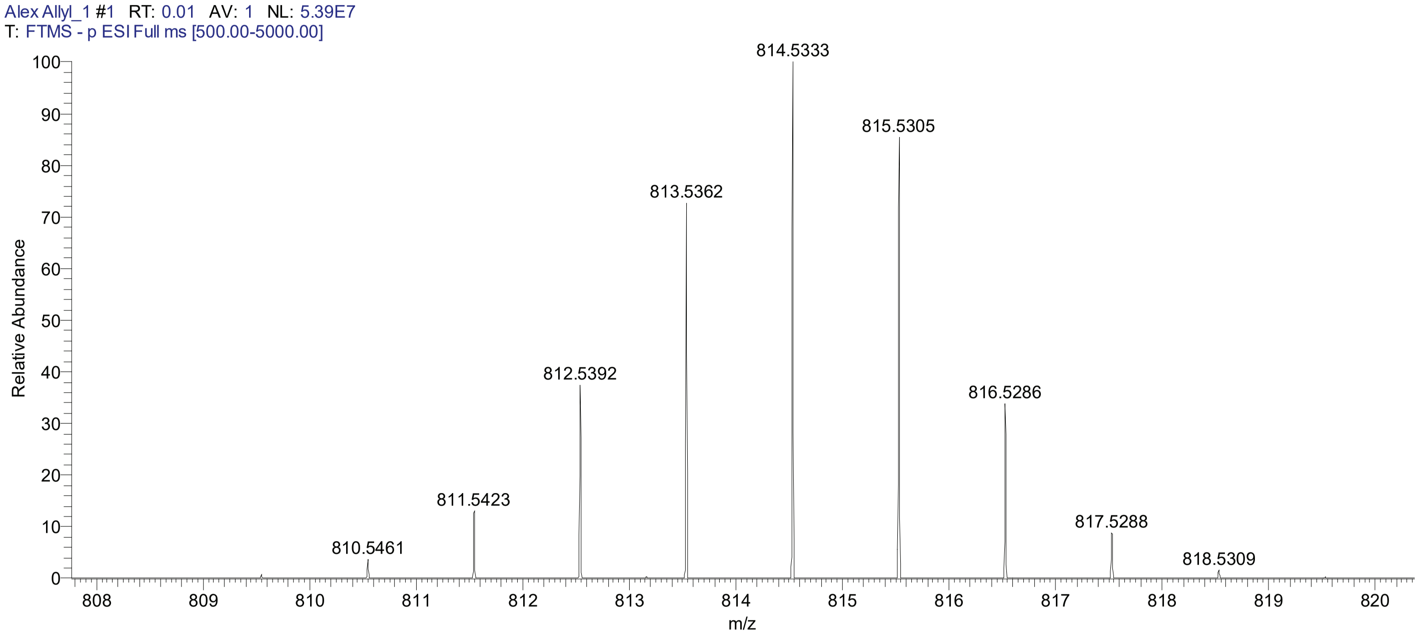

^{11}B {^{1}H} NMR

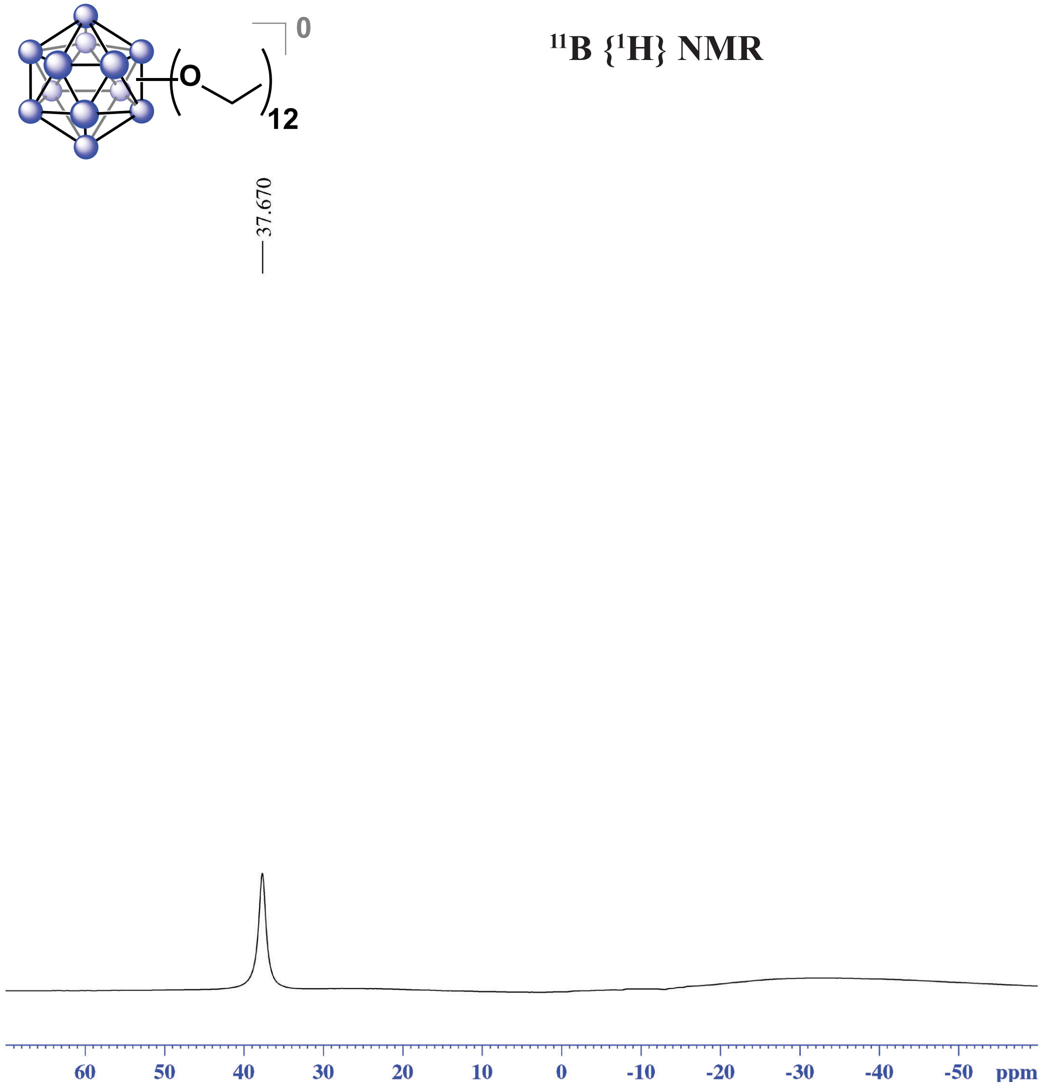

```
Current Data Parameters
NAME        B12(O-Et)12
EXPNO              100
PROCNO               1

F2 - Acquisition Parameters
Date_         20150412
Time             19.11
INSTRUM          av400
PROBHD   5 mm PABBO BB/
PULPROG        zgdc.js
TD                5096
SOLVENT          CDCl3
NS                1024
DS                   0
SWH        51020.406 Hz
FIDRES     10.011854 Hz
AQ         0.0499408 sec
RG              189.85
DW            9.800 usec
DE             6.50 usec
TE             299.1 K
D1        0.00000400 sec
D11       0.03000000 sec
TD0                  1

======== CHANNEL f1 ========
SFO1      128.3776052 MHz
NUC1               11B
P1            10.00 usec
PLW1       52.00000000 W

======== CHANNEL f2 ========
SFO2      400.1324008 MHz
NUC2                1H
CPDPRG[2        waltz16
PCPD2         90.00 usec
PLW2       13.00000000 W
PLW12       0.36111000 W

F2 - Processing parameters
SI               32768
SF        128.3776050 MHz
WDW                 EM
SSB     0
LB            50.00 Hz
GB      0
PC                1.40
```

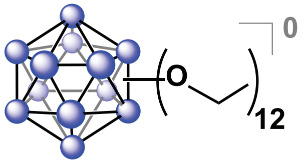

^{13}C NMR

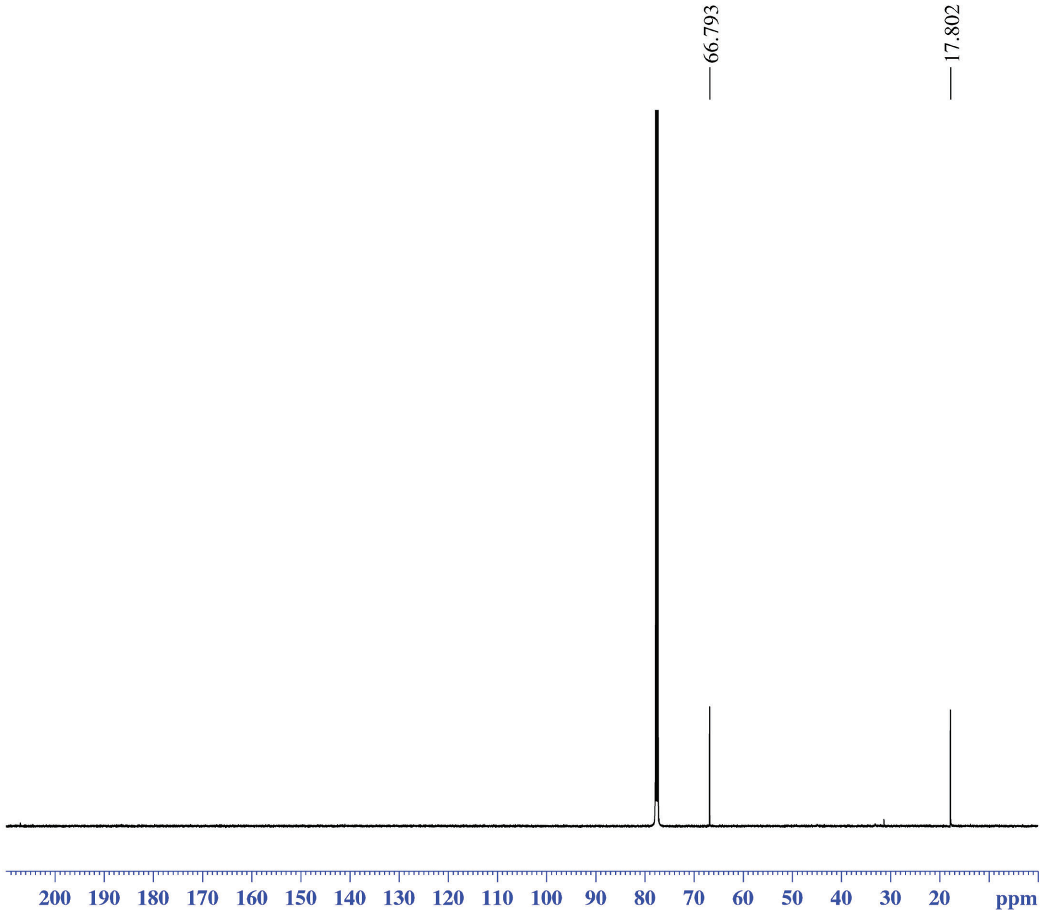

```
Current Data Parameters
NAME       B12(O-Et)12
EXPNO            10
PROCNO            1

F2 - Acquisition Parameters
Date_        20150420
Time           21.23
INSTRUM         av500
PROBHD   5 mm DCH 13C-1
PULPROG        zgpg30
TD            65536
SOLVENT          CDCl3
NS               64
DS                2
SWH         31250.000 Hz
FIDRES       0.476837 Hz
AQ          1.0485760 sec
RG            204.54
DW            16.000 usec
DE             18.00 usec
TE             298.0 K
D1        2.00000000 sec
D11       0.03000000 sec
TD0               1

======== CHANNEL f1 ========
SFO1     125.7722511 MHz
NUC1             13C
P1              9.63 usec
PLW1     23.00000000 W

======== CHANNEL f2 ========
SFO2     500.1330008 MHz
NUC2              1H
CPDPRG[2      waltz16
PCPD2          80.00 usec
PLW2     13.50000000 W
PLW12     0.21094000 W
PLW13     0.13500001 W

F2 - Processing parameters
SI          131072
SF       125.7577890 MHz
WDW              EM
SSB    0
LB              1.00 Hz
GB     0
PC              1.40
```

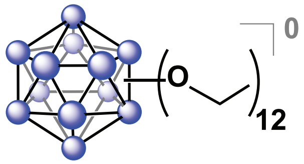

^{1}H NMR

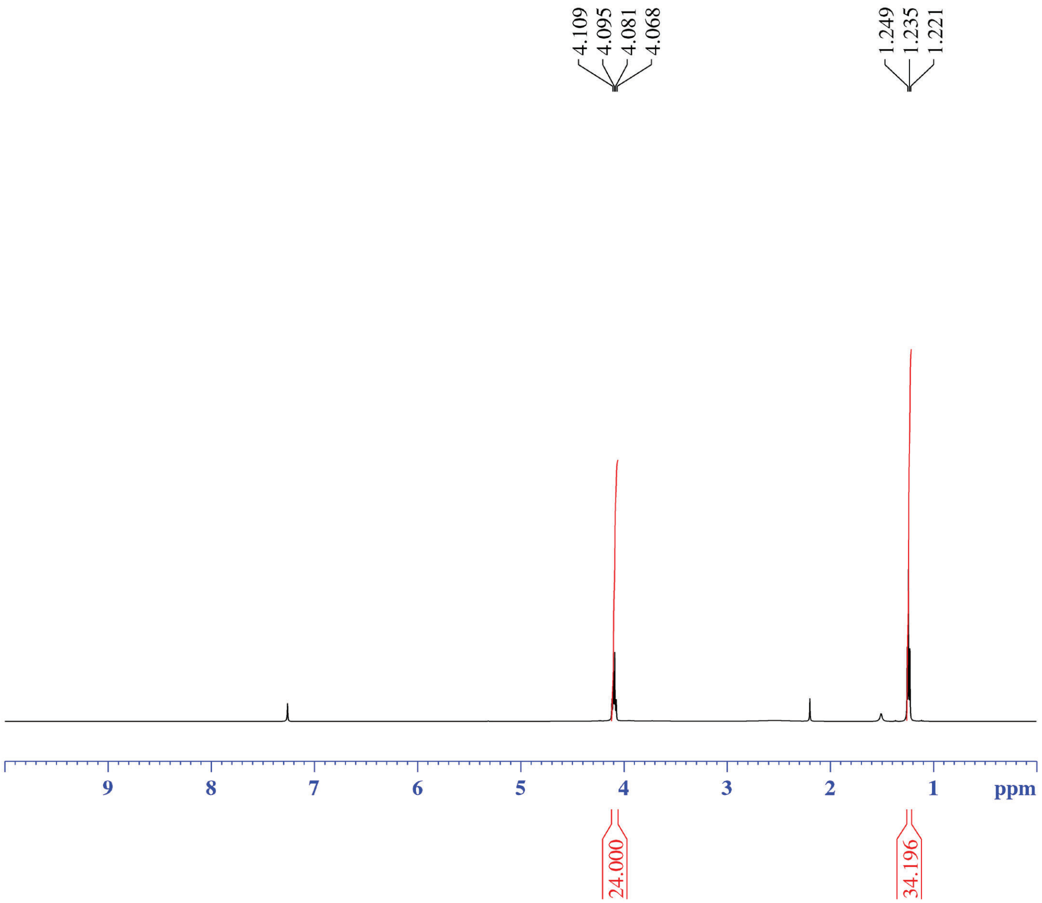

Current Data Parameters
NAME B12(O-Et)12
EXPNO 11
PROCNO 1

F2 - Acquisition Parameters
Date_ 20150420
Time 21.30
INSTRUM av500
PROBHD 5 mm DCH 13C-1
PULPROG zg30
TD 65536
SOLVENT CDCl3
NS 64
DS 0
SWH 10000.000 Hz
FIDRES 0.152588 Hz
AQ 3.2767999 sec
RG 52.41
DW 50.000 usec
DE 10.00 usec
TE 298.0 K
D1 2.00000000 sec
TD0 1

======== CHANNEL f1 ========
SFO1 500.1330008 MHz
NUC1 1H
P1 10.00 usec
PLW1 13.50000000 W

F2 - Processing parameters
SI 65536
SF 500.1300115 MHz
WDW EM
SSB 0
LB 0.30 Hz
GB 0
PC 1.00

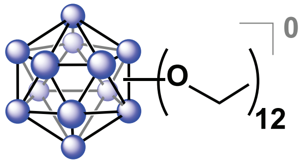

Q Exactive
High-Res Mass Spec

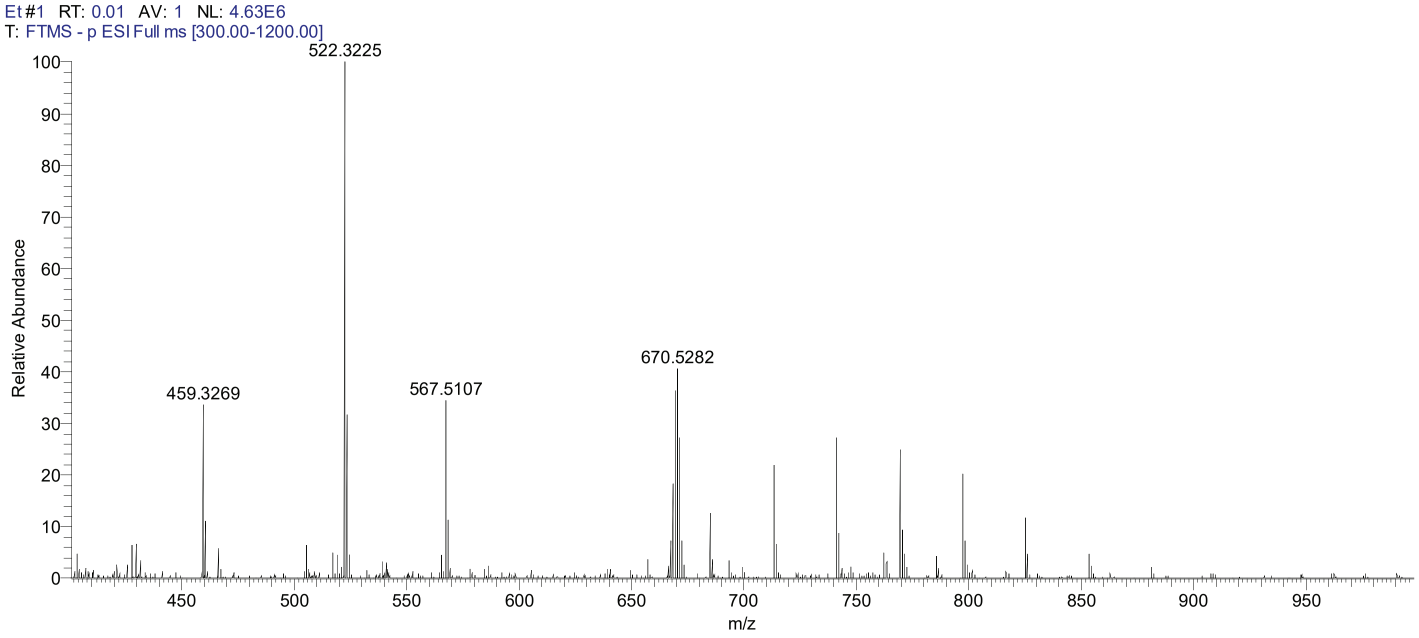

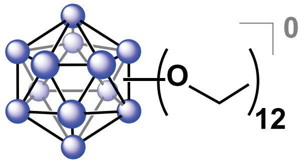

Q Exactive
High-Res Mass Spec

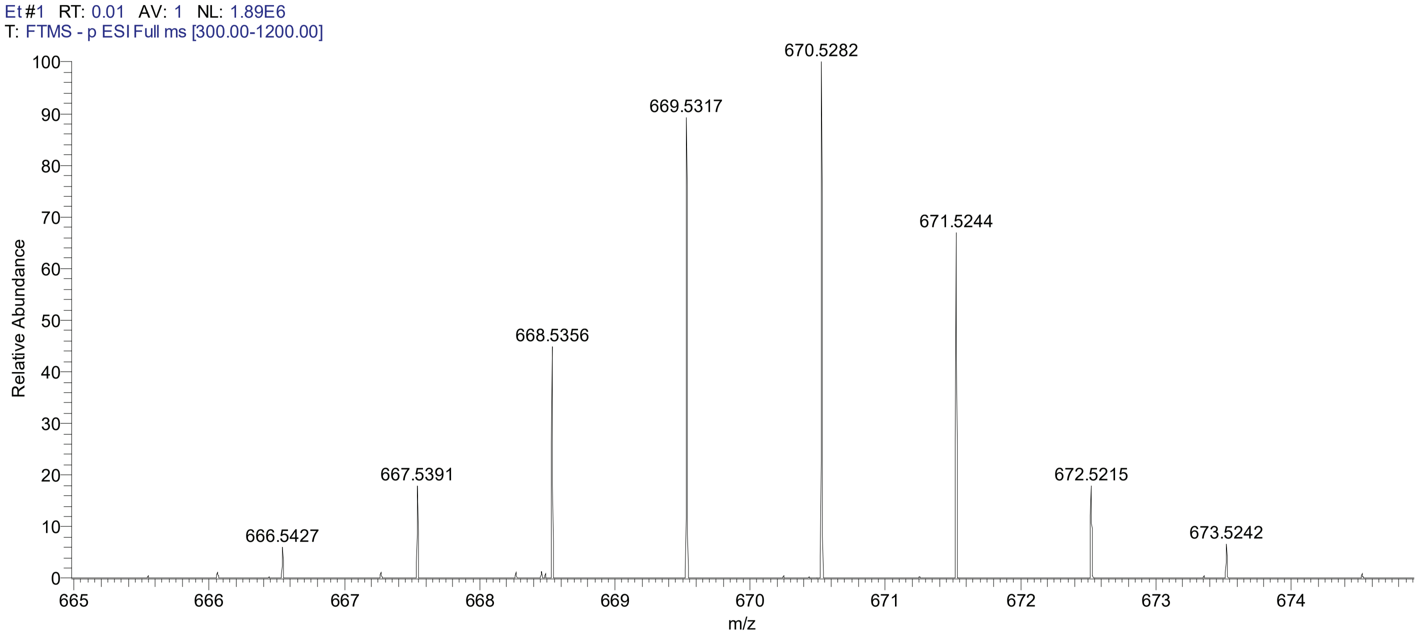

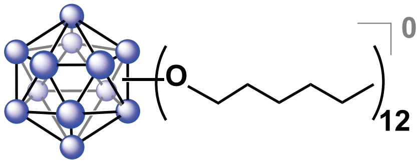

$^{11}B\ \{^1H\}$ NMR

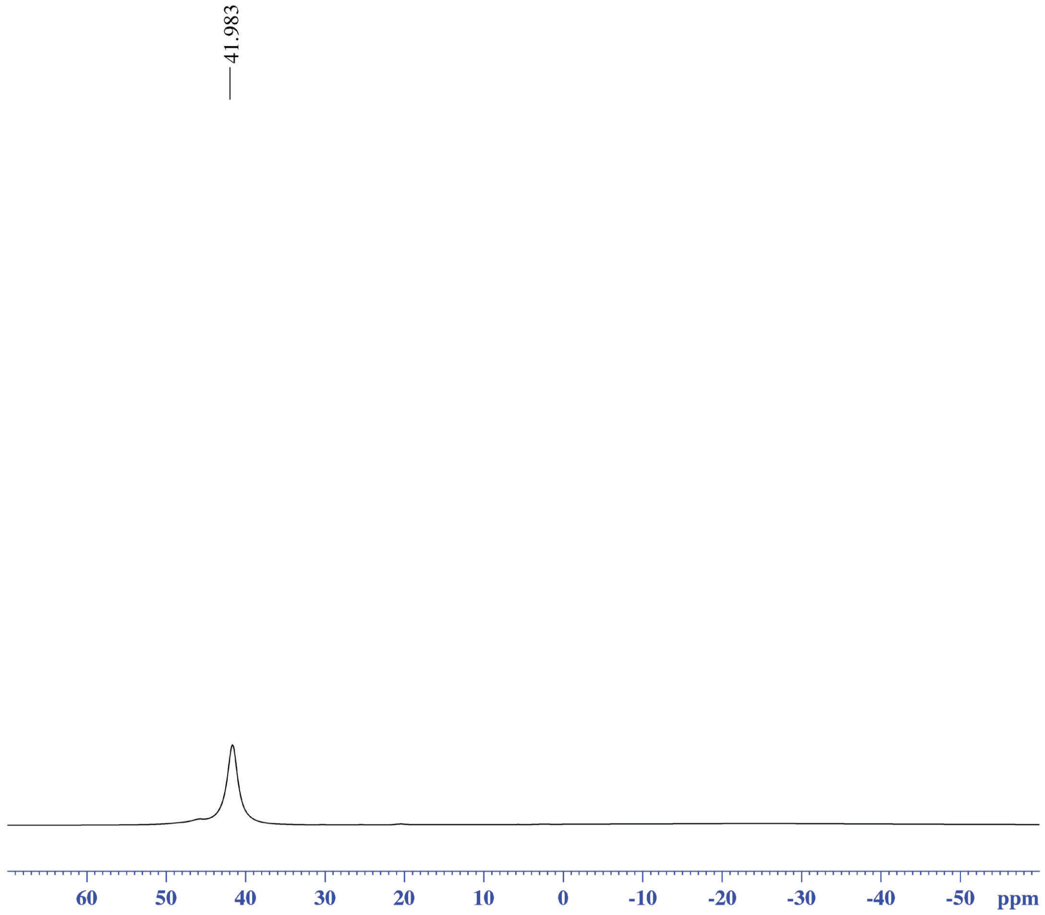

```
Current Data Parameters
NAME     B12(O-Hexyl)12
EXPNO              20
PROCNO              1

F2 - Acquisition Parameters
Date_         20150610
Time             15.09
INSTRUM          av400
PROBHD   5 mm PABBO BB/
PULPROG       zgdc.js
TD               5096
SOLVENT          CDCl3
NS               1024
DS                  0
SWH        51020.406 Hz
FIDRES     10.011854 Hz
AQ         0.0499408 sec
RG             189.85
DW              9.800 usec
DE              6.50 usec
TE             299.2 K
D1        0.00000400 sec
D11       0.03000000 sec
TD0                 1

======== CHANNEL f1 ========
SFO1      128.3776052 MHz
NUC1              11B
P1              10.00 usec
PLW1      52.00000000 W

======== CHANNEL f2 ========
SFO2      400.1324008 MHz
NUC2               1H
CPDPRG[2       waltz16
PCPD2           90.00 usec
PLW2      13.00000000 W
PLW12      0.36111000 W

F2 - Processing parameters
SI              32768
SF        128.3776050 MHz
WDW                EM
SSB     0
LB              50.00 Hz
GB      0
PC               1.40
```

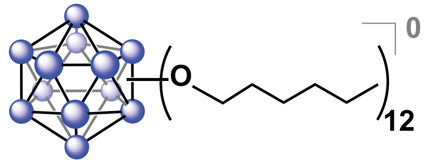

^{13}C NMR

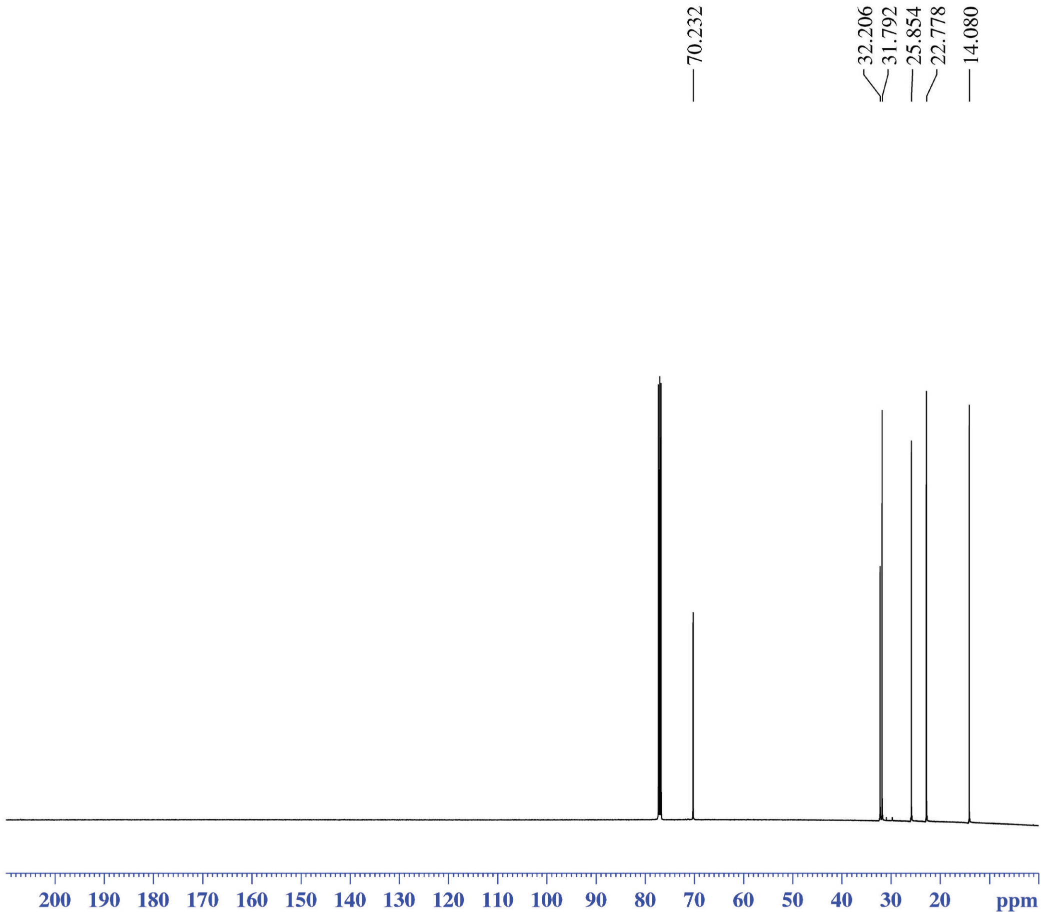

```
Current Data Parameters
NAME     B12(O-Hexyl)12
EXPNO              200
PROCNO               1

F2 - Acquisition Parameters
Date_         20150829
Time             20.52
INSTRUM          av500
PROBHD   5 mm DCH 13C-1
PULPROG        zgpg30
TD              65536
SOLVENT          CDCl3
NS                256
DS                  2
SWH        31250.000 Hz
FIDRES      0.476837 Hz
AQ         1.0485760 sec
RG             204.54
DW            16.000 usec
DE             18.00 usec
TE             298.0 K
D1        2.00000000 sec
D11       0.03000000 sec
TD0                 1

======== CHANNEL f1 ========
SFO1      125.7722511 MHz
NUC1              13C
P1               9.63 usec
PLW1      23.00000000 W

======== CHANNEL f2 ========
SFO2      500.1330008 MHz
NUC2               1H
CPDPRG[2        waltz16
PCPD2           80.00 usec
PLW2      13.50000000 W
PLW12      0.21094000 W
PLW13      0.13500001 W

F2 - Processing parameters
SI              131072
SF        125.7577890 MHz
WDW                 EM
SSB     0
LB             1.00 Hz
GB      0
PC             1.40
```

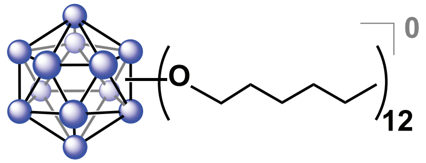

^{1}H NMR

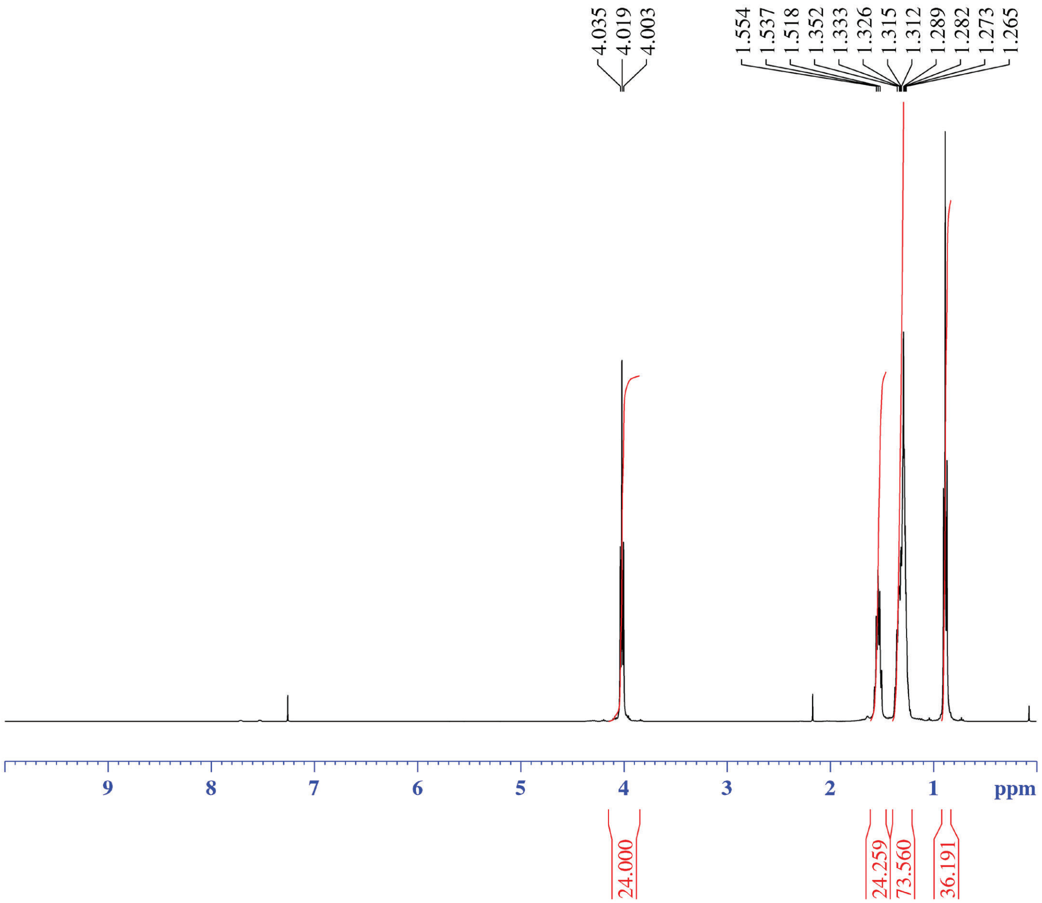

```
Current Data Parameters
NAME         Jun10-2015
EXPNO                11
PROCNO                1

F2 - Acquisition Parameters
Date_          20150610
Time              15.04
INSTRUM           av400
PROBHD   5 mm PABBO BB/
PULPROG            zg30
TD                52882
SOLVENT           CDCl3
NS                    8
DS                    0
SWH          8012.820 Hz
FIDRES       0.151523 Hz
AQ          3.2998369 sec
RG                30.37
DW             62.400 usec
DE               6.50 usec
TE              299.0 K
D1        2.00000000 sec
TD0                   1

======== CHANNEL f1 ========
SFO1       400.1324008 MHz
NUC1                 1H
P1              15.00 usec
PLW1       13.00000000 W

F2 - Processing parameters
SI                65536
SF         400.1300184 MHz
WDW                  EM
SSB      0
LB                 0.30 Hz
GB       0
PC                 1.00
```

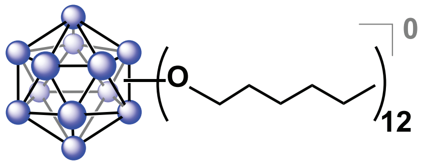

Q Exactive
High-Res Mass Spec

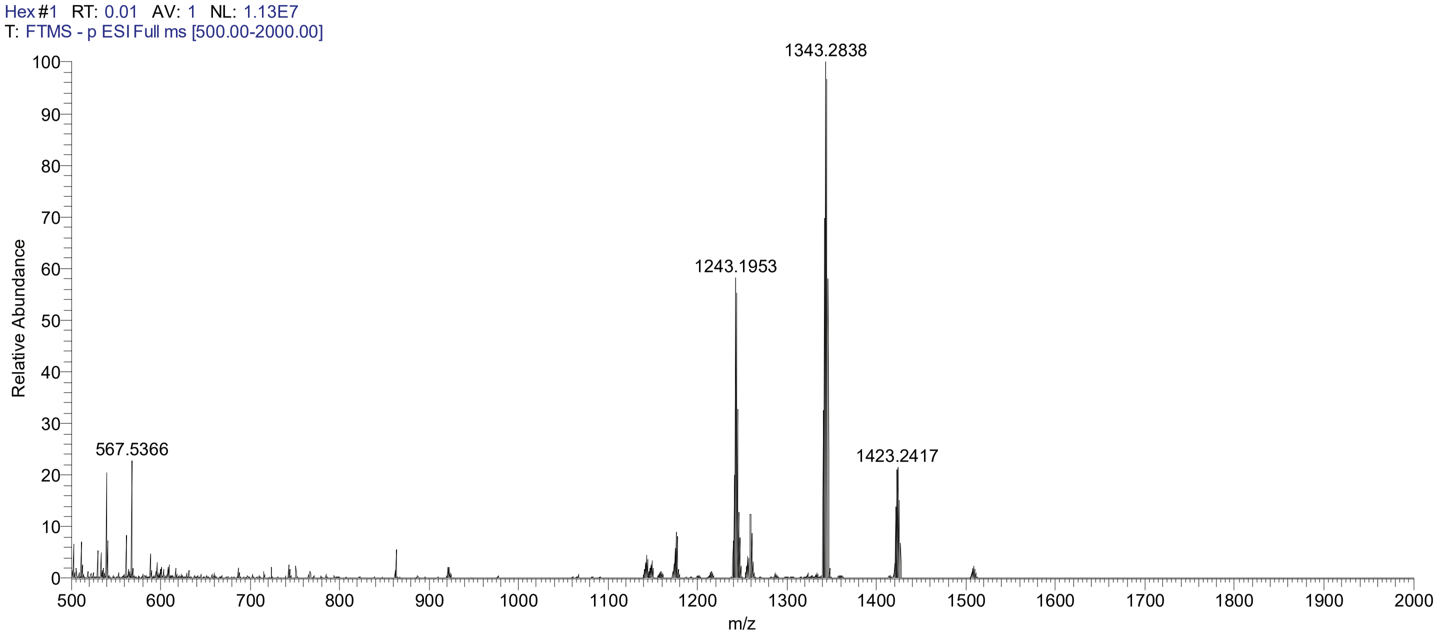

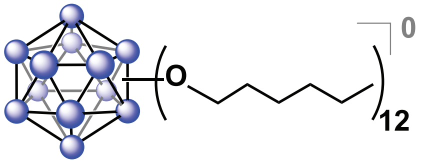

Q Exactive
High-Res Mass Spec

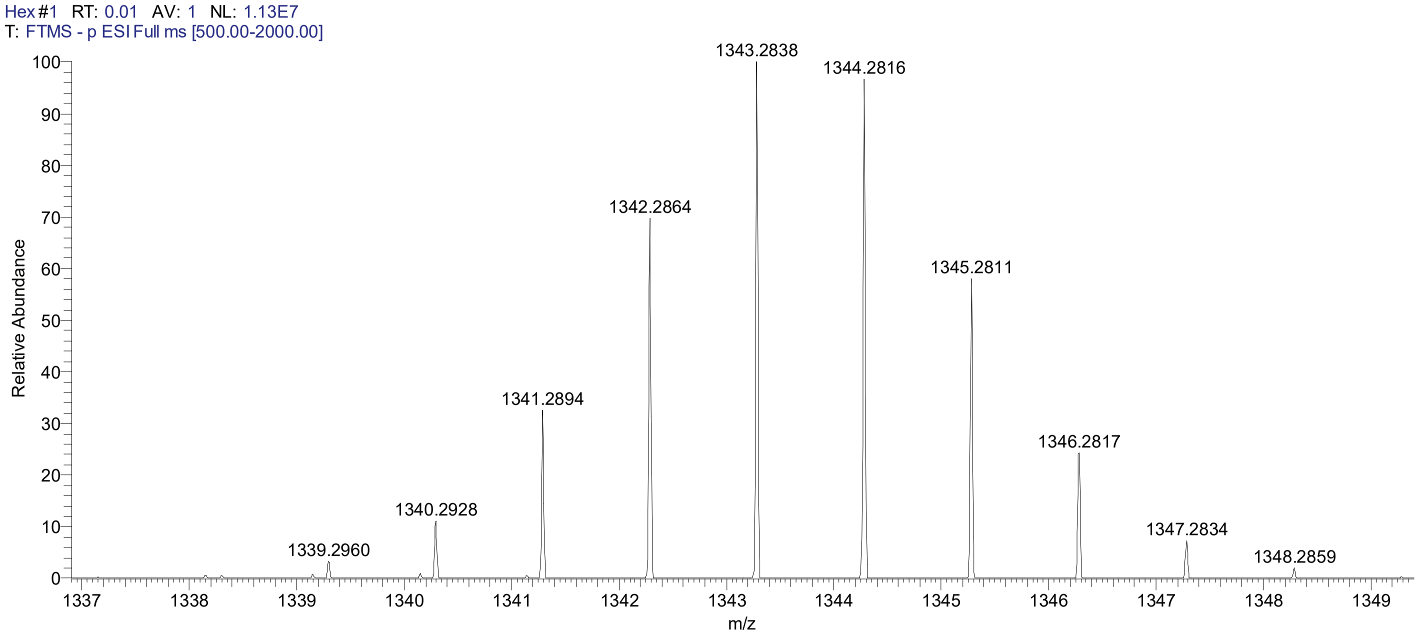

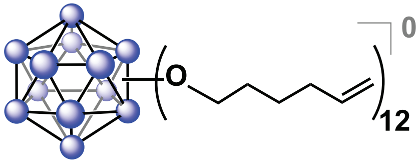

$^{11}B\ \{^{1}H\}$ NMR

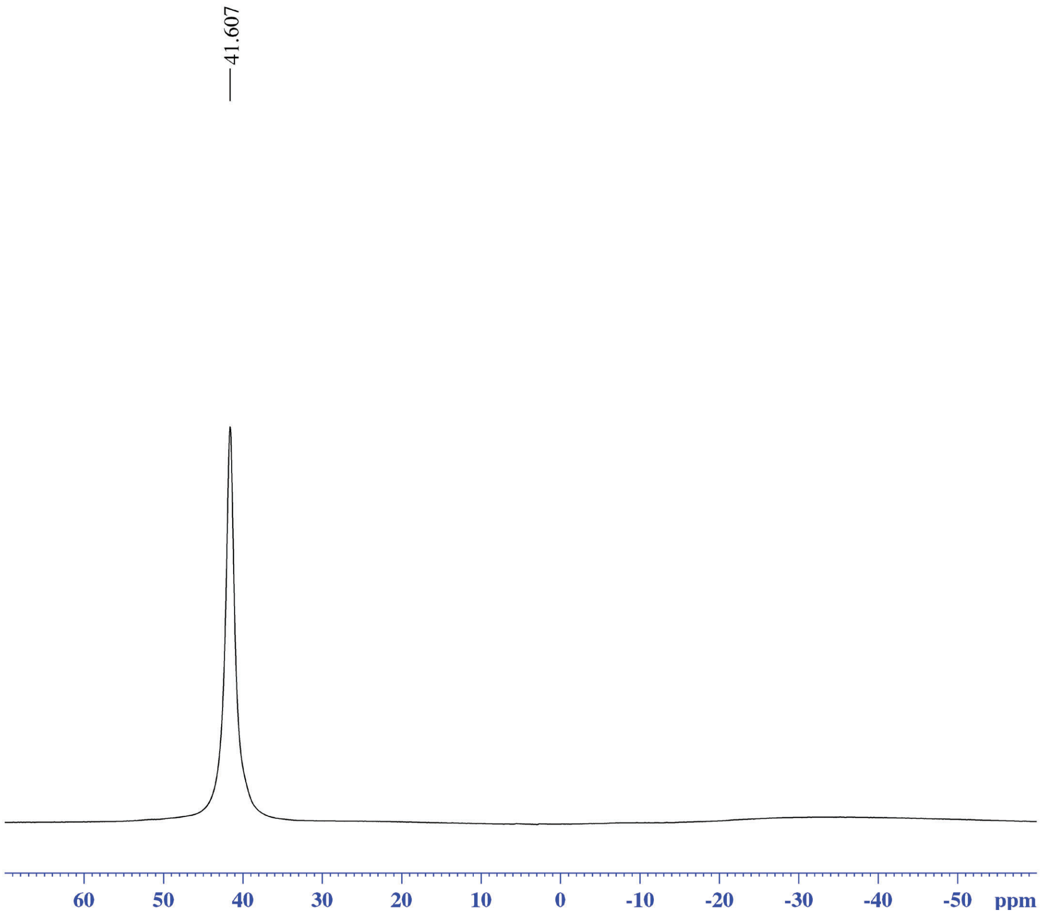

```
Current Data Parameters
NAME          Oct05-2015
EXPNO                 51
PROCNO                 1

F2 - Acquisition Parameters
Date_         20151005
Time             15.01
INSTRUM          av400
PROBHD   5 mm PABBO BB/
PULPROG        zgdc.js
TD                5096
SOLVENT          CDCl3
NS                1024
DS                   0
SWH        51020.406 Hz
FIDRES     10.011854 Hz
AQ         0.0499408 sec
RG              189.85
DW           9.800 usec
DE            6.50 usec
TE             299.1 K
D1      0.05000000 sec
D11     0.03000000 sec
TD0                  1

======== CHANNEL f1 ========
SFO1     128.3776052 MHz
NUC1               11B
P1            10.00 usec
PLW1      52.00000000 W

======== CHANNEL f2 ========
SFO2     400.1324008 MHz
NUC2                1H
CPDPRG[2        waltz16
PCPD2         90.00 usec
PLW2      13.00000000 W
PLW12      0.36111000 W

F2 - Processing parameters
SI               32768
SF       128.3776161 MHz
WDW                 EM
SSB     0
LB            10.00 Hz
GB      0
PC                1.40
```

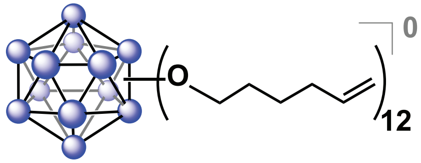

^{13}C NMR

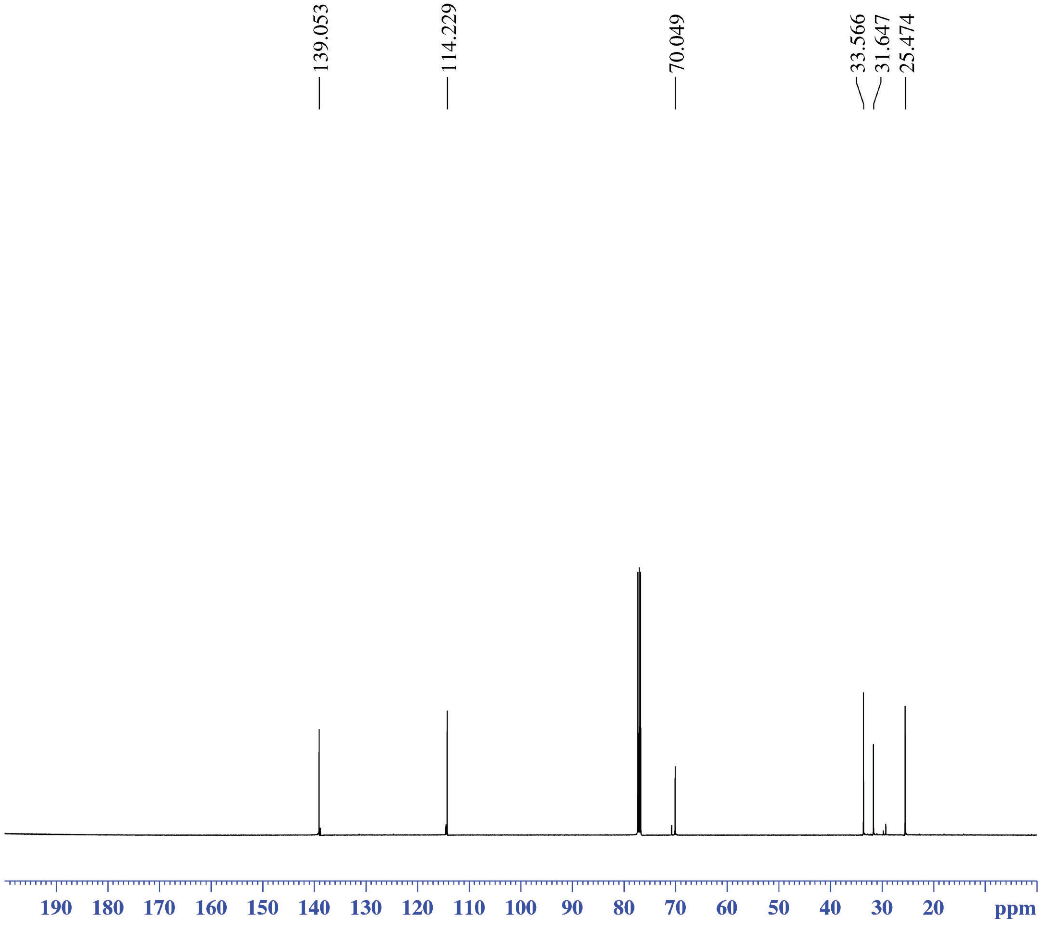

```
Current Data Parameters
NAME     B12(O-Hexene)12
EXPNO              20
PROCNO              1

F2 - Acquisition Parameters
Date_        20151021
Time            17.44
INSTRUM         av500
PROBHD   5 mm DCH 13C-1
PULPROG        zgpg30
TD            65536
SOLVENT         CDCl3
NS              256
DS                2
SWH        31250.000 Hz
FIDRES      0.476837 Hz
AQ         1.0485760 sec
RG            204.54
DW            16.000 usec
DE             18.00 usec
TE             298.0 K
D1        2.00000000 sec
D11       0.03000000 sec
TD0                1

======== CHANNEL f1 ========
SFO1      125.7722511 MHz
NUC1             13C
P1              9.63 usec
PLW1     23.00000000 W

======== CHANNEL f2 ========
SFO2      500.1330008 MHz
NUC2              1H
CPDPRG[2        waltz16
PCPD2           80.00 usec
PLW2      13.50000000 W
PLW12      0.21094000 W
PLW13      0.13500001 W

F2 - Processing parameters
SI            131072
SF       125.7577890 MHz
WDW               EM
SSB     0
LB              1.00 Hz
GB      0
PC              1.40
```

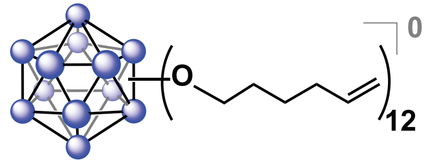

^{1}H NMR

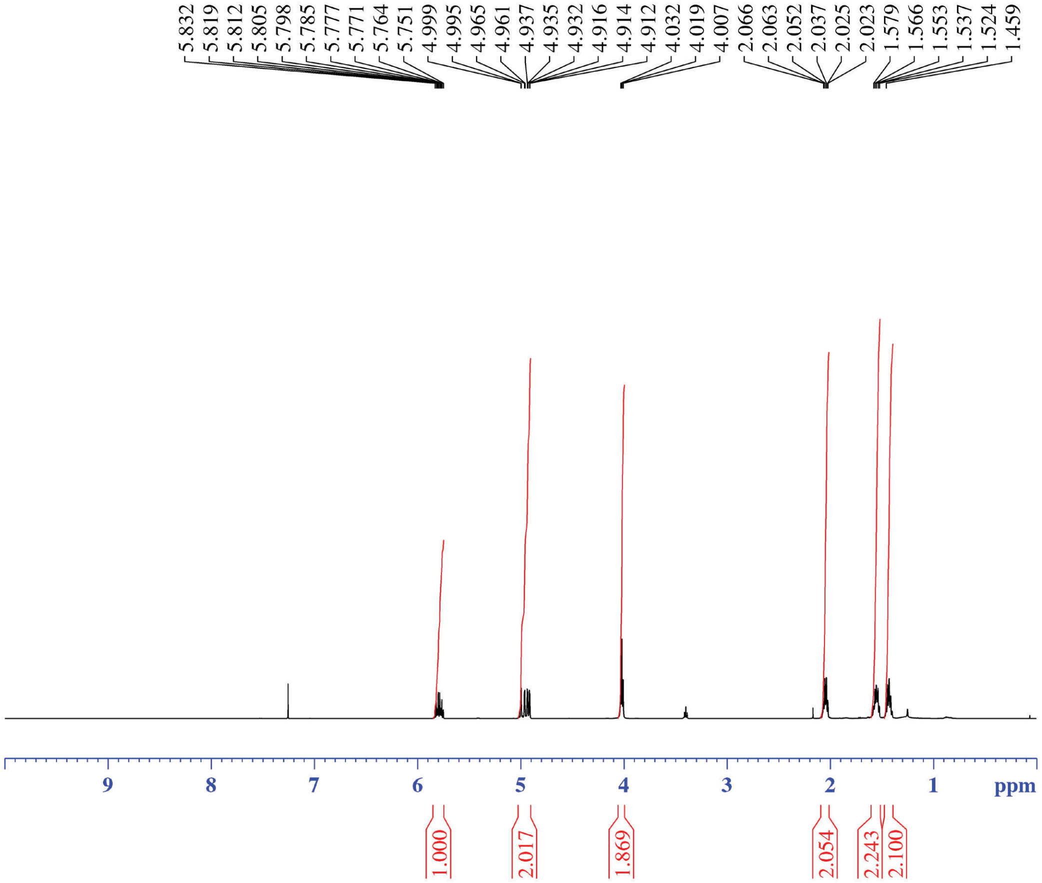

```
Current Data Parameters
NAME     B12(O-Hexene)12
EXPNO              21
PROCNO              1

F2 - Acquisition Parameters
Date_          20151021
Time              17.48
INSTRUM           av500
PROBHD   5 mm DCH 13C-1
PULPROG            zg30
TD                65536
SOLVENT            CDCl3
NS                   32
DS                    0
SWH          10000.000 Hz
FIDRES        0.152588 Hz
AQ           3.2767999 sec
RG                33.91
DW               50.000 usec
DE                10.00 usec
TE                298.0 K
D1          2.00000000 sec
TD0                   1

======== CHANNEL f1 ========
SFO1       500.1330008 MHz
NUC1                 1H
P1                10.00 usec
PLW1        13.50000000 W

F2 - Processing parameters
SI                65536
SF         500.1300146 MHz
WDW                  EM
SSB     0
LB                 0.30 Hz
GB      0
PC                 1.00
```

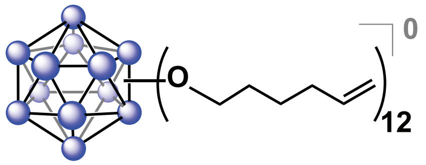

Q Exactive
High-Res Mass Spec

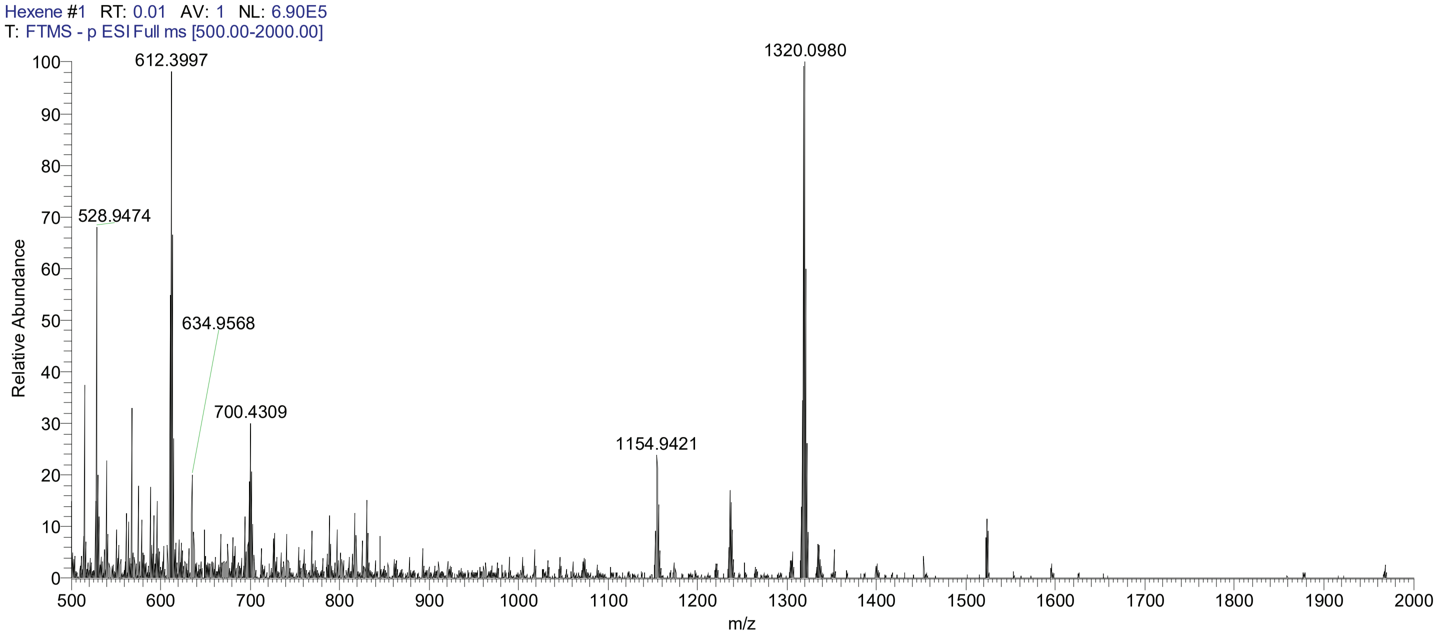

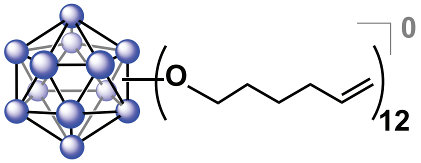

Q Exactive
High-Res Mass Spec

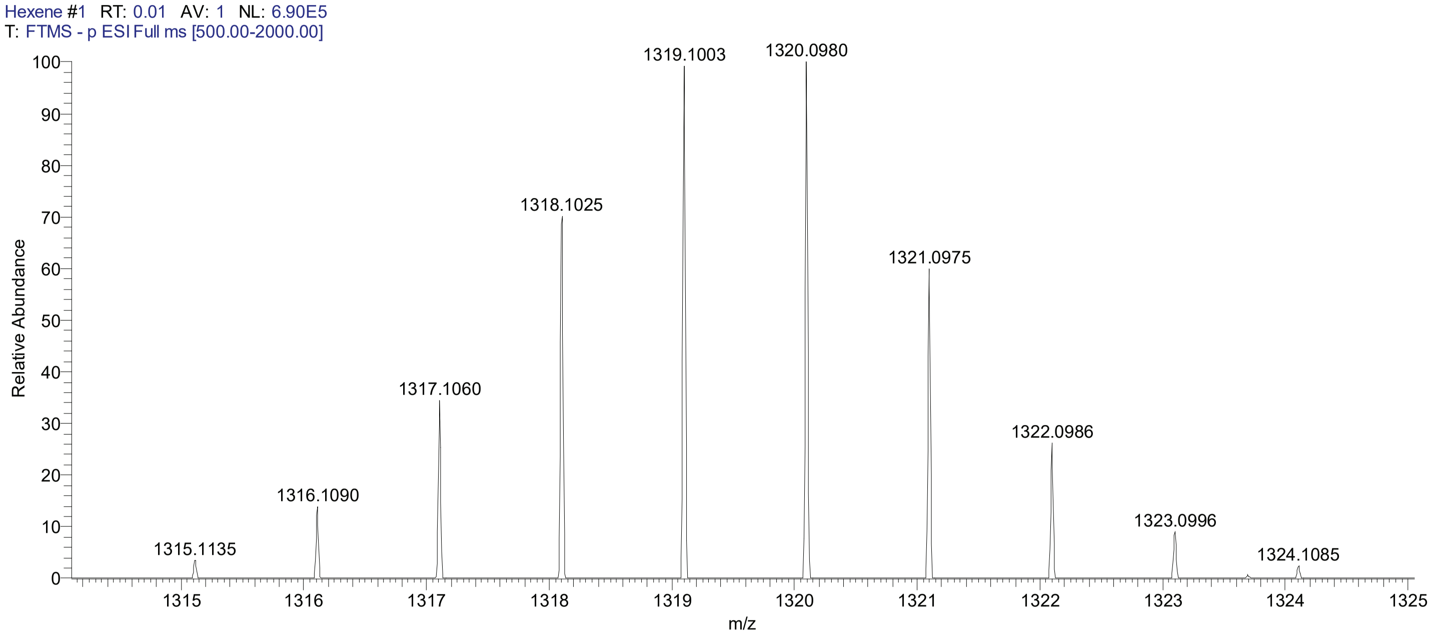

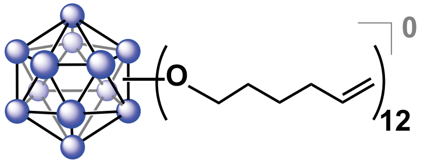

O
0
12

IR

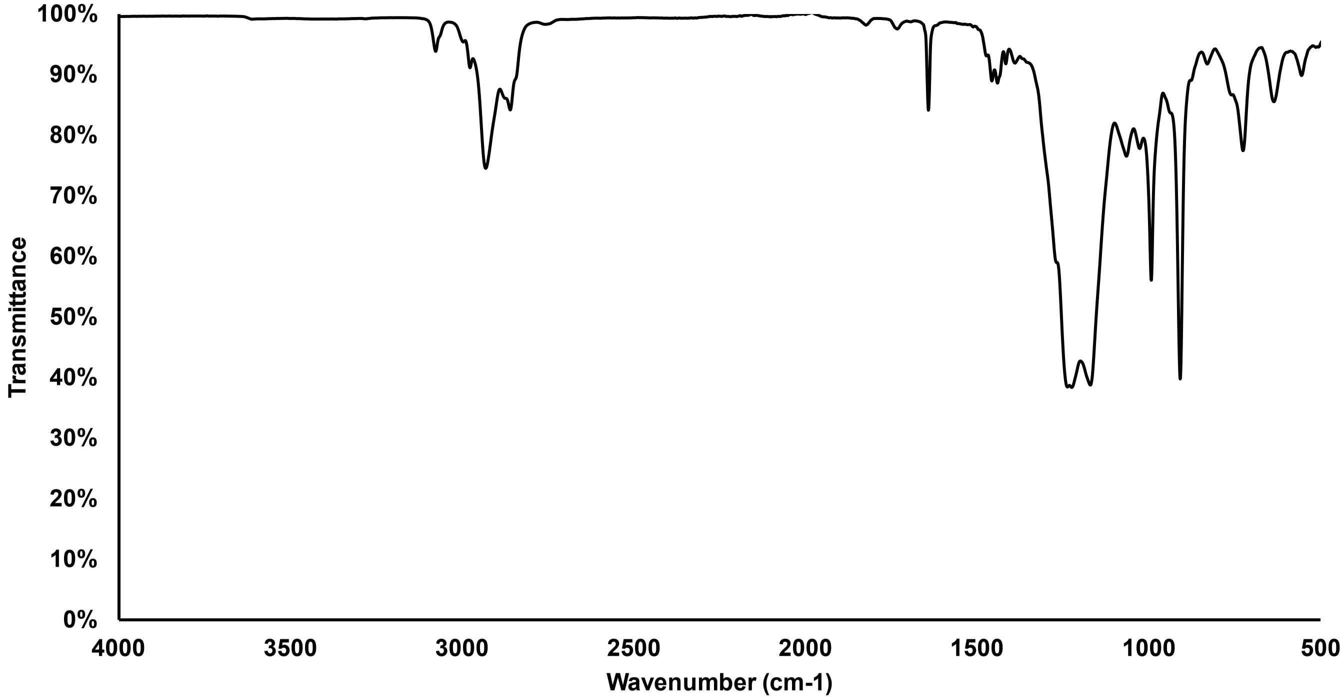

Transmittance
100%
90%
80%
70%
60%
50%
40%
30%
20%
10%
0%
4000
3500
3000
2500
2000
1500
1000
500
Wavenumber (cm-1)

^{11}B {^{1}H} NMR

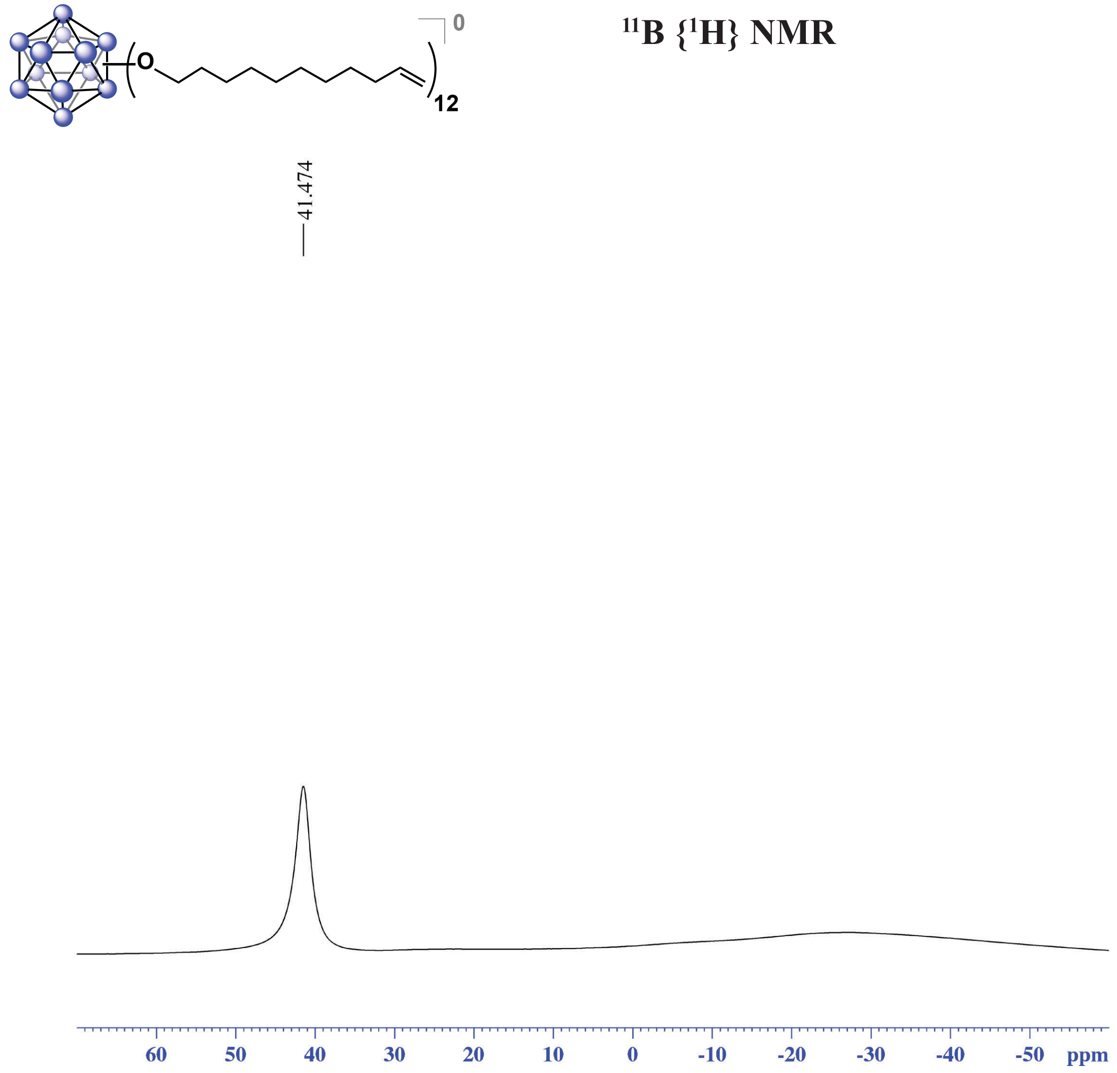

```
Current Data Parameters
NAME     B12(O-1-undecene)12
EXPNO              20
PROCNO              1

F2 - Acquisition Parameters
Date_          20150626
Time              12.16
INSTRUM          av400
PROBHD   5 mm PABBO BB/
PULPROG        zgdc.js
TD                5096
SOLVENT        CD2Cl2
NS                1024
DS                   0
SWH          51020.406 Hz
FIDRES       10.011854 Hz
AQ           0.0499408 sec
RG              189.85
DW               9.800 usec
DE                6.50 usec
TE               299.1 K
D1          0.00000400 sec
D11         0.03000000 sec
TD0                  1

======== CHANNEL f1 ========
SFO1       128.3776052 MHz
NUC1              11B
P1               10.00 usec
PLW1       52.00000000 W

======== CHANNEL f2 ========
SFO2       400.1324008 MHz
NUC2               1H
CPDPRG[2        waltz16
PCPD2            90.00 usec
PLW2       13.00000000 W
PLW12       0.36111000 W

F2 - Processing parameters
SI               32768
SF         128.3776050 MHz
WDW                 EM
SSB      0
LB               50.00 Hz
GB       0
PC                1.40
```

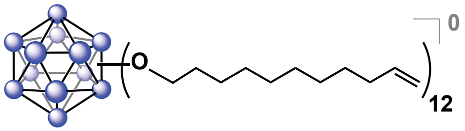

^{13}C NMR

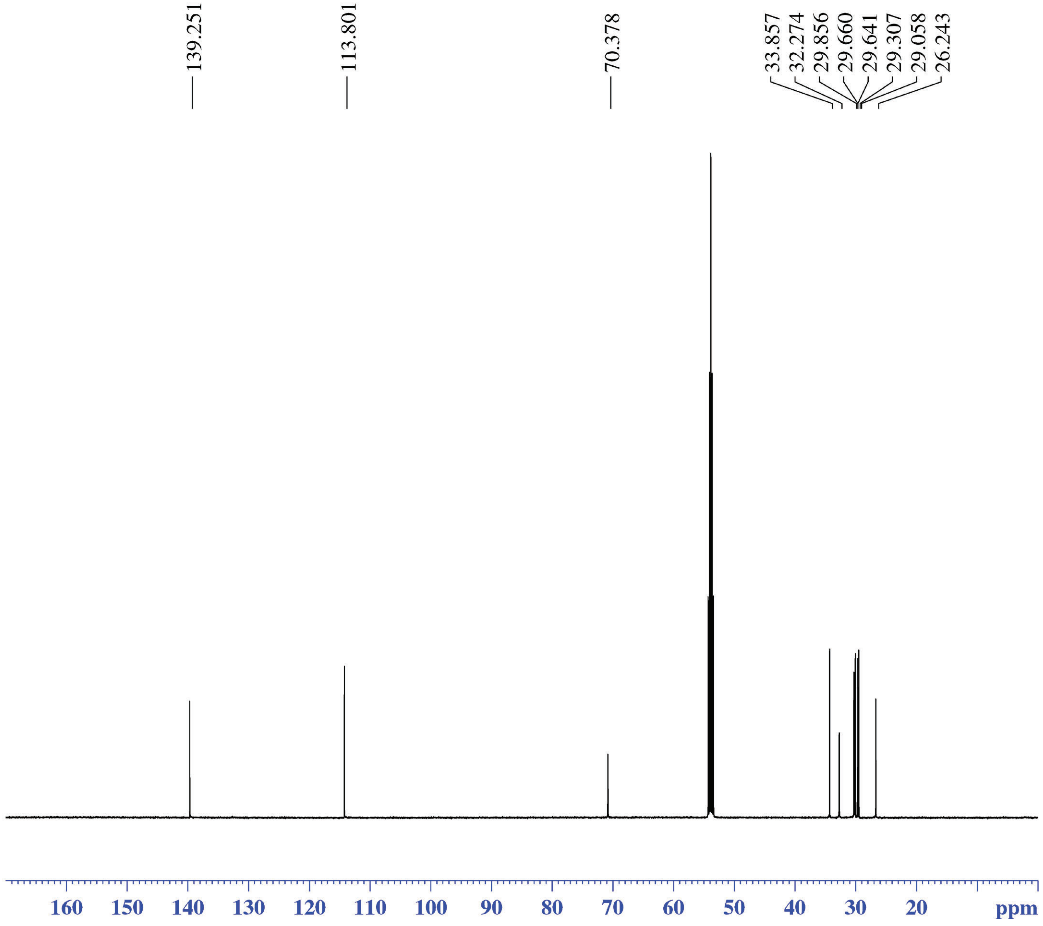

```
Current Data Parameters
NAME        Jun26-2015
EXPNO              10
PROCNO              1

F2 - Acquisition Parameters
Date_        20150626
Time            14.05
INSTRUM         av500
PROBHD   5 mm DCH 13C-1
PULPROG        zgpg30
TD              65536
SOLVENT        CD2Cl2
NS                 64
DS                  2
SWH        31250.000 Hz
FIDRES      0.476837 Hz
AQ         1.0485760 sec
RG             204.54
DW             16.000 usec
DE              18.00 usec
TE              298.0 K
D1        2.00000000 sec
D11       0.03000000 sec
TD0                 1

======== CHANNEL f1 ========
SFO1      125.7722511 MHz
NUC1              13C
P1               9.63 usec
PLW1      23.00000000 W

======== CHANNEL f2 ========
SFO2      500.1330008 MHz
NUC2               1H
CPDPRG[2       waltz16
PCPD2           80.00 usec
PLW2      13.50000000 W
PLW12      0.21094000 W
PLW13      0.13500001 W

F2 - Processing parameters
SI             131072
SF        125.7577890 MHz
WDW                EM
SSB     0
LB             1.00 Hz
GB      0
PC             1.40
```

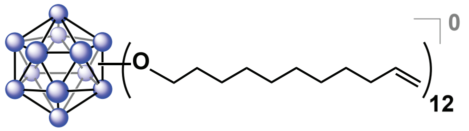

^{1}H NMR

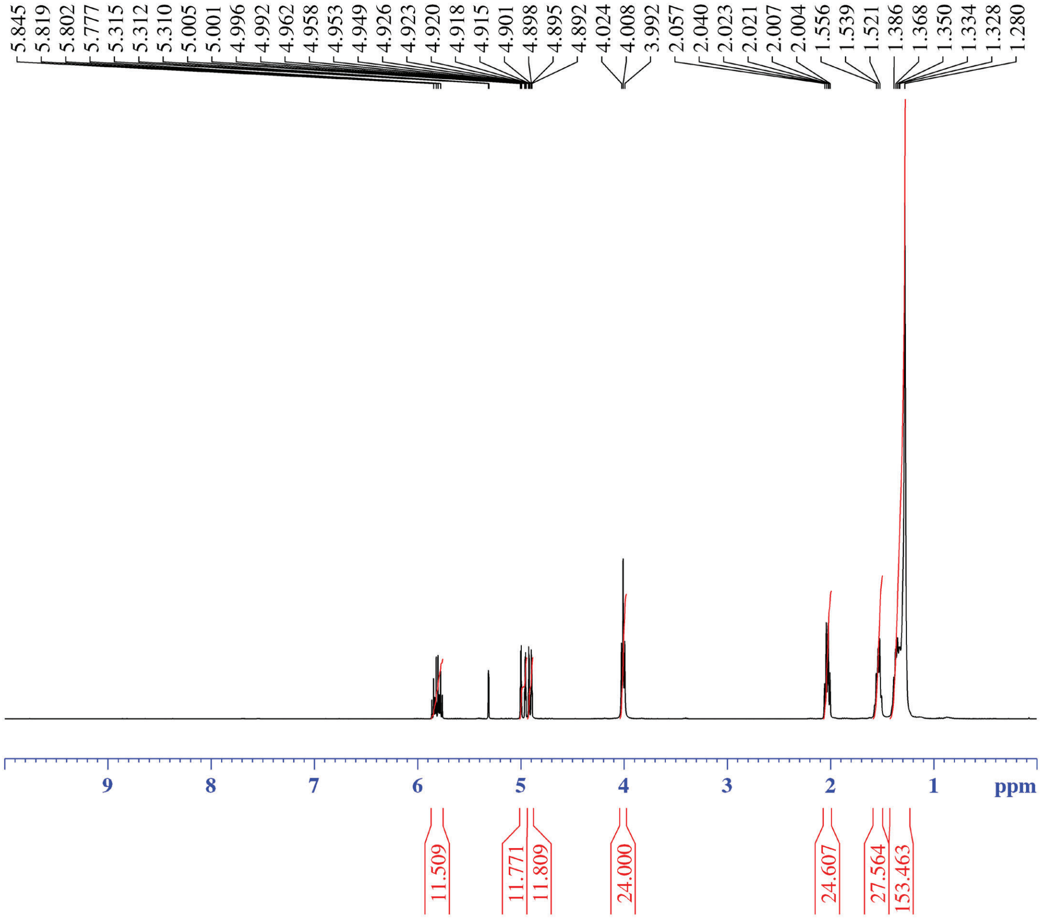

```
Current Data Parameters
NAME     B12(O-1-undecene)12
EXPNO                 21
PROCNO                 1

F2 - Acquisition Parameters
Date_          20150626
Time              12.18
INSTRUM           av400
PROBHD   5 mm PABBO BB/
PULPROG            zg30
TD                52882
SOLVENT          CD2Cl2
NS                    8
DS                    0
SWH          8012.820 Hz
FIDRES       0.151523 Hz
AQ          3.2998369 sec
RG                83.63
DW           62.400 usec
DE             6.50 usec
TE              299.0 K
D1         2.00000000 sec
TD0                   1

======== CHANNEL f1 ========
SFO1      400.1324008 MHz
NUC1                 1H
P1              15.00 usec
PLW1      13.00000000 W

F2 - Processing parameters
SI                65536
SF        400.1300184 MHz
WDW                  EM
SSB    0
LB                0.30 Hz
GB     0
PC                 1.00
```

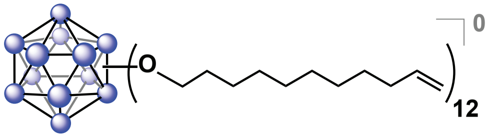
O
12
0

IR

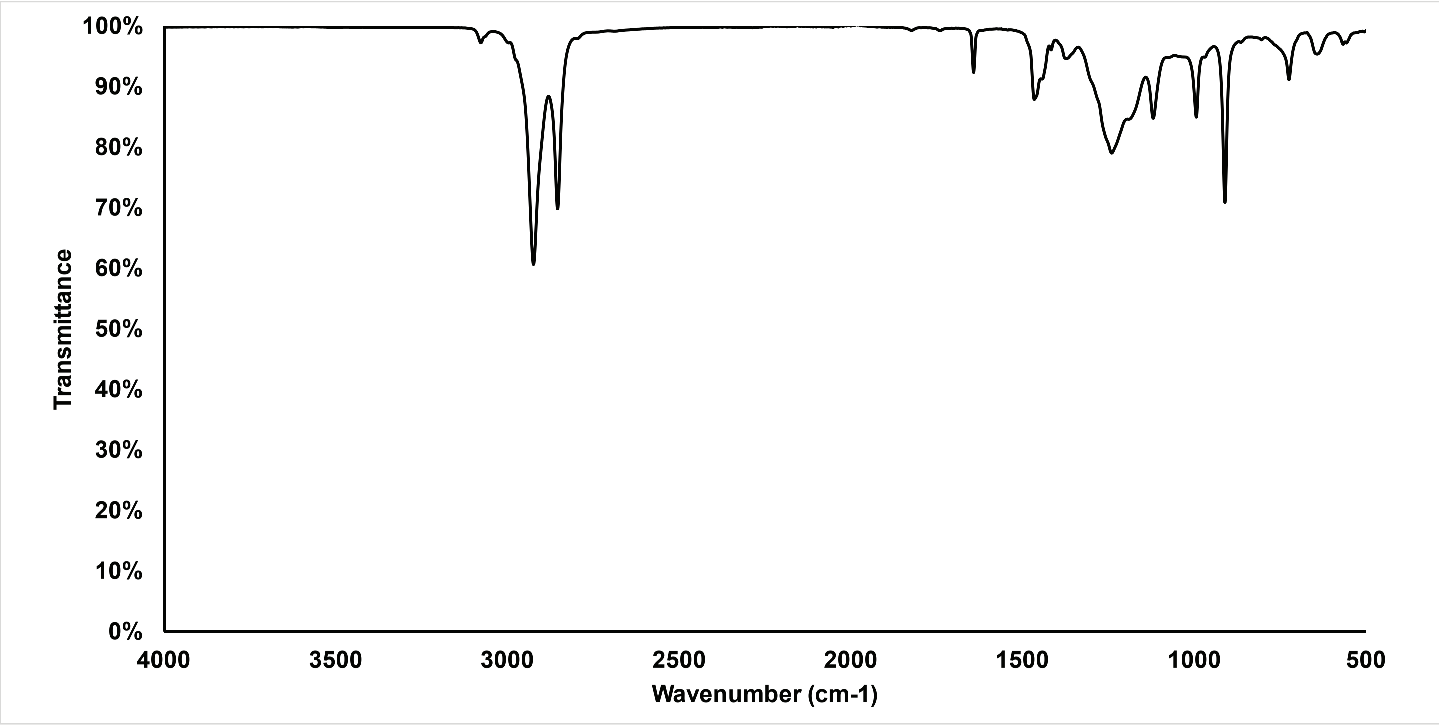
Transmittance
100%
90%
80%
70%
60%
50%
40%
30%
20%
10%
0%
4000
3500
3000
2500
2000
1500
1000
500
Wavenumber (cm-1)

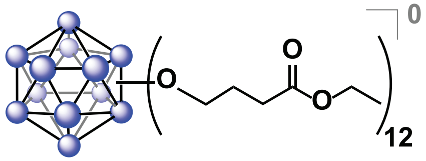

^{11}B {^{1}H} NMR

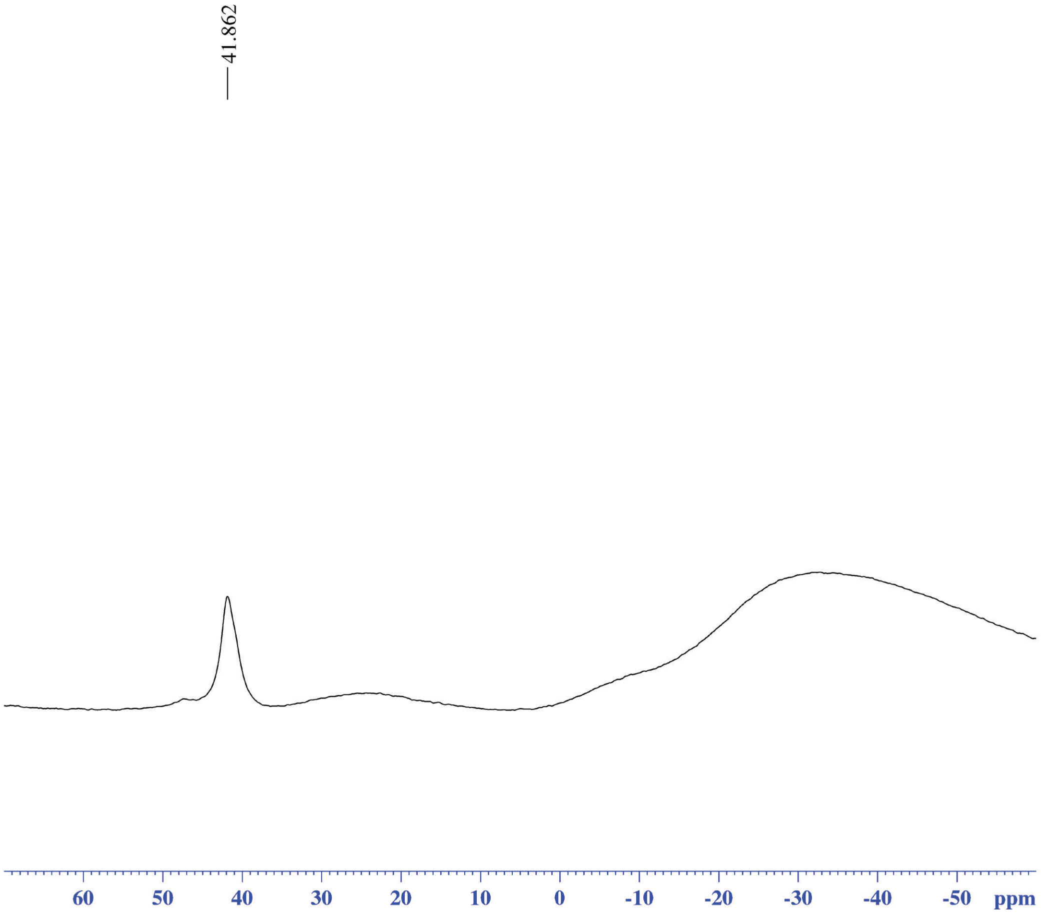

Current Data Parameters
NAME B12(O-EtButyr)12
EXPNO 110
PROCNO 1

F2 - Acquisition Parameters
Date_ 20150412
Time 19.19
INSTRUM av400
PROBHD 5 mm PABBO BB/
PULPROG zgdc.js
TD 5096
SOLVENT CDCl3
NS 1024
DS 0
SWH 51020.406 Hz
FIDRES 10.011854 Hz
AQ 0.0499408 sec
RG 189.85
DW 9.800 usec
DE 6.50 usec
TE 299.1 K
D1 0.00000400 sec
D11 0.03000000 sec
TD0 1

======== CHANNEL f1 ========
SFO1 128.3776052 MHz
NUC1 11B
P1 10.00 usec
PLW1 52.00000000 W

======== CHANNEL f2 ========
SFO2 400.1324008 MHz
NUC2 1H
CPDPRG[2 waltz16
PCPD2 90.00 usec
PLW2 13.00000000 W
PLW12 0.36111000 W

F2 - Processing parameters
SI 32768
SF 128.3776050 MHz
WDW EM
SSB 0
LB 50.00 Hz
GB 0
PC 1.40

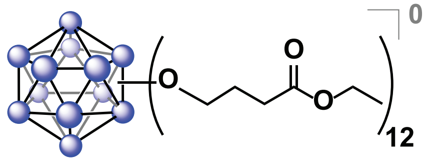

^{13}C NMR

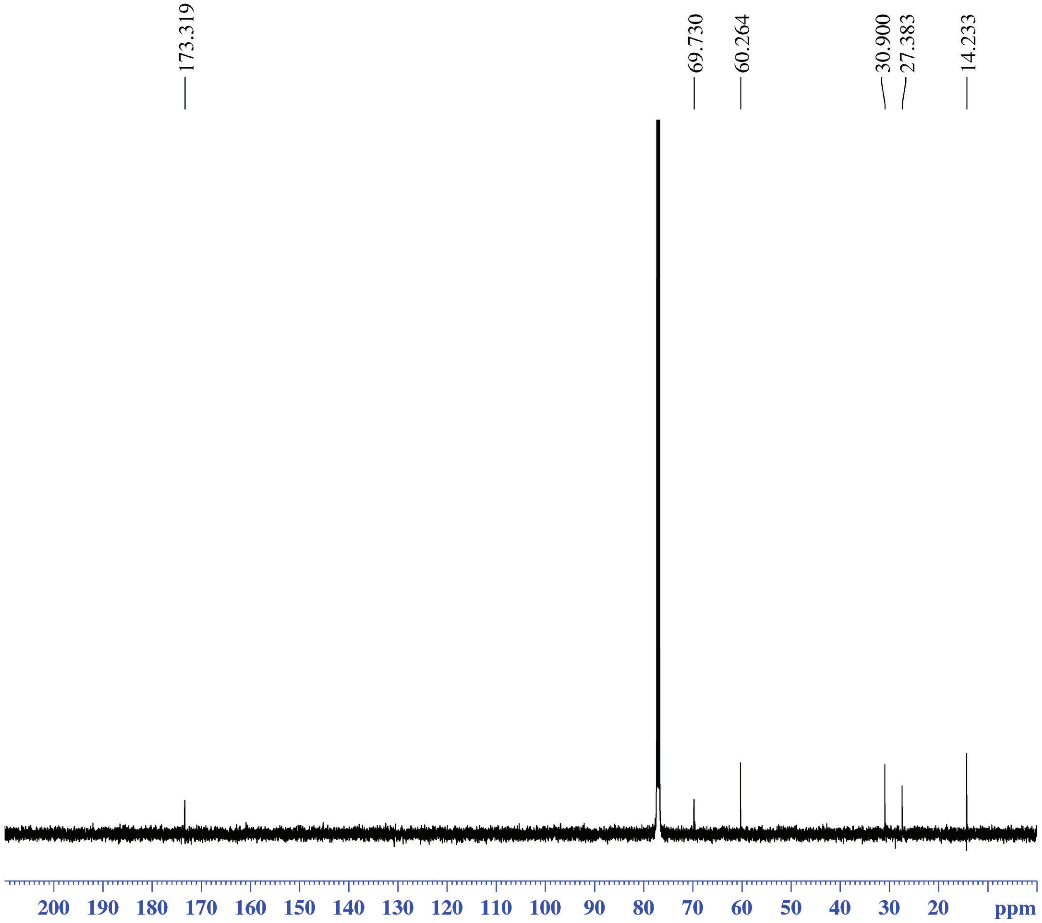

```
Current Data Parameters
NAME     B12(O-EtButyr)12
EXPNO              60
PROCNO              1

F2 - Acquisition Parameters
Date_        20150406
Time            23.42
INSTRUM         av500
PROBHD   5 mm DCH 13C-1
PULPROG        zgpg30
TD              65536
SOLVENT         CDCl3
NS                 64
DS                  2
SWH        31250.000 Hz
FIDRES      0.476837 Hz
AQ         1.0485760 sec
RG             204.54
DW             16.000 usec
DE              18.00 usec
TE              298.0 K
D1         2.00000000 sec
D11        0.03000000 sec
TD0                 1

======== CHANNEL f1 ========
SFO1      125.7722511 MHz
NUC1              13C
P1               9.63 usec
PLW1      23.00000000 W

======== CHANNEL f2 ========
SFO2      500.1330008 MHz
NUC2               1H
CPDPRG[2        waltz16
PCPD2           80.00 usec
PLW2      13.50000000 W
PLW12      0.21094000 W
PLW13      0.13500001 W

F2 - Processing parameters
SI             131072
SF        125.7577890 MHz
WDW                EM
SSB     0
LB               1.00 Hz
GB      0
PC               1.40
```

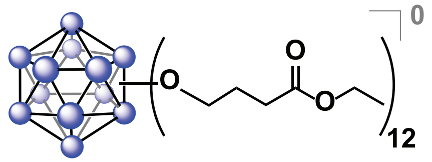

^{1}H NMR

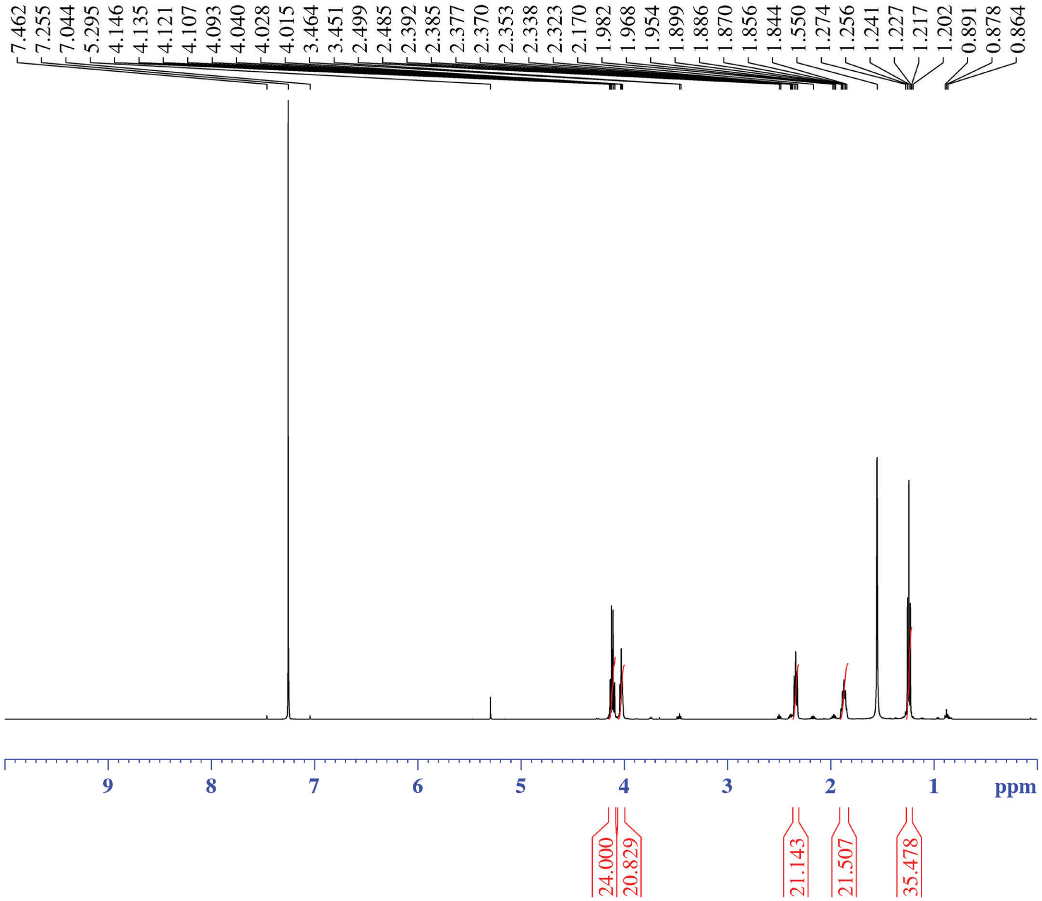

```
Current Data Parameters
NAME     B12(O-EtButyr)12
EXPNO               61
PROCNO               1

F2 - Acquisition Parameters
Date_         20150406
Time             23.44
INSTRUM          av500
PROBHD  5 mm DCH 13C-1
PULPROG           zg30
TD               65536
SOLVENT          CDCl3
NS                   8
DS                   0
SWH        10000.000 Hz
FIDRES      0.152588 Hz
AQ         3.2767999 sec
RG               59.34
DW           50.000 usec
DE           10.00 usec
TE             298.0 K
D1       2.00000000 sec
TD0                  1

======== CHANNEL f1 ========
SFO1     500.1330008 MHz
NUC1                1H
P1          10.00 usec
PLW1      13.50000000 W

F2 - Processing parameters
SI               65536
SF       500.1300146 MHz
WDW                 EM
SSB    0
LB             0.30 Hz
GB     0
PC                1.00
```

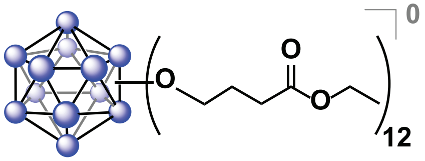

Q Exactive
High-Res Mass Spec

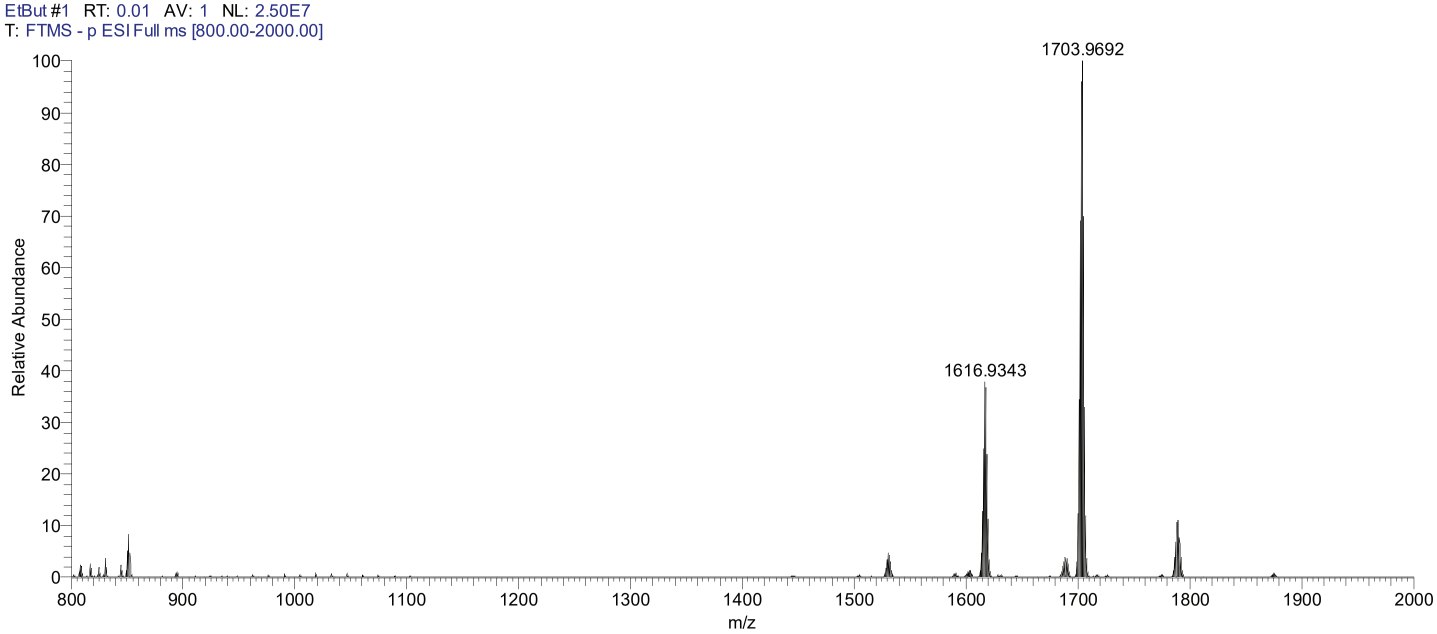

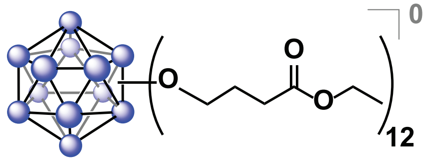

Q Exactive
High-Res Mass Spec

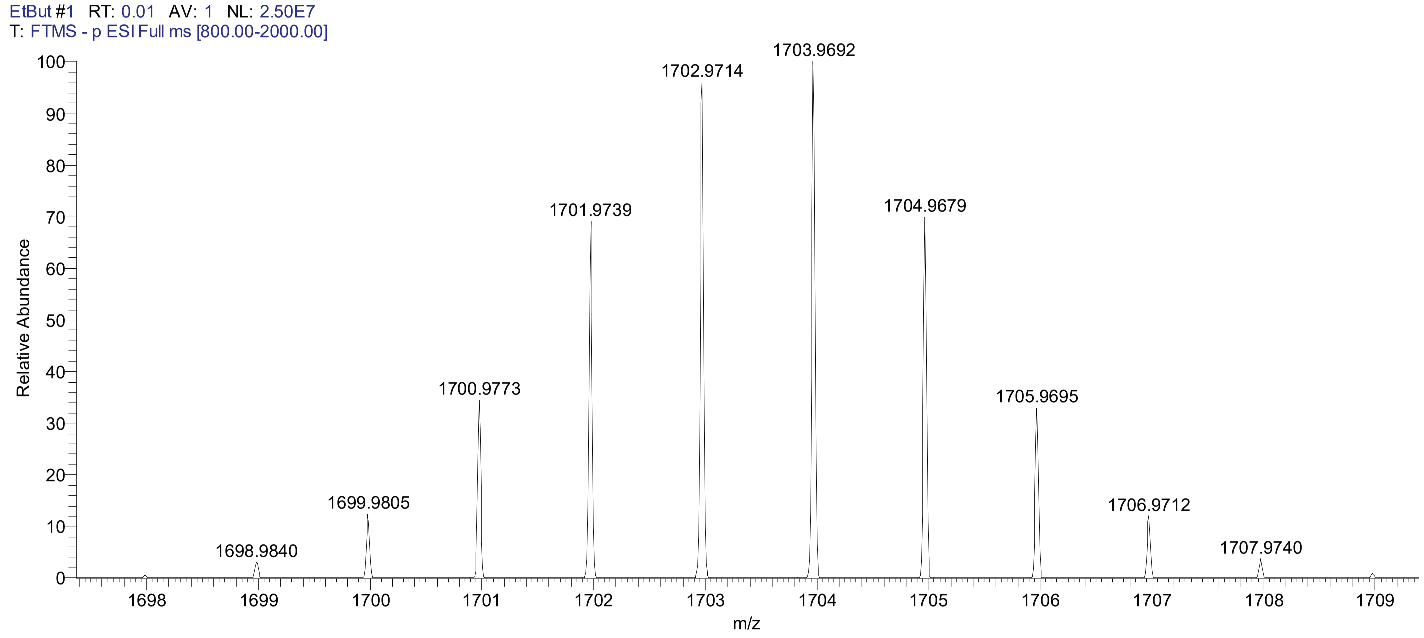

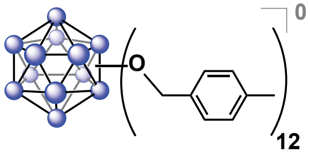

$^{11}B\ \{^1H\}$ NMR

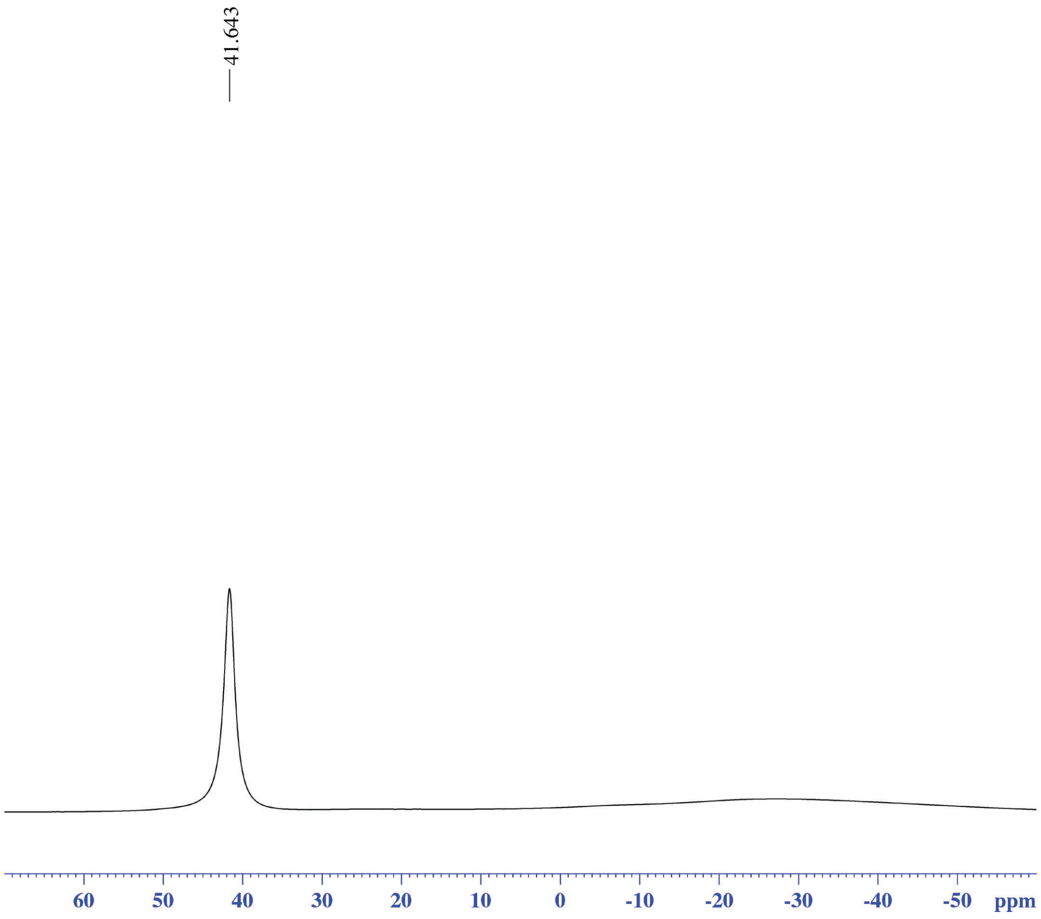

Current Data Parameters

NAME	Aug29-2015
EXPNO	160
PROCNO	1

F2 - Acquisition Parameters

Date_	20150829
Time	21.02
INSTRUM	av400
PROBHD	5 mm PABBO BB/
PULPROG	zgdc.js
TD	5096
SOLVENT	CDCl3
NS	1024
DS	0
SWH	51020.406 Hz
FIDRES	10.011854 Hz
AQ	0.0499408 sec
RG	189.85
DW	9.800 usec
DE	6.50 usec
TE	299.3 K
D1	0.00000400 sec
D11	0.03000000 sec
TD0	1

======== CHANNEL f1 ========

SFO1	128.3776052 MHz
NUC1	11B
P1	10.00 usec
PLW1	52.00000000 W

======== CHANNEL f2 ========

SFO2	400.1324008 MHz
NUC2	1H
CPDPRG[2	waltz16
PCPD2	90.00 usec
PLW2	13.00000000 W
PLW12	0.36111000 W

F2 - Processing parameters

SI	32768
SF	128.3776050 MHz
WDW	EM
SSB	0
LB	50.00 Hz
GB	0
PC	1.40

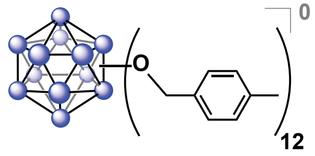

^{13}C NMR

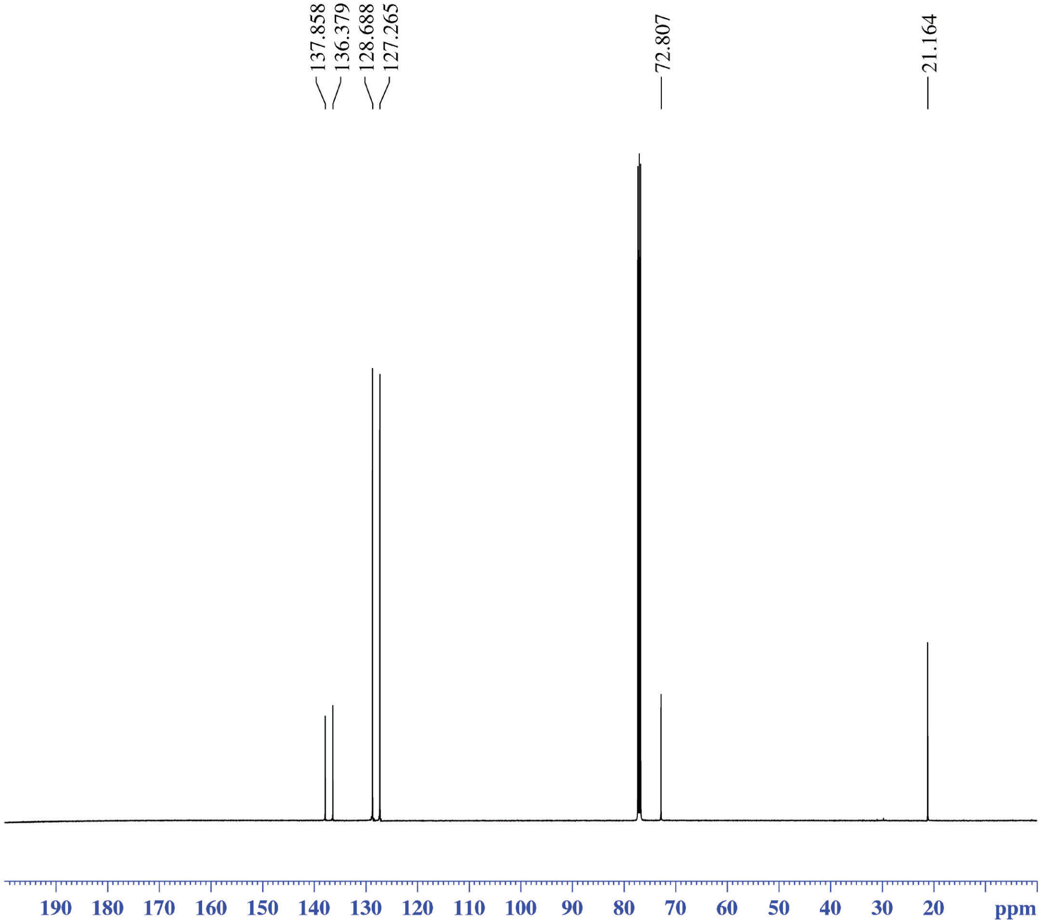

Current Data Parameters
NAME B12(O-4-MeBn)12
EXPNO 60
PROCNO 1

F2 - Acquisition Parameters
Date_ 20150829
Time 22.04
INSTRUM av500
PROBHD 5 mm DCH 13C-1
PULPROG zgpg30
TD 65536
SOLVENT CDCl3
NS 256
DS 2
SWH 31250.000 Hz
FIDRES 0.476837 Hz
AQ 1.0485760 sec
RG 204.54
DW 16.000 usec
DE 18.00 usec
TE 298.0 K
D1 2.00000000 sec
D11 0.03000000 sec
TD0 1

======== CHANNEL f1 ========
SFO1 125.7722511 MHz
NUC1 13C
P1 9.63 usec
PLW1 23.00000000 W

======== CHANNEL f2 ========
SFO2 500.1330008 MHz
NUC2 1H
CPDPRG[2 waltz16
PCPD2 80.00 usec
PLW2 13.50000000 W
PLW12 0.21094000 W
PLW13 0.13500001 W

F2 - Processing parameters
SI 131072
SF 125.7577890 MHz
WDW EM
SSB 0
LB 1.00 Hz
GB 0
PC 1.40

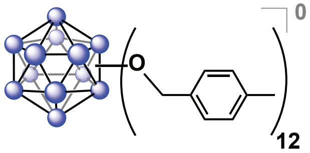

^{1}H NMR

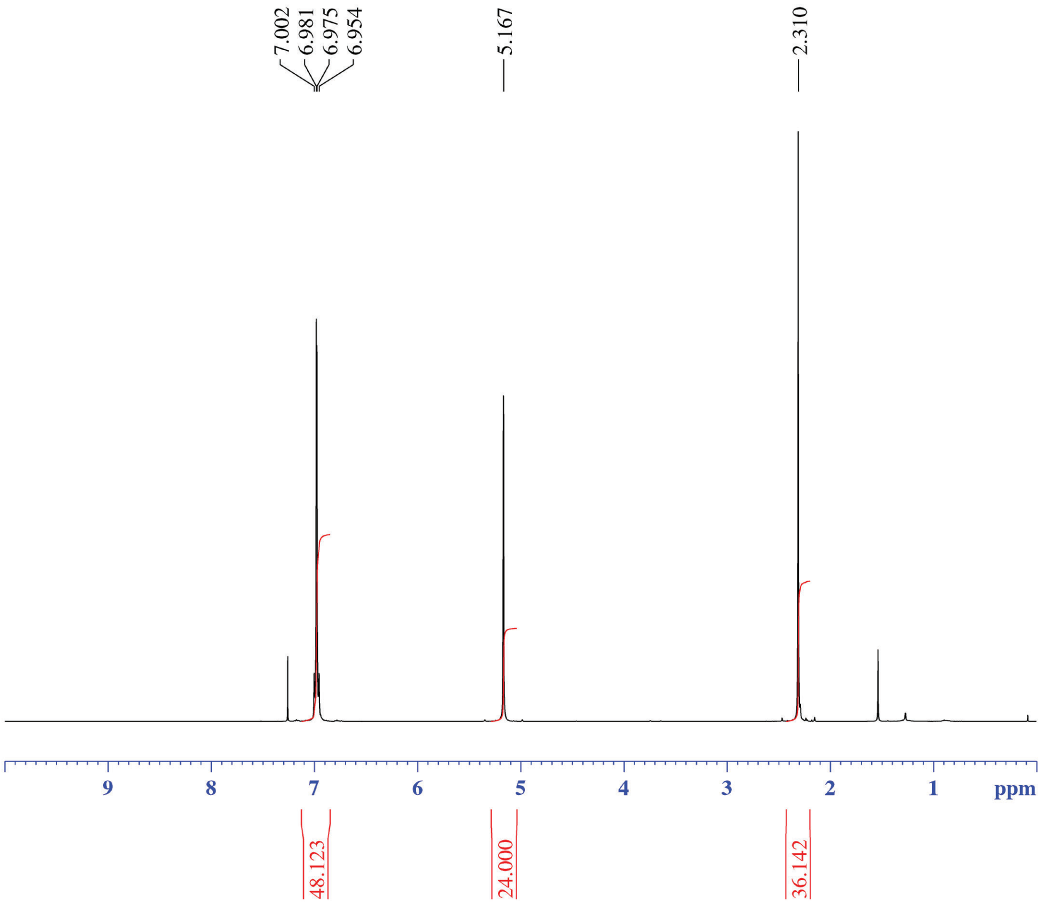

Current Data Parameters
NAME B12(O-4-MeBn)12
EXPNO 161
PROCNO 1

F2 - Acquisition Parameters
Date_ 20150829
Time 21.05
INSTRUM av400
PROBHD 5 mm PABBO BB/
PULPROG zg30
TD 52882
SOLVENT CDCl3
NS 32
DS 0
SWH 8012.820 Hz
FIDRES 0.151523 Hz
AQ 3.2998369 sec
RG 155.85
DW 62.400 usec
DE 6.50 usec
TE 299.0 K
D1 2.00000000 sec
TD0 1

======== CHANNEL f1 ========
SFO1 400.1324008 MHz
NUC1 1H
P1 15.00 usec
PLW1 13.00000000 W

F2 - Processing parameters
SI 65536
SF 400.1300184 MHz
WDW EM
SSB 0
LB 0.30 Hz
GB 0
PC 1.00

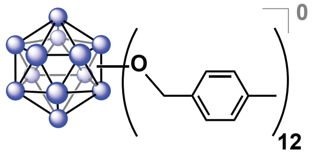

Q Exactive
High-Res Mass Spec

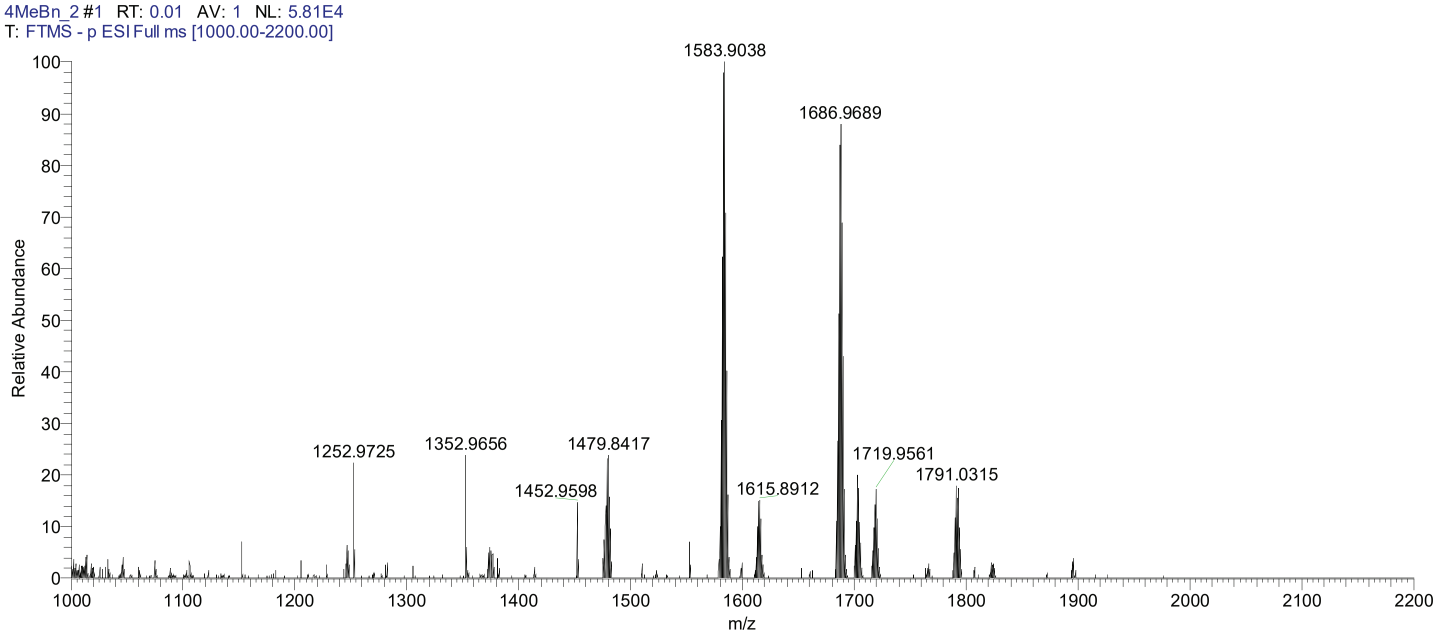

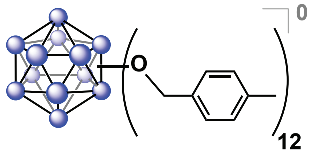

Q Exactive
High-Res Mass Spec

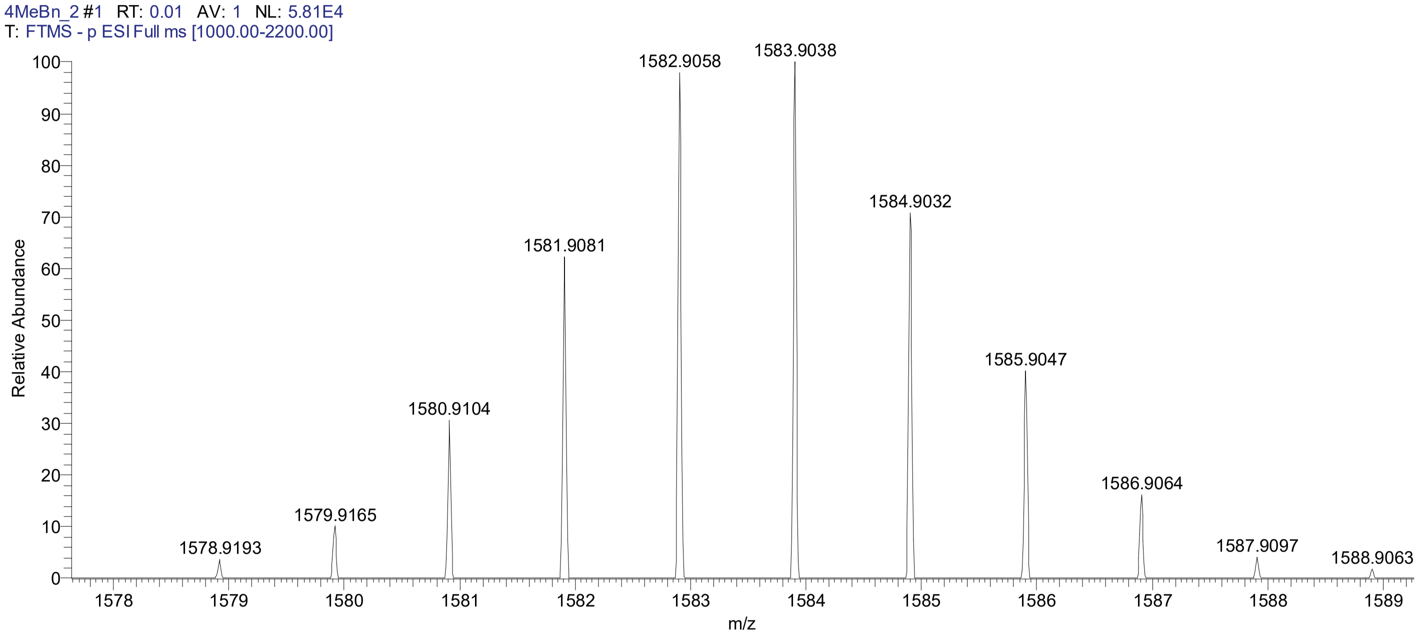

$^{11}B\ \{^1H\}$ NMR

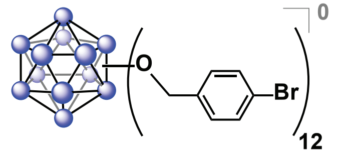

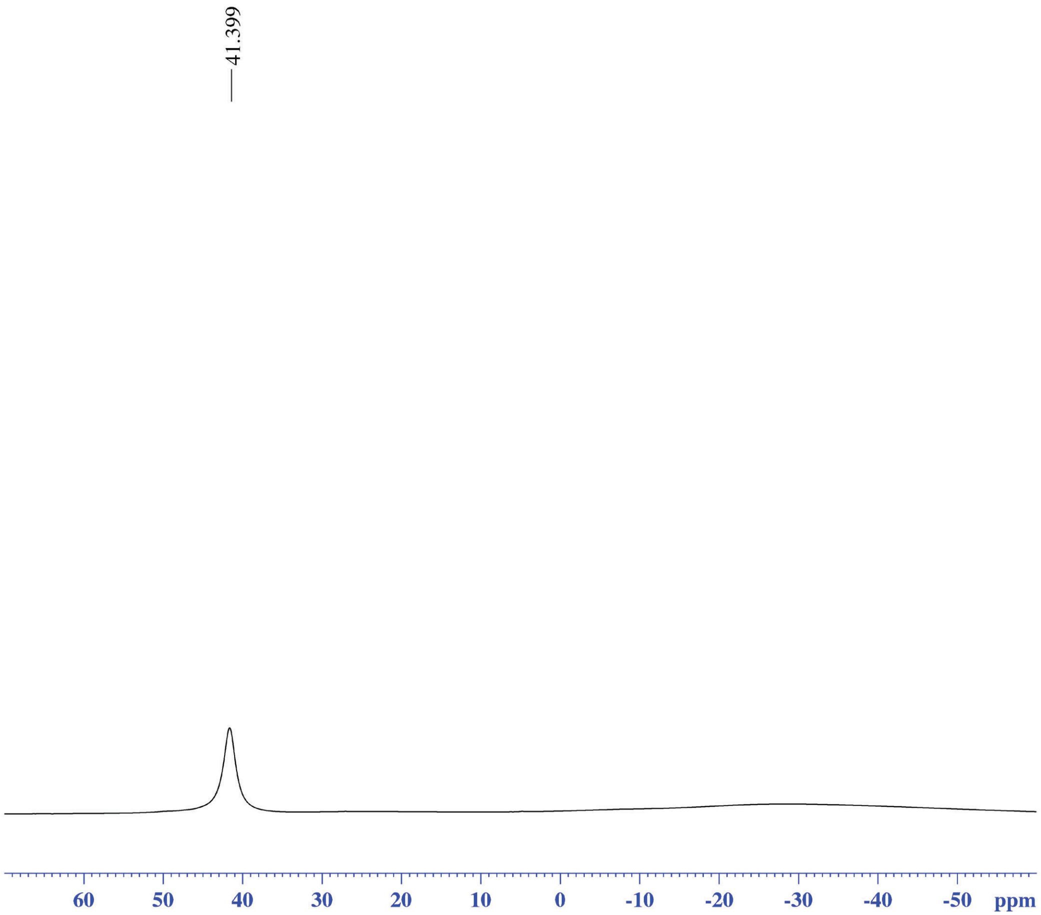

```
Current Data Parameters
NAME     B12(O-4-BrBn)12
EXPNO              10
PROCNO              1

F2 - Acquisition Parameters
Date_         20150624
Time             10.50
INSTRUM          av400
PROBHD   5 mm PABBO BB/
PULPROG        zgdc.js
TD                5096
SOLVENT          CDCl3
NS                1024
DS                   0
SWH       51020.406 Hz
FIDRES    10.011854 Hz
AQ        0.0499408 sec
RG              189.85
DW           9.800 usec
DE            6.50 usec
TE             299.1 K
D1       0.00000400 sec
D11      0.03000000 sec
TD0                  1

======== CHANNEL f1 ========
SFO1      128.3776052 MHz
NUC1                  11B
P1             10.00 usec
PLW1        52.00000000 W

======== CHANNEL f2 ========
SFO2      400.1324008 MHz
NUC2                   1H
CPDPRG[2          waltz16
PCPD2          90.00 usec
PLW2        13.00000000 W
PLW12        0.36111000 W

F2 - Processing parameters
SI               32768
SF      128.3776050 MHz
WDW                 EM
SSB     0
LB            50.00 Hz
GB      0
PC                1.40
```

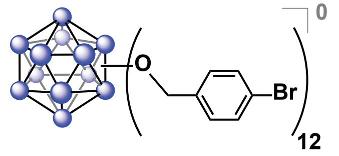

^{13}C NMR

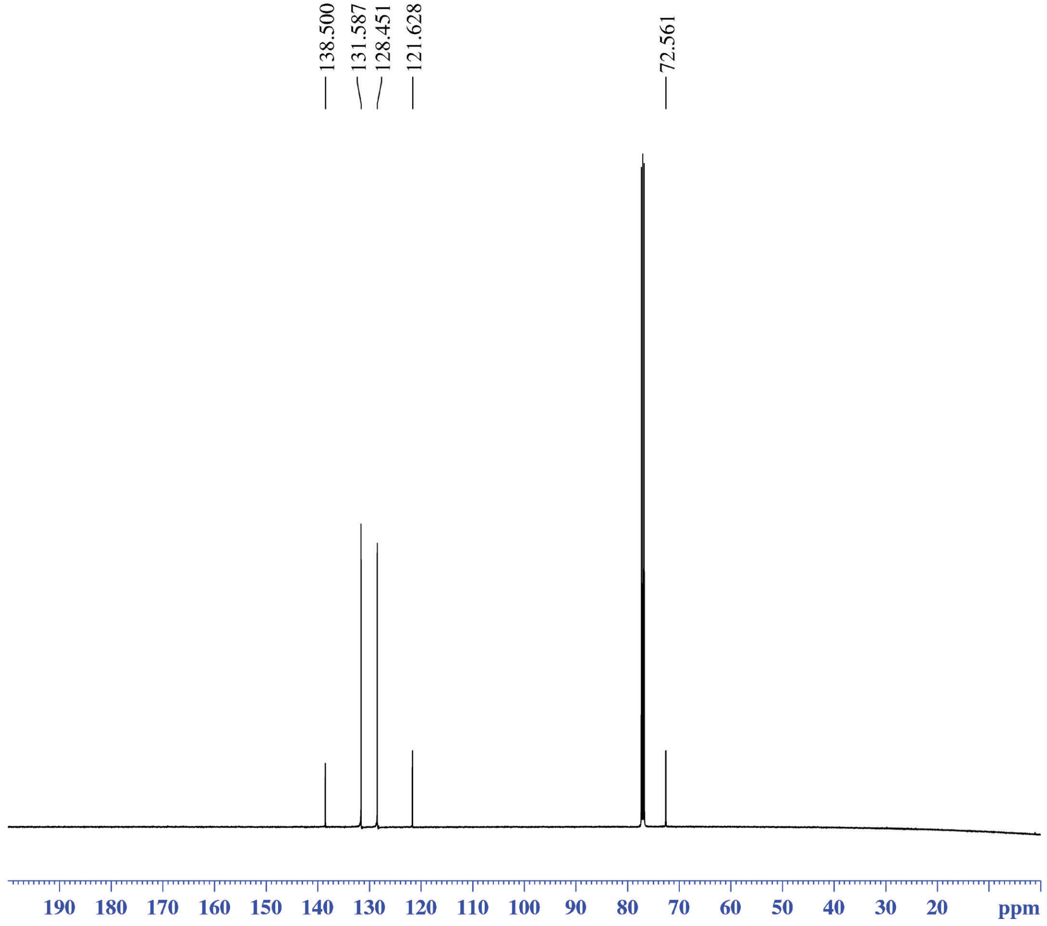

```
Current Data Parameters
NAME     Jan13-2016-awixtrom
EXPNO              10
PROCNO              1

F2 - Acquisition Parameters
Date_        20160113
Time            15.37
INSTRUM         av500
PROBHD   5 mm DCH 13C-1
PULPROG        zgpg30
TD              65536
SOLVENT         CDCl3
NS                256
DS                  2
SWH        31250.000 Hz
FIDRES      0.476837 Hz
AQ         1.0485760 sec
RG             204.54
DW             16.000 usec
DE              18.00 usec
TE              298.0 K
D1         2.00000000 sec
D11        0.03000000 sec
TD0                 1

======== CHANNEL f1 ========
SFO1      125.7722511 MHz
NUC1              13C
P1               9.63 usec
PLW1      23.00000000 W

======== CHANNEL f2 ========
SFO2      500.1330008 MHz
NUC2               1H
CPDPRG[2       waltz16
PCPD2           80.00 usec
PLW2      13.50000000 W
PLW12      0.21094000 W
PLW13      0.13500001 W

F2 - Processing parameters
SI             131072
SF        125.7577890 MHz
WDW                EM
SSB     0
LB               1.00 Hz
GB      0
PC               1.40
```

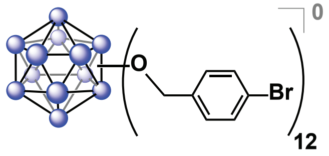

^{1}H NMR

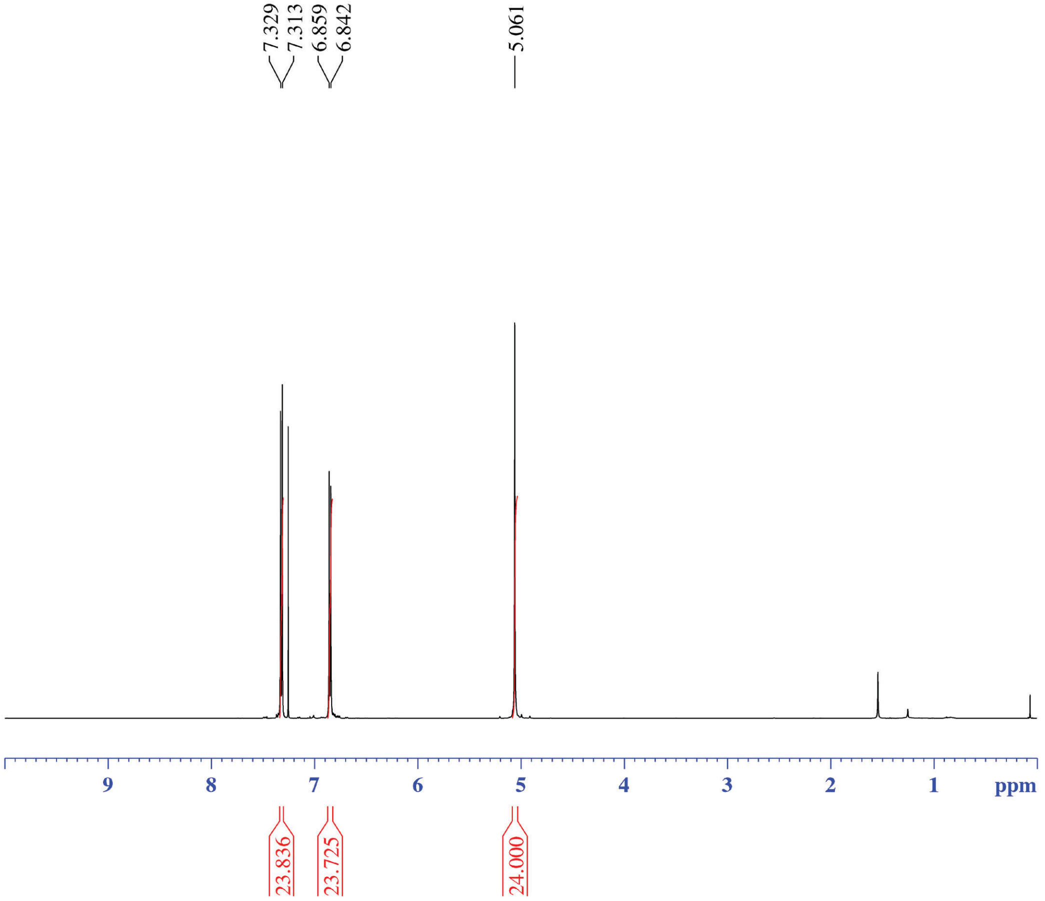

Current Data Parameters
NAME Jan13-2016-awixtrom
EXPNO 11
PROCNO 1

F2 - Acquisition Parameters
Date_ 20160113
Time 15.40
INSTRUM av500
PROBHD 5 mm DCH 13C-1
PULPROG zg30
TD 65536
SOLVENT CDCl3
NS 16
DS 0
SWH 10000.000 Hz
FIDRES 0.152588 Hz
AQ 3.2767999 sec
RG 52.41
DW 50.000 usec
DE 10.00 usec
TE 298.0 K
D1 2.00000000 sec
TD0 1

======== CHANNEL f1 ========
SFO1 500.1330008 MHz
NUC1 1H
P1 10.00 usec
PLW1 13.50000000 W

F2 - Processing parameters
SI 65536
SF 500.1300146 MHz
WDW EM
SSB 0
LB 0.30 Hz
GB 0
PC 1.00

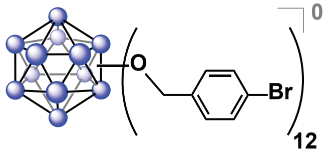

Q Exactive
High-Res Mass Spec

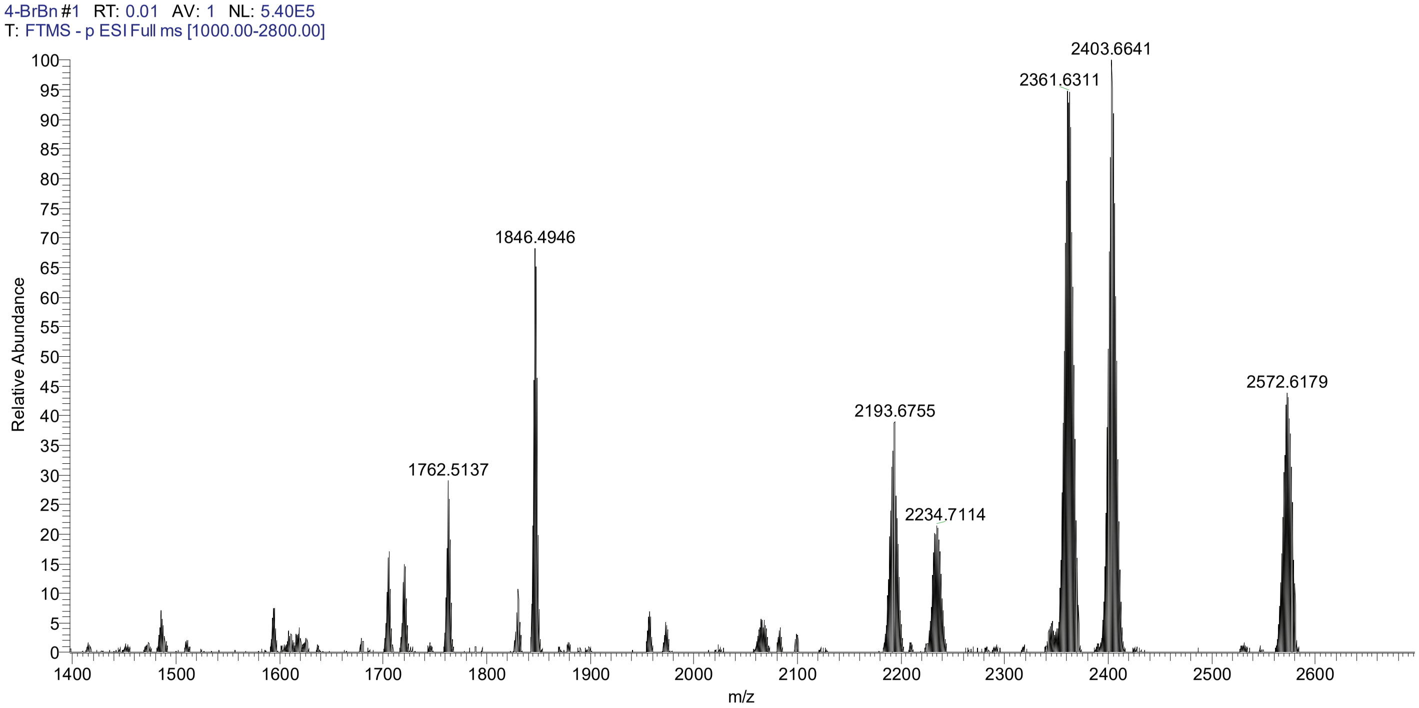

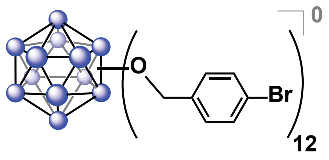

Q Exactive
High-Res Mass Spec

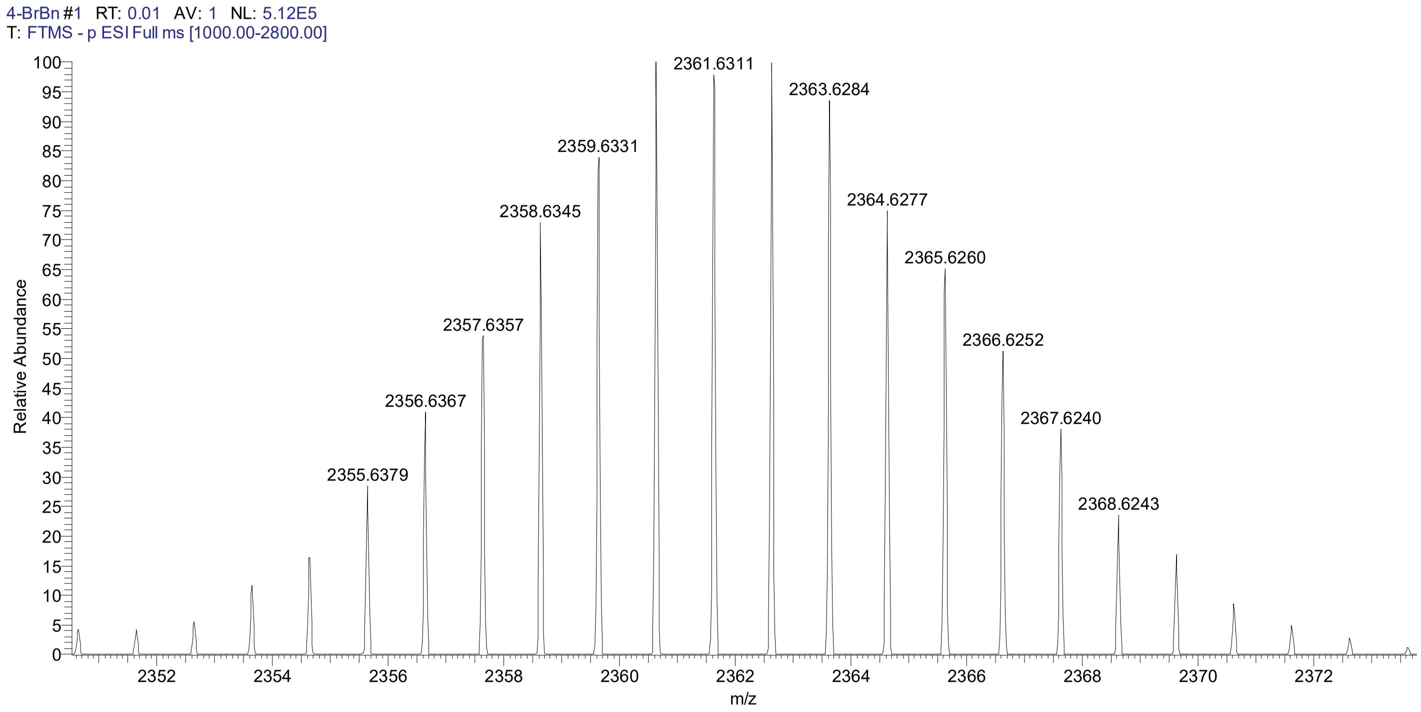

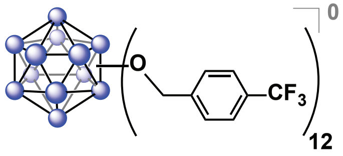

$^{11}B\ \{^1H\}$ NMR

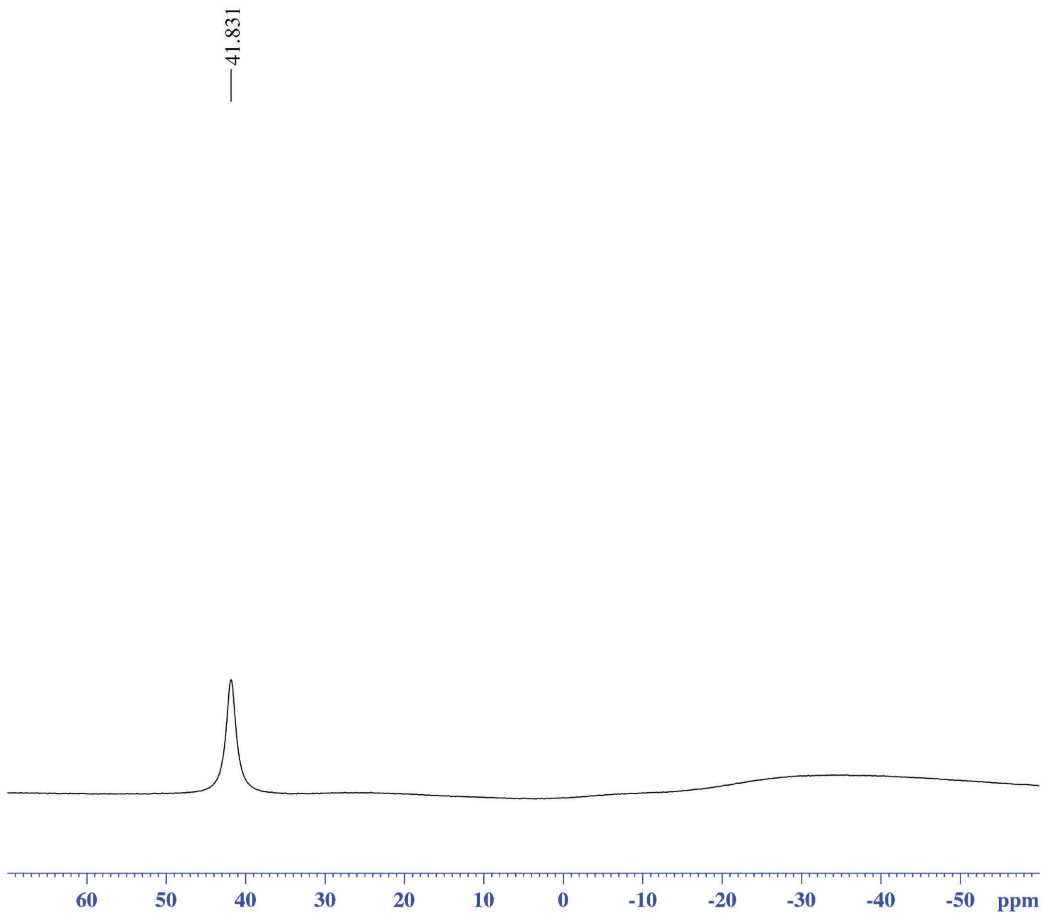

```
Current Data Parameters
NAME     B12(O-4-TFMBn)12
EXPNO              40
PROCNO              1

F2 - Acquisition Parameters
Date_        20150927
Time            14.58
INSTRUM         av400
PROBHD   5 mm PABBO BB/
PULPROG       zgdc.js
TD               5096
SOLVENT         CDCl3
NS               1024
DS                  0
SWH      51020.406 Hz
FIDRES   10.011854 Hz
AQ       0.0499408 sec
RG             189.85
DW          9.800 usec
DE           6.50 usec
TE            299.3 K
D1     0.05000000 sec
D11    0.03000000 sec
TD0                 1

======== CHANNEL f1 ========
SFO1   128.3776052 MHz
NUC1              11B
P1         10.00 usec
PLW1    52.00000000 W

======== CHANNEL f2 ========
SFO2   400.1324008 MHz
NUC2               1H
CPDPRG[2      waltz16
PCPD2      90.00 usec
PLW2    13.00000000 W
PLW12    0.36111000 W

F2 - Processing parameters
SI              32768
SF     128.3776161 MHz
WDW                EM
SSB    0
LB           10.00 Hz
GB     0
PC               1.40
```

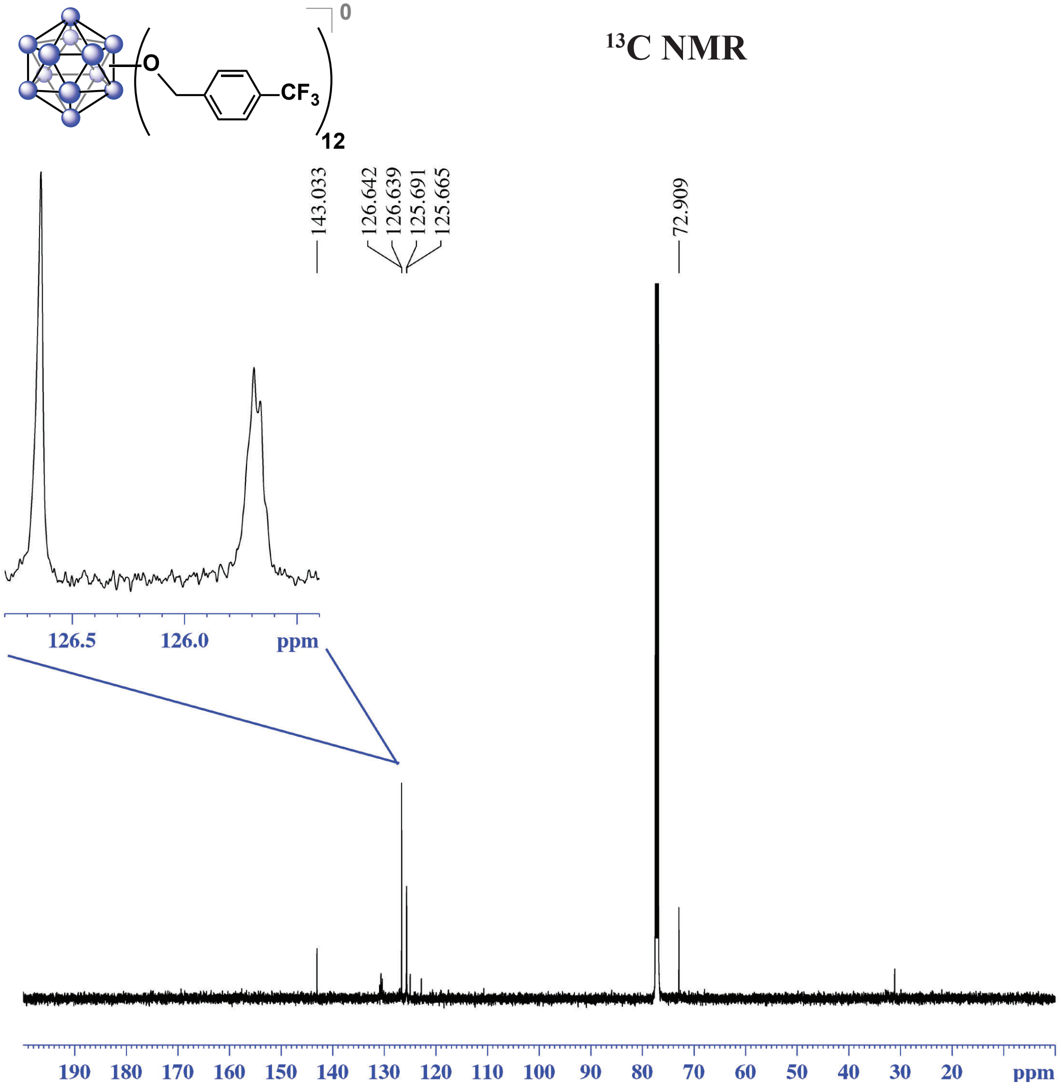

^{13}C NMR

```
Current Data Parameters
NAME     B12(O-4-TFMBn)12
EXPNO              20
PROCNO              1

F2 - Acquisition Parameters
Date_        20150928
Time            13.45
INSTRUM         av500
PROBHD   5 mm DCH 13C-1
PULPROG        zgpg30
TD              65536
SOLVENT         CDCl3
NS                 64
DS                  2
SWH        31250.000 Hz
FIDRES      0.476837 Hz
AQ         1.0485760 sec
RG             204.54
DW             16.000 usec
DE              18.00 usec
TE              298.0 K
D1         2.00000000 sec
D11        0.03000000 sec
TD0                 1

======== CHANNEL f1 ========
SFO1      125.7722511 MHz
NUC1              13C
P1               9.63 usec
PLW1      23.00000000 W

======== CHANNEL f2 ========
SFO2      500.1330008 MHz
NUC2               1H
CPDPRG[2        waltz16
PCPD2           80.00 usec
PLW2      13.50000000 W
PLW12      0.21094000 W
PLW13      0.13500001 W

F2 - Processing parameters
SI             131072
SF        125.7577722 MHz
WDW                EM
SSB     0
LB               1.00 Hz
GB      0
PC               1.40
```

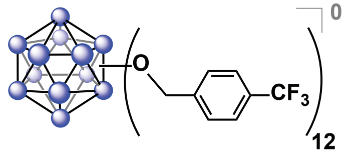

^{19}F NMR

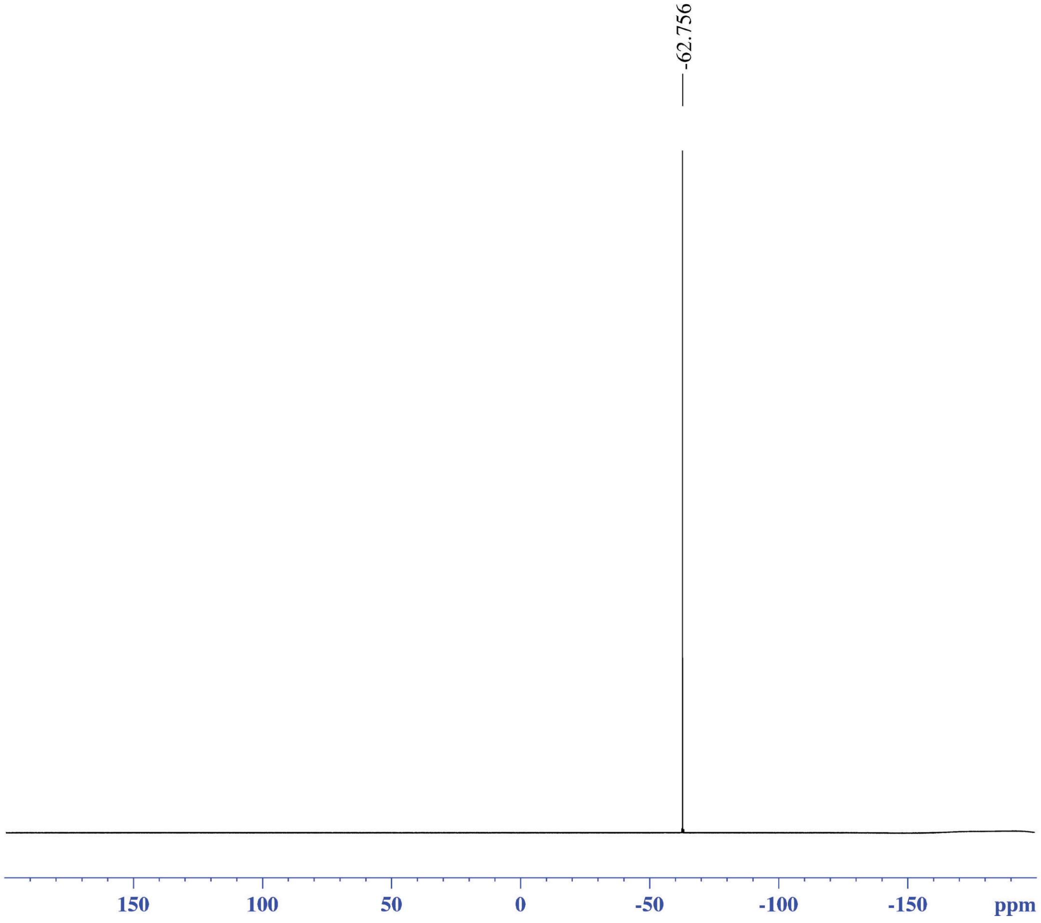

```
Current Data Parameters
NAME     B12(O-4-TFMBn)12
EXPNO              42
PROCNO              1

F2 - Acquisition Parameters
Date_         20150927
Time              15.05
INSTRUM          av400
PROBHD   5 mm PABBO BB/
PULPROG        zgflqn30
TD             262144
SOLVENT          CDCl3
NS                 64
DS                  0
SWH        150000.000 Hz
FIDRES        0.572205 Hz
AQ          0.8738133 sec
RG             189.85
DW              3.333 usec
DE              6.50 usec
TE              299.0 K
D1         2.00000000 sec
TD0                 1

======== CHANNEL f1 ========
SFO1      376.4983660 MHz
NUC1              19F
P1              14.50 usec
PLW1      17.00000000 W

F2 - Processing parameters
SI              262144
SF         376.4983660 MHz
WDW                EM
SSB     0
LB                1.00 Hz
GB      0
PC                1.00
```

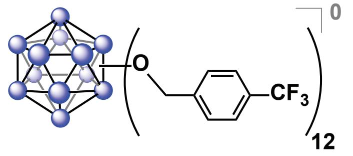

^{1}H NMR

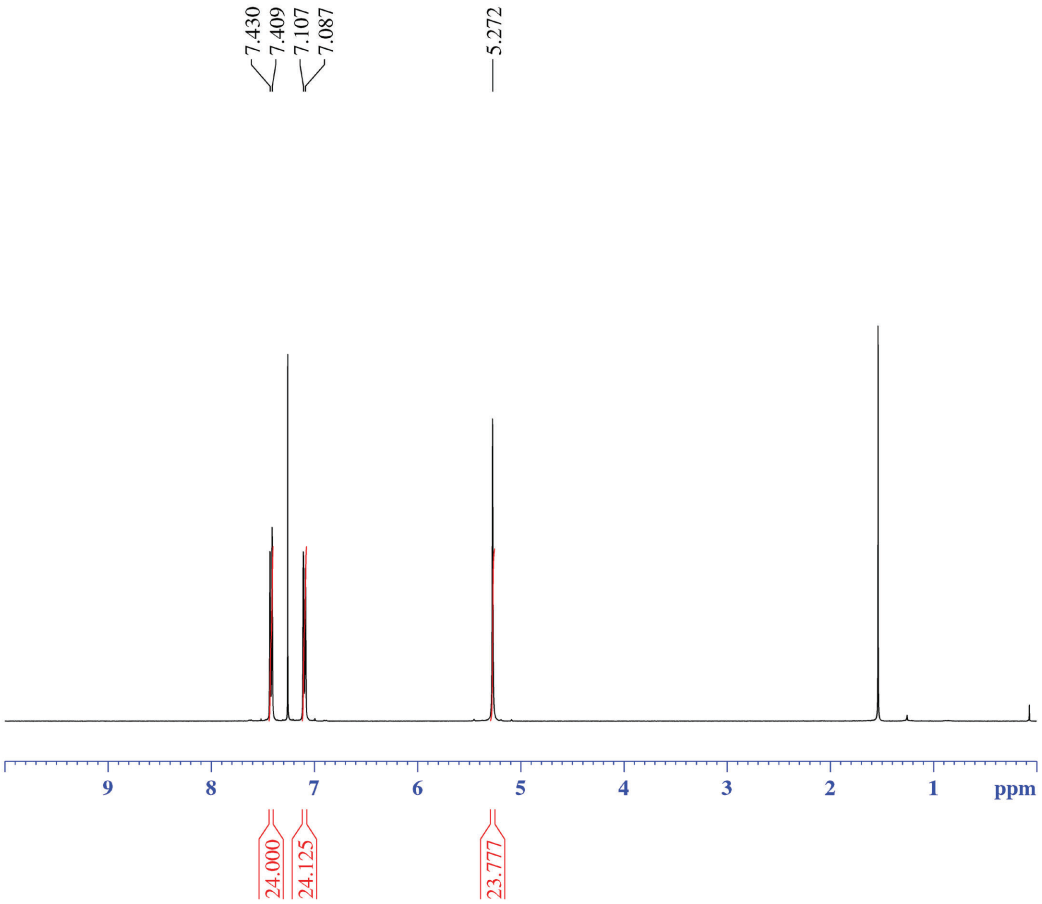

Current Data Parameters
NAME B12(O-4-TFMBn)12
EXPNO 41
PROCNO 1

F2 - Acquisition Parameters
Date_ 20150927
Time 15.01
INSTRUM av400
PROBHD 5 mm PABBO BB/
PULPROG zg30
TD 52882
SOLVENT CDCl3
NS 32
DS 0
SWH 8012.820 Hz
FIDRES 0.151523 Hz
AQ 3.2998369 sec
RG 189.85
DW 62.400 usec
DE 6.50 usec
TE 299.0 K
D1 2.00000000 sec
TD0 1

======== CHANNEL f1 ========
SFO1 400.1324008 MHz
NUC1 1H
P1 15.00 usec
PLW1 13.00000000 W

F2 - Processing parameters
SI 65536
SF 400.1300184 MHz
WDW EM
SSB 0
LB 0.30 Hz
GB 0
PC 1.00

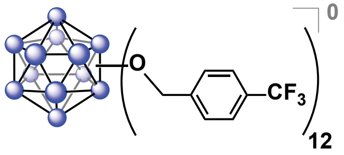

Q Exactive
High-Res Mass Spec

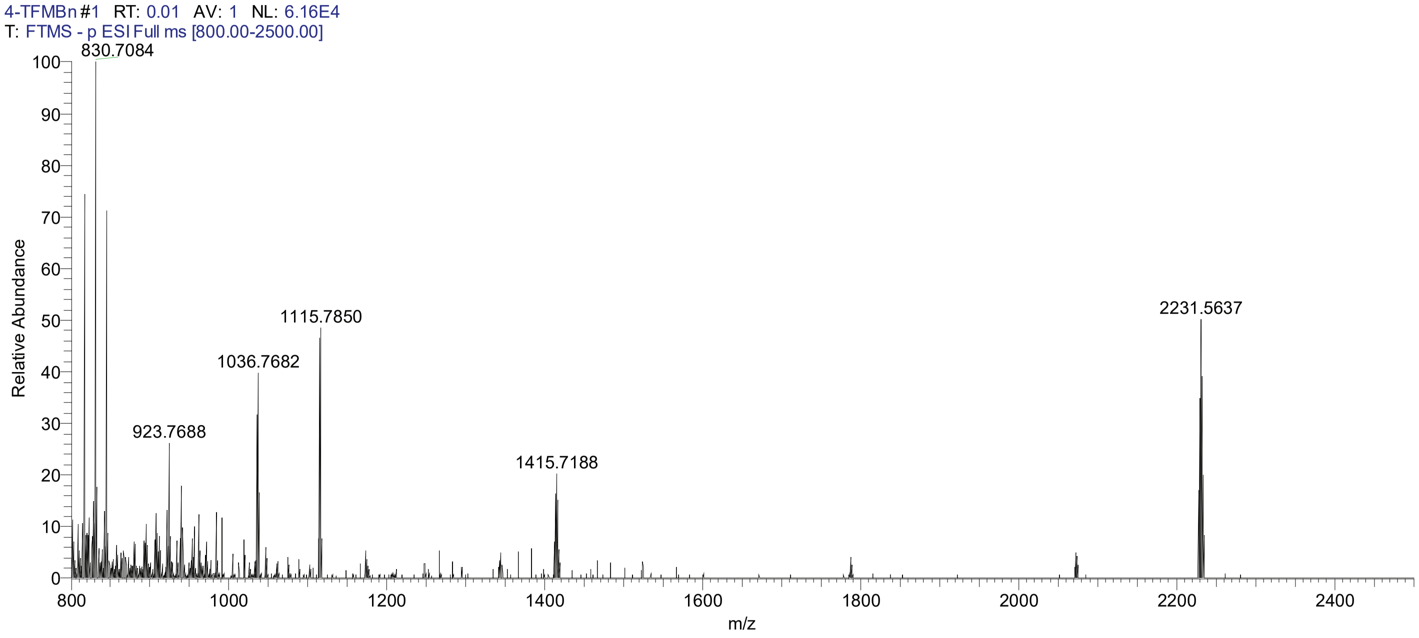

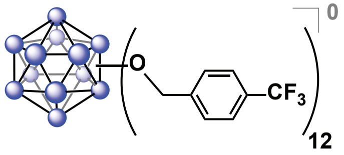

Q Exactive
High-Res Mass Spec

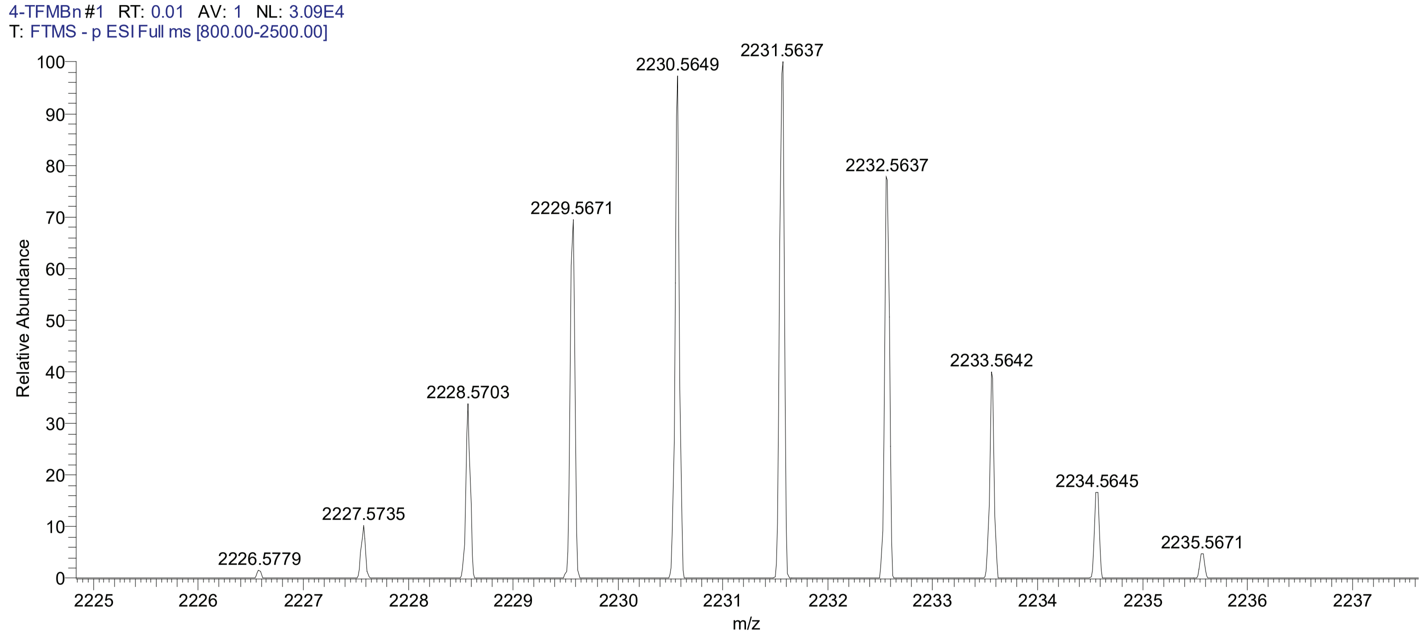

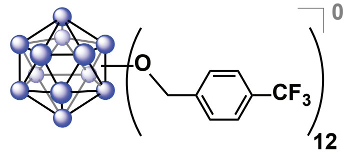
0
O
CF3
12

IR

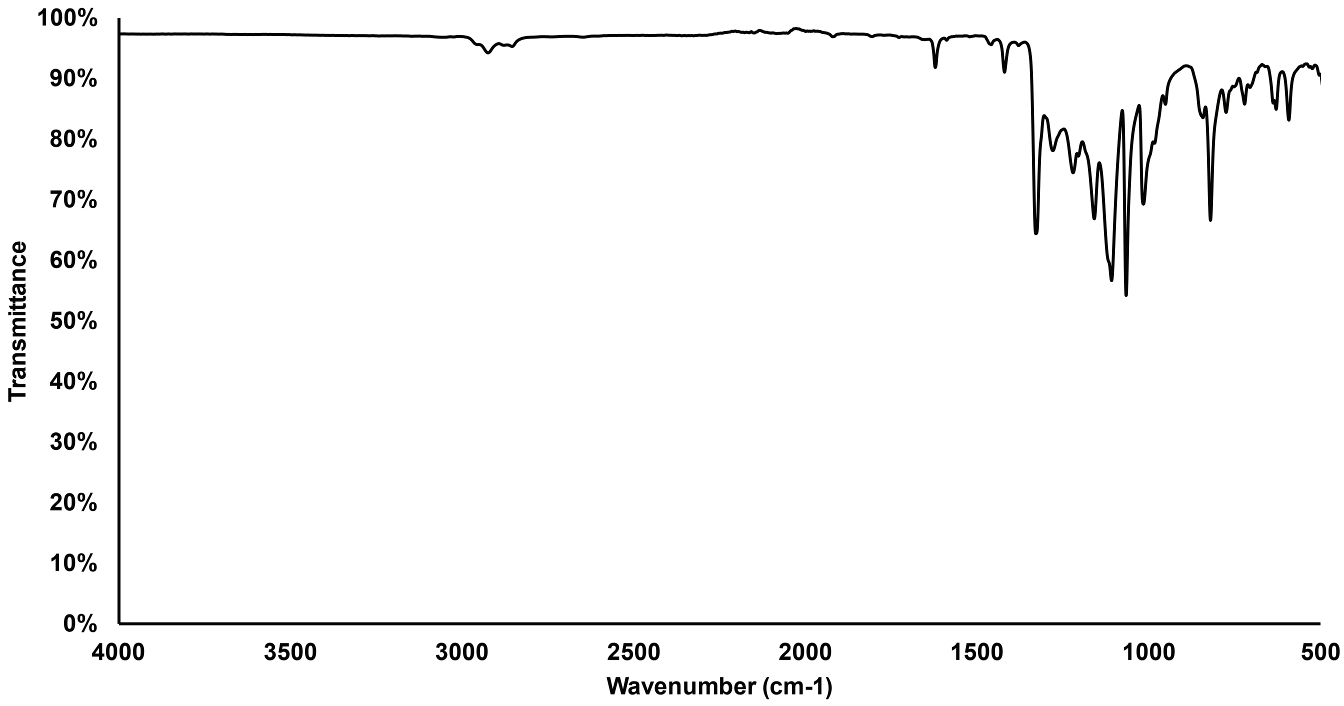
Transmittance
100%
90%
80%
70%
60%
50%
40%
30%
20%
10%
0%
4000
3500
3000
2500
2000
1500
1000
500
Wavenumber (cm-1)

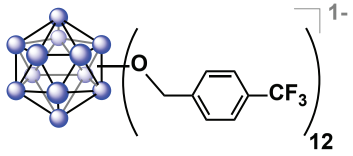
O
CF3
12
1-

IR

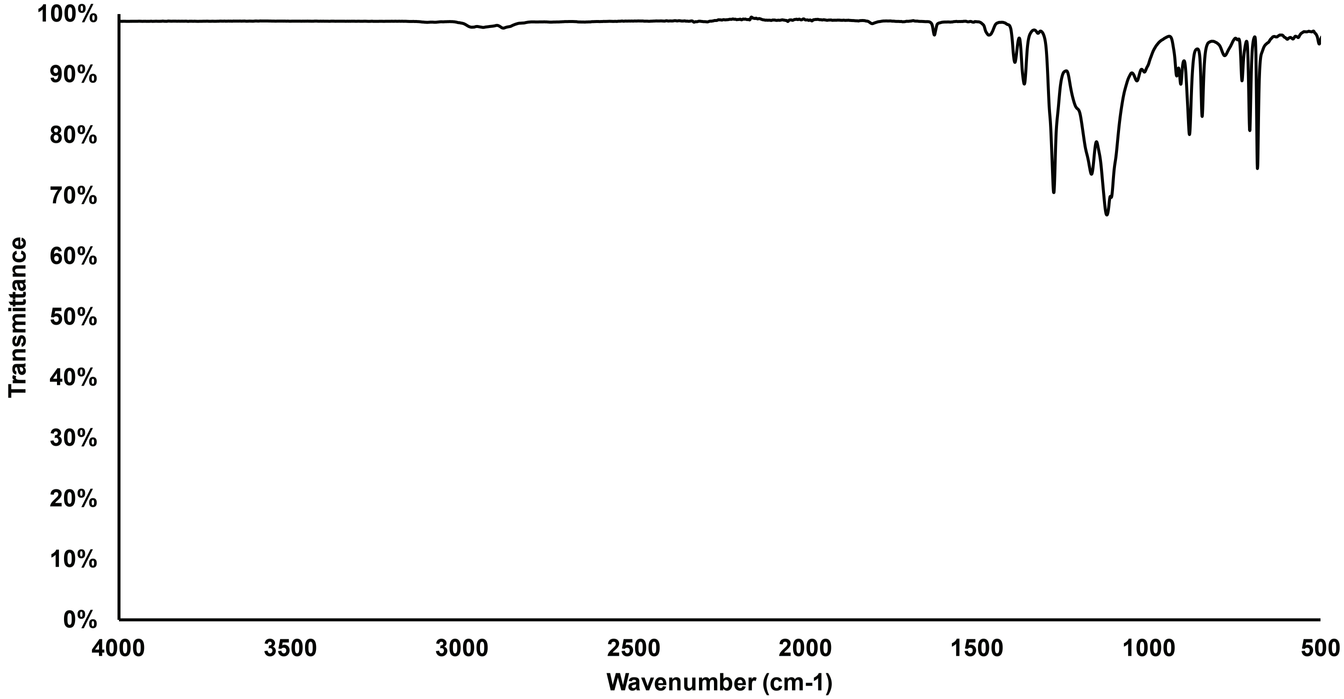
Transmittance
100%
90%
80%
70%
60%
50%
40%
30%
20%
10%
0%
4000
3500
3000
2500
2000
1500
1000
500
Wavenumber (cm-1)

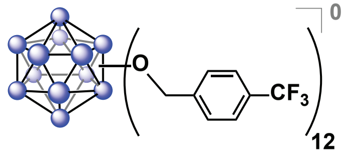
O
CF3
12
0

IR

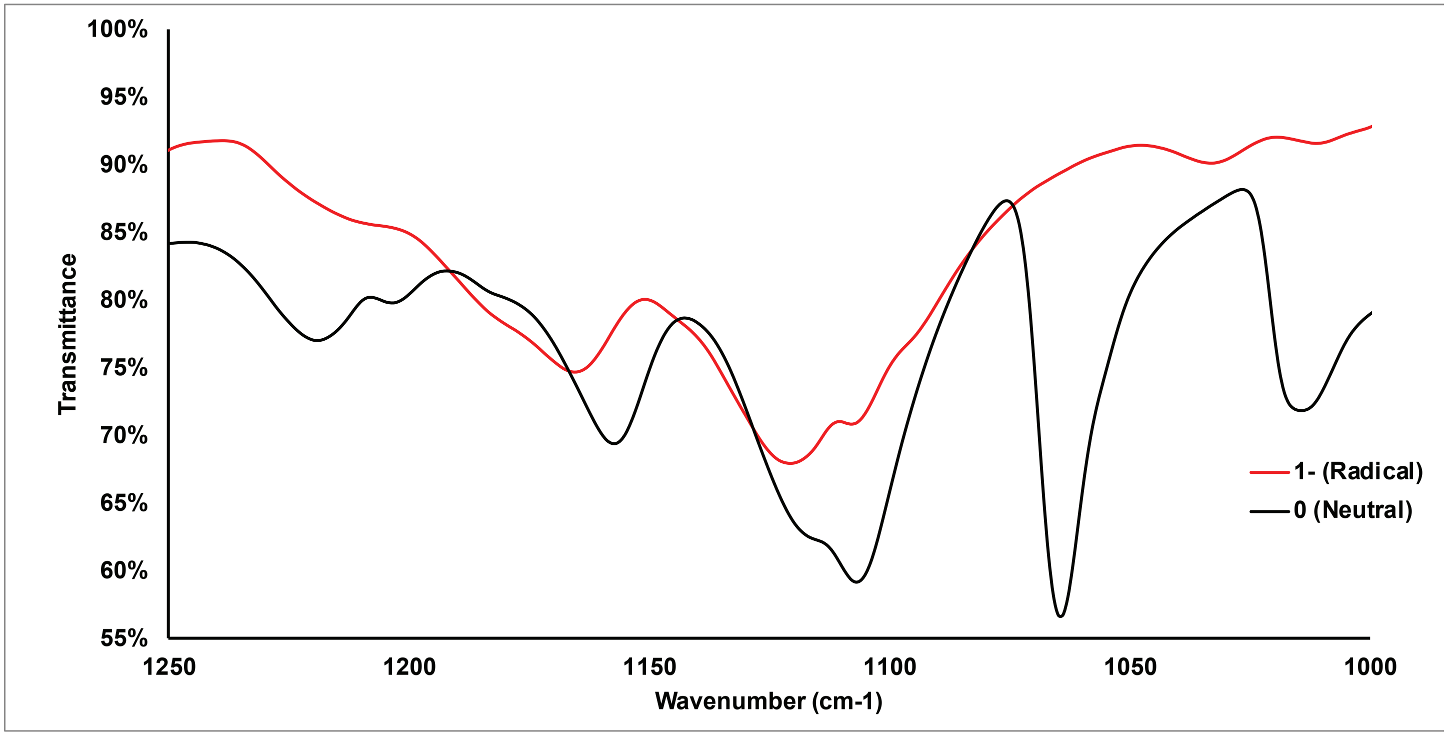
Transmittance
100%
95%
90%
85%
80%
75%
70%
65%
60%
55%
1250
1200
1150
1100
1050
1000
Wavenumber (cm-1)
1- (Radical)
0 (Neutral)

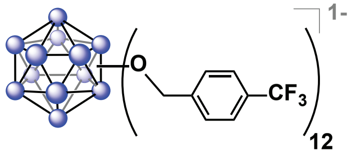

EPR

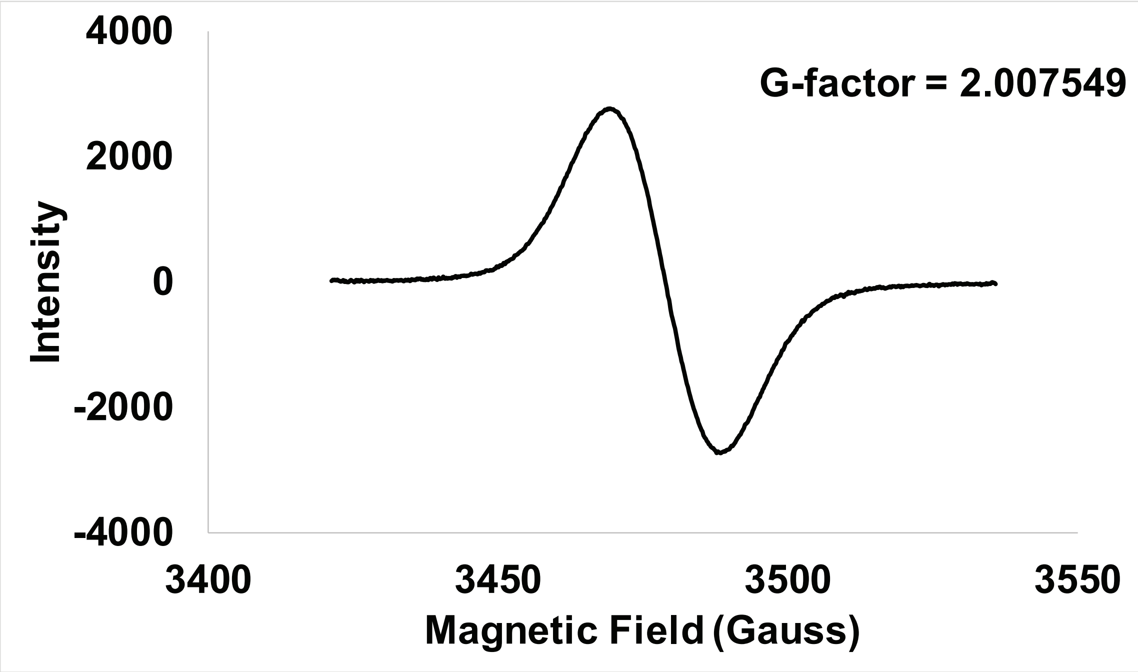

DOS	Format
ANZ	1024
MIN	-2733.186523
MAX	2772.813477
JSS	0
GST	3421.274884
GSI	114.543004
JUN	G
JON	Bruker BioSpin GmbH
JDA	9/25/2015
JTM	13:33
JRE	c:\programfiles\bruker-emx\syscal\st0103.cal
JEX	field-sweep
JSD	1
HCF	3478.546386
HSW	114.543004
EMF	0
RCT	20.48
RTC	20.48
RRG	8.93E+03
RMA	4
MF	9.773981
MP	6.38E-01
MPD	25

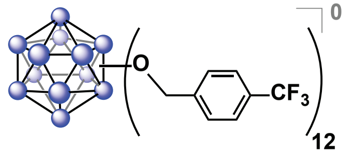

B 1s XPS

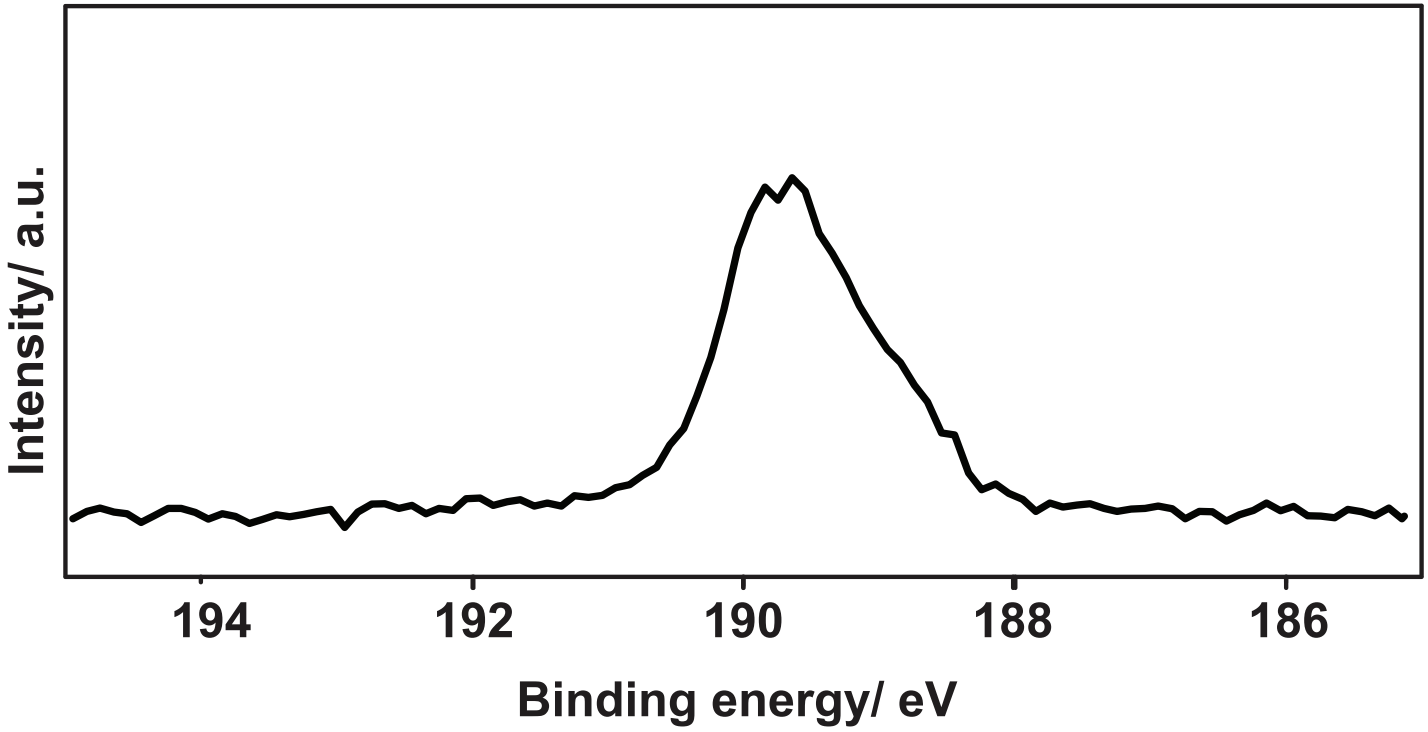

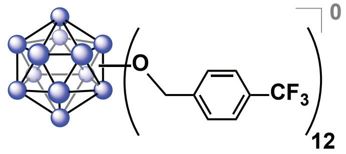

Cyclic voltammetry

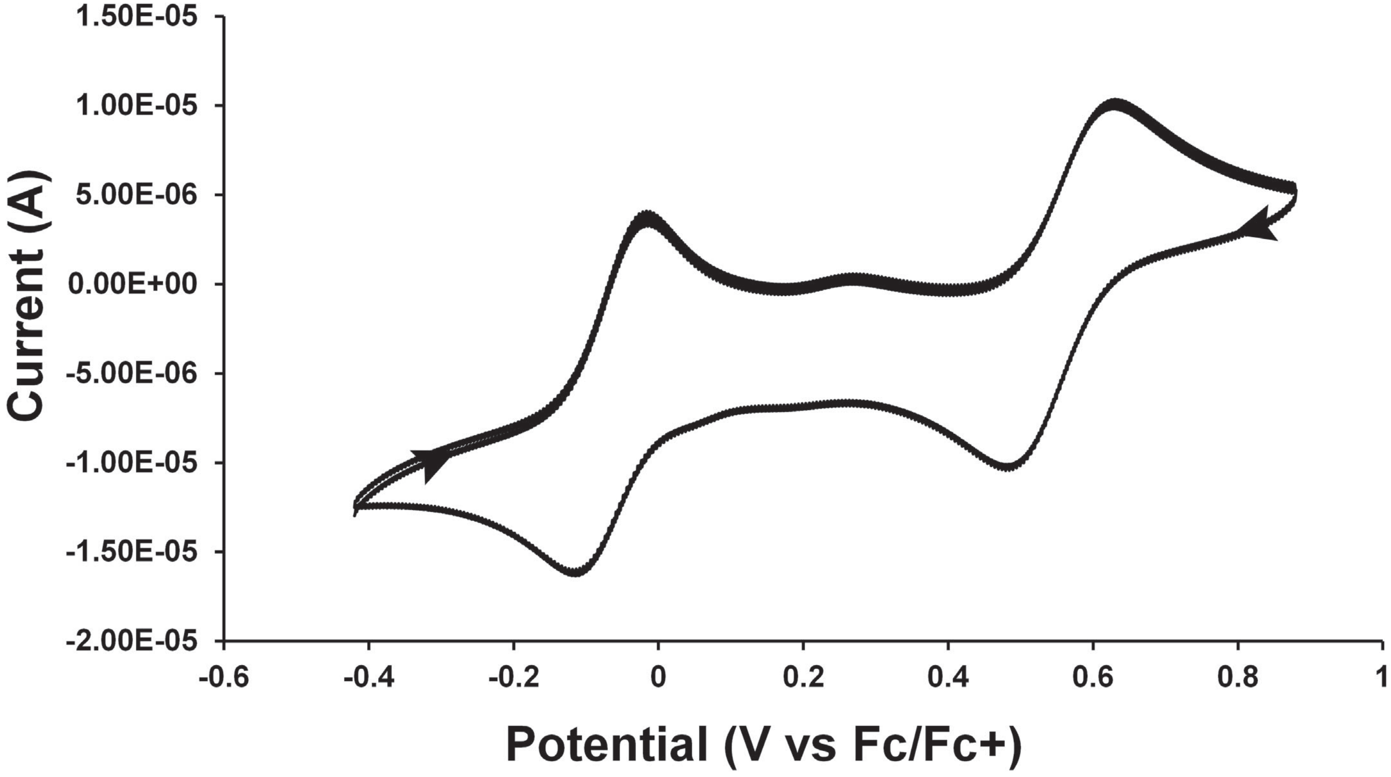

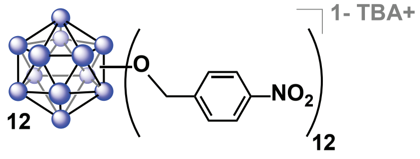

^{11}B {^{1}H} NMR

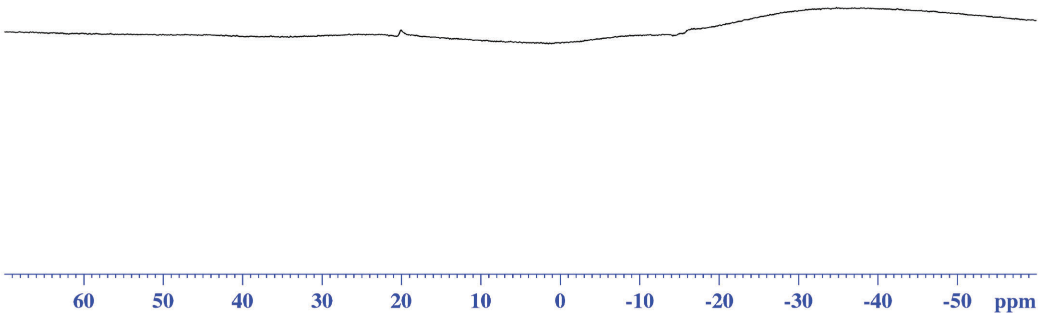

```
Current Data Parameters
NAME     B12(O-4-NO2Bn)12
EXPNO              60
PROCNO              1

F2 - Acquisition Parameters
Date_         20151101
Time              19.40
INSTRUM          av400
PROBHD   5 mm PABBO BB/
PULPROG        zgdc.js
TD               5096
SOLVENT         Acetone
NS               1024
DS                  0
SWH         51020.406 Hz
FIDRES      10.011854 Hz
AQ          0.0499408 sec
RG             189.85
DW             9.800 usec
DE              6.50 usec
TE             299.0 K
D1         0.05000000 sec
D11        0.03000000 sec
TD0                 1

======== CHANNEL f1 ========
SFO1      128.3776052 MHz
NUC1              11B
P1              10.00 usec
PLW1      52.00000000 W

======== CHANNEL f2 ========
SFO2      400.1324008 MHz
NUC2               1H
CPDPRG[2        waltz16
PCPD2           90.00 usec
PLW2      13.00000000 W
PLW12      0.36111000 W

F2 - Processing parameters
SI              32768
SF        128.3776161 MHz
WDW                EM
SSB     0
LB              10.00 Hz
GB      0
PC               1.40
```

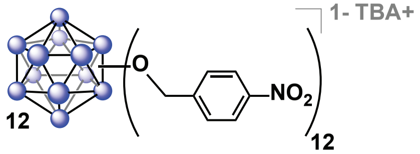

^{13}C NMR

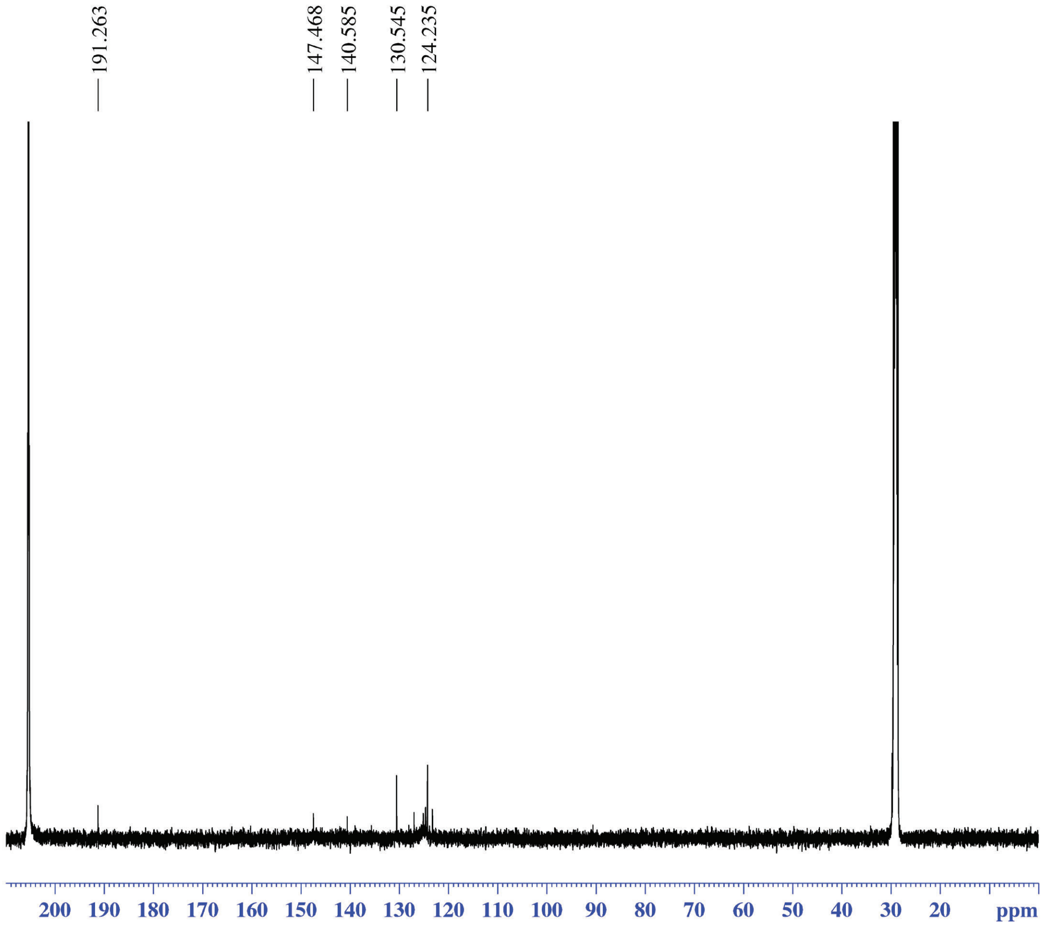

```
Current Data Parameters
NAME     B12(O-4-NO2Bn)12
EXPNO                 10
PROCNO                 1

F2 - Acquisition Parameters
Date_        20151103
Time            11.12
INSTRUM         av500
PROBHD   5 mm DCH 13C-1
PULPROG        zgpg30
TD              65536
SOLVENT       Acetone
NS                128
DS                  2
SWH        31250.000 Hz
FIDRES      0.476837 Hz
AQ         1.0485760 sec
RG             204.54
DW             16.000 usec
DE              18.00 usec
TE              298.0 K
D1         2.00000000 sec
D11        0.03000000 sec
TD0                 1

======== CHANNEL f1 ========
SFO1      125.7722511 MHz
NUC1              13C
P1               9.63 usec
PLW1      23.00000000 W

======== CHANNEL f2 ========
SFO2      500.1330008 MHz
NUC2               1H
CPDPRG[2         waltz16
PCPD2           80.00 usec
PLW2      13.50000000 W
PLW12      0.21094000 W
PLW13      0.13500001 W

F2 - Processing parameters
SI             131072
SF        125.7577890 MHz
WDW                EM
SSB     0
LB               1.00 Hz
GB      0
PC               1.40
```

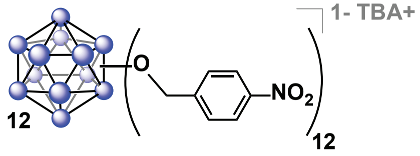

^{1}H NMR

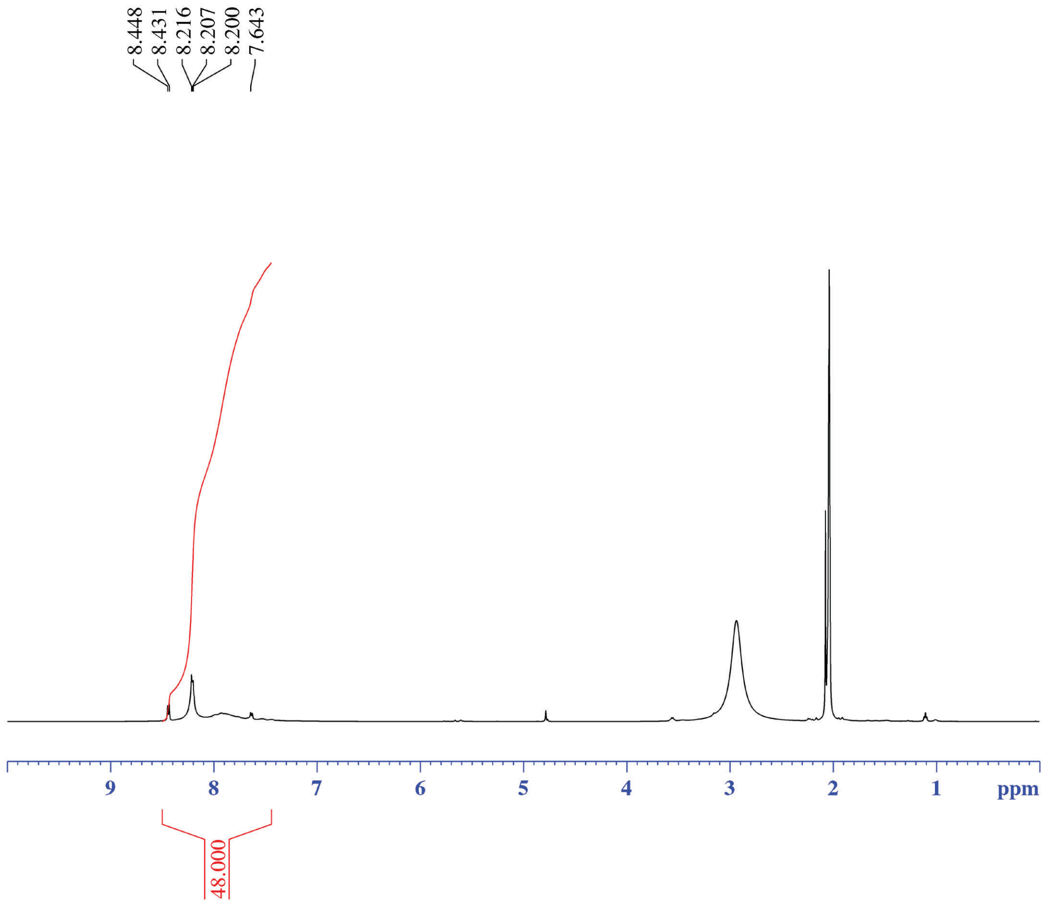

```
Current Data Parameters
NAME     B12(O-4-NO2Bn)12
EXPNO              11
PROCNO              1

F2 - Acquisition Parameters
Date_         20151103
Time            11.16
INSTRUM          av500
PROBHD  5 mm DCH 13C-1
PULPROG          zg30
TD             65536
SOLVENT        Acetone
NS                32
DS                 0
SWH        10000.000 Hz
FIDRES      0.152588 Hz
AQ         3.2767999 sec
RG             52.41
DW            50.000 usec
DE            10.00 usec
TE             298.0 K
D1        2.00000000 sec
TD0                1

======== CHANNEL f1 ========
SFO1      500.1330008 MHz
NUC1              1H
P1             10.00 usec
PLW1       13.50000000 W

F2 - Processing parameters
SI             65536
SF        500.1300146 MHz
WDW               EM
SSB     0
LB              0.30 Hz
GB      0
PC              1.00
```

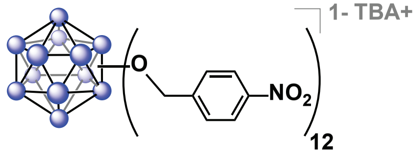
O
NO2
12
1- TBA+

Q Exactive
High-Res Mass Spec

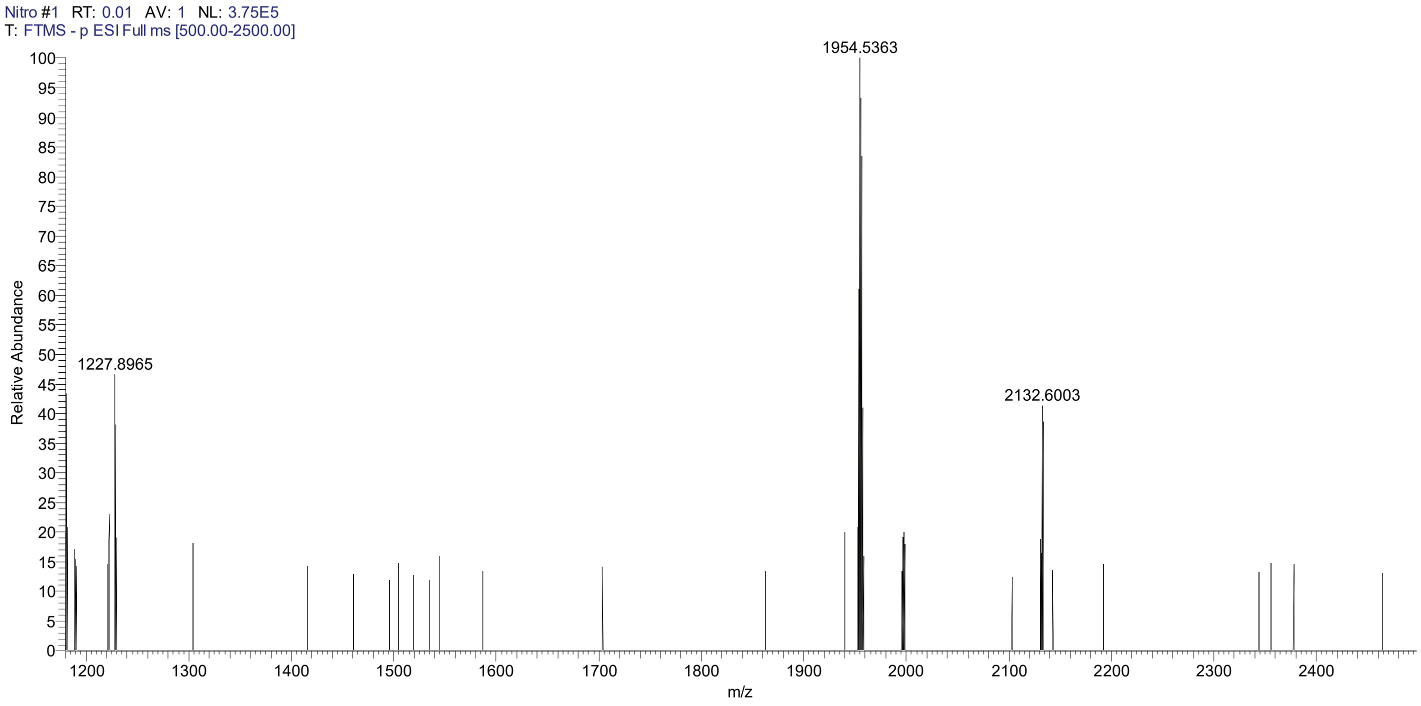

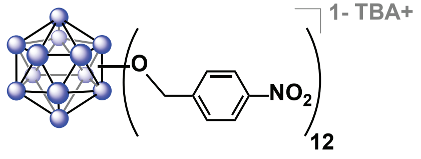
1- TBA+
O
NO2
12

Q Exactive
High-Res Mass Spec

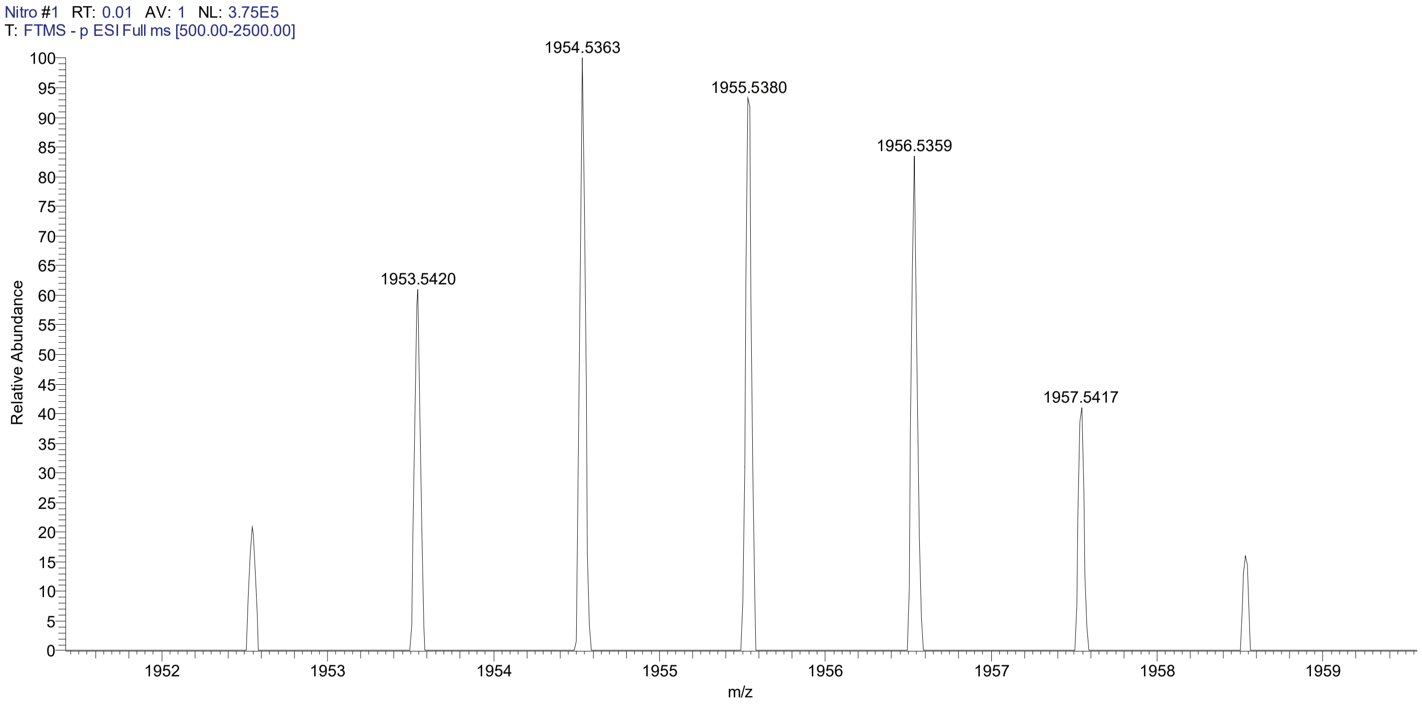

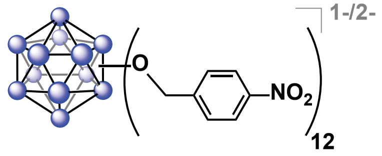
O
NO2
12
1-/2-

IR

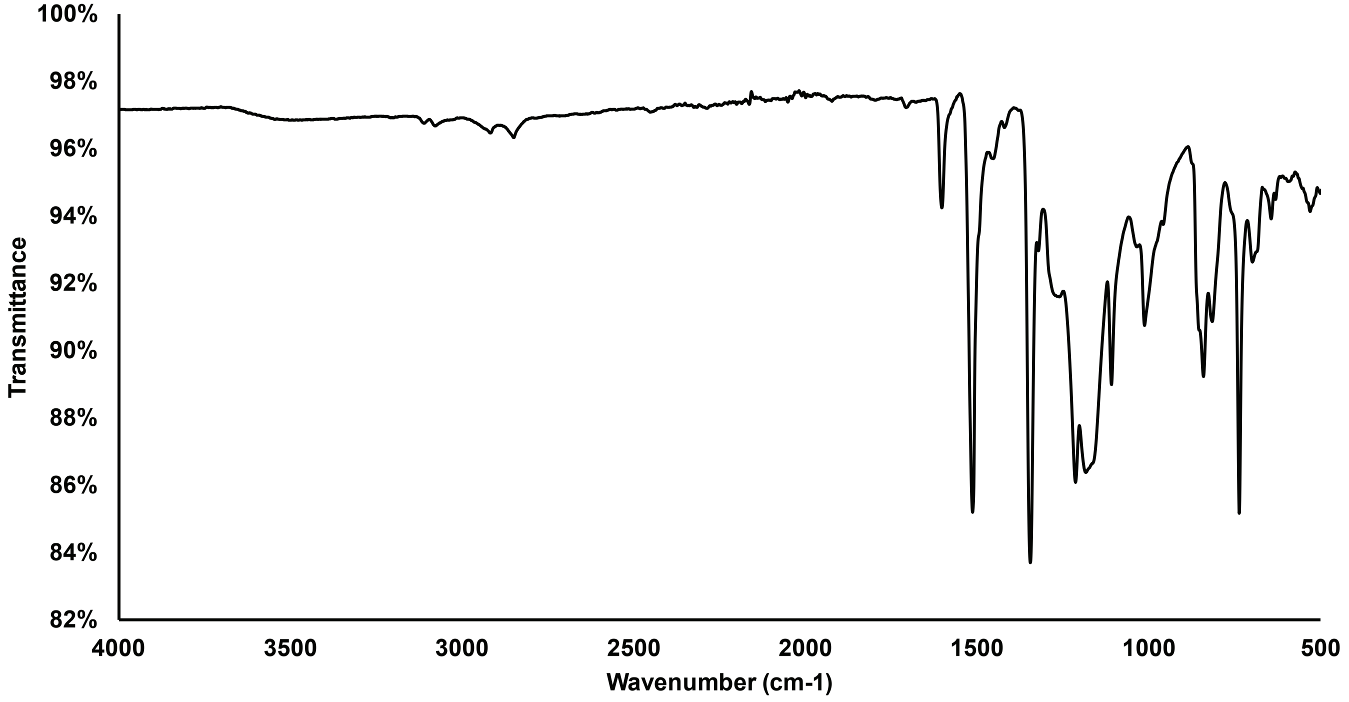
Transmittance
100%
98%
96%
94%
92%
90%
88%
86%
84%
82%
4000
3500
3000
2500
2000
1500
1000
500
Wavenumber (cm-1)

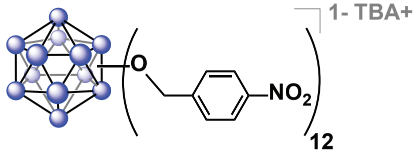

EPR

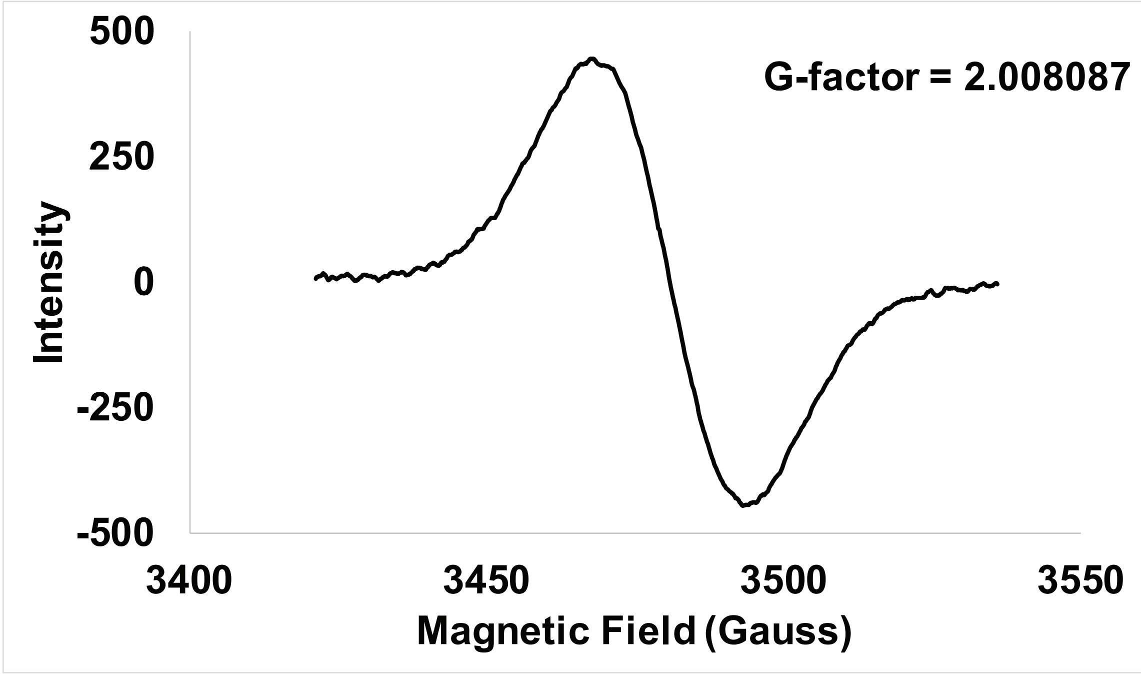

DOS	Format
ANZ	1024
MIN	-445.813477
MAX	444.186523
JSS	0
GST	3421.28
GSI	114.54
JUN	G
JON	Bruker BioSpin GmbH
JDA	9/29/2015
JTM	16:26
JRE	c:\programfiles\bruker-emx\syscal\st0103.cal
JEX	field-sweep
JSD	1
HCF	3478.55
HSW	114.54
EMF	0
RCT	20.48
RTC	163.84
RRG	8.93E+03
RMA	4
MF	9.776609
MP	6.38E-01
MPD	25

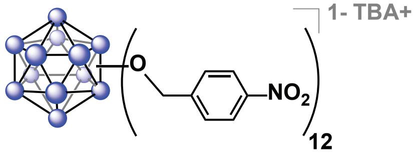
O
NO_2
12
1- TBA+

B 1s XPS

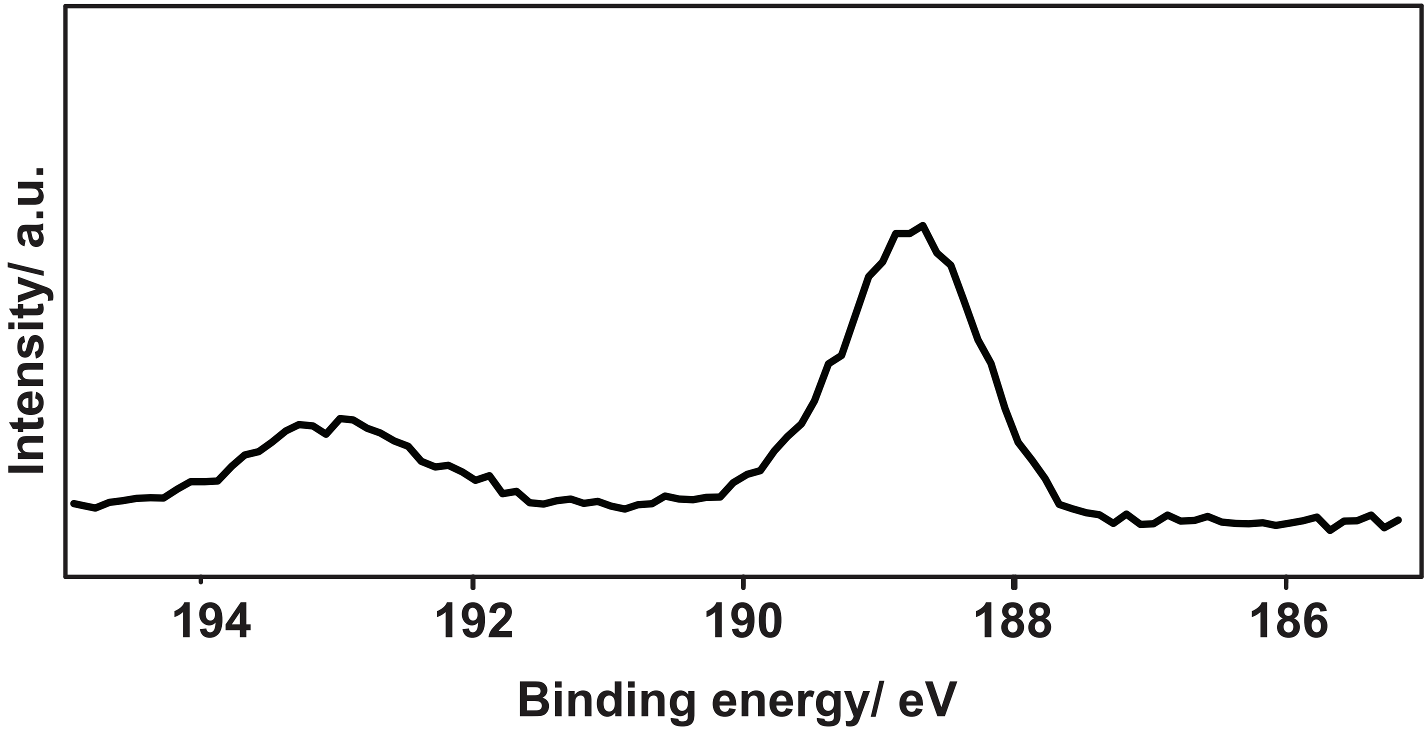
Intensity/ a.u.
194
192
190
188
186
Binding energy/ eV

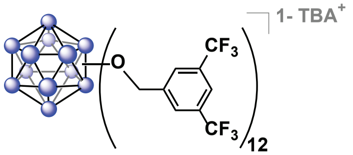

^{11}B {^{1}H} NMR

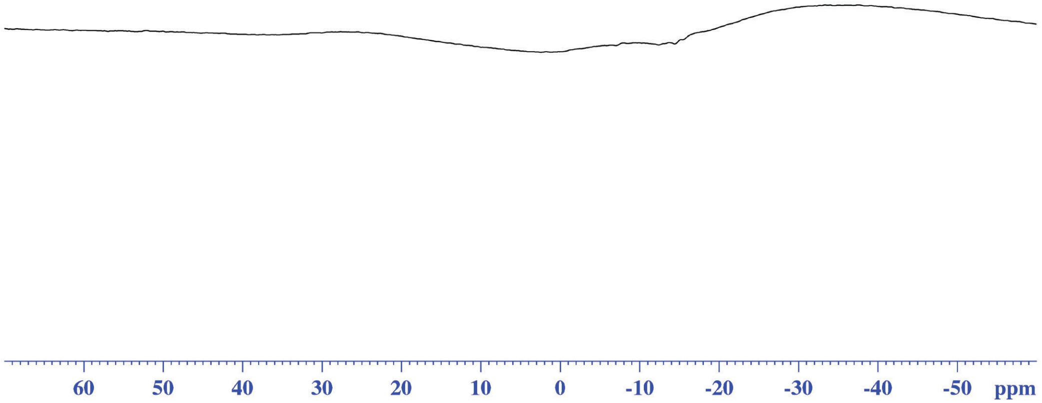

```
Current Data Parameters
NAME     B12(O-3,5-bisTFMBn)12
EXPNO             210
PROCNO              1

F2 - Acquisition Parameters
Date_          20150824
Time              20.51
INSTRUM           av400
PROBHD   5 mm PABBO BB/
PULPROG         zgdc.js
TD                 5096
SOLVENT           CDCl3
NS                 1024
DS                    0
SWH        51020.406 Hz
FIDRES     10.011854 Hz
AQ        0.0499408 sec
RG               189.85
DW           9.800 usec
DE            6.50 usec
TE              299.2 K
D1       0.00000400 sec
D11      0.03000000 sec
TD0                   1

======== CHANNEL f1 ========
SFO1     128.3776052 MHz
NUC1                 11B
P1            10.00 usec
PLW1       52.00000000 W

======== CHANNEL f2 ========
SFO2     400.1324008 MHz
NUC2                  1H
CPDPRG[2         waltz16
PCPD2         90.00 usec
PLW2       13.00000000 W
PLW12       0.36111000 W

F2 - Processing parameters
SI                 32768
SF       128.3776050 MHz
WDW                   EM
SSB      0
LB              50.00 Hz
GB       0
PC                  1.40
```

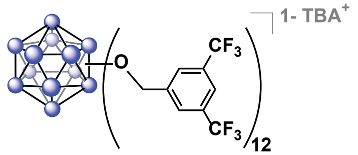

^{13}C NMR

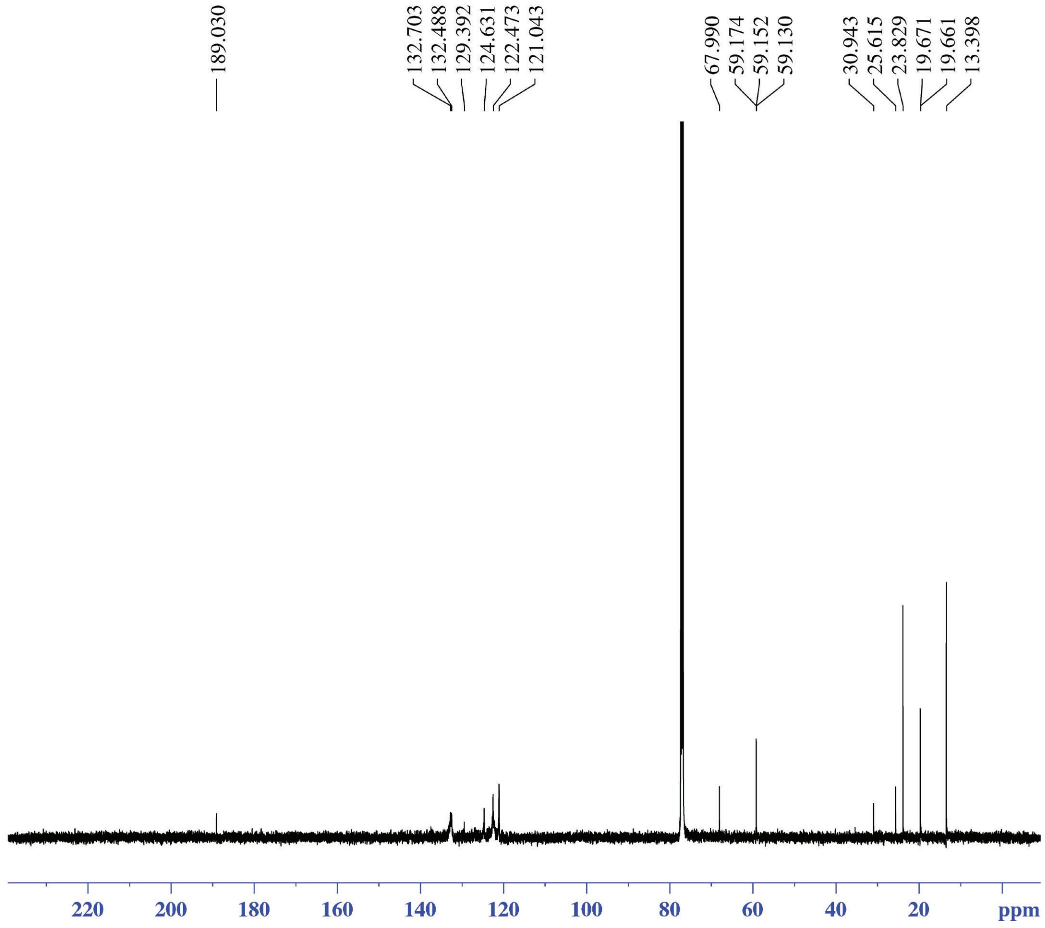

```
Current Data Parameters
NAME     B12(O-3,5-bisTFMBn)12
EXPNO              300
PROCNO               1

F2 - Acquisition Parameters
Date_        20150829
Time            21.11
INSTRUM         av500
PROBHD   5 mm DCH 13C-1
PULPROG        zgpg30
TD            65536
SOLVENT          CDCl3
NS              256
DS                2
SWH         31250.000 Hz
FIDRES       0.476837 Hz
AQ          1.0485760 sec
RG            204.54
DW            16.000 usec
DE             18.00 usec
TE             298.0 K
D1        2.00000000 sec
D11       0.03000000 sec
TD0                1

======== CHANNEL f1 ========
SFO1       125.7722511 MHz
NUC1               13C
P1               9.63 usec
PLW1       23.00000000 W

======== CHANNEL f2 ========
SFO2       500.1330008 MHz
NUC2                1H
CPDPRG[2        waltz16
PCPD2          80.00 usec
PLW2       13.50000000 W
PLW12       0.21094000 W
PLW13       0.13500001 W

F2 - Processing parameters
SI           131072
SF       125.7577890 MHz
WDW              EM
SSB     0
LB             1.00 Hz
GB      0
PC             1.40
```

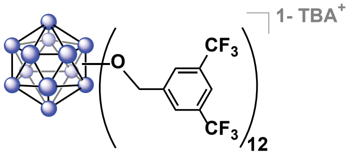

^{19}F NMR

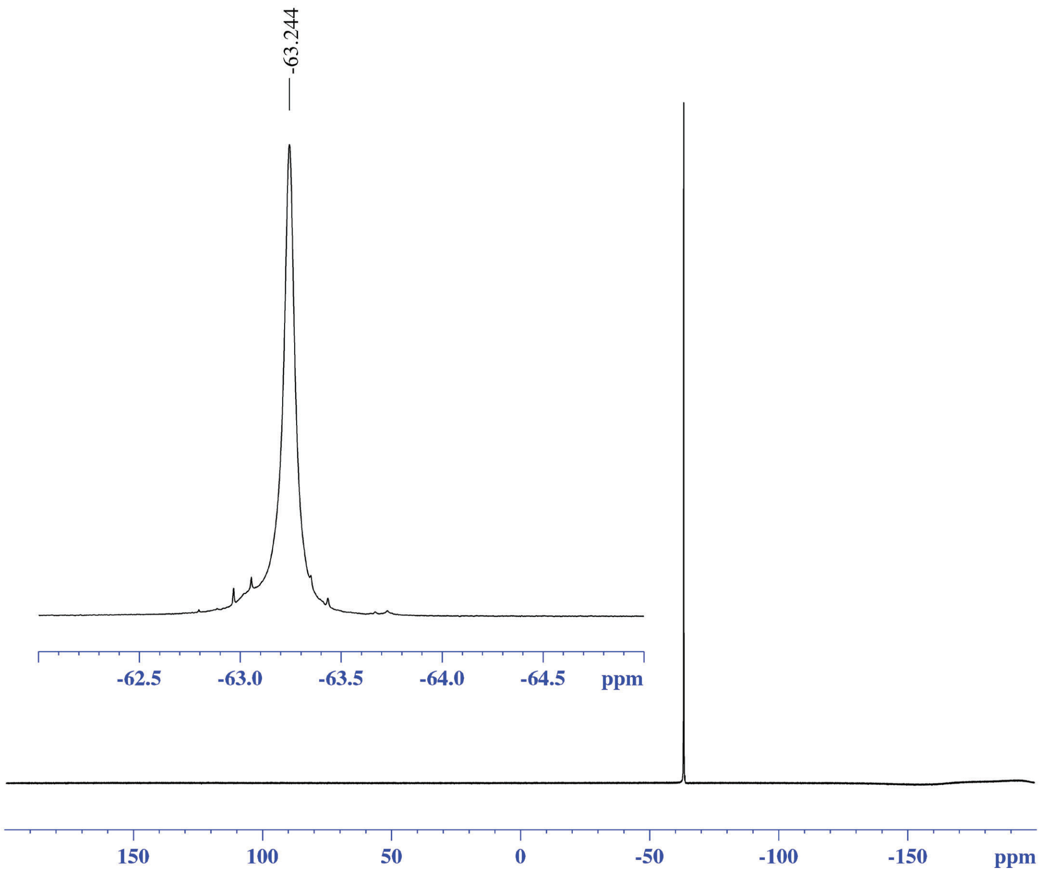

```
Current Data Parameters
NAME     B12(O-3,5-bisTFMBn)12
EXPNO              212
PROCNO               1

F2 - Acquisition Parameters
Date_         20150824
Time             21.00
INSTRUM          av400
PROBHD   5 mm PABBO BB/
PULPROG       zgflqn30
TD              262144
SOLVENT          CDCl3
NS                  64
DS                   0
SWH        150000.000 Hz
FIDRES        0.572205 Hz
AQ           0.8738133 sec
RG              189.85
DW               3.333 usec
DE                6.50 usec
TE               299.0 K
D1          2.00000000 sec
TD0                  1

======== CHANNEL f1 ========
SFO1       376.4983660 MHz
NUC1               19F
P1               14.50 usec
PLW1       17.00000000 W

F2 - Processing parameters
SI              262144
SF         376.4983660 MHz
WDW                 EM
SSB      0
LB                1.00 Hz
GB       0
PC                1.00
```

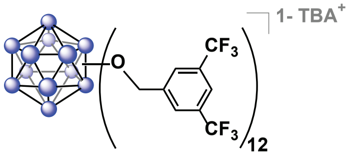

^{1}H NMR

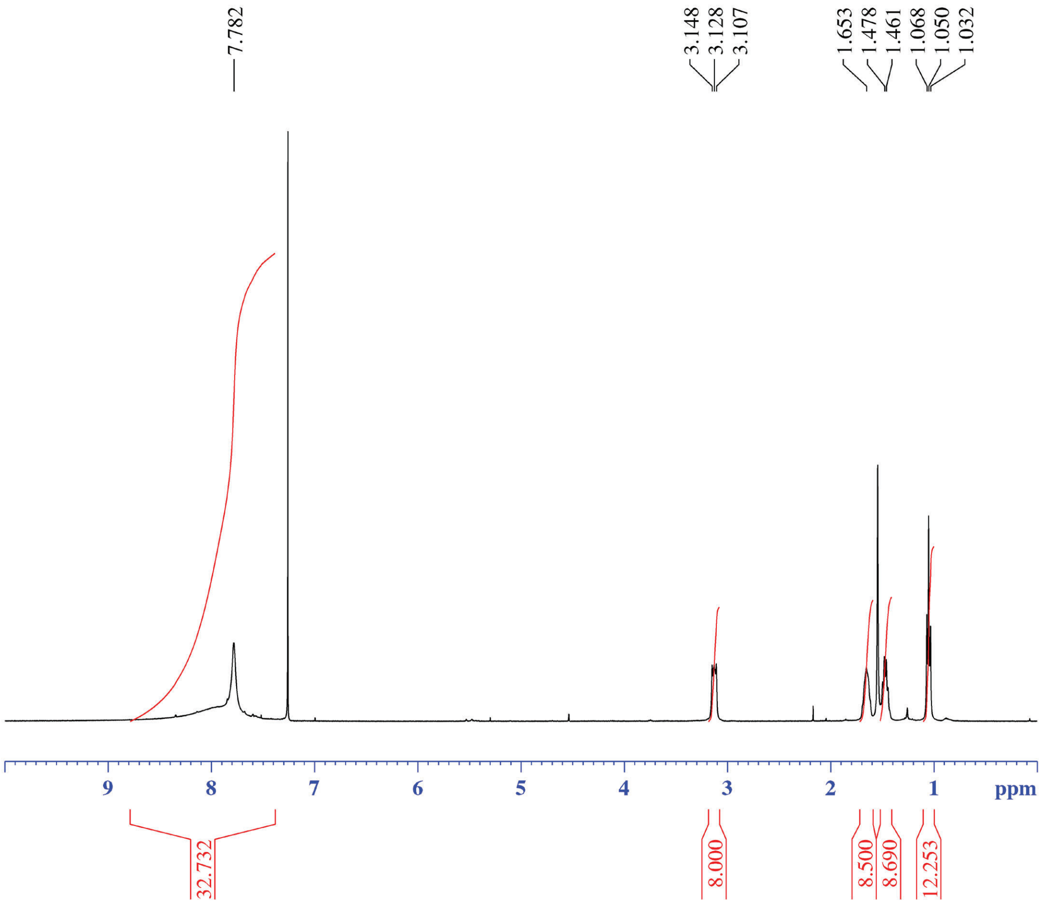

```
Current Data Parameters
NAME     B12(O-3,5-bisTFMBn)12
EXPNO              211
PROCNO               1

F2 - Acquisition Parameters
Date_          20150824
Time              20.54
INSTRUM           av400
PROBHD   5 mm PABBO BB/
PULPROG            zg30
TD                52882
SOLVENT           CDCl3
NS                   32
DS                    0
SWH          8012.820 Hz
FIDRES       0.151523 Hz
AQ          3.2998369 sec
RG               189.85
DW           62.400 usec
DE             6.50 usec
TE              299.0 K
D1        2.00000000 sec
TD0                   1

======== CHANNEL f1 ========
SFO1      400.1324008 MHz
NUC1                 1H
P1             15.00 usec
PLW1        13.00000000 W

F2 - Processing parameters
SI                65536
SF        400.1300184 MHz
WDW                  EM
SSB     0
LB              0.30 Hz
GB      0
PC                 1.00
```

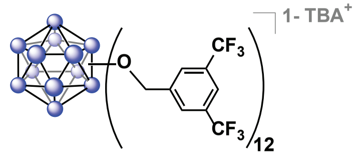
O
CF3
CF3
12
1- TBA+

Q Exactive
High-Res Mass Spec

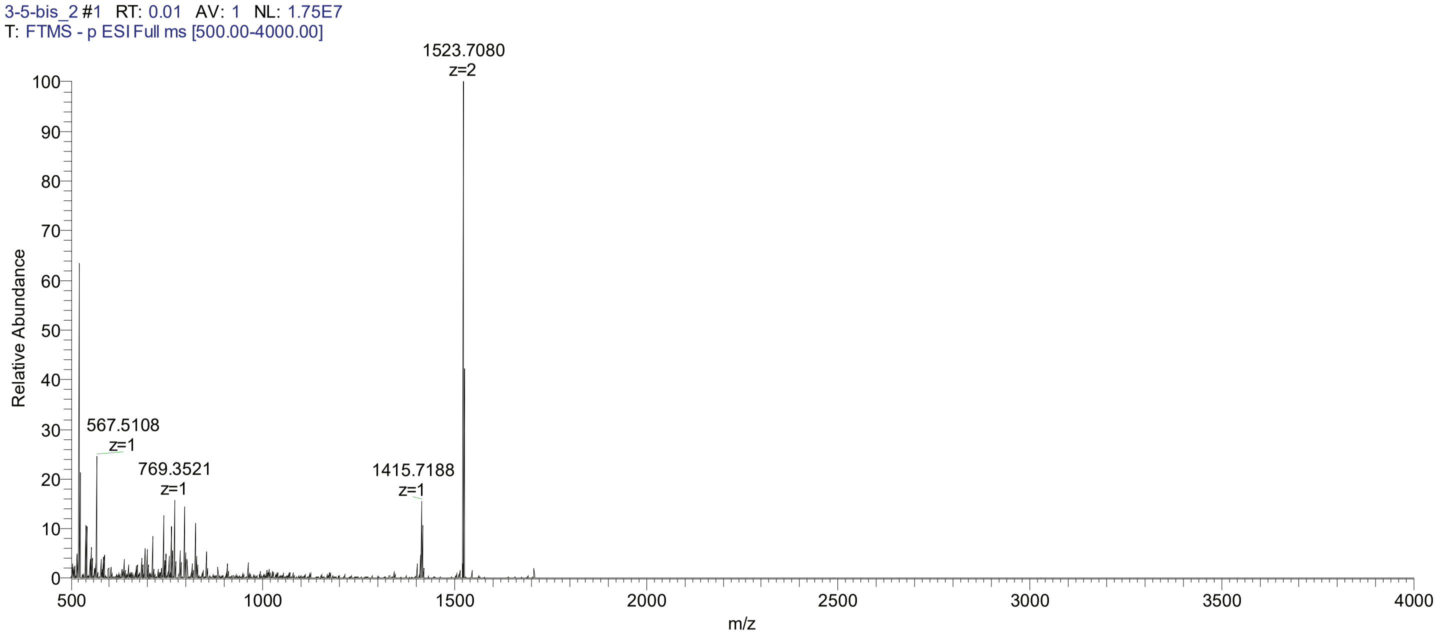

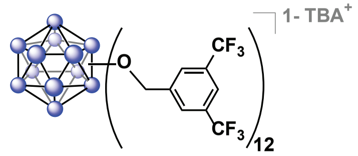
O
CF3
CF3
12
1- TBA+

Q Exactive
High-Res Mass Spec

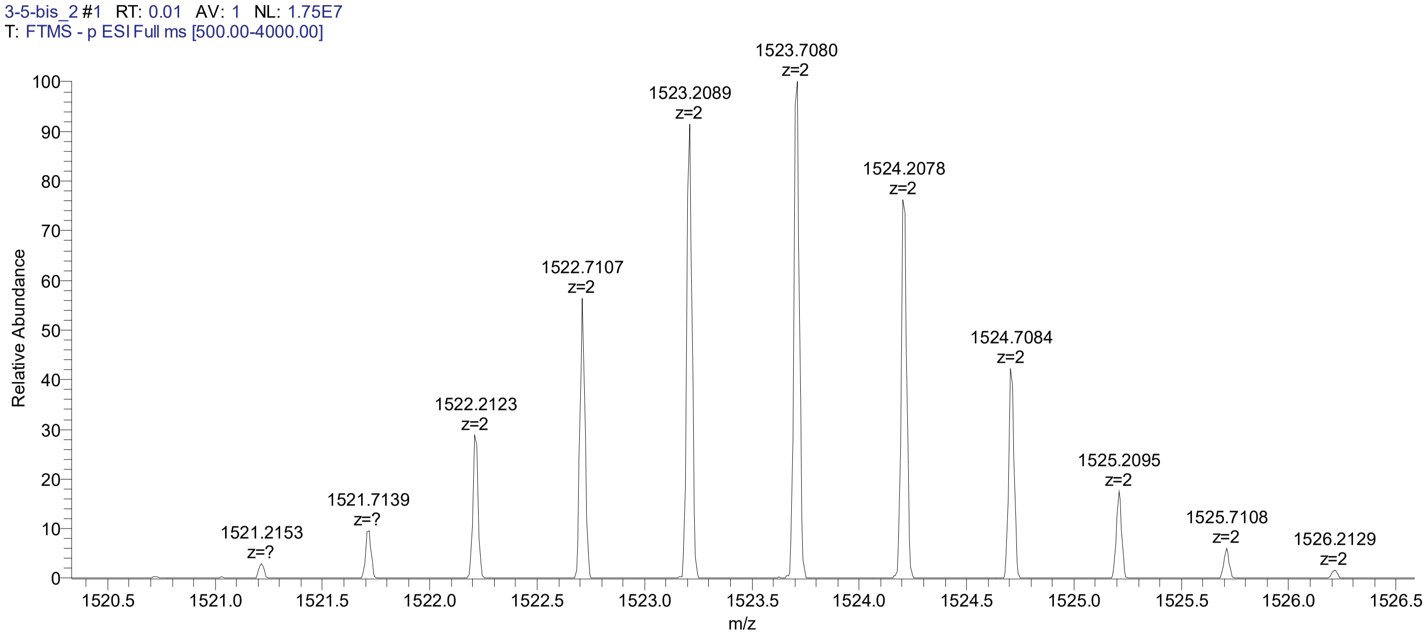

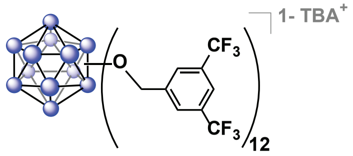
O
CF3
CF3
12
1- TBA+

IR

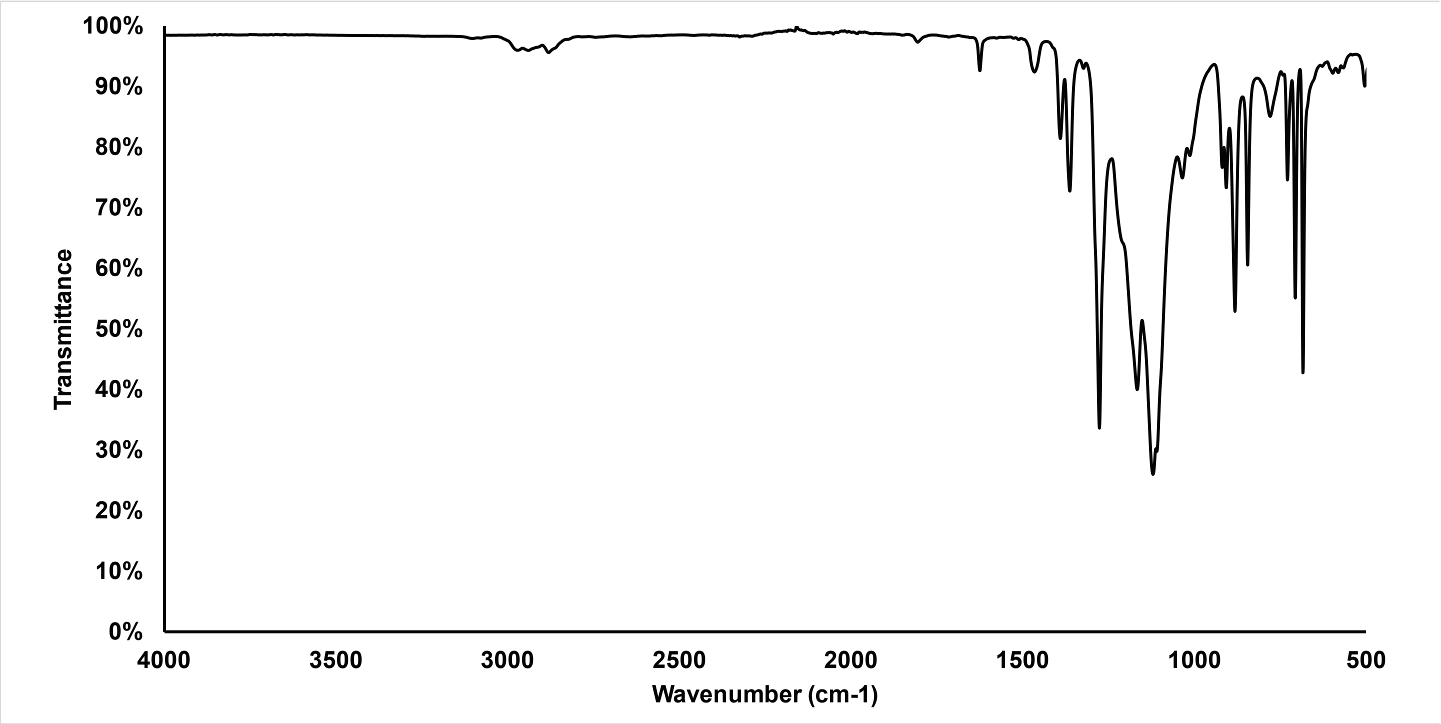
Transmittance
100%
90%
80%
70%
60%
50%
40%
30%
20%
10%
0%
4000
3500
3000
2500
2000
1500
1000
500
Wavenumber (cm-1)

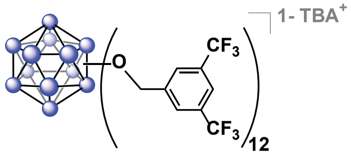

EPR

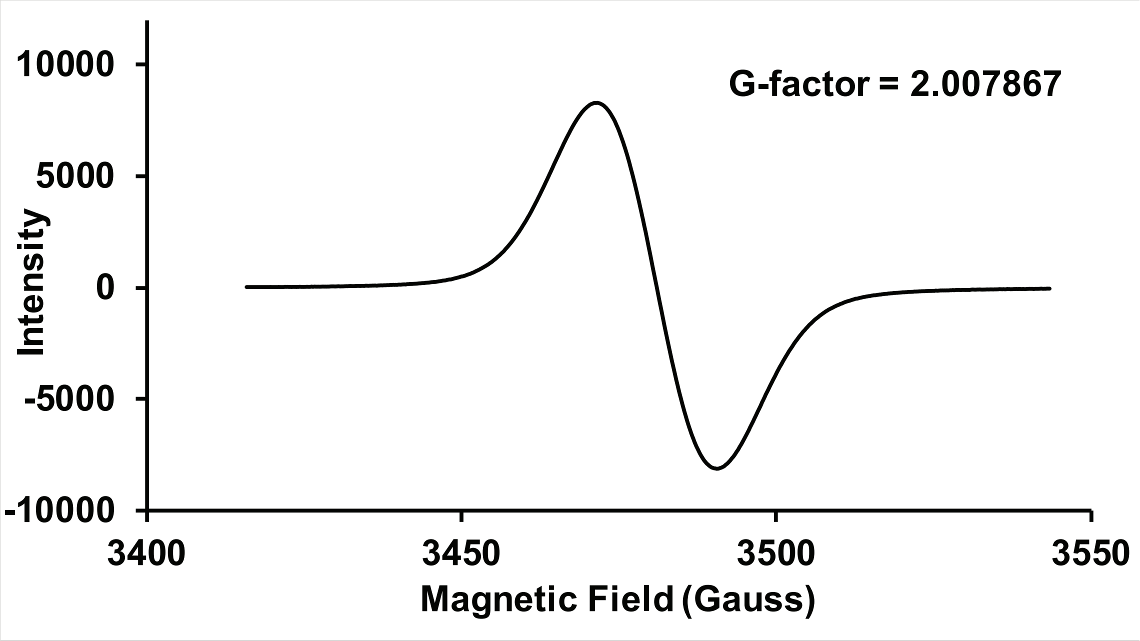

DOS	Format
ANZ	1024
MIN	-8134.161133
MAX	8283.838867
JSS	0
GST	3415.875
GSI	127.47
JUN	G
JON	Bruker BioSpin GmbH
JDA	6/4/2015
JTM	16:02
JRE	c:\programfiles\bruker-emx\syscal\st0103.cal
JEX	field-sweep
JSD	1
HCF	3479.61
HSW	127.47
EMF	0
RCT	20.48
RTC	20.48
RRG	2.83E+03
RMA	4
MF	9.778519
MP	6.38E-01

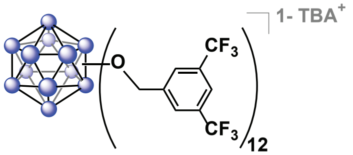
O
CF3
CF3
12
1- TBA+

B 1s XPS

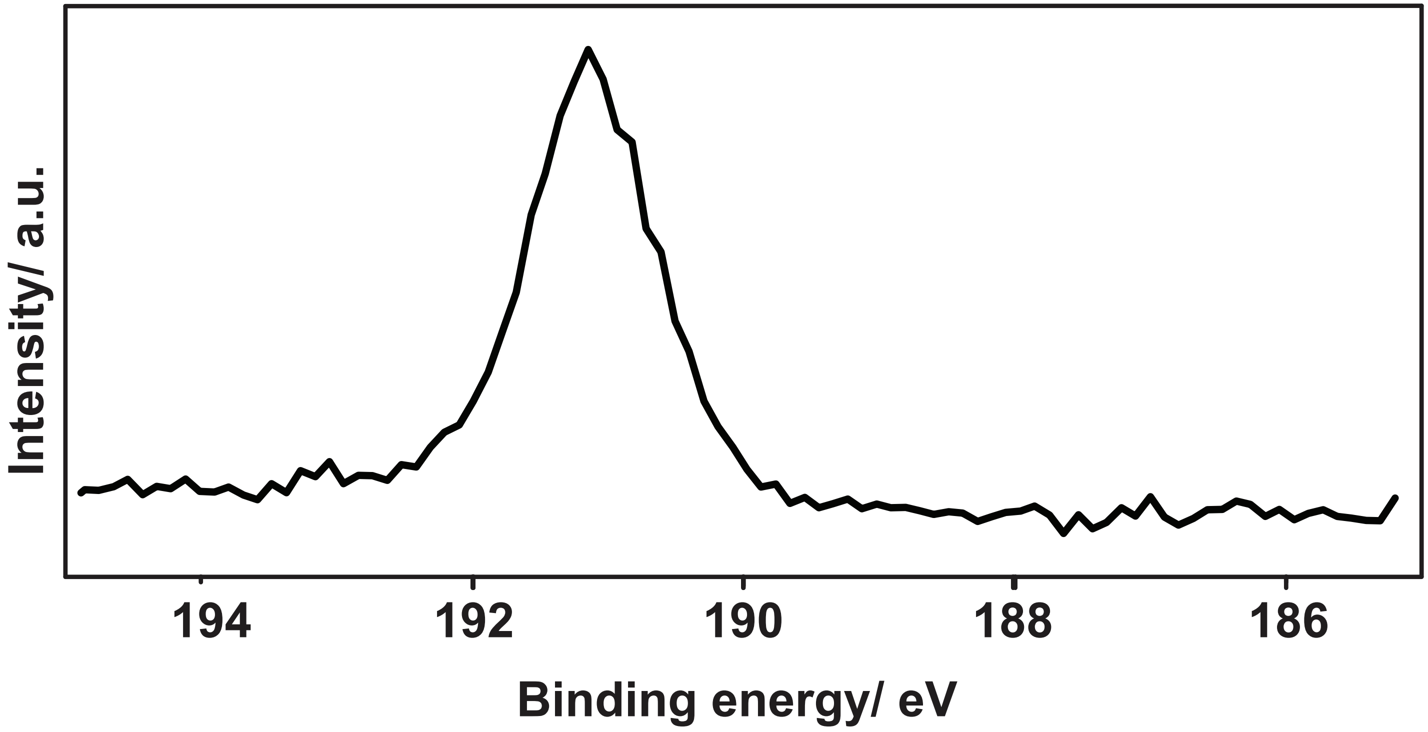
Intensity/ a.u.
194
192
190
188
186
Binding energy/ eV

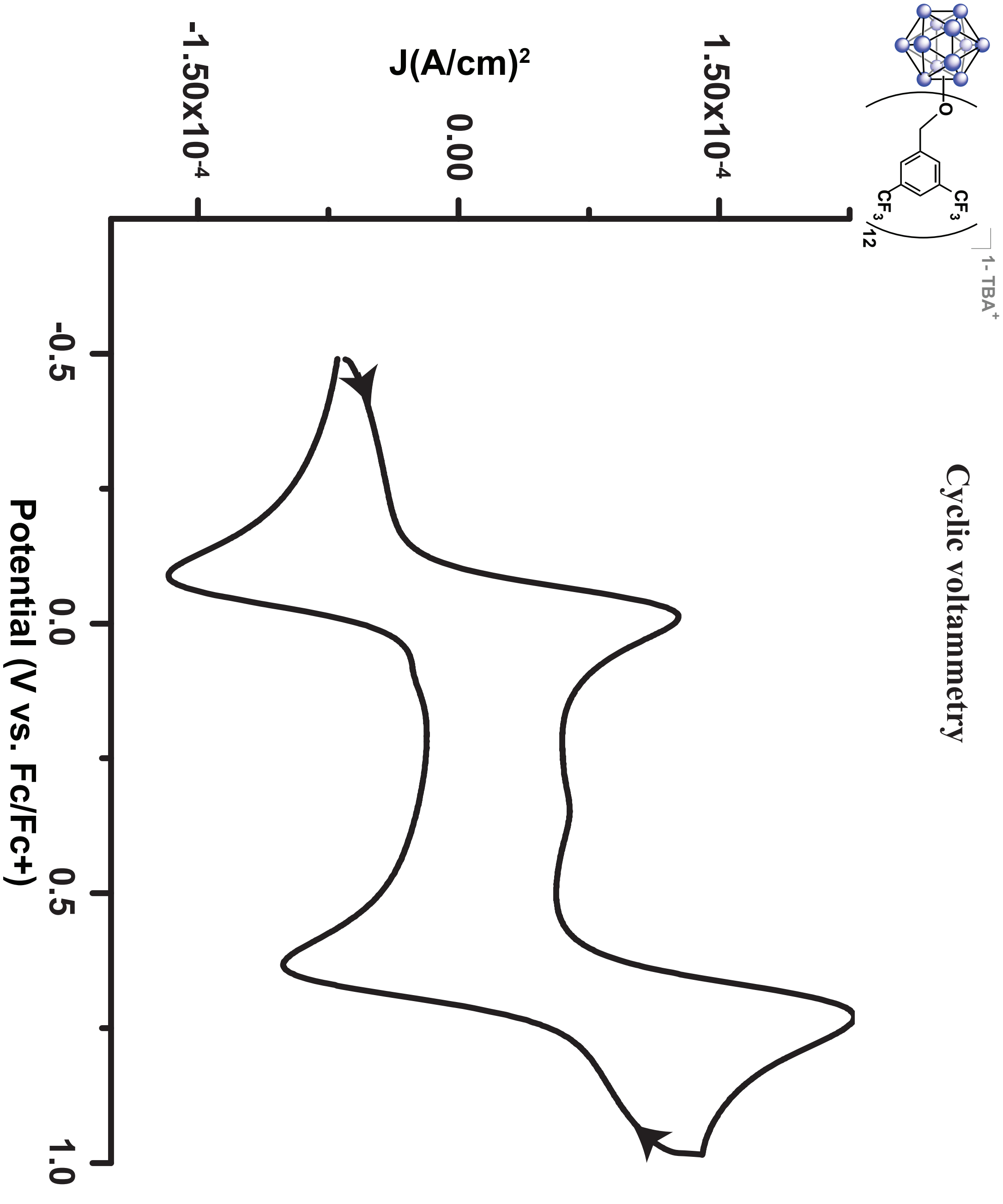
Cyclic voltammetry
J(A/cm)²
1.50x10⁻⁴
0.00
-1.50x10⁻⁴
Potential (V vs. Fc/Fc+)
-0.5
0.0
0.5
1.0
O
CF₃
CF₃
12
1- TBA⁺

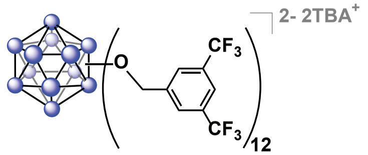

^{13}C NMR

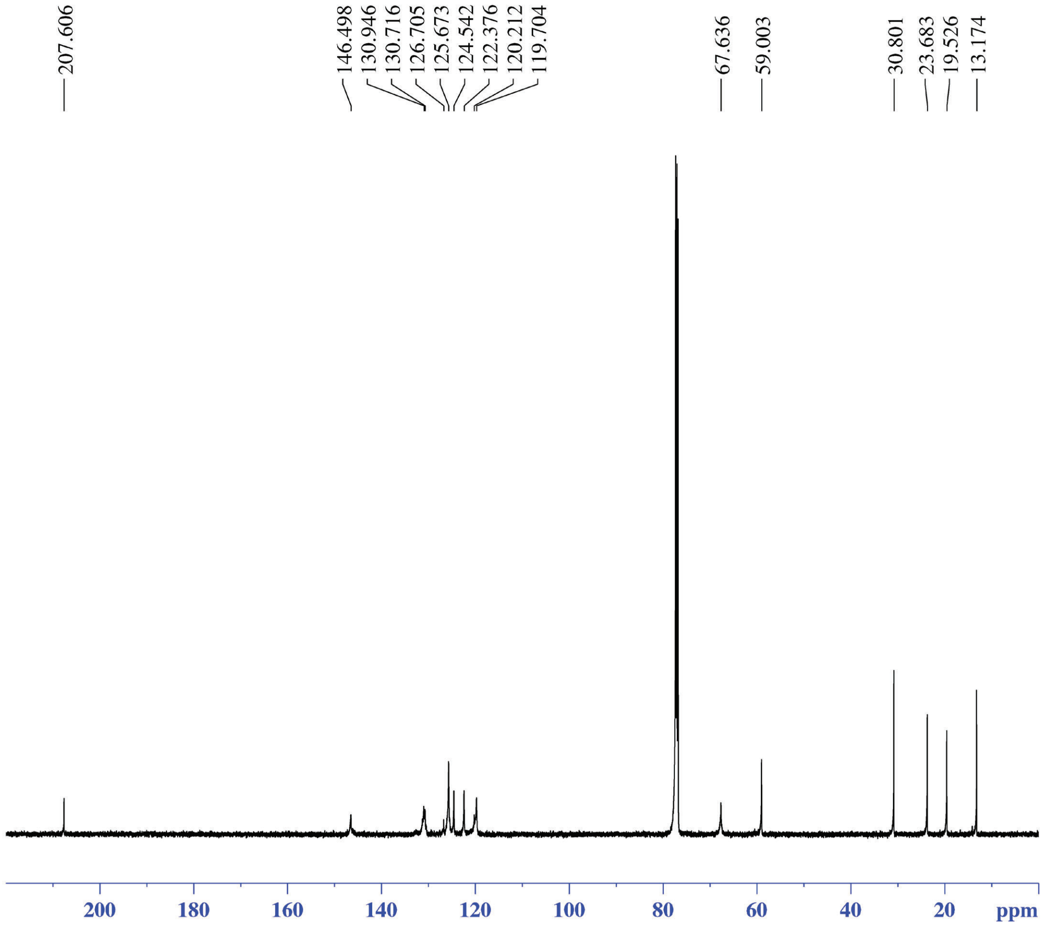

```
Current Data Parameters
NAME     B12(O-3,5-bisTFMBn)12
EXPNO              700
PROCNO               1

F2 - Acquisition Parameters
Date_        20150829
Time            22.21
INSTRUM         av500
PROBHD   5 mm DCH 13C-1
PULPROG        zgpg30
TD              65536
SOLVENT          CDCl3
NS                256
DS                  2
SWH        31250.000 Hz
FIDRES      0.476837 Hz
AQ         1.0485760 sec
RG             204.54
DW             16.000 usec
DE              18.00 usec
TE              298.0 K
D1        2.00000000 sec
D11       0.03000000 sec
TD0                 1

======== CHANNEL f1 ========
SFO1      125.7722511 MHz
NUC1              13C
P1               9.63 usec
PLW1      23.00000000 W

======== CHANNEL f2 ========
SFO2      500.1330008 MHz
NUC2               1H
CPDPRG[2       waltz16
PCPD2           80.00 usec
PLW2      13.50000000 W
PLW12      0.21094000 W
PLW13      0.13500001 W

F2 - Processing parameters
SI             131072
SF        125.7577890 MHz
WDW                EM
SSB      0
LB               1.00 Hz
GB       0
PC               1.40
```

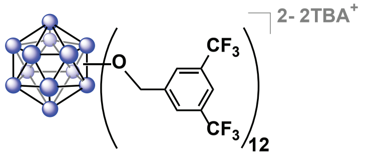

^{19}F NMR

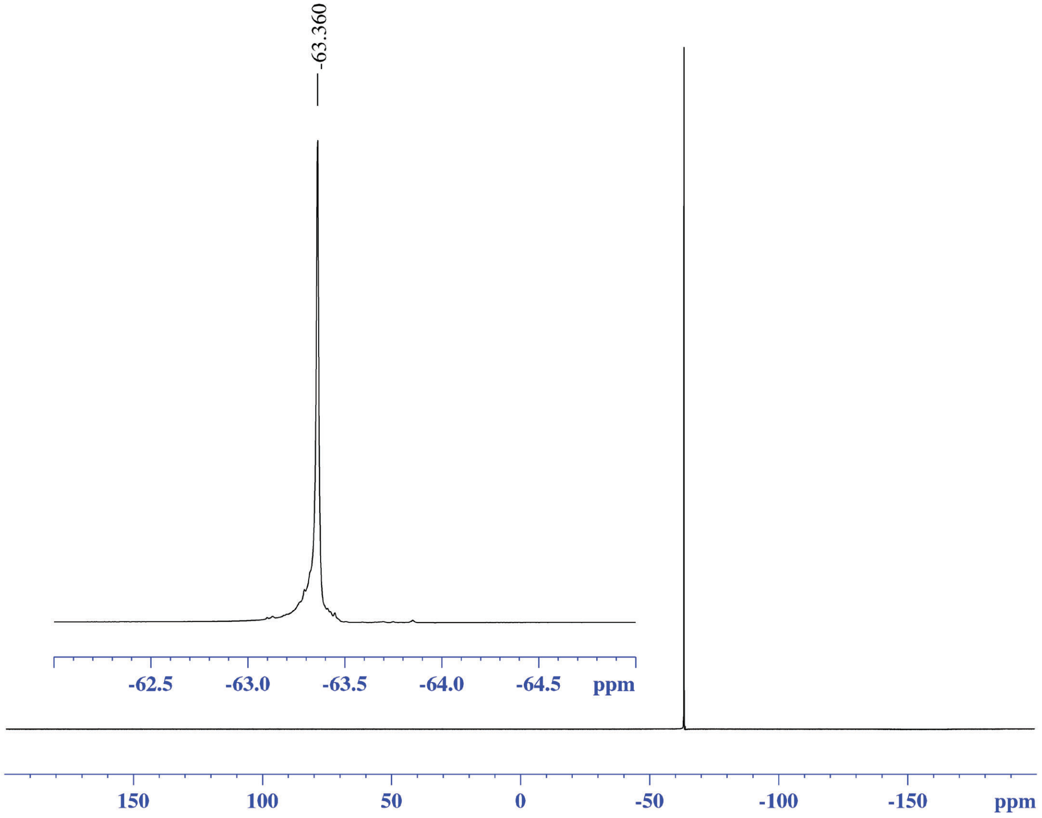

```
Current Data Parameters
NAME     B12(O-3,5-bisTFMBn)12
EXPNO              121
PROCNO               1

F2 - Acquisition Parameters
Date_          20150824
Time              17.26
INSTRUM           av400
PROBHD   5 mm PABBO BB/
PULPROG        zgflqn30
TD               262144
SOLVENT           CDCl3
NS                   32
DS                    0
SWH         150000.000 Hz
FIDRES        0.572205 Hz
AQ           0.8738133 sec
RG               189.85
DW                3.333 usec
DE                 6.50 usec
TE                299.0 K
D1           2.00000000 sec
TD0                   1

======== CHANNEL f1 ========
SFO1       376.4983660 MHz
NUC1                19F
P1                14.50 usec
PLW1        17.00000000 W

F2 - Processing parameters
SI               262144
SF         376.4983660 MHz
WDW                  EM
SSB     0
LB                 1.00 Hz
GB      0
PC                 1.00
```

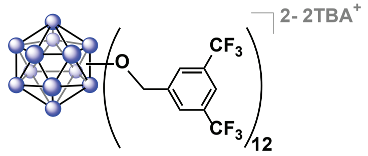

^{1}H NMR

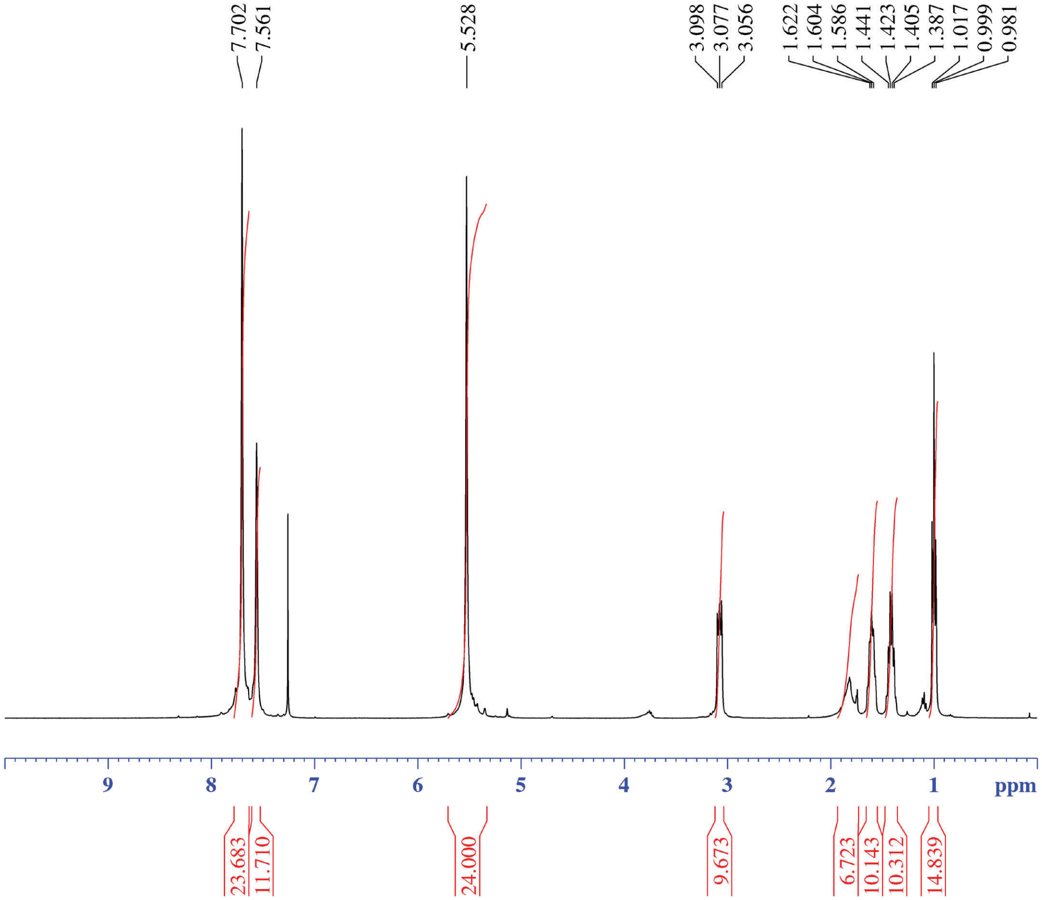

Current Data Parameters
NAME B12(O-3,5-bisTFMBn)12
EXPNO 122
PROCNO 1

F2 - Acquisition Parameters
Date_ 20150824
Time 17.32
INSTRUM av400
PROBHD 5 mm PABBO BB/
PULPROG zg30
TD 52882
SOLVENT CDCl3
NS 64
DS 0
SWH 8012.820 Hz
FIDRES 0.151523 Hz
AQ 3.2998369 sec
RG 155.85
DW 62.400 usec
DE 6.50 usec
TE 299.0 K
D1 2.00000000 sec
TD0 1

======== CHANNEL f1 ========
SFO1 400.1324008 MHz
NUC1 1H
P1 15.00 usec
PLW1 13.00000000 W

F2 - Processing parameters
SI 65536
SF 400.1300184 MHz
WDW EM
SSB 0
LB 0.30 Hz
GB 0
PC 1.00

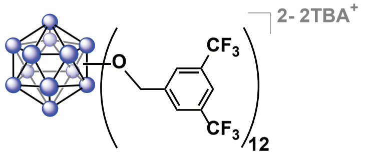

^{11}B {^{1}H} NMR

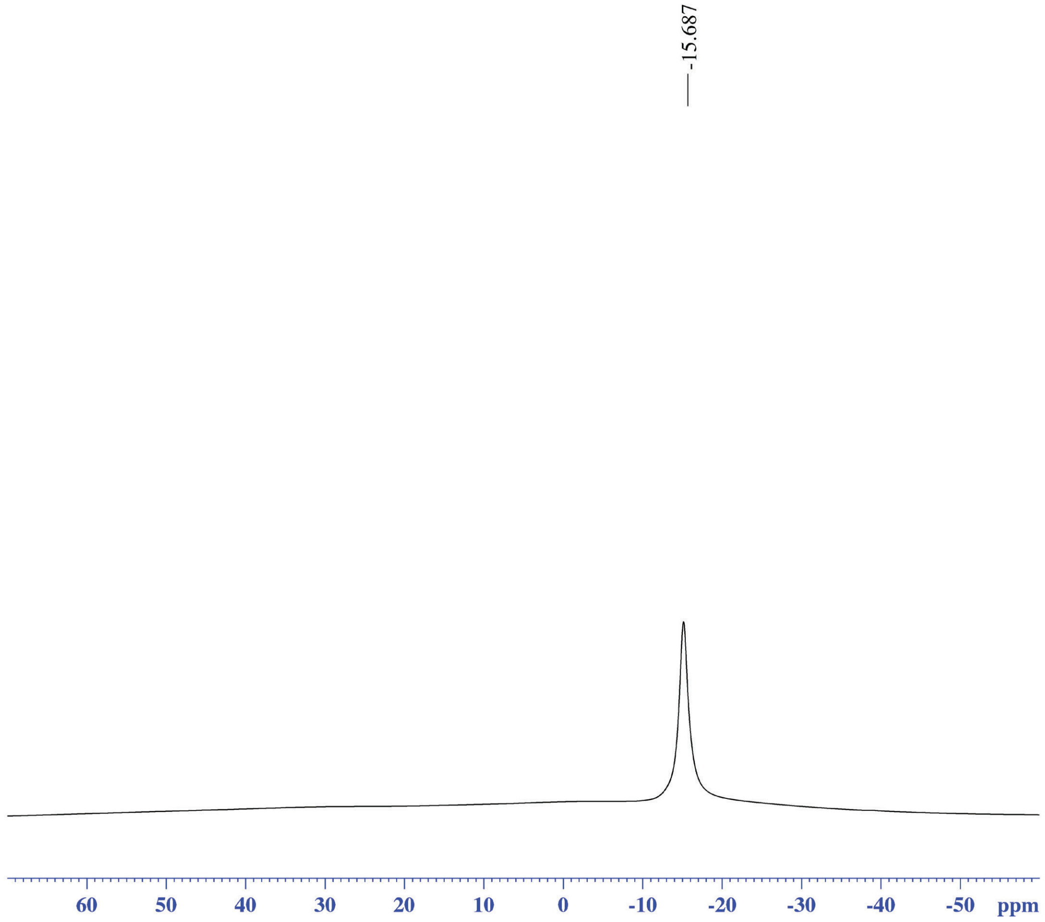

```
Current Data Parameters
NAME     B12(O-3,5-bisTFMBn)12
EXPNO              120
PROCNO               1

F2 - Acquisition Parameters
Date_          20150824
Time              17.23
INSTRUM           av400
PROBHD   5 mm PABBO BB/
PULPROG         zgdc.js
TD                5096
SOLVENT           CDCl3
NS                1024
DS                   0
SWH          51020.406 Hz
FIDRES       10.011854 Hz
AQ           0.0499408 sec
RG              189.85
DW               9.800 usec
DE                6.50 usec
TE               299.2 K
D1          0.00000400 sec
D11         0.03000000 sec
TD0                  1

======== CHANNEL f1 ========
SFO1      128.3776052 MHz
NUC1              11B
P1              10.00 usec
PLW1      52.00000000 W

======== CHANNEL f2 ========
SFO2      400.1324008 MHz
NUC2               1H
CPDPRG[2        waltz16
PCPD2           90.00 usec
PLW2      13.00000000 W
PLW12      0.36111000 W

F2 - Processing parameters
SI              32768
SF        128.3776050 MHz
WDW                EM
SSB     0
LB              50.00 Hz
GB      0
PC               1.40
```

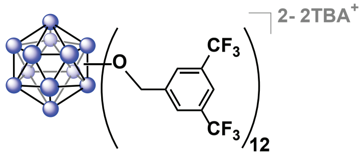
O
CF$_3$
CF$_3$
12
2- 2TBA$^+$

IR

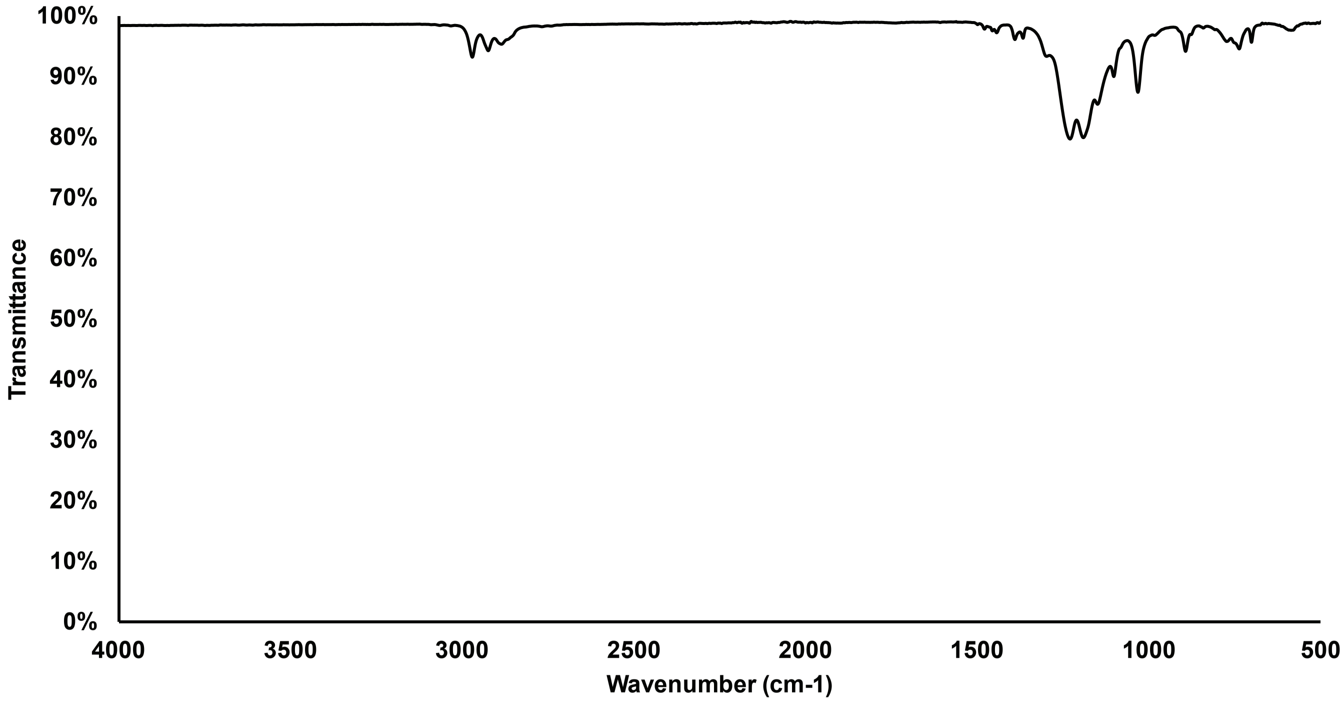
Transmittance
100%
90%
80%
70%
60%
50%
40%
30%
20%
10%
0%
4000
3500
3000
2500
2000
1500
1000
500
Wavenumber (cm-1)

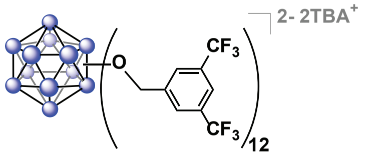
O
CF$_3$
CF$_3$
12
2- 2TBA$^+$

B 1s XPS

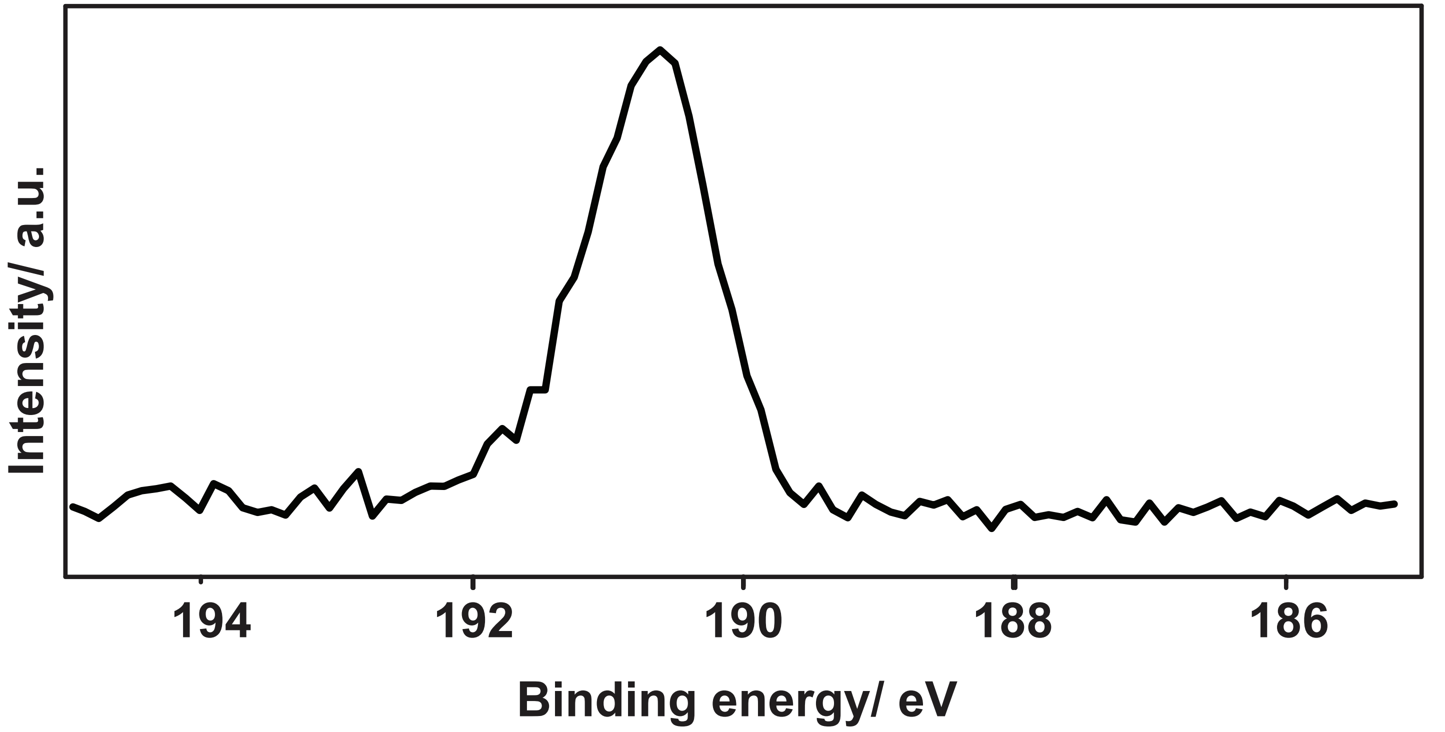
Intensity/ a.u.
194
192
190
188
186
Binding energy/ eV

$^{11}B\ \{^1H\}$ NMR

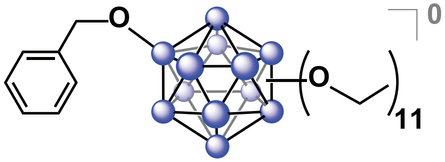

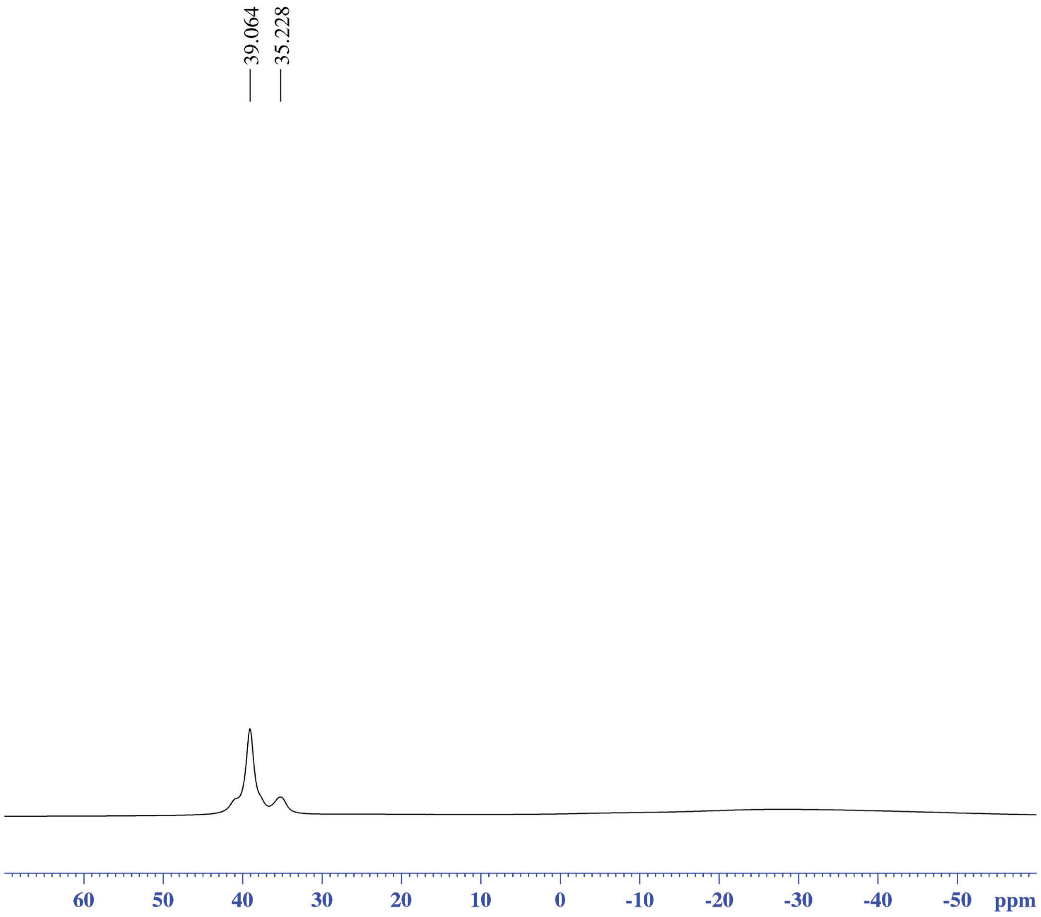

```
Current Data Parameters
NAME     B12(O-Bn)(O-Et)11
EXPNO              30
PROCNO              1

F2 - Acquisition Parameters
Date_         20150517
Time              15.01
INSTRUM          av400
PROBHD   5 mm PABBO BB/
PULPROG        zgdc.js
TD              5096
SOLVENT          CDCl3
NS              1024
DS                 0
SWH         51020.406 Hz
FIDRES      10.011854 Hz
AQ         0.0499408 sec
RG             189.85
DW             9.800 usec
DE              6.50 usec
TE             299.1 K
D1        0.00000400 sec
D11       0.03000000 sec
TD0                1

======== CHANNEL f1 ========
SFO1       128.3776052 MHz
NUC1              11B
P1              10.00 usec
PLW1       52.00000000 W

======== CHANNEL f2 ========
SFO2       400.1324008 MHz
NUC2               1H
CPDPRG[2        waltz16
PCPD2           90.00 usec
PLW2       13.00000000 W
PLW12       0.36111000 W

F2 - Processing parameters
SI              32768
SF         128.3776050 MHz
WDW                EM
SSB      0
LB              50.00 Hz
GB       0
PC               1.40
```

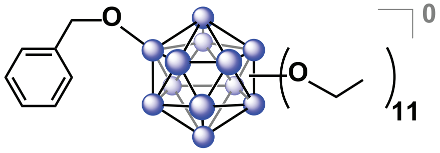

^{13}C NMR

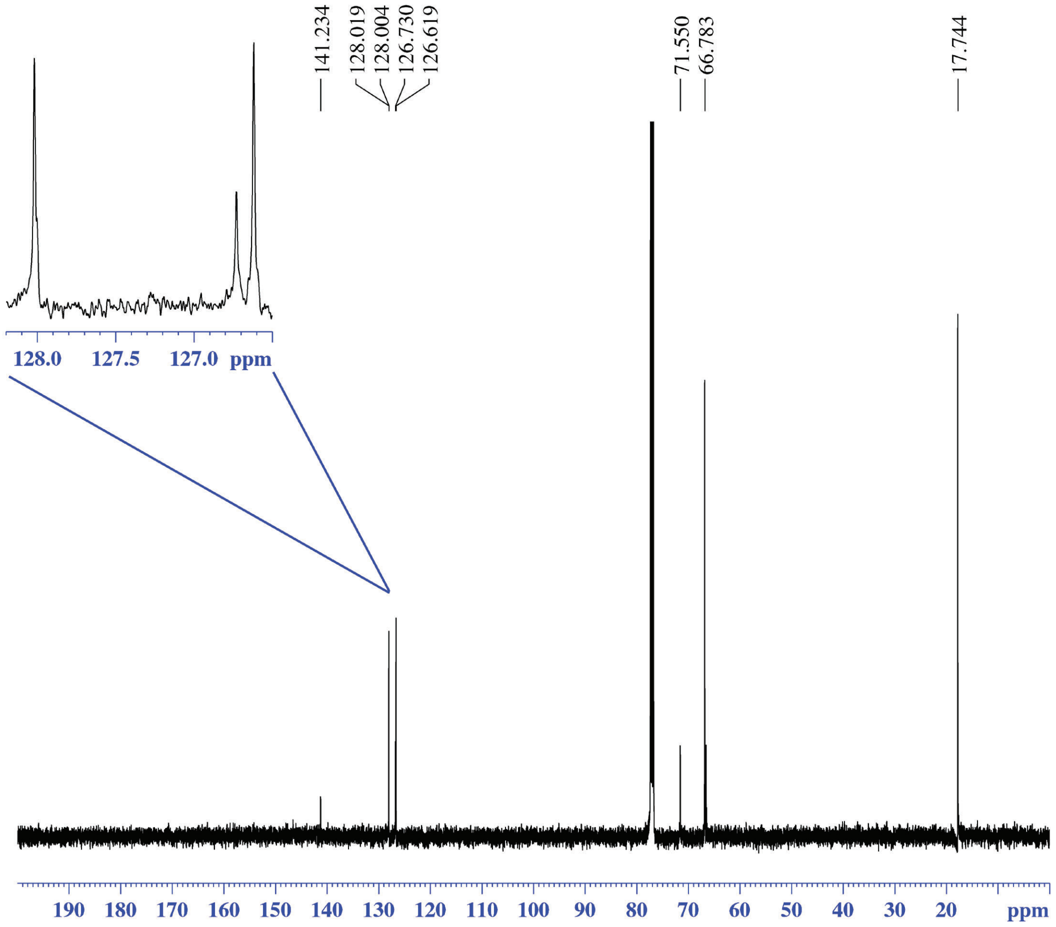

```
Current Data Parameters
NAME     B12(O-Bn)(O-Et)11
EXPNO              2
PROCNO             1

F2 - Acquisition Parameters
Date_        20150517
Time            16.29
INSTRUM         av500
PROBHD   5 mm DCH 13C-1
PULPROG        zgpg30
TD             65536
SOLVENT         CDCl3
NS                64
DS                 2
SWH        31250.000 Hz
FIDRES      0.476837 Hz
AQ         1.0485760 sec
RG             13.13
DW            16.000 usec
DE             18.00 usec
TE             298.0 K
D1        2.00000000 sec
D11       0.03000000 sec
TD0                1

======== CHANNEL f1 ========
SFO1      125.7722511 MHz
NUC1              13C
P1               9.63 usec
PLW1      23.00000000 W

======== CHANNEL f2 ========
SFO2      500.1330008 MHz
NUC2               1H
CPDPRG[2        waltz16
PCPD2           80.00 usec
PLW2      13.50000000 W
PLW12      0.21094000 W
PLW13      0.13500001 W

F2 - Processing parameters
SI            131072
SF        125.7577892 MHz
WDW               EM
SSB      0
LB              1.00 Hz
GB       0
PC              1.40
```

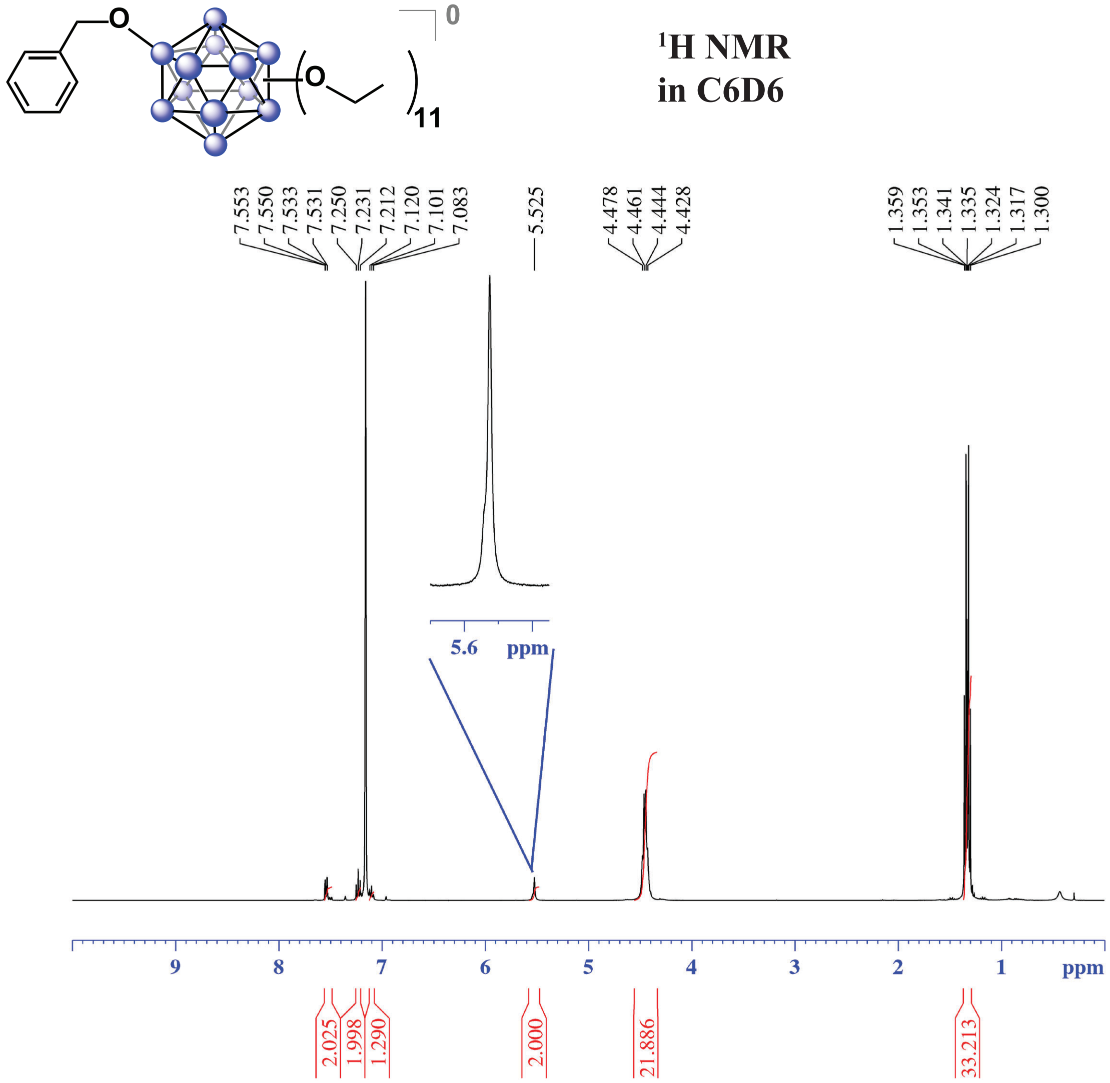

^{1}H NMR
in C6D6

Current Data Parameters
NAME Jan14-2016
EXPNO 100
PROCNO 1

F2 - Acquisition Parameters
Date_ 20160114
Time 14.59
INSTRUM av400
PROBHD 5 mm PABBO BB/
PULPROG zg30
TD 52882
SOLVENT C6D6
NS 32
DS 0
SWH 8012.820 Hz
FIDRES 0.151523 Hz
AQ 3.2998369 sec
RG 155.85
DW 62.400 usec
DE 6.50 usec
TE 299.0 K
D1 2.00000000 sec
TD0 1

======== CHANNEL f1 ========
SFO1 400.1324008 MHz
NUC1 1H
P1 15.00 usec
PLW1 13.00000000 W

F2 - Processing parameters
SI 65536
SF 400.1299967 MHz
WDW EM
SSB 0
LB 0.30 Hz
GB 0
PC 1.00

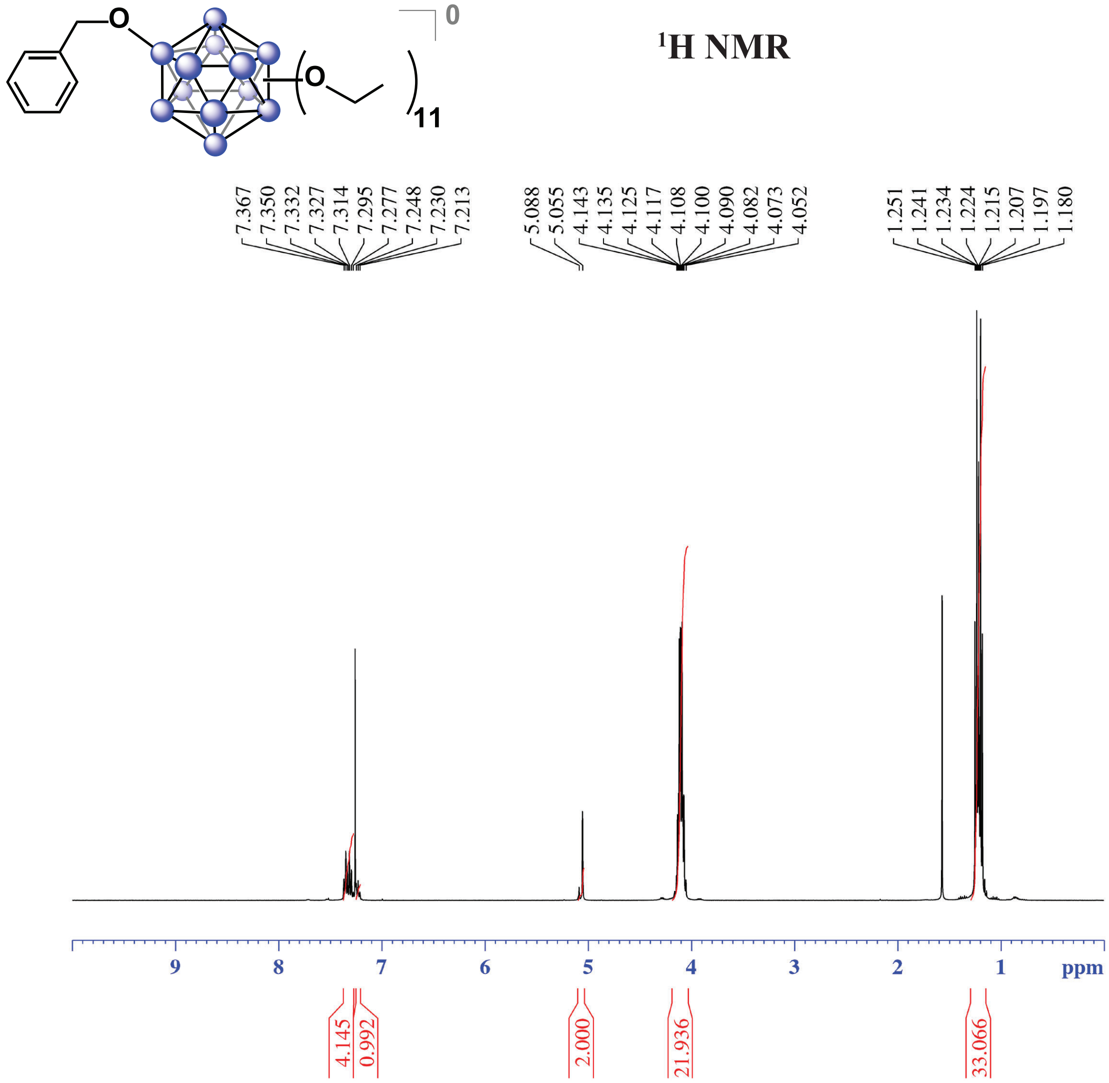

```
Current Data Parameters
NAME        Jan13-2016
EXPNO              142
PROCNO               1

F2 - Acquisition Parameters
Date_        20160113
Time            20.50
INSTRUM         av400
PROBHD  5 mm PABBO BB/
PULPROG          zg30
TD              52882
SOLVENT         CDCl3
NS                 32
DS                  0
SWH       8012.820 Hz
FIDRES    0.151523 Hz
AQ       3.2998369 sec
RG             155.85
DW         62.400 usec
DE           6.50 usec
TE            299.0 K
D1     2.00000000 sec
TD0                 1

======== CHANNEL f1 ========
SFO1    400.1324008 MHz
NUC1                 1H
P1           15.00 usec
PLW1      13.00000000 W

F2 - Processing parameters
SI              65536
SF     400.1300184 MHz
WDW                EM
SSB    0
LB            0.30 Hz
GB     0
PC               1.00
```

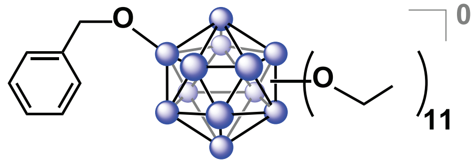

DART
High-Res Mass Spec

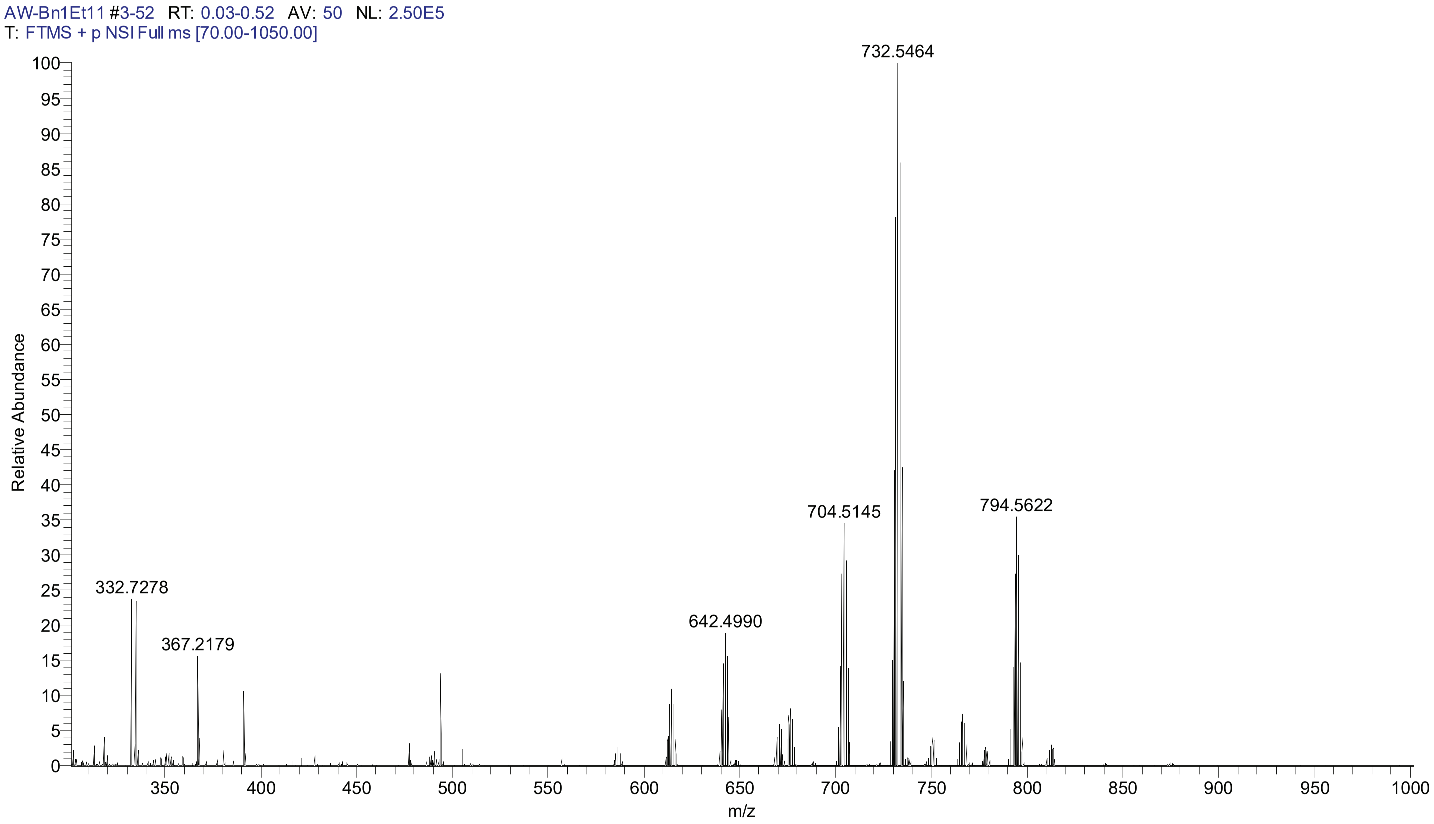

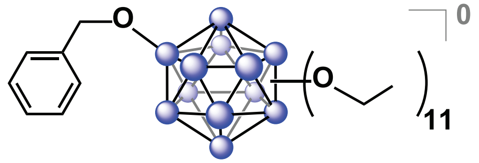

DART
High-Res Mass Spec

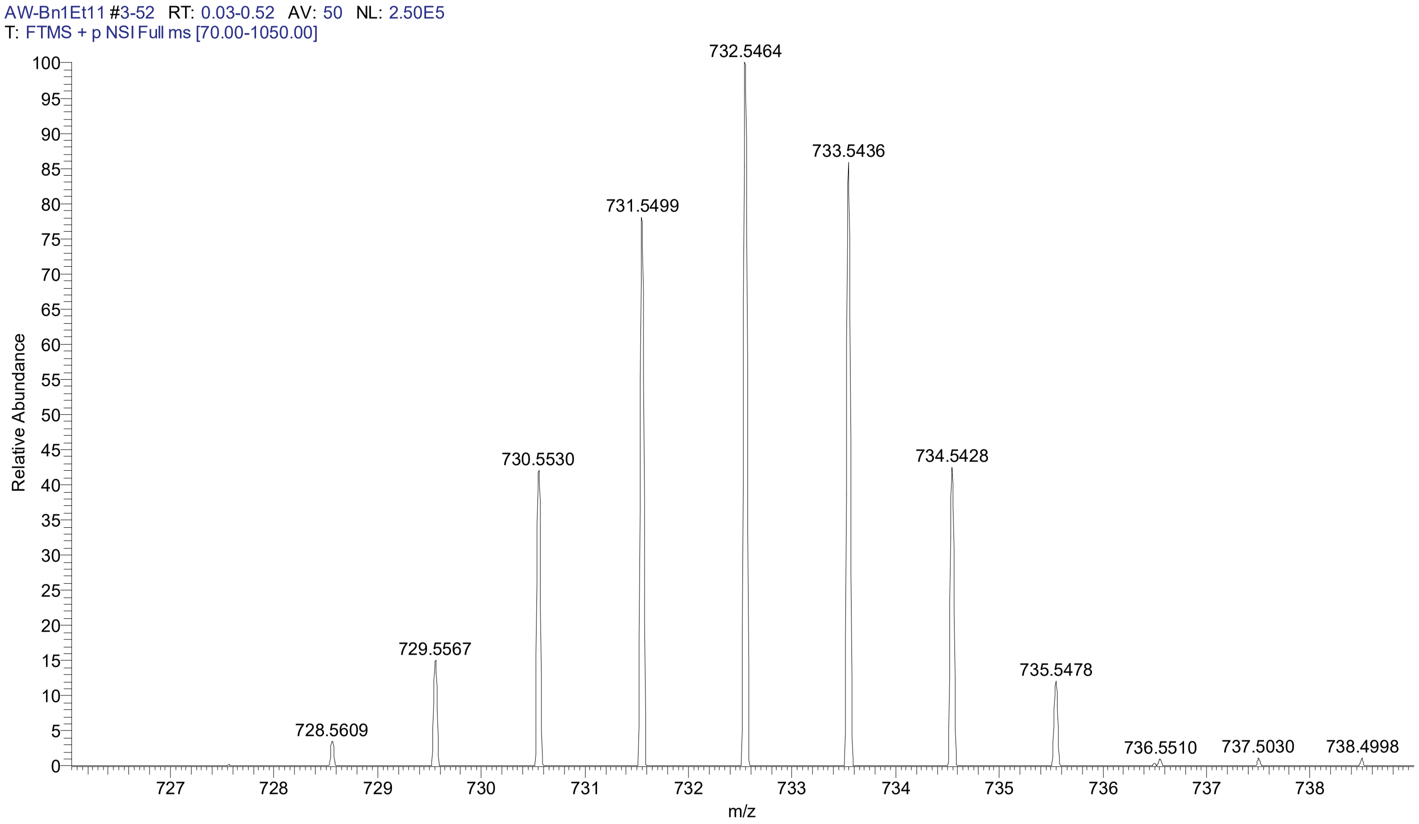

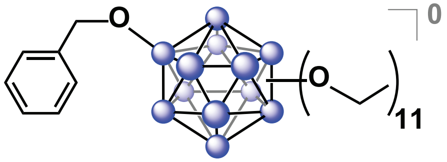
O
O
11
0

IR

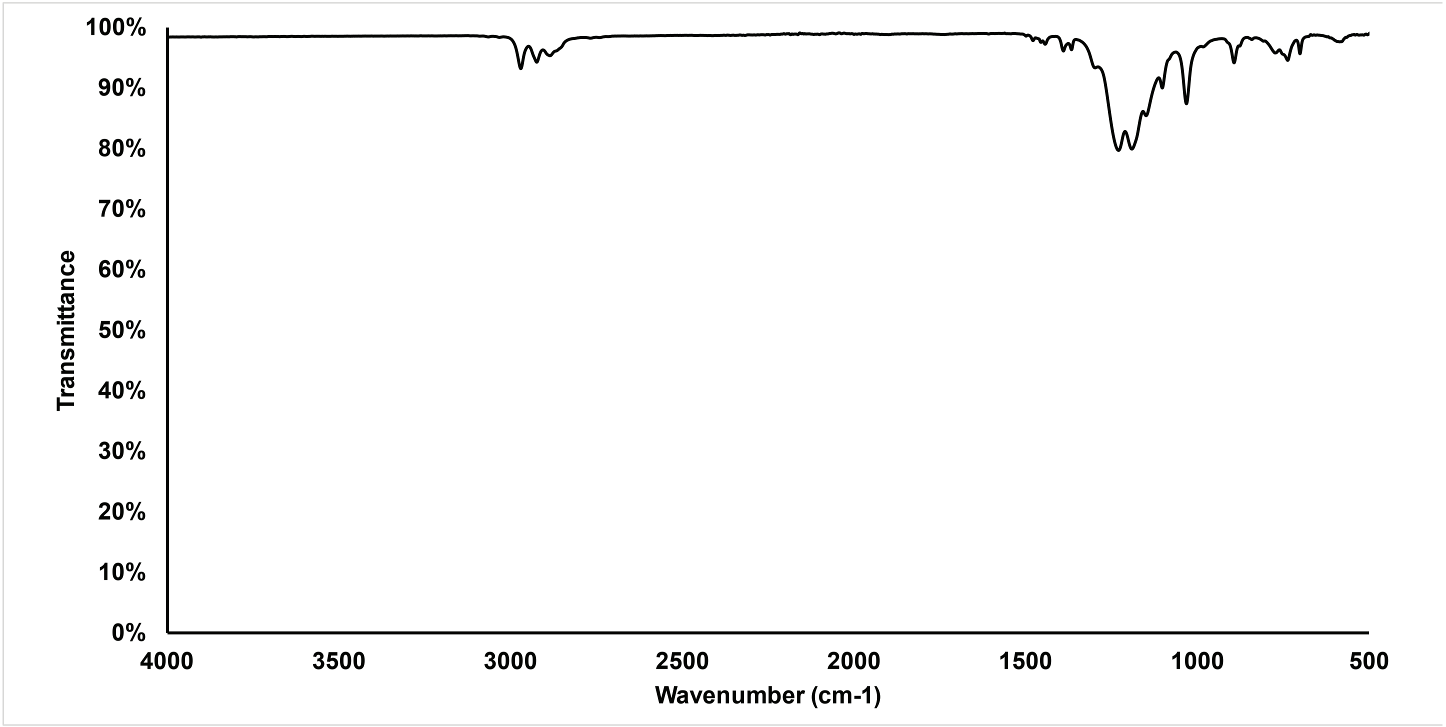
Transmittance
100%
90%
80%
70%
60%
50%
40%
30%
20%
10%
0%
4000
3500
3000
2500
2000
1500
1000
500
Wavenumber (cm-1)

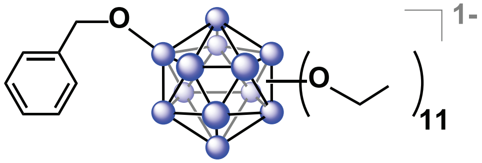

EPR

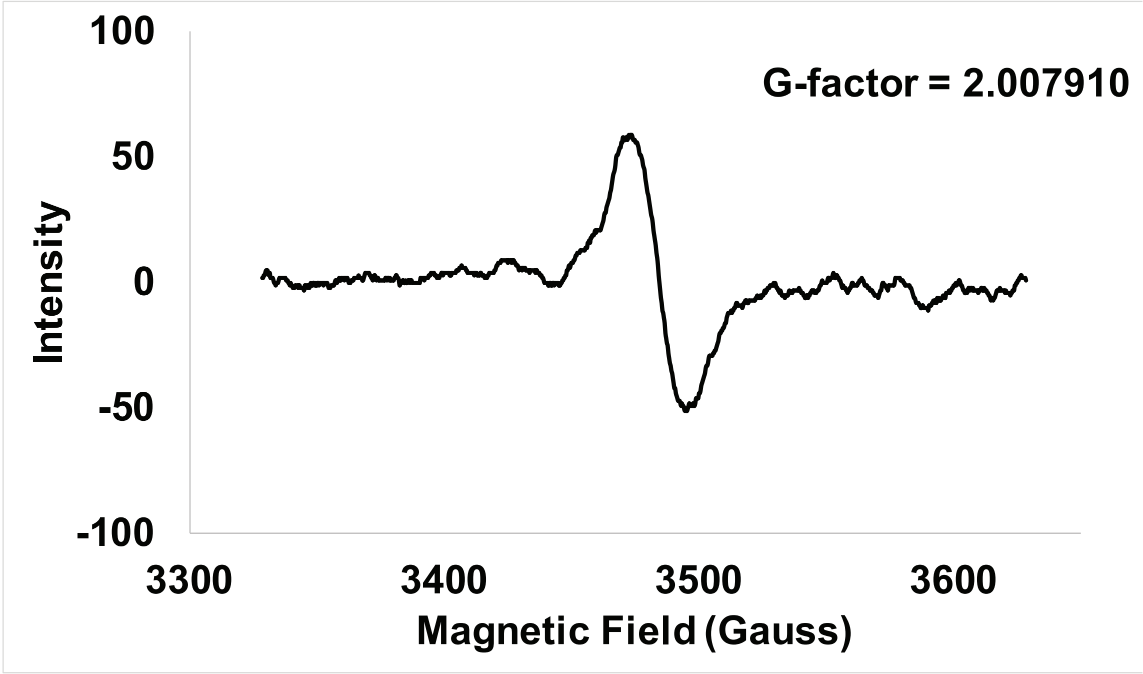

DOS	Format
ANZ	1024
MIN	-51.404297
MAX	58.595703
JSS	0
GST	3328.55
GSI	300
JUN	G
JON	Bruker BioSpin GmbH
JDA	11/2/2015
JTM	20:39
JRE	c:\programfiles\bruker-emx\syscal\st0103.cal
JEX	field-sweep
JSD	1
HCF	3478.55
HSW	300
EMF	0
RCT	20.48
RTC	327.68
RRG	8.93E+03
RMA	4
MF	9.77575
MP	2.54E+00
MPD	19

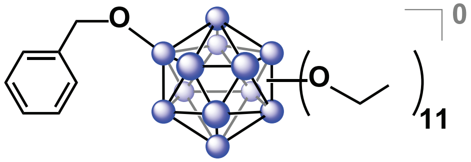

Cyclic voltammetry

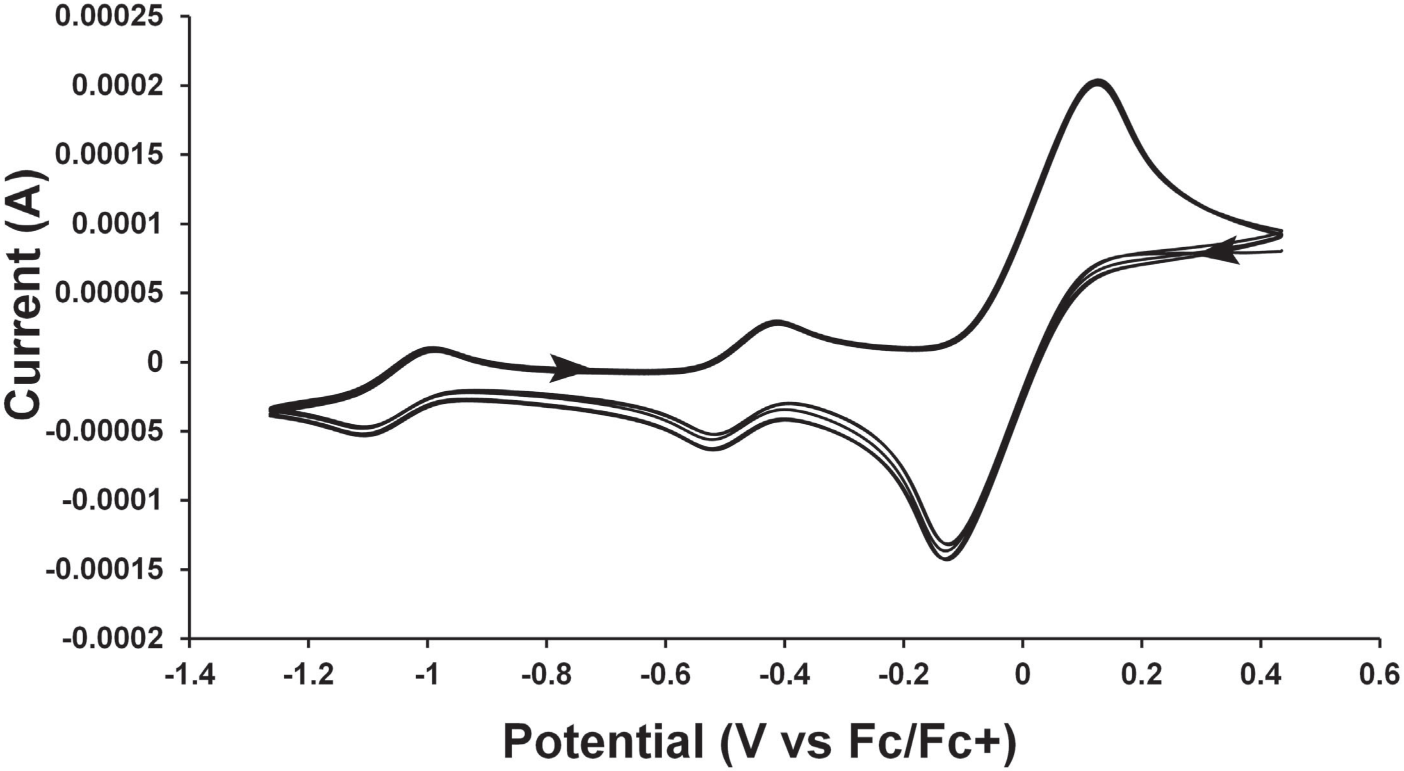

Supplemental spectra & data for Chapter 3

^{11}B NMR Spectra of **[2a]**

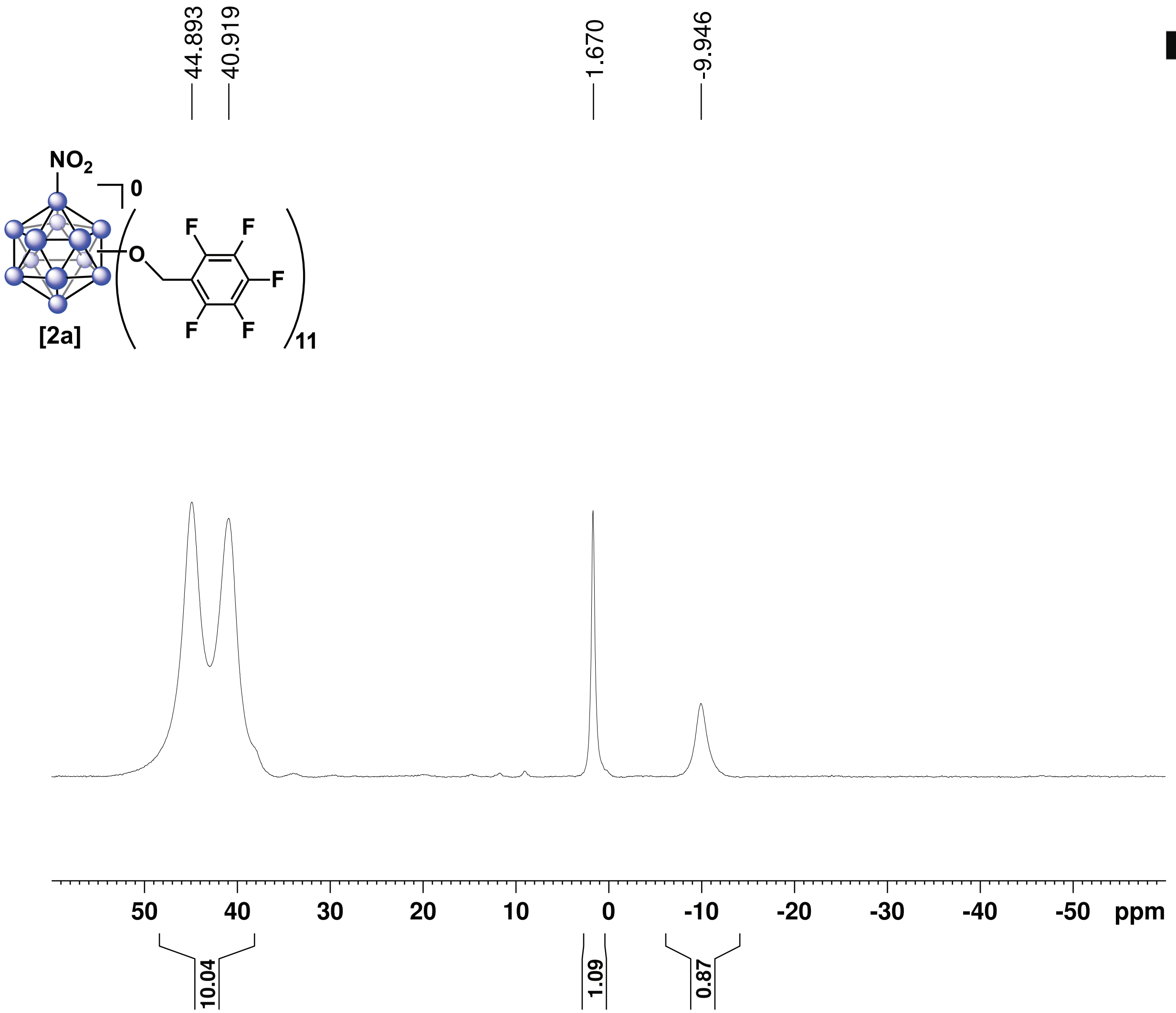

```
Current Data Parameters
NAME         Jan09-2018
EXPNO                21
PROCNO                1

F2 - Acquisition Parameters
Date_          20180109
Time              10.09
INSTRUM           av400
PROBHD   5 mm PABBO BB/
PULPROG              zg
TD                 5096
SOLVENT          CD2Cl2
NS                 1024
DS                    0
SWH       51020.406 Hz
FIDRES     10.011854 Hz
AQ        0.0499408 sec
RG               189.85
DW           9.800 usec
DE            6.50 usec
TE              297.9 K
D1      0.05000000 sec
TD0                   1

======== CHANNEL f1 ========
SFO1     128.3776052 MHz
NUC1                 11B
P1            10.00 usec
PLW1       52.00000000 W

F2 - Processing parameters
SI                32768
SF       128.3776547 MHz
WDW                  EM
SSB     0
LB             10.00 Hz
GB      0
PC                 1.40
```

^{19}F NMR Spectra of **[2a]**

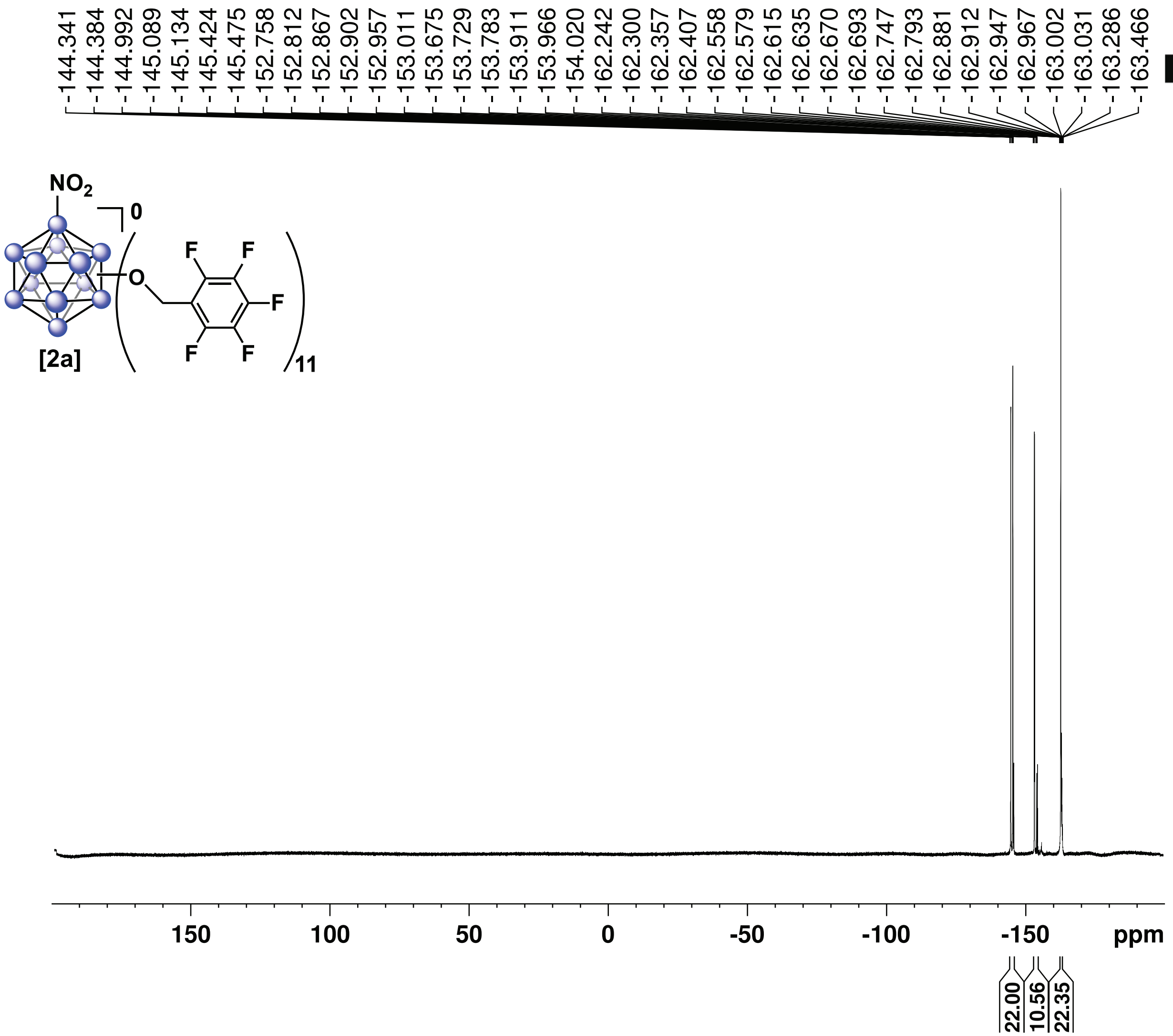

```
Current Data Parameters
NAME        Jan09-2018
EXPNO              22
PROCNO              1

F2 - Acquisition Parameters
Date_         20180109
Time            10.12
INSTRUM         av400
PROBHD   5 mm PABBO BB/
PULPROG       zgflqn30
TD             262144
SOLVENT         CD2Cl2
NS                 32
DS                  0
SWH        150000.000 Hz
FIDRES       0.572205 Hz
AQ          0.8738133 sec
RG             189.85
DW              3.333 usec
DE               6.50 usec
TE              297.9 K
D1         2.00000000 sec
TD0                 1

======== CHANNEL f1 ========
SFO1      376.4983660 MHz
NUC1              19F
P1              14.50 usec
PLW1      17.00000000 W

F2 - Processing parameters
SI             262144
SF        376.4984698 MHz
WDW                EM
SSB     0
LB               1.00 Hz
GB      0
PC               1.00
```

^{1}H NMR Spectra of **[2a]**

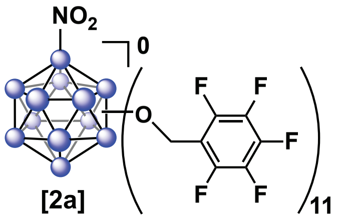

[2a]

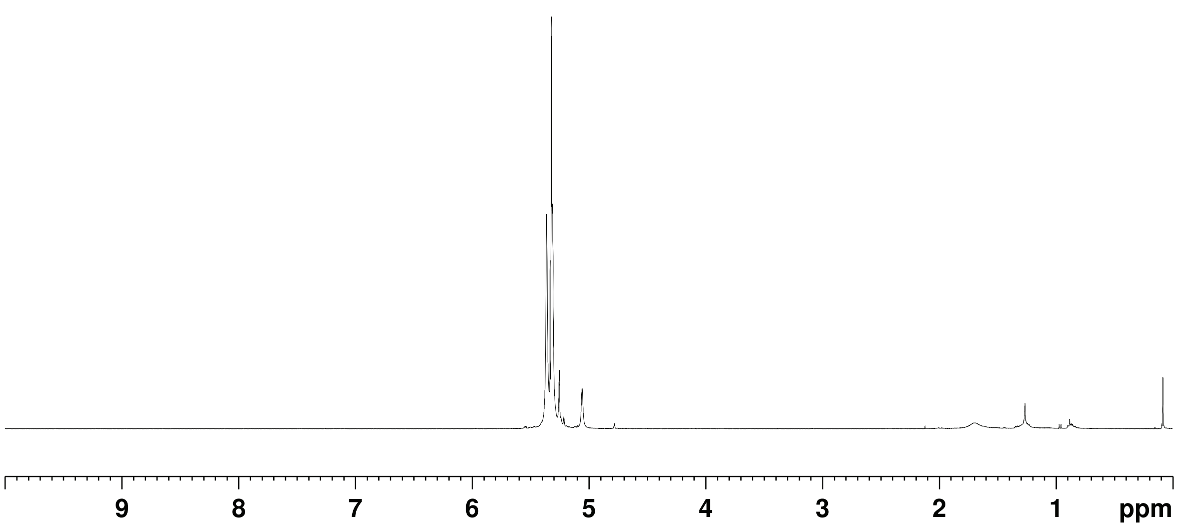

```
Current Data Parameters
NAME        Jan09-2018
EXPNO               20
PROCNO               1

F2 - Acquisition Parameters
Date_         20180109
Time             10.06
INSTRUM          av400
PROBHD   5 mm PABBO BB/
PULPROG           zg30
TD               52882
SOLVENT         CD2Cl2
NS                  32
DS                   0
SWH         8012.820 Hz
FIDRES      0.151523 Hz
AQ        3.2998369 sec
RG              189.85
DW          62.400 usec
DE            6.50 usec
TE             297.8 K
D1       2.00000000 sec
TD0                  1

======== CHANNEL f1 ========
SFO1      400.1324008 MHz
NUC1                 1H
P1             15.00 usec
PLW1       13.00000000 W

F2 - Processing parameters
SI               65536
SF       400.1300154 MHz
WDW                 EM
SSB      0
LB             0.30 Hz
GB       0
PC                1.00
```

^{1}H NMR Spectra of **[2a]**

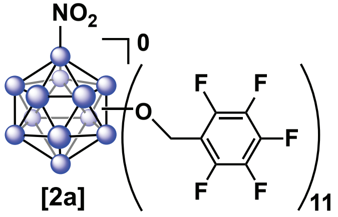

[2a]

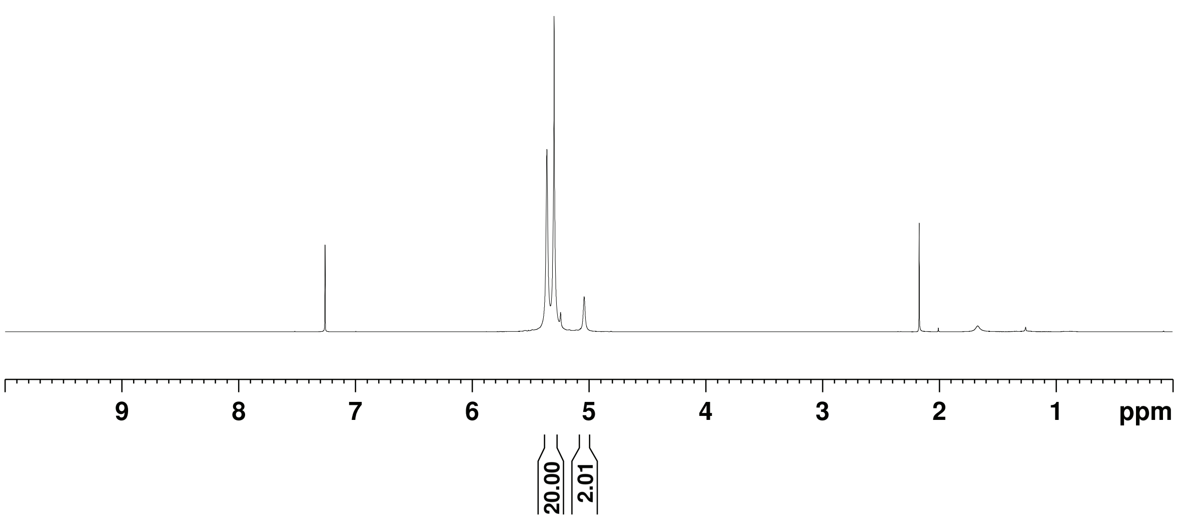

```
Current Data Parameters
NAME        Jul02-2017
EXPNO               51
PROCNO               1

F2 - Acquisition Parameters
Date_         20170702
Time             19.00
INSTRUM          av400
PROBHD  5 mm PABBO BB/
PULPROG           zg30
TD               52882
SOLVENT          CDCl3
NS                  32
DS                   0
SWH        8012.820 Hz
FIDRES     0.151523 Hz
AQ       3.2998369 sec
RG              155.85
DW          62.400 usec
DE            6.50 usec
TE             298.3 K
D1      2.00000000 sec
TD0                  1

======== CHANNEL f1 ========
SFO1      400.1324008 MHz
NUC1               1H
P1              15.00 usec
PLW1     13.00000000 W

F2 - Processing parameters
SI              65536
SF       400.1300180 MHz
WDW                EM
SSB    0
LB               0.30 Hz
GB     0
PC               1.00
```

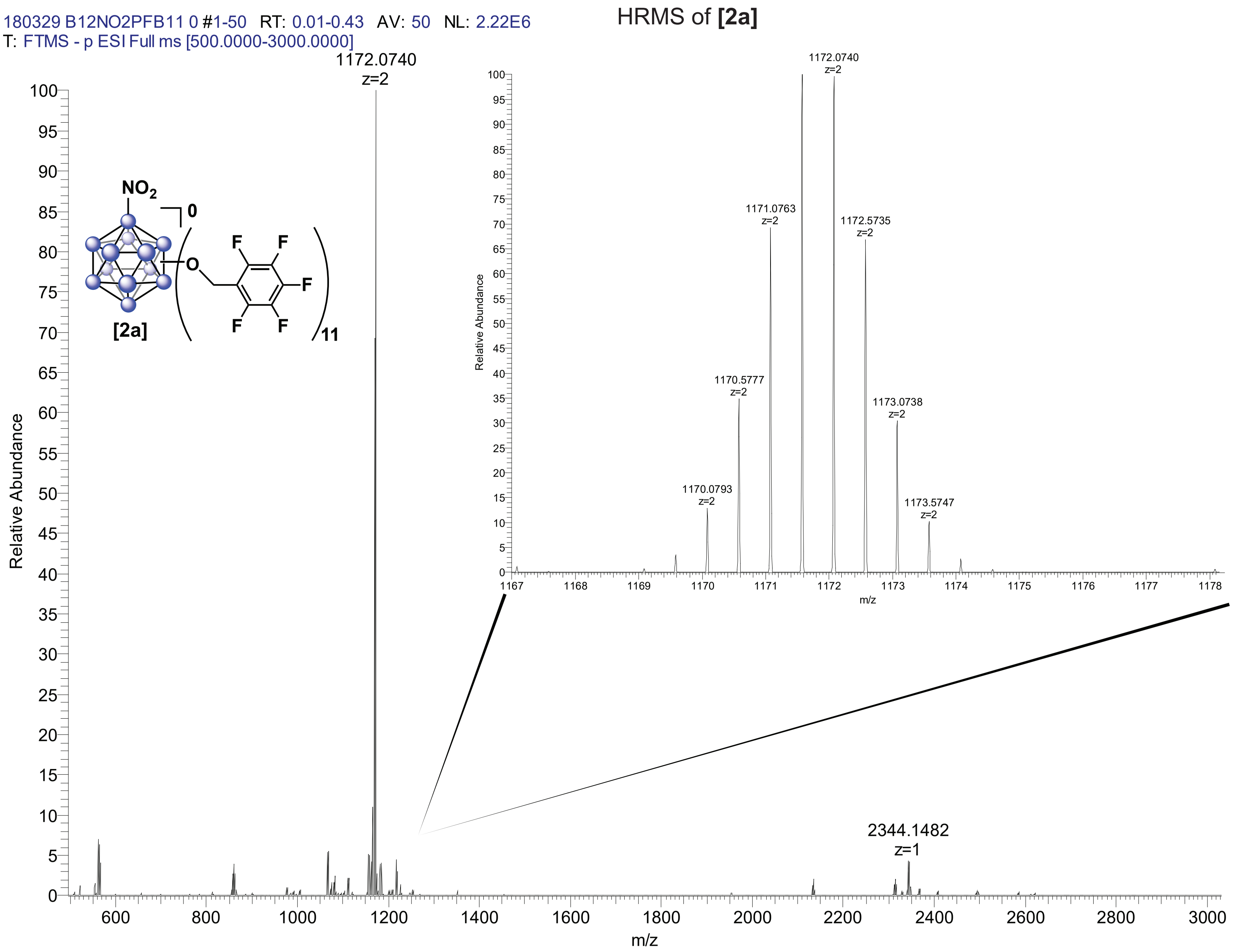
HRMS of **[2a]**

180329 B12NO2PFB11 0 #1-50 RT: 0.01-0.43 AV: 50 NL: 2.22E6
T: FTMS - p ESI Full ms [500.0000-3000.0000]
Relative Abundance
m/z
1172.0740
z=2
2344.1482
z=1
NO2
0
O
F
11
[2a]
1170.0793
z=2
1170.5777
z=2
1171.0763
z=2
1172.0740
z=2
1172.5735
z=2
1173.0738
z=2
1173.5747
z=2

IR Spectra of **[2a]**

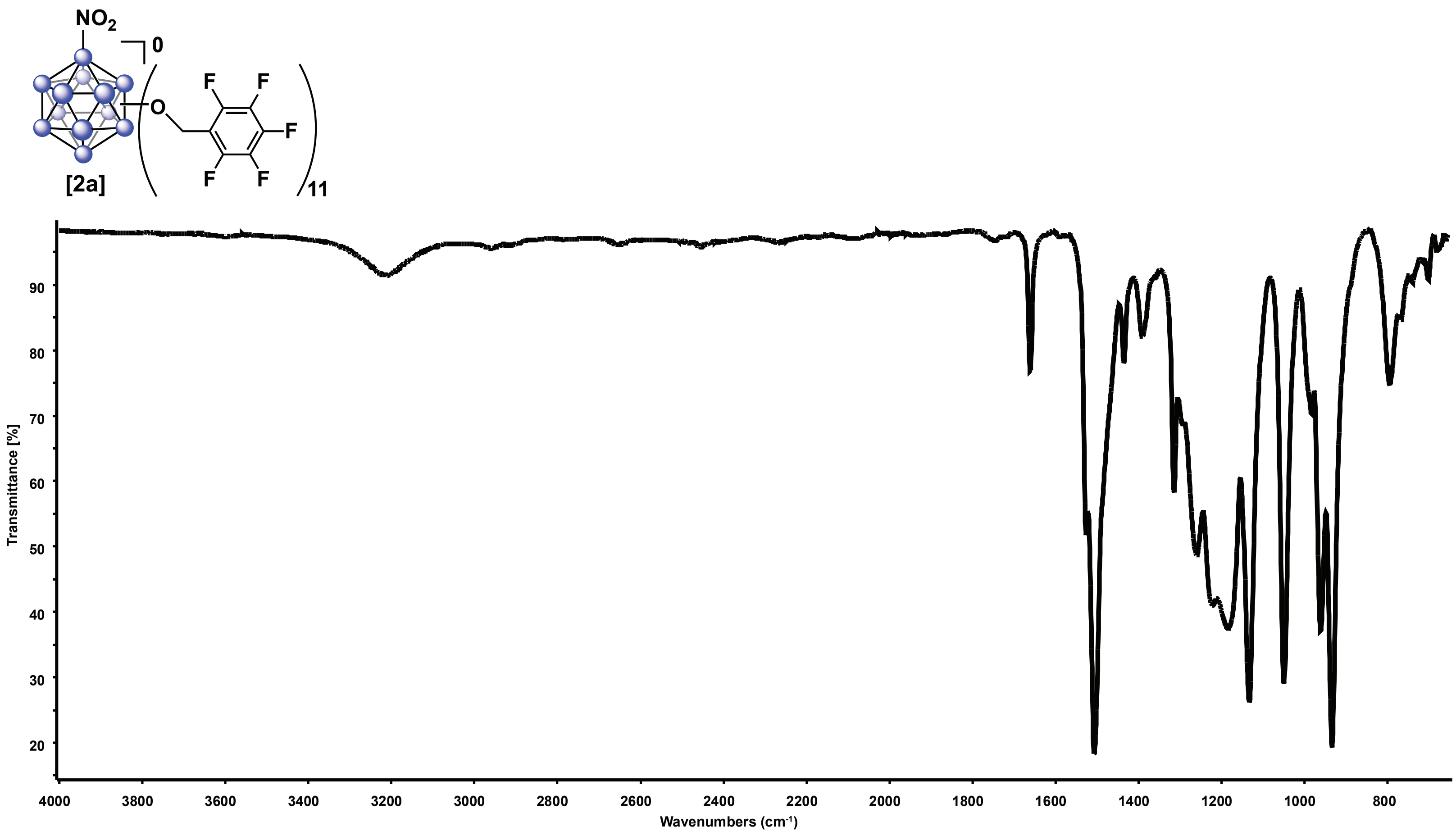

^{11}B NMR Spectra of **[2b]**

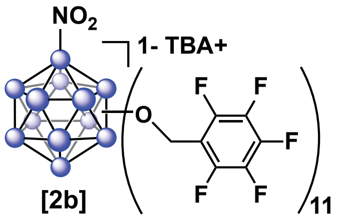

[2b]

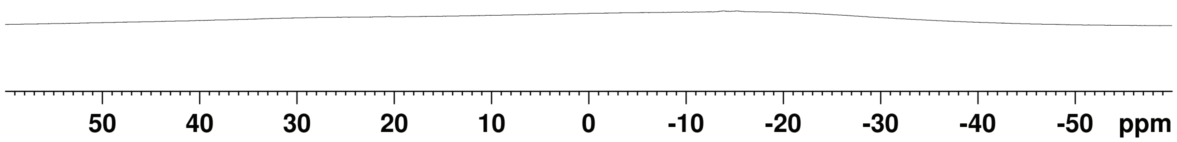

```
Current Data Parameters
NAME         Jan16-2018
EXPNO               172
PROCNO                1

F2 - Acquisition Parameters
Date_          20180117
Time               0.15
INSTRUM           av400
PROBHD   5 mm PABBO BB/
PULPROG              zg
TD                 5096
SOLVENT           CD3CN
NS                 1024
DS                    0
SWH          51020.406 Hz
FIDRES       10.011854 Hz
AQ           0.0499408 sec
RG               189.85
DW                9.800 usec
DE                 6.50 usec
TE                298.2 K
D1           0.05000000 sec
TD0                   1

======== CHANNEL f1 ========
SFO1        128.3776052 MHz
NUC1                11B
P1                10.00 usec
PLW1        52.00000000 W

F2 - Processing parameters
SI                32768
SF          128.3775340 MHz
WDW                  EM
SSB      0
LB                10.00 Hz
GB       0
PC                 1.40
```

^{19}F NMR Spectra of **[2b]**

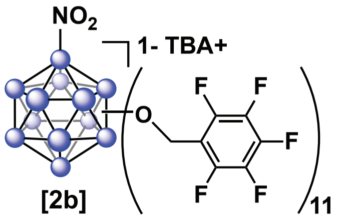

[2b]

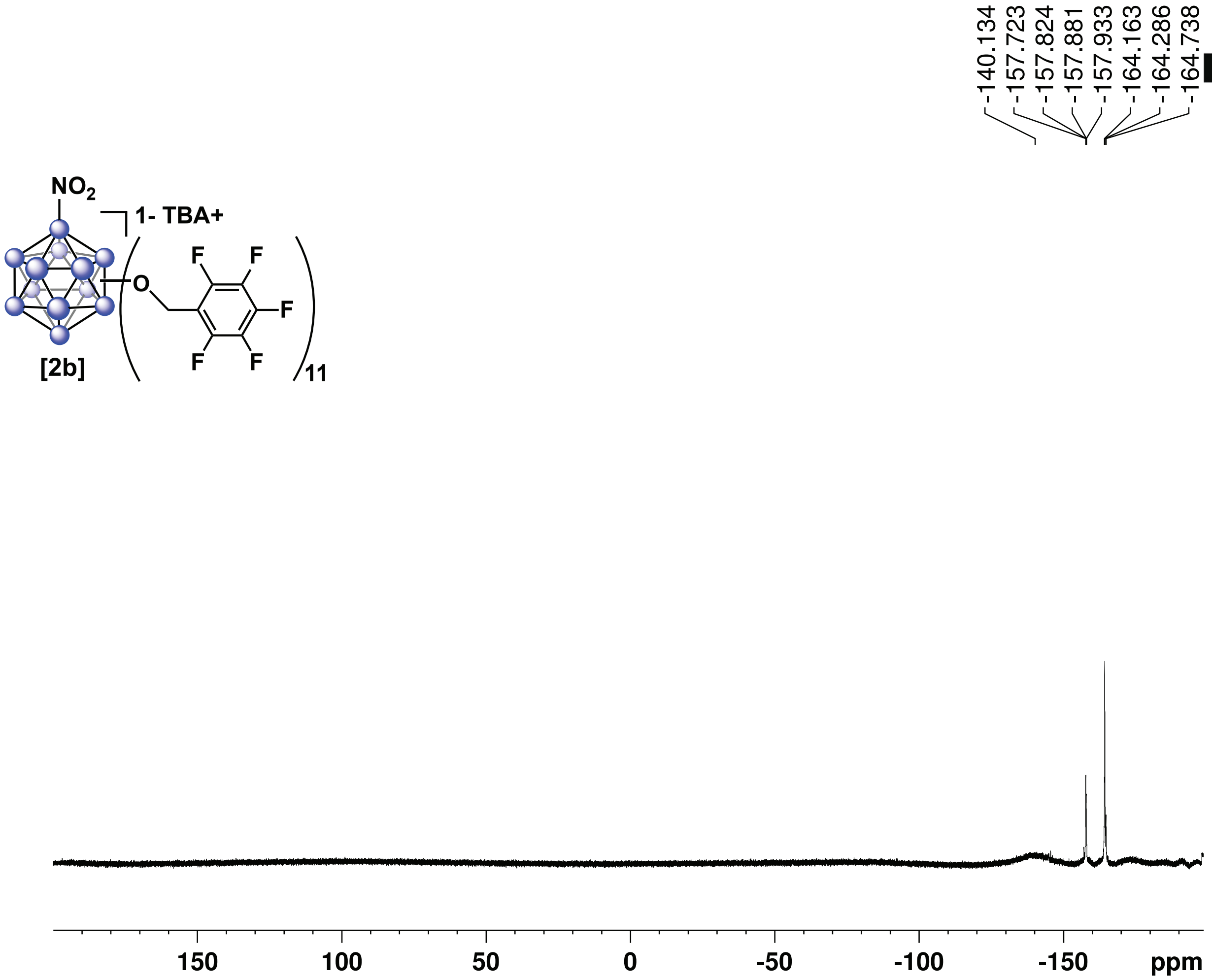

```
Current Data Parameters
NAME          Jan16-2018
EXPNO                171
PROCNO                 1

F2 - Acquisition Parameters
Date_           20180117
Time                0.12
INSTRUM            av400
PROBHD   5 mm PABBO BB/
PULPROG         zgflqn30
TD                262144
SOLVENT            CD3CN
NS                    32
DS                     0
SWH          150000.000 Hz
FIDRES         0.572205 Hz
AQ            0.8738133 sec
RG                189.85
DW                 3.333 usec
DE                  6.50 usec
TE                 298.2 K
D1           2.00000000 sec
TD0                    1

======== CHANNEL f1 ========
SFO1        376.4983660 MHz
NUC1                 19F
P1                 14.50 usec
PLW1         17.00000000 W

F2 - Processing parameters
SI                262144
SF          376.4981063 MHz
WDW                   EM
SSB      0
LB                  1.00 Hz
GB       0
PC                  1.00
```

^{1}H NMR Spectra of **[2b]**

[2b]

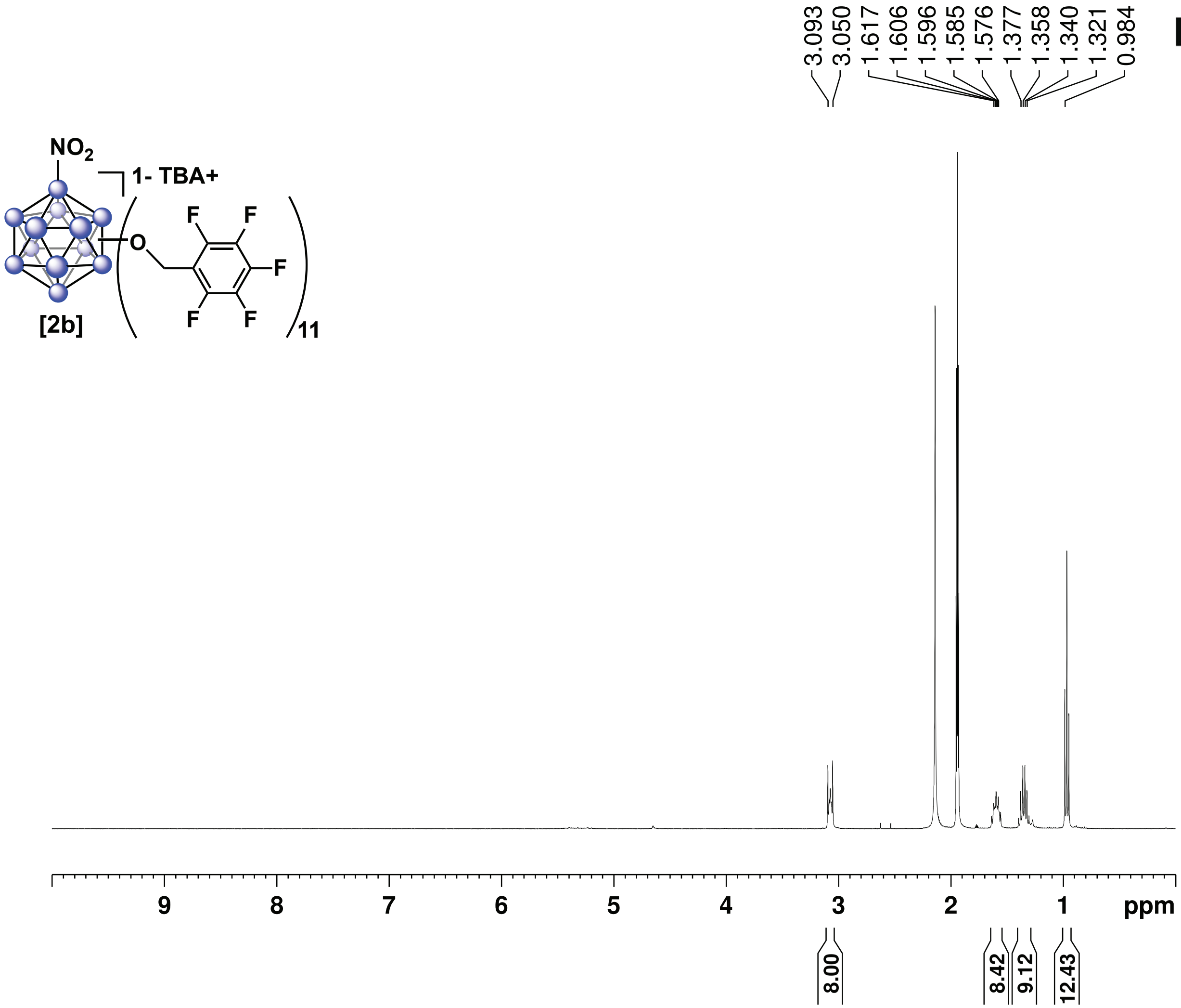

```
Current Data Parameters
NAME        Jan16-2018
EXPNO              170
PROCNO               1

F2 - Acquisition Parameters
Date_         20180117
Time              0.09
INSTRUM          av400
PROBHD   5 mm PABBO BB/
PULPROG           zg30
TD               52882
SOLVENT          CD3CN
NS                  32
DS                   0
SWH          8012.820 Hz
FIDRES       0.151523 Hz
AQ          3.2998369 sec
RG              189.85
DW              62.400 usec
DE                6.50 usec
TE               298.2 K
D1         2.00000000 sec
TD0                  1

======== CHANNEL f1 ========
SFO1       400.1324008 MHz
NUC1                1H
P1               15.00 usec
PLW1       13.00000000 W

F2 - Processing parameters
SI               65536
SF         400.1300113 MHz
WDW                 EM
SSB      0
LB                0.30 Hz
GB       0
PC                1.00
```

HRMS of **[2b]**

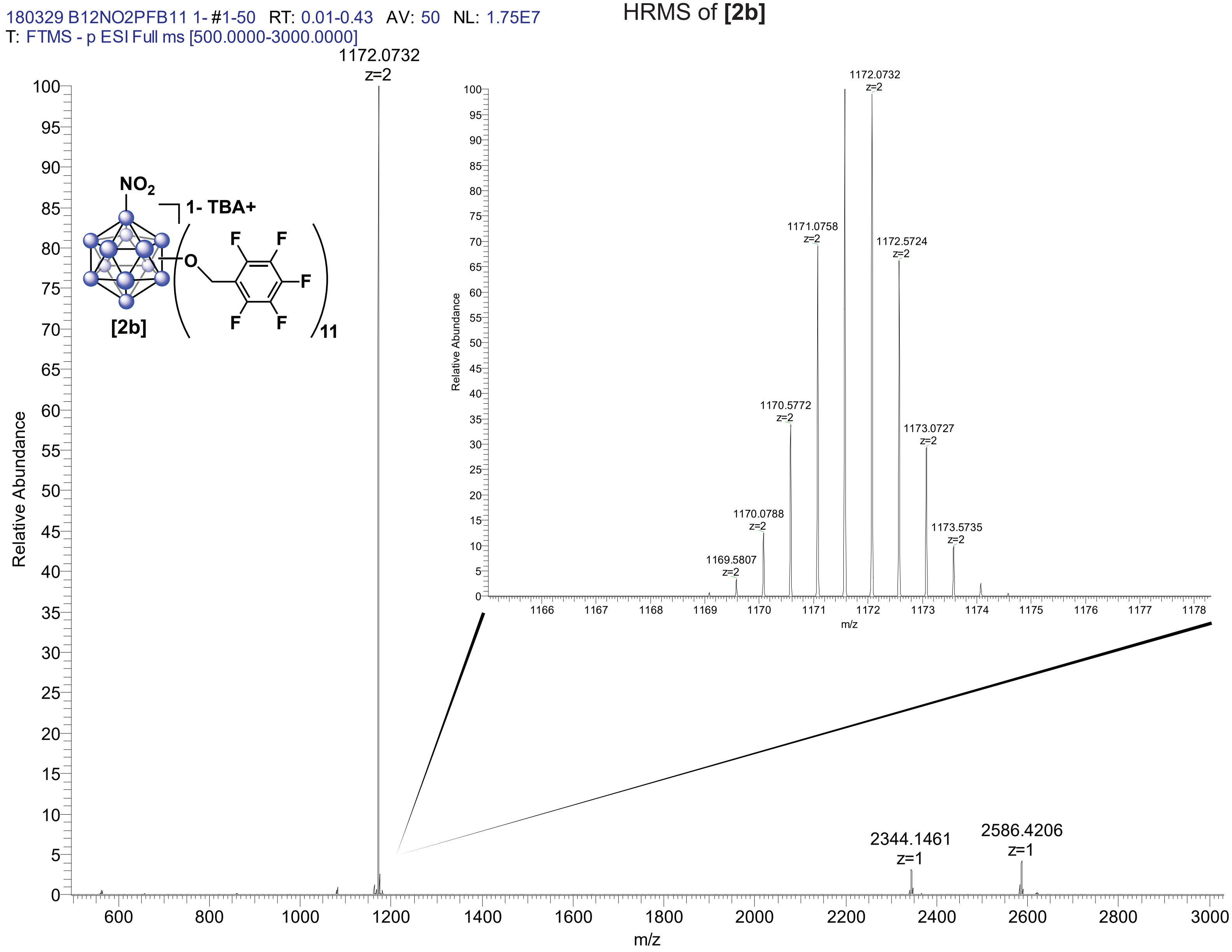
180329 B12NO2PFB11 1- #1-50 RT: 0.01-0.43 AV: 50 NL: 1.75E7
T: FTMS - p ESI Full ms [500.0000-3000.0000]
1172.0732
z=2
Relative Abundance
0
5
10
15
20
25
30
35
40
45
50
55
60
65
70
75
80
85
90
95
100
NO2
1- TBA+
O
F
F
F
F
F
11
[2b]
600
800
1000
1200
1400
1600
1800
2000
2200
2400
2600
2800
3000
m/z
2344.1461
z=1
2586.4206
z=1
1169.5807
z=2
1170.0788
z=2
1170.5772
z=2
1171.0758
z=2
1172.0732
z=2
1172.5724
z=2
1173.0727
z=2
1173.5735
z=2
1166
1167
1168
1169
1170
1171
1172
1173
1174
1175
1176
1177
1178

IR Spectra of **[2b]**

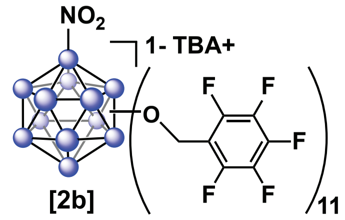
NO2
1- TBA+
O
F
F
F
F
F
11

[2b]

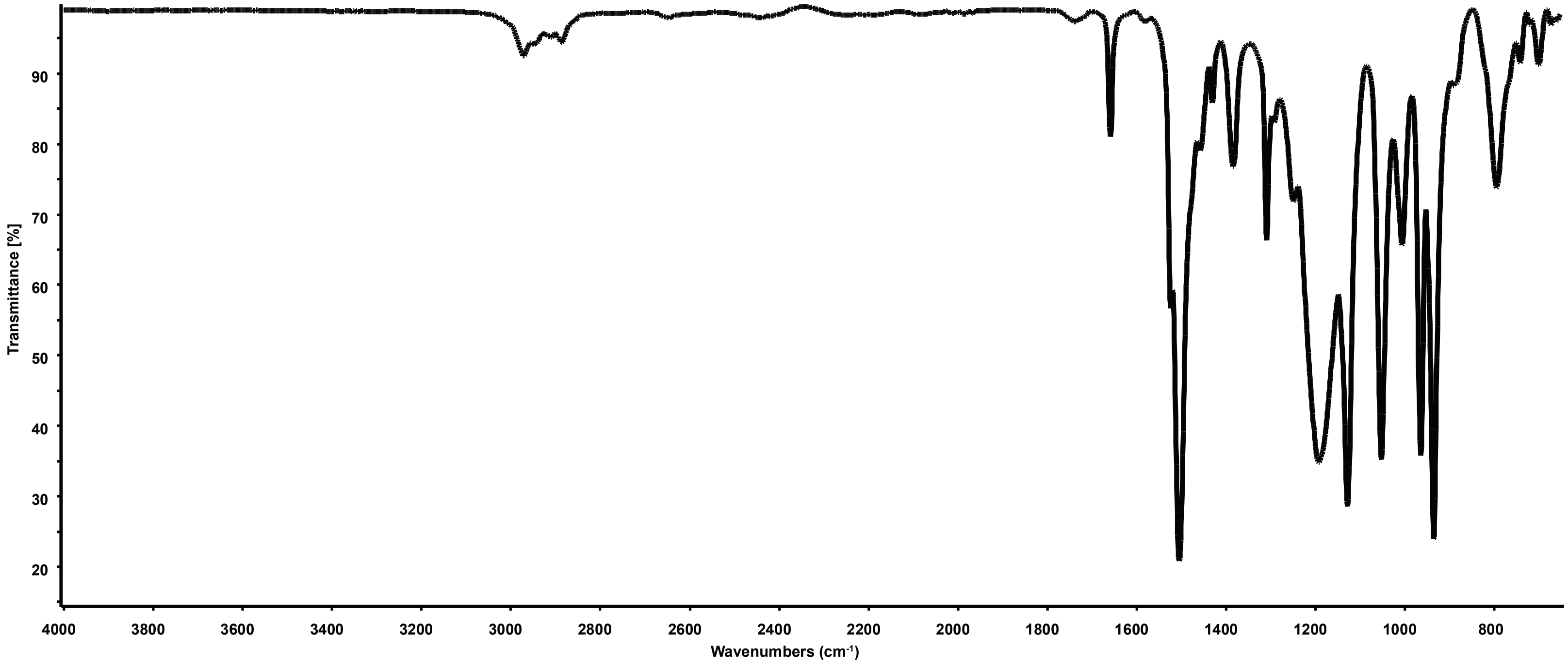

^{11}B NMR Spectra of **[2c]**

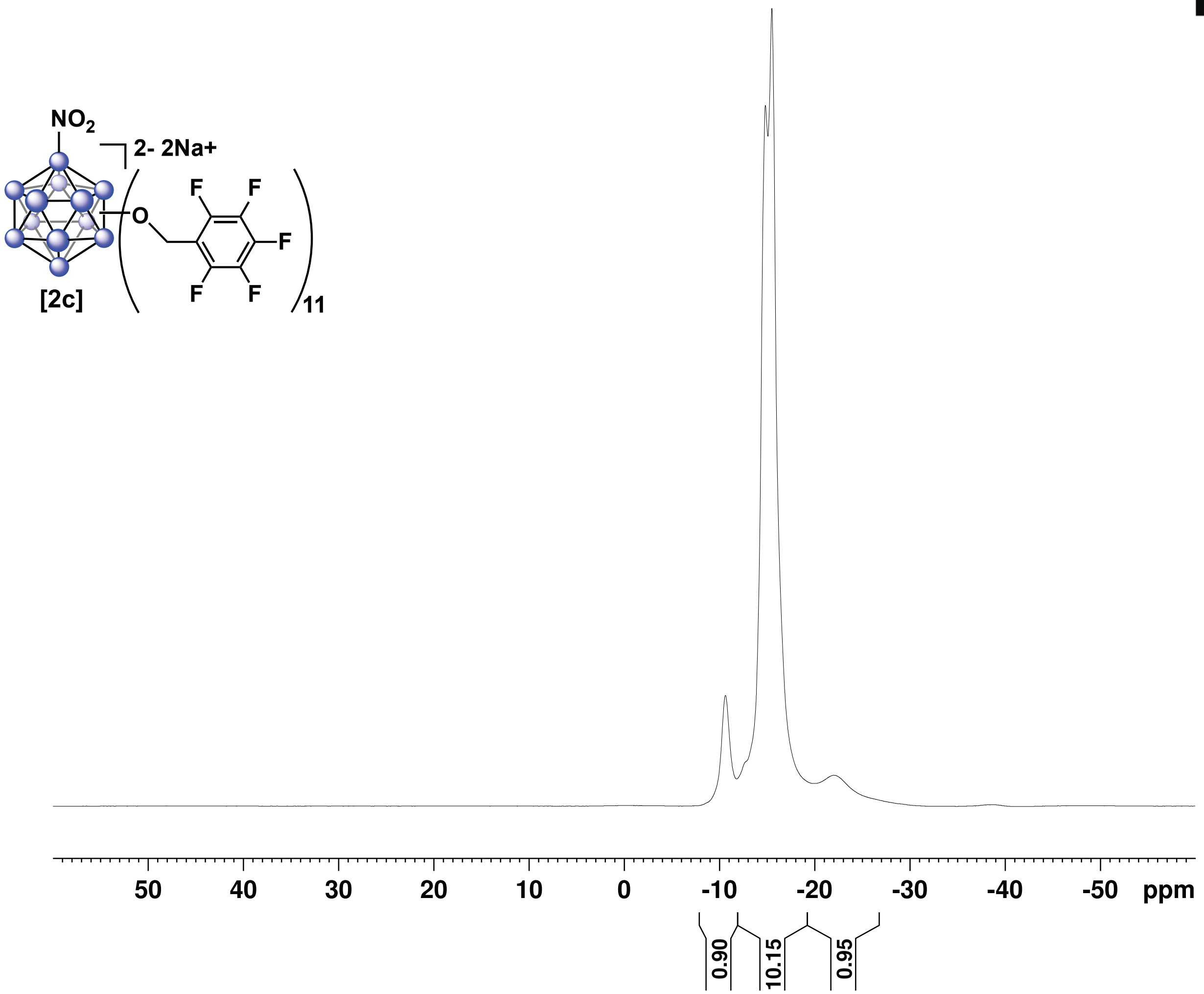

[2c]

```
Current Data Parameters
NAME         Jan12-2018
EXPNO                71
PROCNO                1

F2 - Acquisition Parameters
Date_          20180112
Time              14.26
INSTRUM           av400
PROBHD   5 mm PABBO BB/
PULPROG              zg
TD                 5096
SOLVENT           CD3CN
NS                 1024
DS                    0
SWH          51020.406 Hz
FIDRES       10.011854 Hz
AQ          0.0499408 sec
RG               189.85
DW                9.800 usec
DE                 6.50 usec
TE                298.2 K
D1         0.05000000 sec
TD0                   1

======== CHANNEL f1 ========
SFO1       128.3776052 MHz
NUC1                11B
P1                10.00 usec
PLW1        52.00000000 W

F2 - Processing parameters
SI                32768
SF          128.3776161 MHz
WDW                  EM
SSB     0
LB                10.00 Hz
GB      0
PC                 1.40
```

^{19}F NMR Spectra of **[2c]**

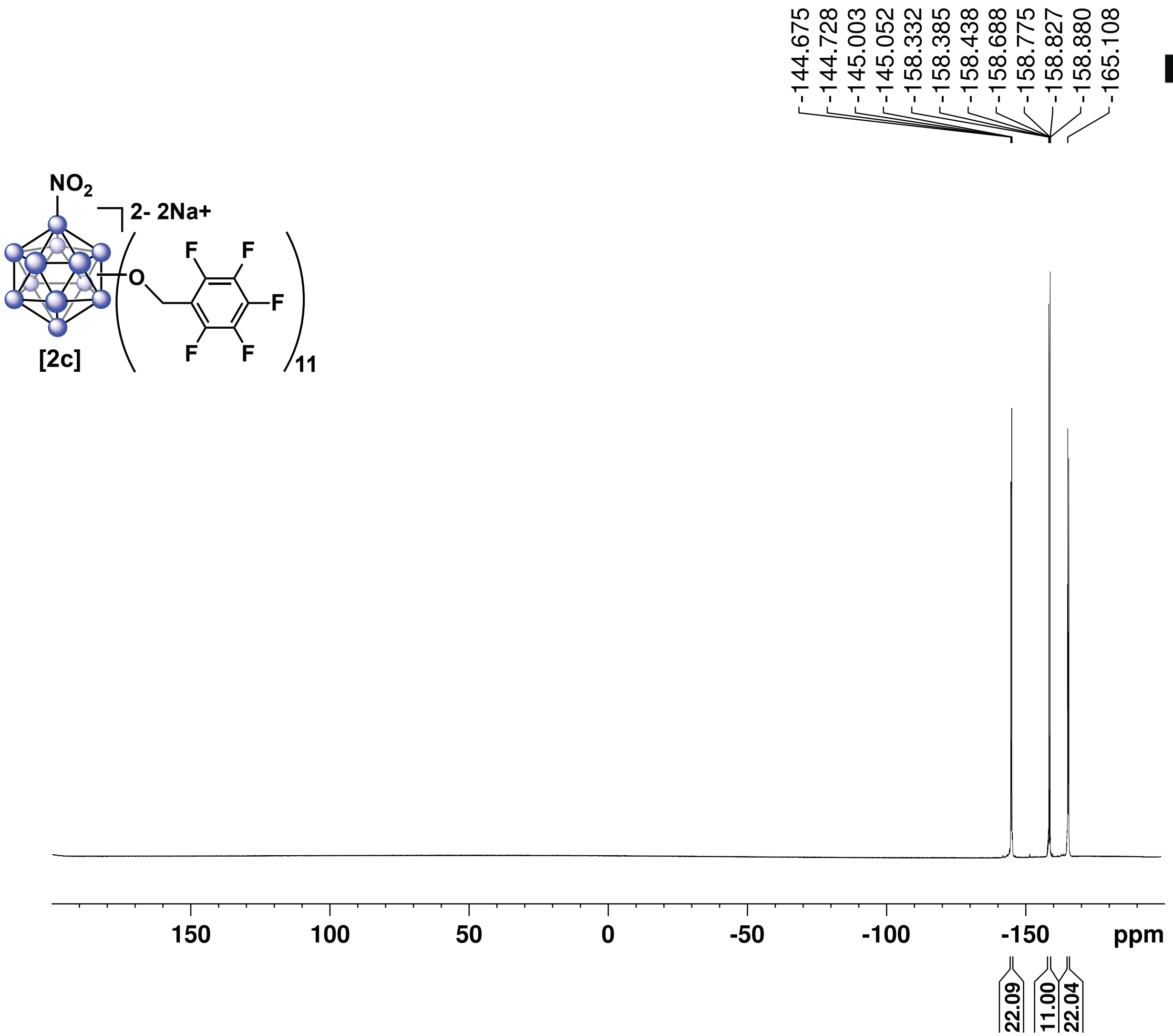

```
Current Data Parameters
NAME        Jan12-2018
EXPNO               72
PROCNO               1

F2 - Acquisition Parameters
Date_         20180112
Time             14.31
INSTRUM          av400
PROBHD   5 mm PABBO BB/
PULPROG        zgflqn30
TD              262144
SOLVENT          CD3CN
NS                  32
DS                   0
SWH        150000.000 Hz
FIDRES       0.572205 Hz
AQ          0.8738133 sec
RG              189.85
DW               3.333 usec
DE                6.50 usec
TE               298.2 K
D1         2.00000000 sec
TD0                  1

======== CHANNEL f1 ========
SFO1      376.4983660 MHz
NUC1               19F
P1               14.50 usec
PLW1       17.00000000 W

F2 - Processing parameters
SI              262144
SF        376.4981932 MHz
WDW                 EM
SSB     0
LB                1.00 Hz
GB      0
PC                1.00
```

^{1}H NMR Spectra of **[2c]**

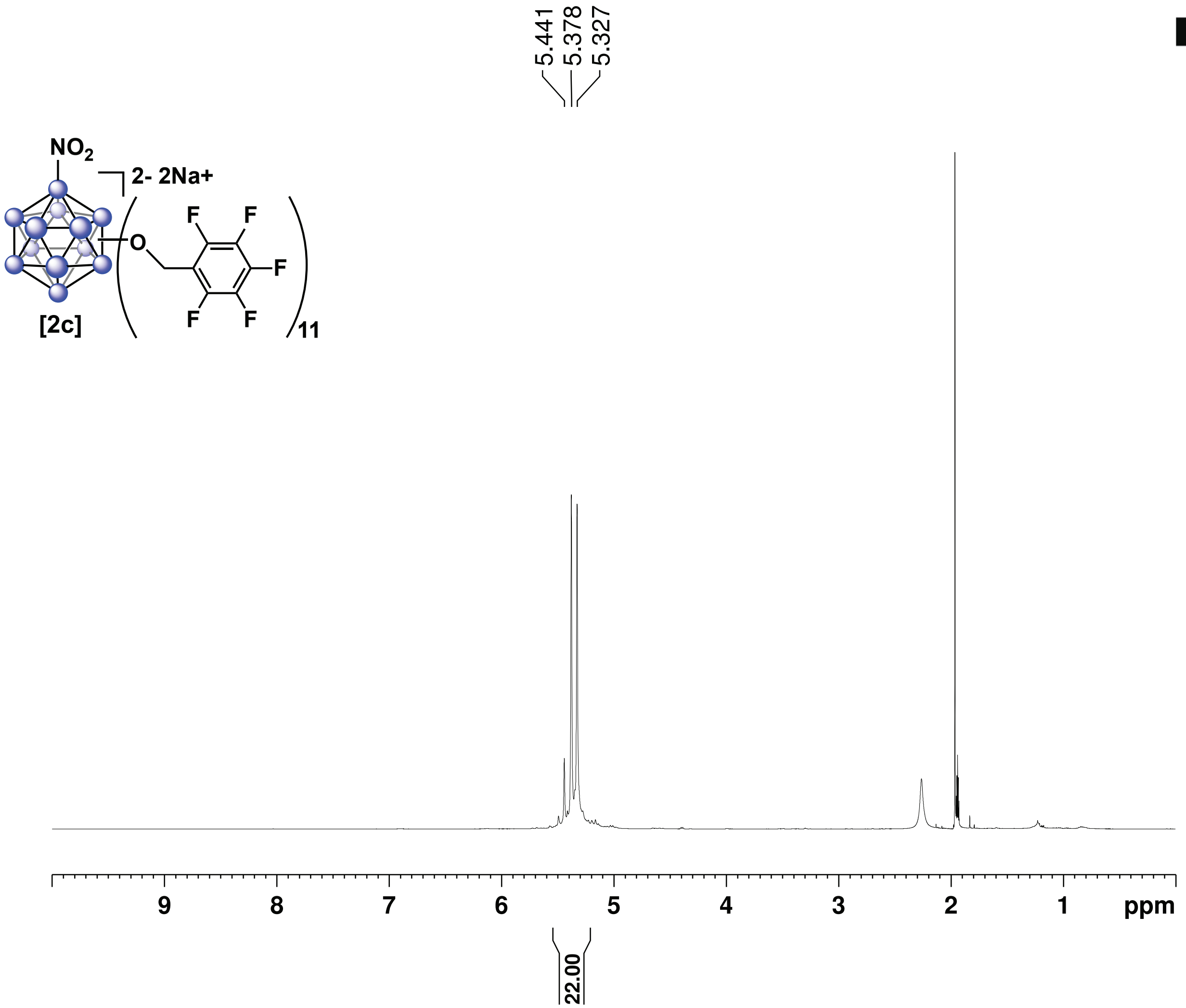

[2c]

Current Data Parameters
NAME Jan12-2018
EXPNO 70
PROCNO 1

F2 - Acquisition Parameters
Date_ 20180112
Time 14.23
INSTRUM av400
PROBHD 5 mm PABBO BB/
PULPROG zg30
TD 52882
SOLVENT CD3CN
NS 32
DS 0
SWH 8012.820 Hz
FIDRES 0.151523 Hz
AQ 3.2998369 sec
RG 94.6
DW 62.400 usec
DE 6.50 usec
TE 298.1 K
D1 2.00000000 sec
TD0 1

======== CHANNEL f1 ========
SFO1 400.1324008 MHz
NUC1 1H
P1 15.00 usec
PLW1 13.00000000 W

F2 - Processing parameters
SI 65536
SF 400.1300114 MHz
WDW EM
SSB 0
LB 0.30 Hz
GB 0
PC 1.00

^{11}B-^{11}B COSY NMR Spectra of **[2c]**

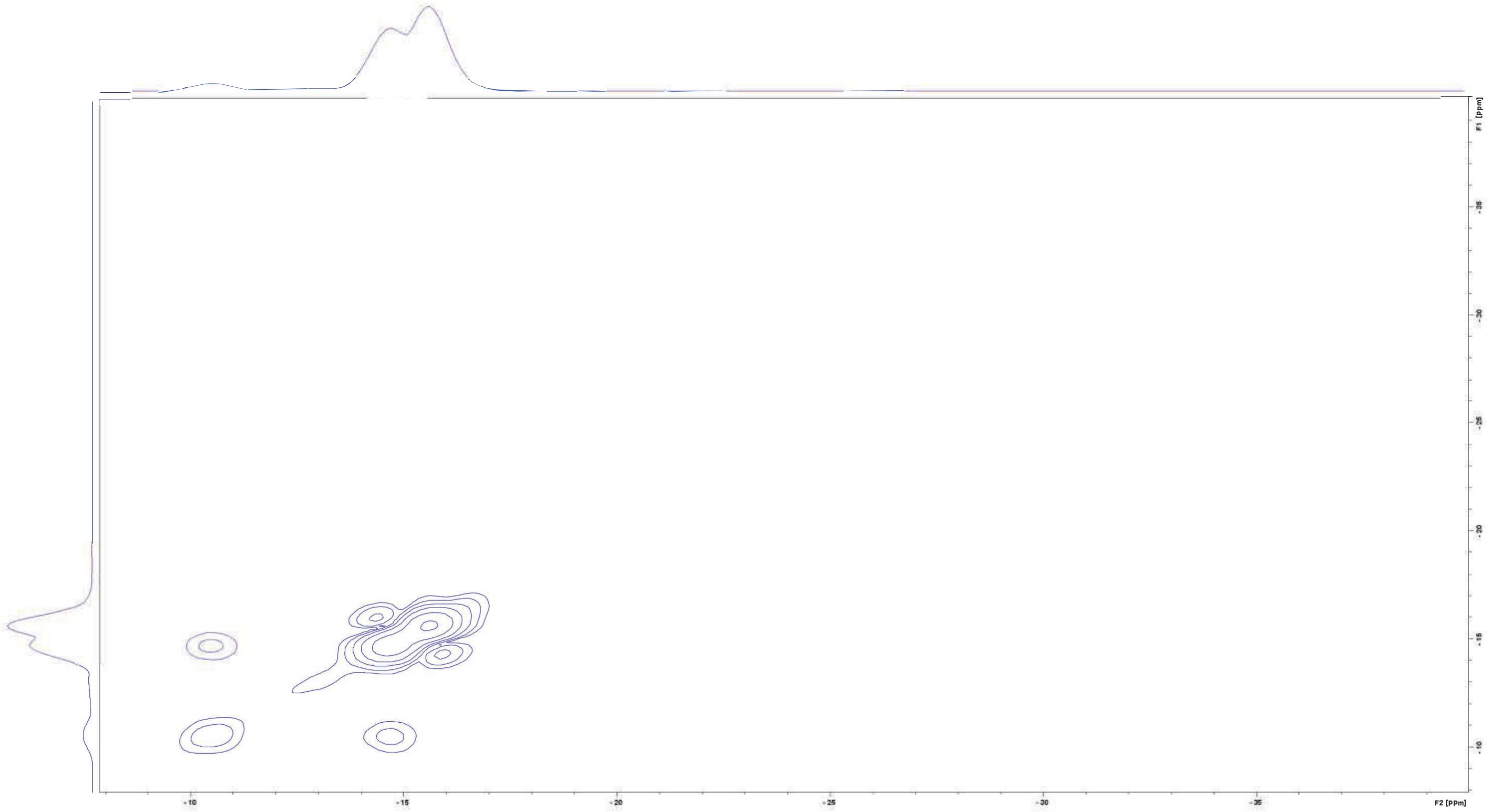

HRMS of **[2c]**

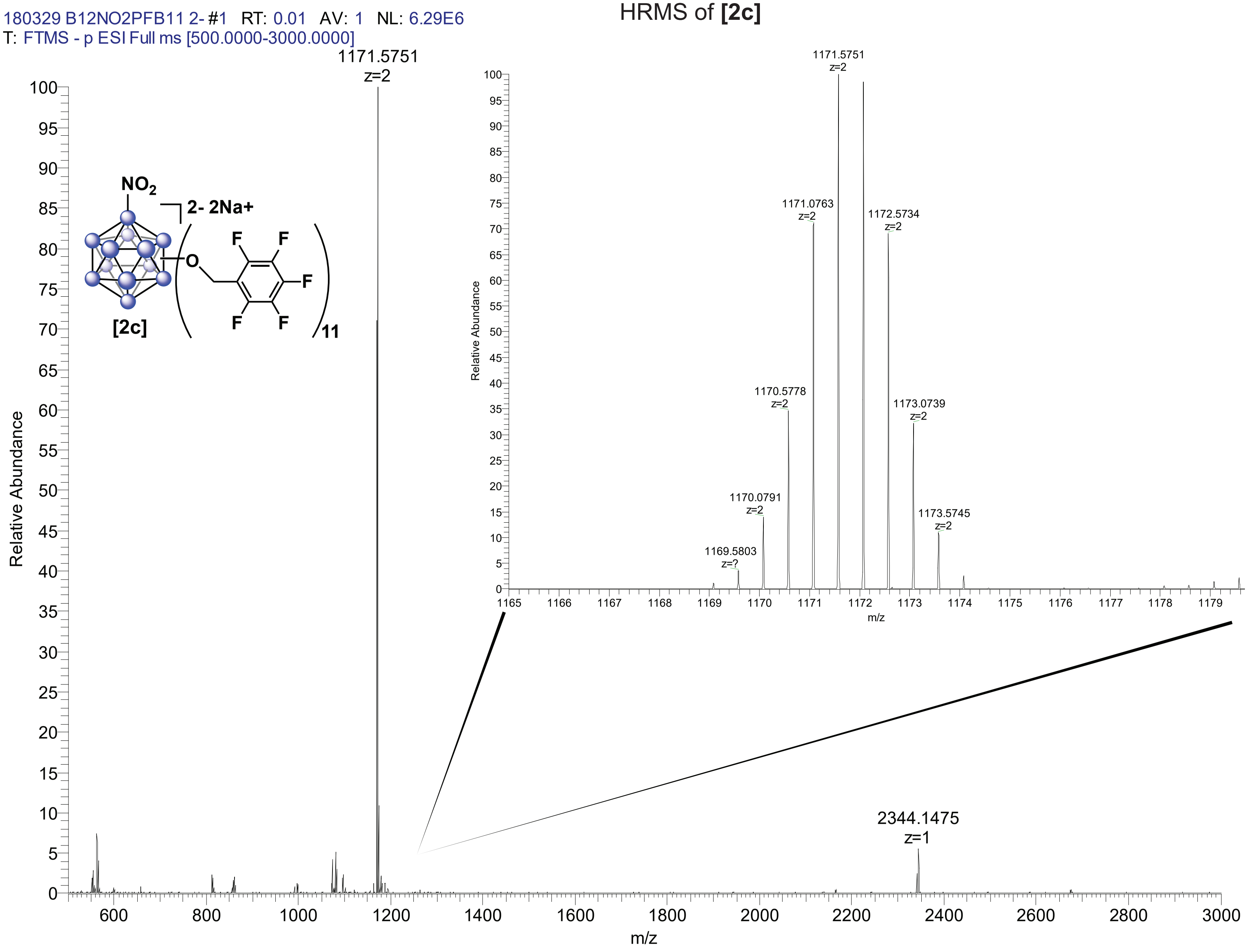
180329 B12NO2PFB11 2- #1 RT: 0.01 AV: 1 NL: 6.29E6
T: FTMS - p ESI Full ms [500.0000-3000.0000]
1171.5751
z=2
2344.1475
z=1
Relative Abundance
m/z
NO2
2- 2Na+
O
F
F
F
F
F
11
[2c]
1169.5803
z=?
1170.0791
z=2
1170.5778
z=2
1171.0763
z=2
1171.5751
z=2
1172.5734
z=2
1173.0739
z=2
1173.5745
z=2
Relative Abundance
m/z

UV-vis spectra of **[2c]**$^{2-}$ and **[3]**$^{2-}$

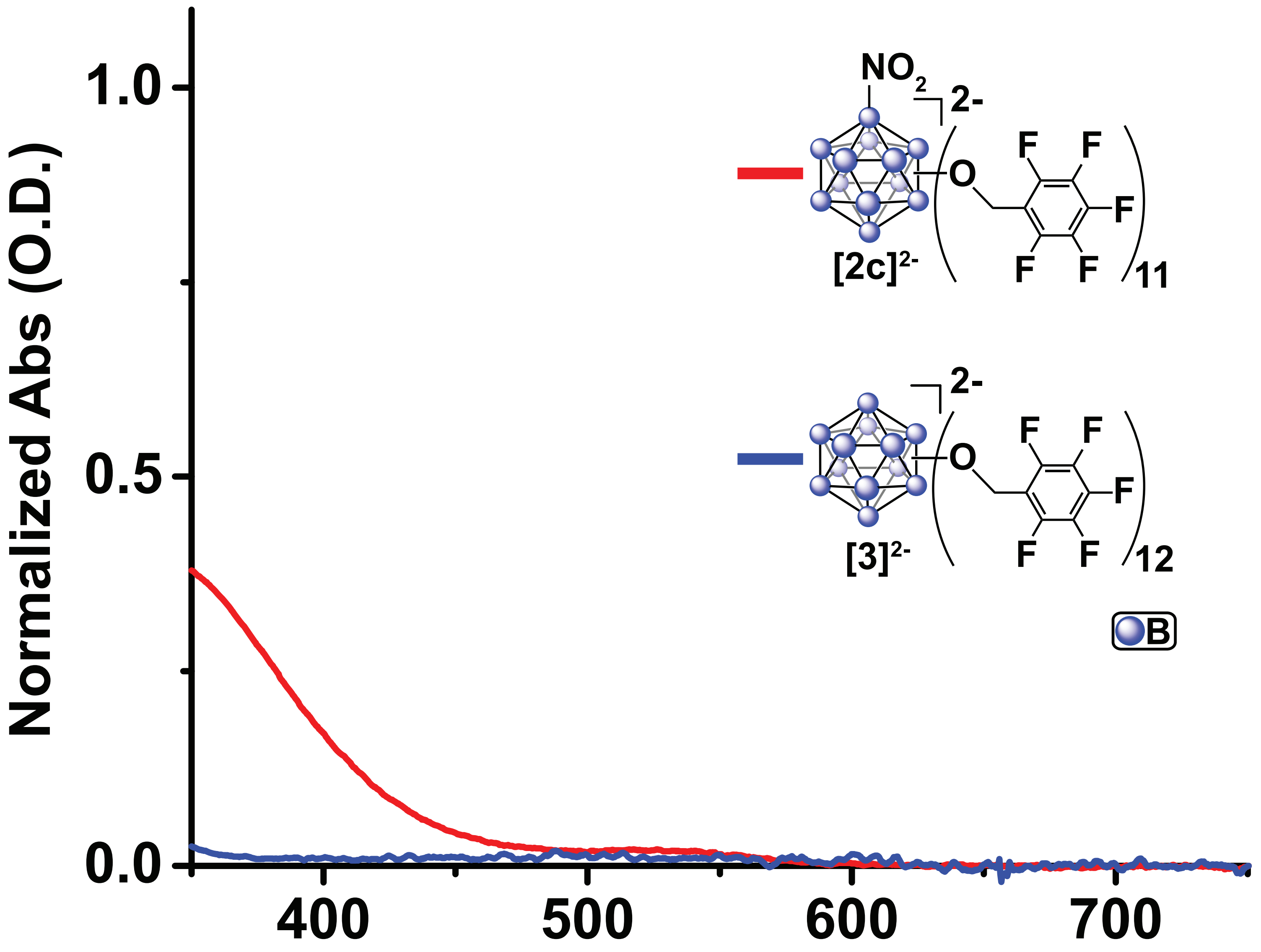

IR Spectra of **[2c]**

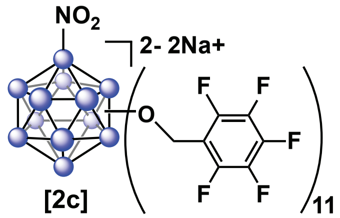
NO2
2- 2Na+
O
F
F
F
F
F
11

[2c]

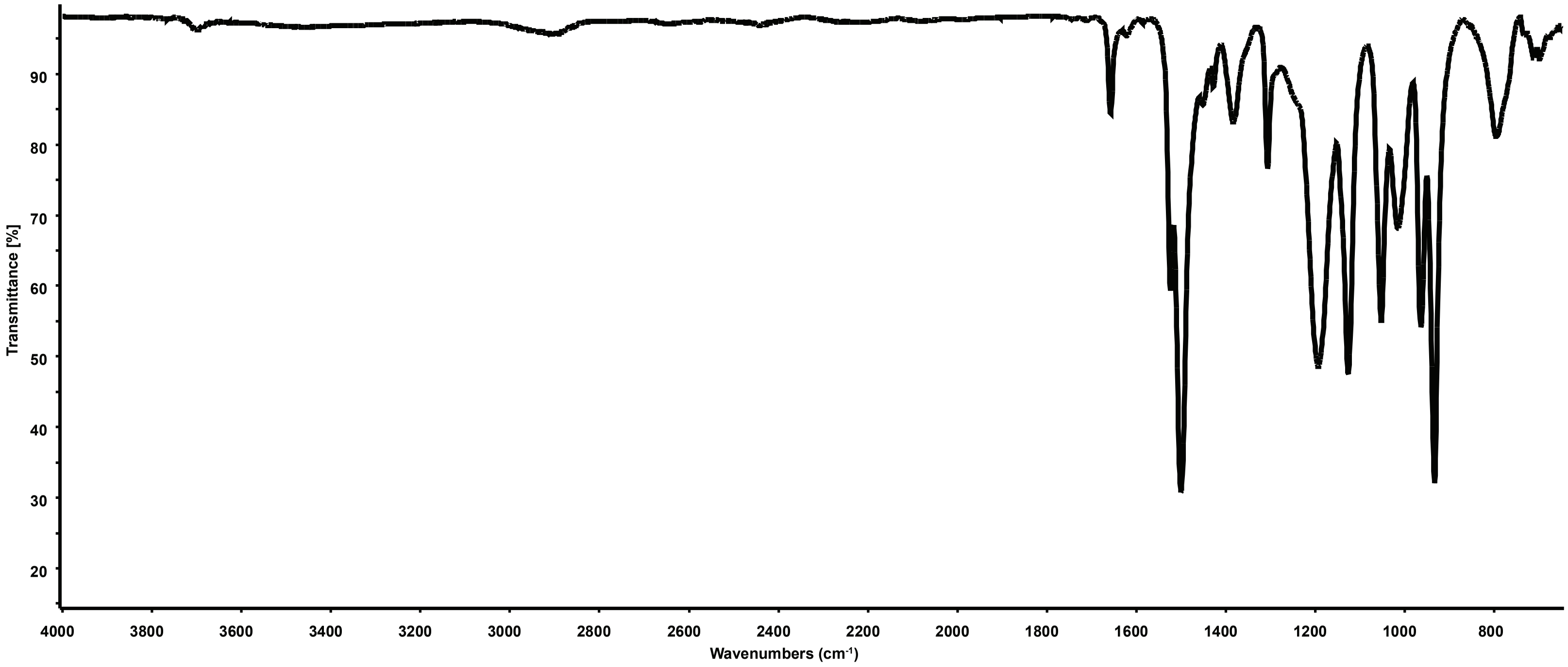

^{11}B NMR Spectra of **[2c]-ME**

[2c]-ME

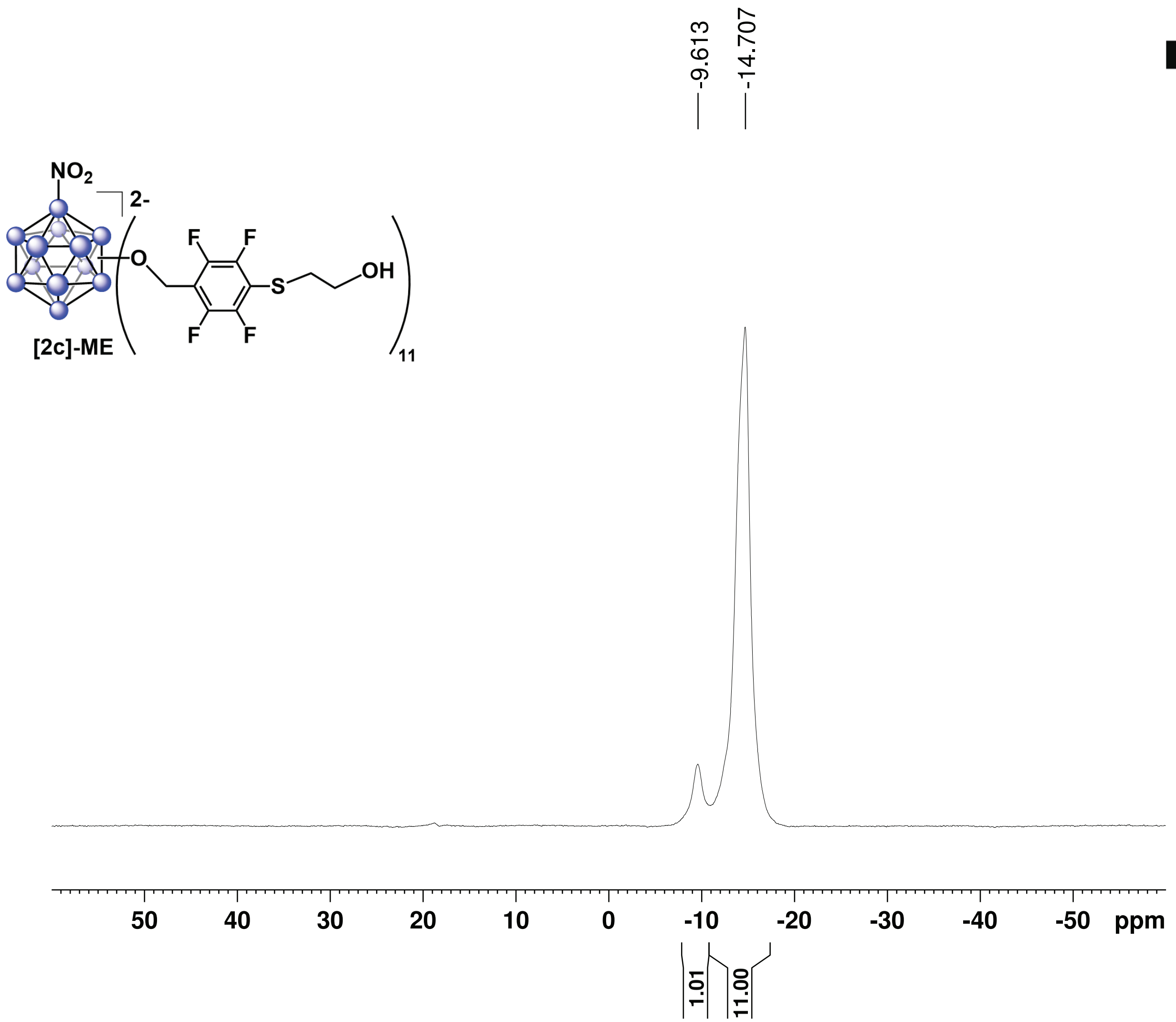

```
Current Data Parameters
NAME        Feb28-2018
EXPNO               80
PROCNO               1

F2 - Acquisition Parameters
Date_         20180228
Time             11.43
INSTRUM          av400
PROBHD   5 mm PABBO BB/
PULPROG             zg
TD               5096
SOLVENT           MeOD
NS               1024
DS                  0
SWH        51020.406 Hz
FIDRES     10.011854 Hz
AQ        0.0499408 sec
RG             189.85
DW            9.800 usec
DE            6.50 usec
TE             297.3 K
D1        0.05000000 sec
TD0                 1

======== CHANNEL f1 ========
SFO1      128.3776052 MHz
NUC1              11B
P1            10.00 usec
PLW1       52.00000000 W

F2 - Processing parameters
SI              32768
SF        128.3775591 MHz
WDW                EM
SSB     0
LB             10.00 Hz
GB      0
PC              1.40
```

^{19}F NMR Spectra of **[2c]-ME**

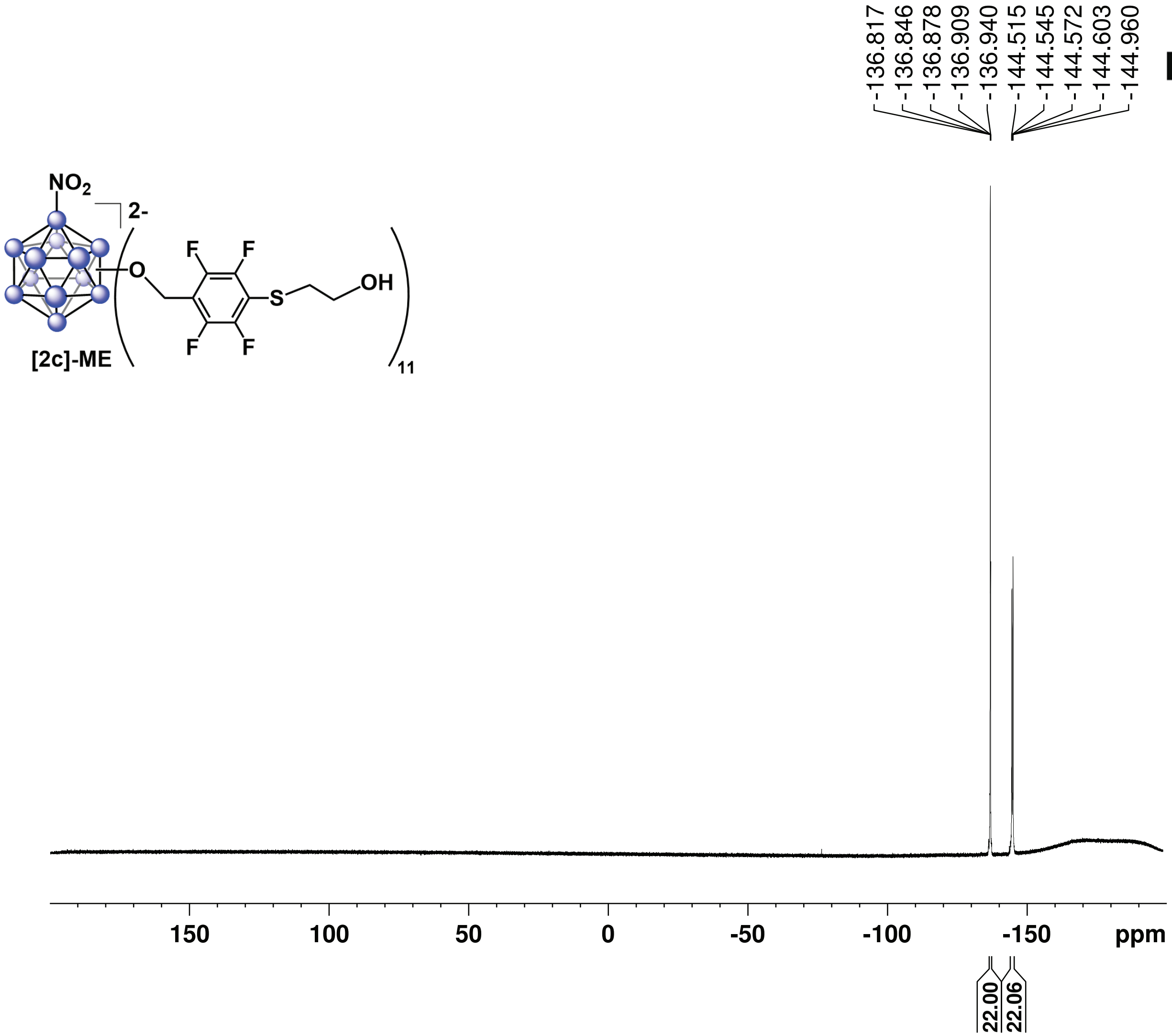

[2c]-ME

```
Current Data Parameters
NAME        Feb28-2018
EXPNO              81
PROCNO              1

F2 - Acquisition Parameters
Date_        20180228
Time            11.48
INSTRUM         av400
PROBHD   5 mm PABBO BB/
PULPROG       zgflqn30
TD             262144
SOLVENT          MeOD
NS                 64
DS                  0
SWH       150000.000 Hz
FIDRES      0.572205 Hz
AQ         0.8738133 sec
RG             189.85
DW              3.333 usec
DE               6.50 usec
TE              297.3 K
D1         2.00000000 sec
TD0                 1

======== CHANNEL f1 ========
SFO1      376.4983660 MHz
NUC1              19F
P1              14.50 usec
PLW1      17.00000000 W

F2 - Processing parameters
SI             262144
SF        376.4981771 MHz
WDW                EM
SSB     0
LB               1.00 Hz
GB      0
PC               1.00
```

^{1}H NMR Spectra of **[2c]-ME**

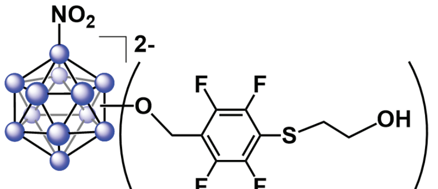

[2c]-ME

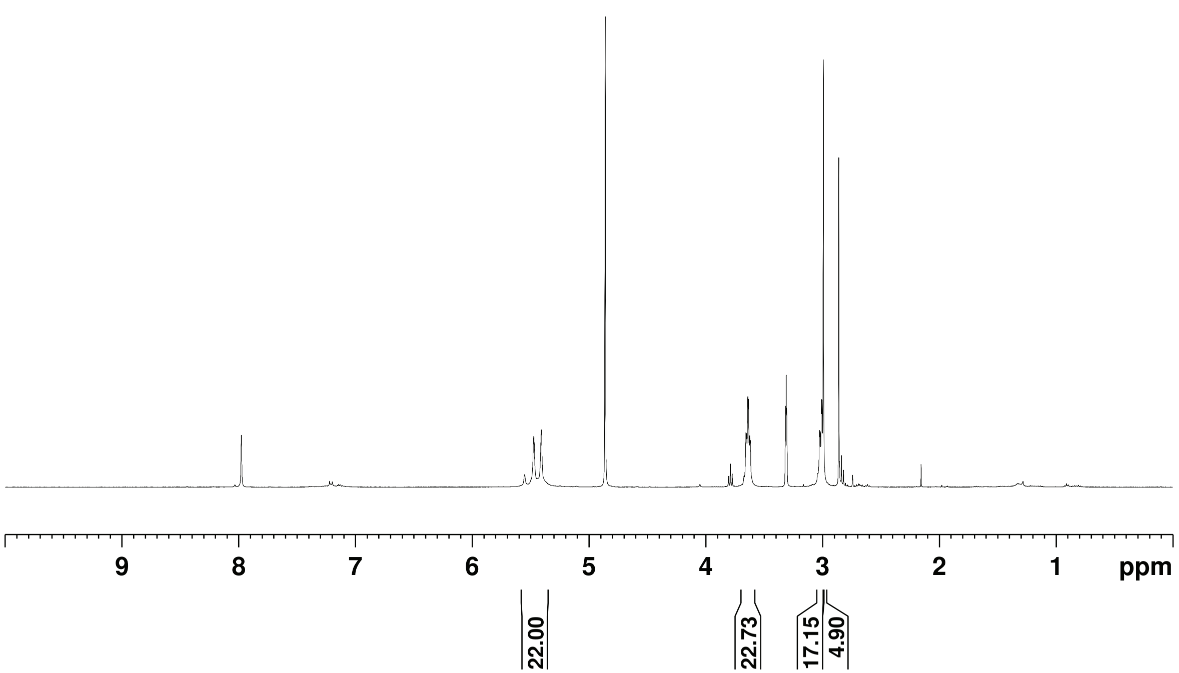

```
Current Data Parameters
NAME        Feb28-2018
EXPNO               82
PROCNO               1

F2 - Acquisition Parameters
Date_         20180228
Time             11.51
INSTRUM          av400
PROBHD   5 mm PABBO BB/
PULPROG           zg30
TD               52882
SOLVENT           MeOD
NS                  32
DS                   0
SWH         8012.820 Hz
FIDRES      0.151523 Hz
AQ        3.2998369 sec
RG              155.85
DW          62.400 usec
DE            6.50 usec
TE             297.3 K
D1       2.00000000 sec
TD0                  1

======== CHANNEL f1 ========
SFO1     400.1324008 MHz
NUC1                1H
P1             15.00 usec
PLW1       13.00000000 W

F2 - Processing parameters
SI               65536
SF       400.1300078 MHz
WDW                 EM
SSB      0
LB             0.30 Hz
GB       0
PC                1.00
```

HRMS of **[2c]-ME**

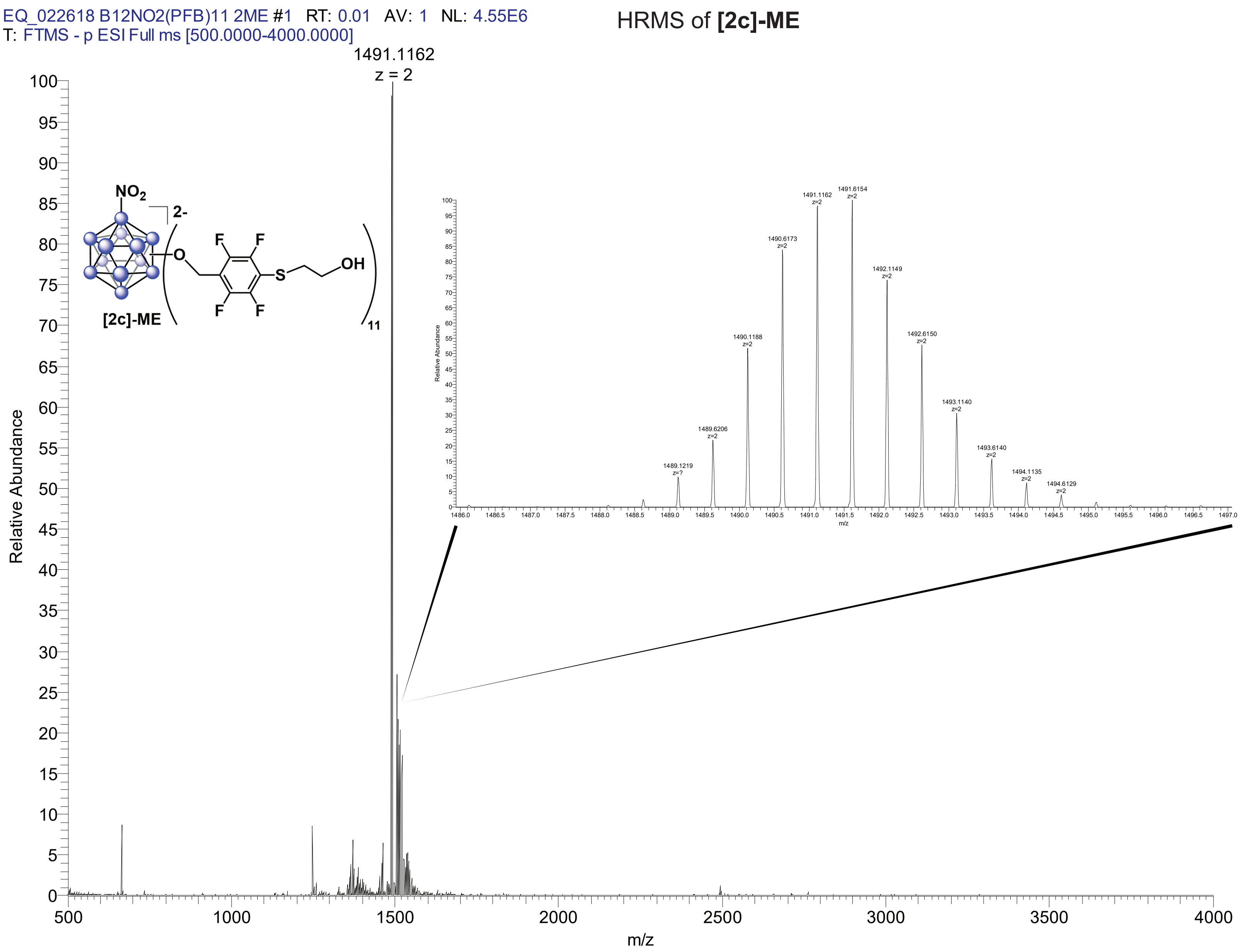

EQ_022618 B12NO2(PFB)11 2ME #1 RT: 0.01 AV: 1 NL: 4.55E6
T: FTMS - p ESI Full ms [500.0000-4000.0000]
1491.1162
z = 2
NO2
2-
O
F
F
F
F
S
OH
11
[2c]-ME
Relative Abundance
m/z
0
5
10
15
20
25
30
35
40
45
50
55
60
65
70
75
80
85
90
95
100
500
1000
1500
2000
2500
3000
3500
4000
1489.1219
z=?
1489.6206
z=2
1490.1188
z=2
1490.6173
z=2
1491.1162
z=2
1491.6154
z=2
1492.1149
z=2
1492.6150
z=2
1493.1140
z=2
1493.6140
z=2
1494.1135
z=2
1494.6129
z=2
1486.0
1486.5
1487.0
1487.5
1488.0
1488.5
1489.0
1489.5
1490.0
1490.5
1491.0
1491.5
1492.0
1492.5
1493.0
1493.5
1494.0
1494.5
1495.0
1495.5
1496.0
1496.5
1497.0

CV of **[2c]-ME**

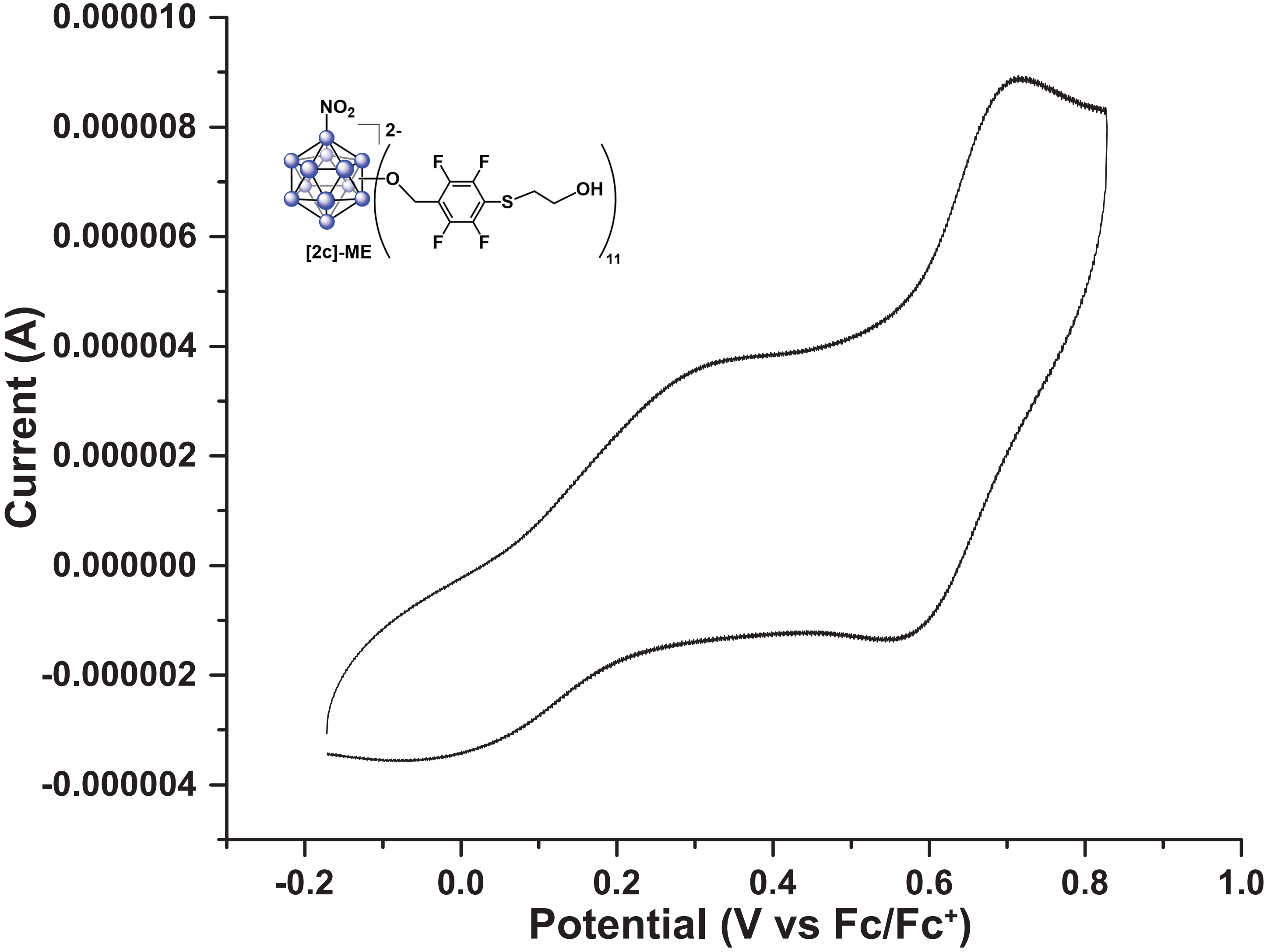
Current (A)
0.000010
0.000008
0.000006
0.000004
0.000002
0.000000
-0.000002
-0.000004
Potential (V vs Fc/Fc⁺)
-0.2
0.0
0.2
0.4
0.6
0.8
1.0
NO2
2-
O
F
F
F
F
S
OH
11
[2c]-ME

Supplemental spectra & data for Chapter 4

$^{11}B\{^{1}H\}$ NMR of $[1]^{2-}$

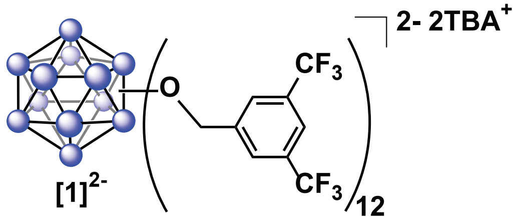

$[1]^{2-}$

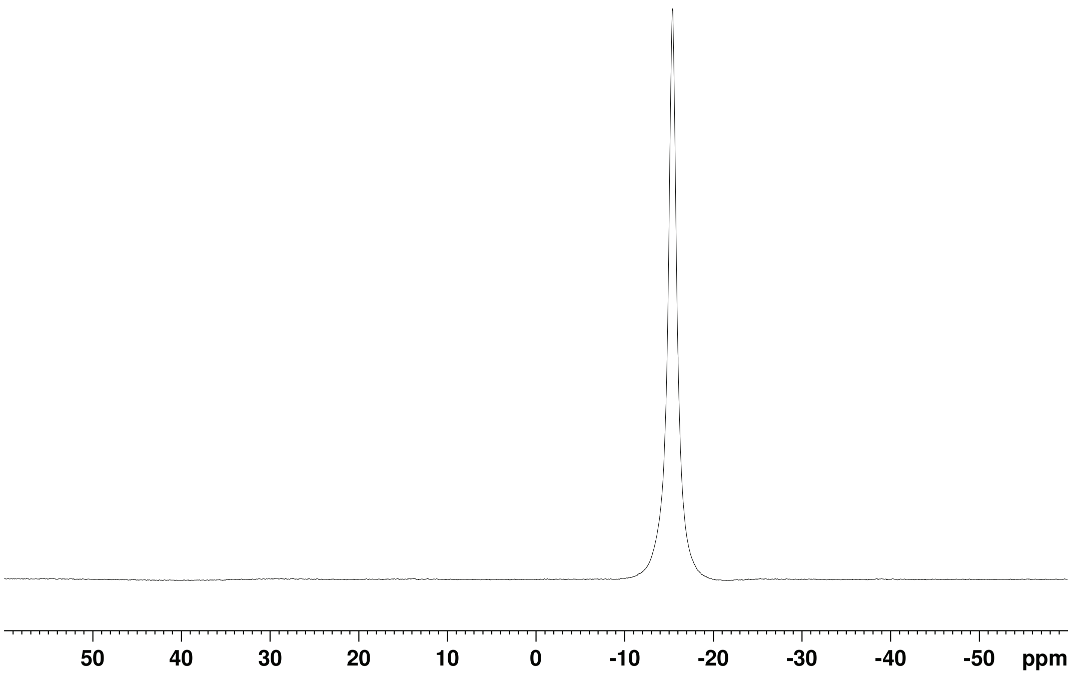

```
Current Data Parameters
NAME        Jul06-2018
EXPNO               40
PROCNO               1

F2 - Acquisition Parameters
Date_         20180706
Time             12.42
INSTRUM          av400
PROBHD   5 mm PABBO BB/
PULPROG        zgdc.js
TD                5096
SOLVENT          CDCl3
NS                1024
DS                   0
SWH       51020.406 Hz
FIDRES    10.011854 Hz
AQ       0.0499408 sec
RG              189.85
DW           9.800 usec
DE            6.50 usec
TE             299.2 K
D1      0.05000000 sec
D11     0.03000000 sec
TD0                  1

======== CHANNEL f1 ========
SFO1    128.3776052 MHz
NUC1               11B
P1          10.00 usec
PLW1    52.00000000 W

======== CHANNEL f2 ========
SFO2    400.1324008 MHz
NUC2                1H
CPDPRG[2       waltz16
PCPD2       90.00 usec
PLW2    13.00000000 W
PLW12    0.36111000 W

F2 - Processing parameters
SI               32768
SF      128.3776483 MHz
WDW                 EM
SSB     0
LB            10.00 Hz
GB      0
PC                1.40
```

^{1}H NMR of [1]$^{2-}$

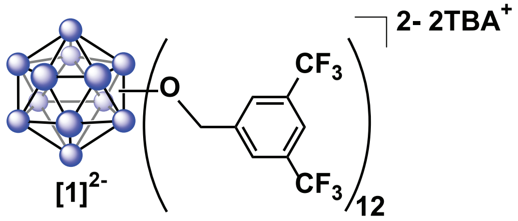

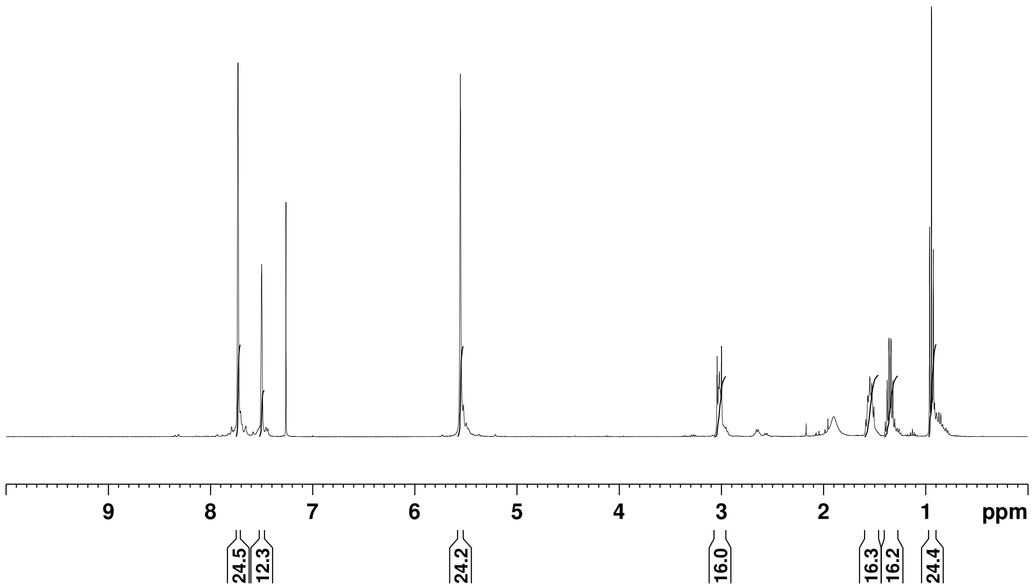

```
Current Data Parameters
NAME        Jul06-2018
EXPNO               41
PROCNO               1

F2 - Acquisition Parameters
Date_         20180706
Time             12.46
INSTRUM          av400
PROBHD   5 mm PABBO BB/
PULPROG           zg30
TD               52882
SOLVENT          CDCl3
NS                  32
DS                   0
SWH        8012.820 Hz
FIDRES     0.151523 Hz
AQ       3.2998369 sec
RG              155.85
DW          62.400 usec
DE            6.50 usec
TE             298.7 K
D1      2.00000000 sec
TD0                  1

======== CHANNEL f1 ========
SFO1    400.1324008 MHz
NUC1                 1H
P1           15.00 usec
PLW1      13.00000000 W

F2 - Processing parameters
SI                65536
SF      400.1300175 MHz
WDW                  EM
SSB     0
LB              0.30 Hz
GB      0
PC                 1.00
```

^{19}F NMR of $[1]^{2-}$

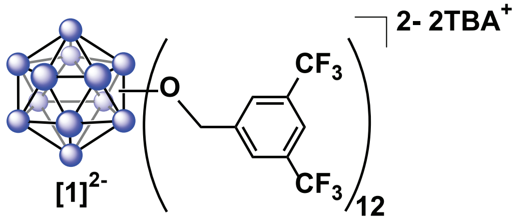

$[1]^{2-}$

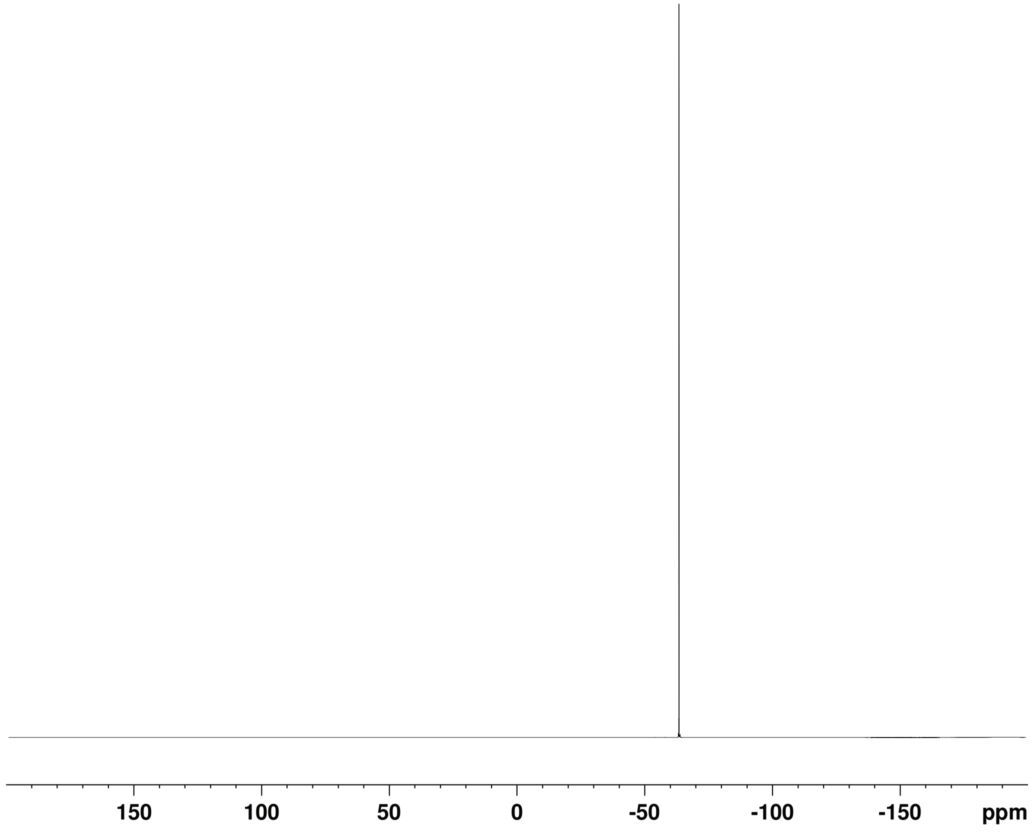

Current Data Parameters
NAME Jul06-2018
EXPNO 42
PROCNO 1

F2 - Acquisition Parameters
Date_ 20180706
Time 12.51
INSTRUM av400
PROBHD 5 mm PABBO BB/
PULPROG zgflqn30
TD 262144
SOLVENT CDCl3
NS 64
DS 0
SWH 150000.000 Hz
FIDRES 0.572205 Hz
AQ 0.8738133 sec
RG 189.85
DW 3.333 usec
DE 6.50 usec
TE 298.7 K
D1 2.00000000 sec
TD0 1

======== CHANNEL f1 ========
SFO1 376.4983660 MHz
NUC1 19F
P1 14.50 usec
PLW1 17.00000000 W

F2 - Processing parameters
SI 262144
SF 376.4984557 MHz
WDW EM
SSB 0
LB 1.00 Hz
GB 0
PC 1.00

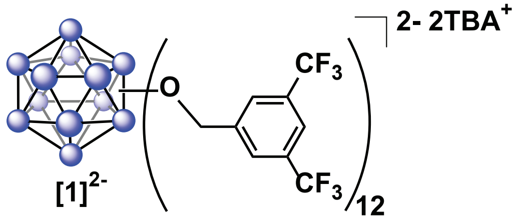
O
CF$_3$
CF$_3$
12
2- 2TBA$^+$
[1]$^{2-}$

Mass Spectrum of [1]$^{2-}$

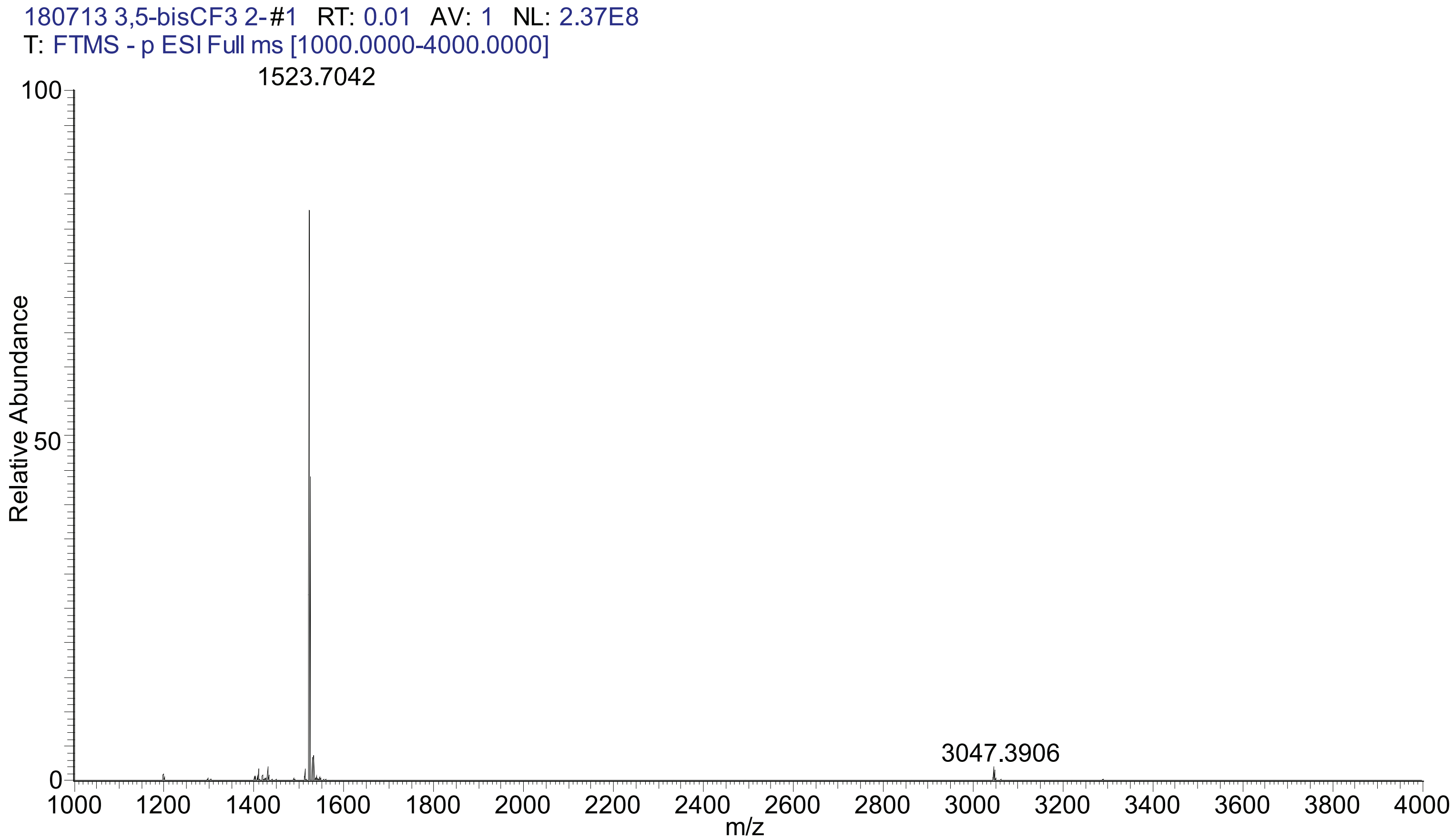

$^{11}B\ \{^{1}H\}$ NMR of $[1]^{1-}$

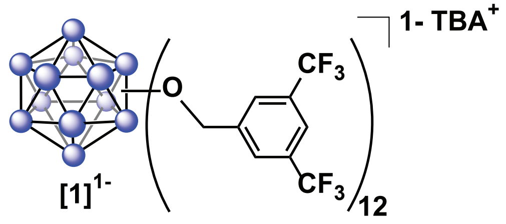

$[1]^{1-}$

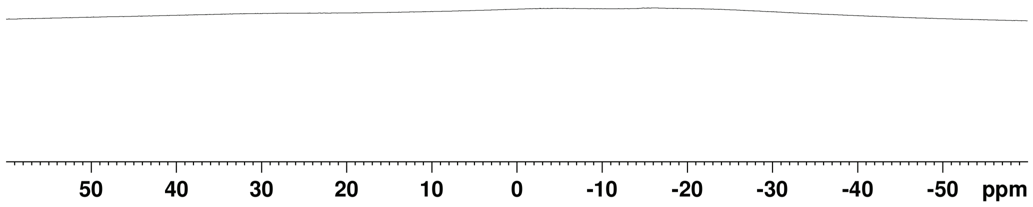

Current Data Parameters
NAME Jul06-2018
EXPNO 50
PROCNO 1

F2 - Acquisition Parameters
Date_ 20180706
Time 12.57
INSTRUM av400
PROBHD 5 mm PABBO BB/
PULPROG zgdc.js
TD 5096
SOLVENT CDCl3
NS 1024
DS 0
SWH 51020.406 Hz
FIDRES 10.011854 Hz
AQ 0.0499408 sec
RG 189.85
DW 9.800 usec
DE 6.50 usec
TE 299.3 K
D1 0.05000000 sec
D11 0.03000000 sec
TD0 1

======== CHANNEL f1 ========
SFO1 128.3776052 MHz
NUC1 11B
P1 10.00 usec
PLW1 52.00000000 W

======== CHANNEL f2 ========
SFO2 400.1324008 MHz
NUC2 1H
CPDPRG[2 waltz16
PCPD2 90.00 usec
PLW2 13.00000000 W
PLW12 0.36111000 W

F2 - Processing parameters
SI 32768
SF 128.3776438 MHz
WDW EM
SSB 0
LB 10.00 Hz
GB 0
PC 1.40

^{1}H NMR of $[1]^{1-}$

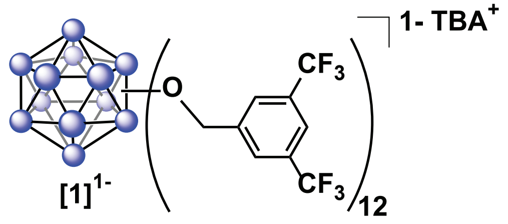

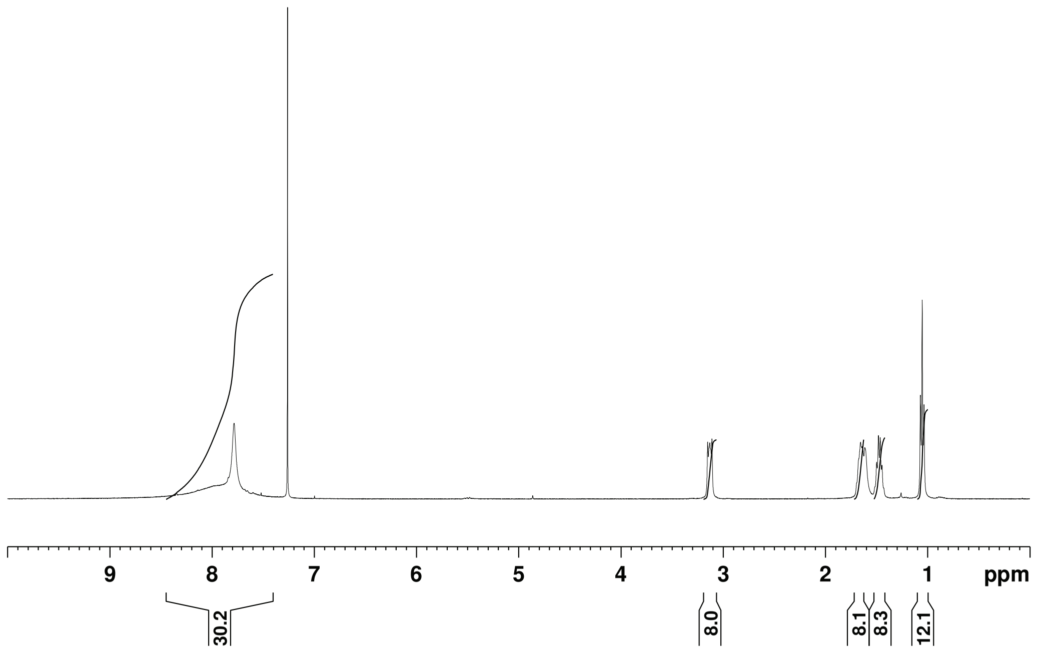

BRUKER

Current Data Parameters

NAME	Jul06-2018
EXPNO	51
PROCNO	1

F2 - Acquisition Parameters

Date_	20180706
Time	13.00
INSTRUM	av400
PROBHD	5 mm PABBO BB/
PULPROG	zg30
TD	52882
SOLVENT	CDCl3
NS	32
DS	0
SWH	8012.820 Hz
FIDRES	0.151523 Hz
AQ	3.2998369 sec
RG	189.85
DW	62.400 usec
DE	6.50 usec
TE	298.8 K
D1	2.00000000 sec
TD0	1

======== CHANNEL f1 ========

SFO1	400.1324008 MHz
NUC1	1H
P1	15.00 usec
PLW1	13.00000000 W

F2 - Processing parameters

SI	65536
SF	400.1300175 MHz
WDW	EM
SSB	0
LB	0.30 Hz
GB	0
PC	1.00

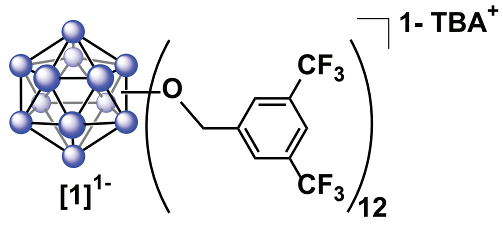

$[1]^{1-}$

^{19}F NMR of $[1]^{1-}$

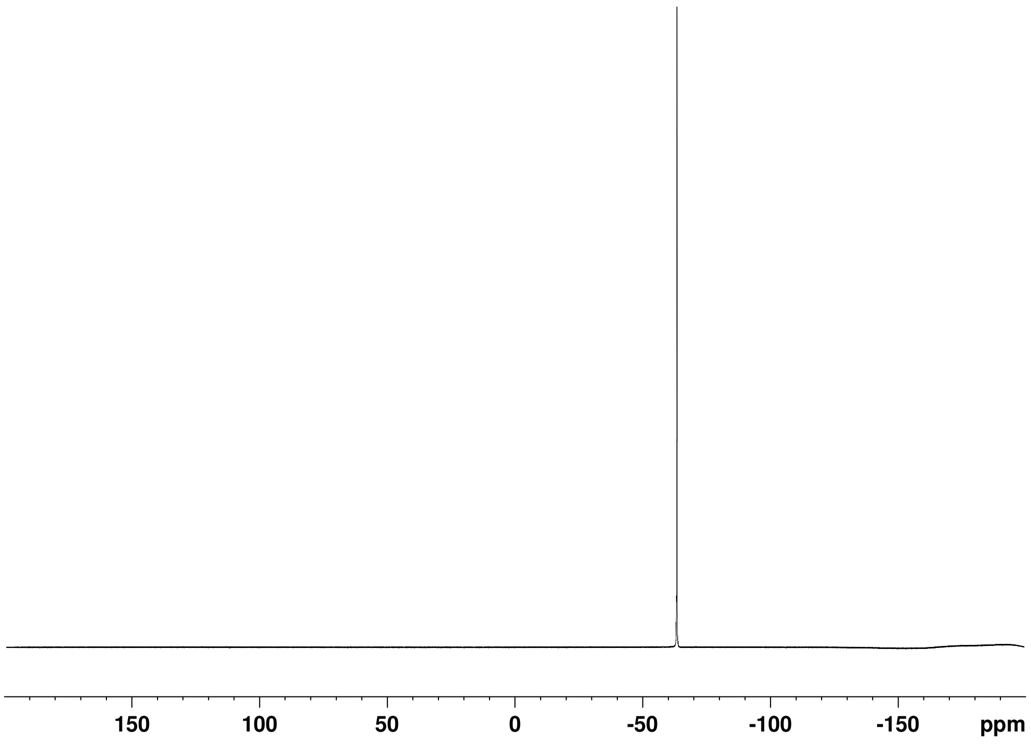

```
Current Data Parameters
NAME        Jul06-2018
EXPNO               52
PROCNO               1

F2 - Acquisition Parameters
Date_         20180706
Time             13.05
INSTRUM          av400
PROBHD   5 mm PABBO BB/
PULPROG        zgflqn30
TD              262144
SOLVENT          CDCl3
NS                  64
DS                   0
SWH      150000.000 Hz
FIDRES     0.572205 Hz
AQ       0.8738133 sec
RG              189.85
DW           3.333 usec
DE            6.50 usec
TE              298.7 K
D1      2.00000000 sec
TD0                  1

======== CHANNEL f1 ========
SFO1     376.4983660 MHz
NUC1               19F
P1           14.50 usec
PLW1      17.00000000 W

F2 - Processing parameters
SI              262144
SF       376.4984454 MHz
WDW                 EM
SSB     0
LB             1.00 Hz
GB      0
PC                1.00
```

Mass Spectrum of $[1]^{1-}$

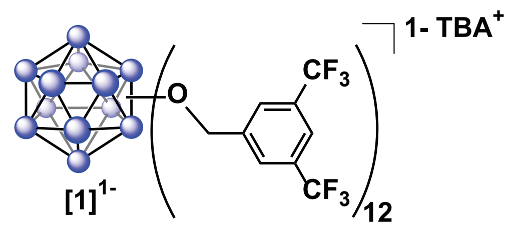
O
CF3
CF3
12
1- TBA+

$[1]^{1-}$

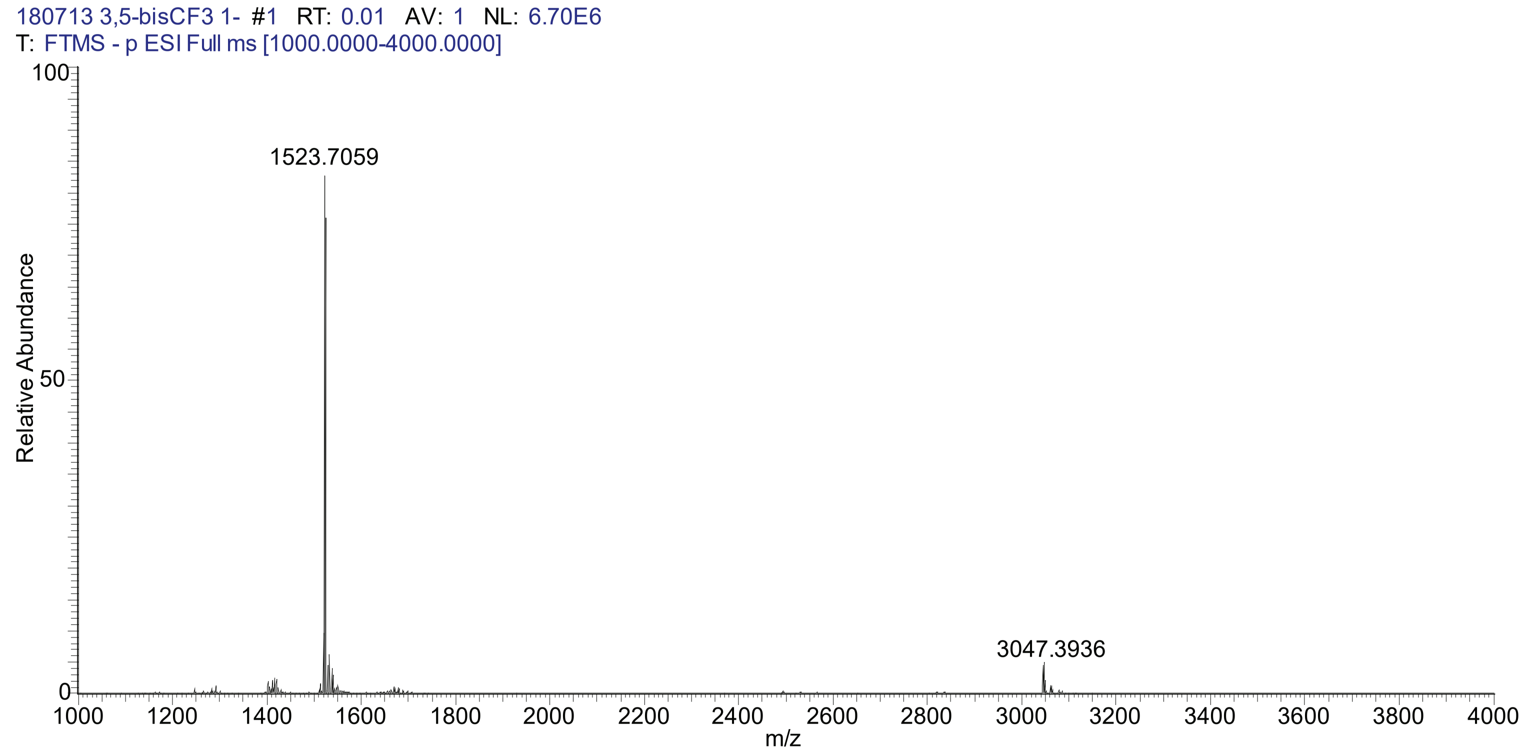

^{11}B {^{1}H} NMR of [2]^{0}

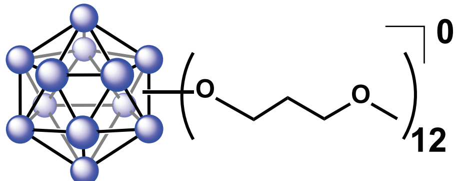

[2]^{0}

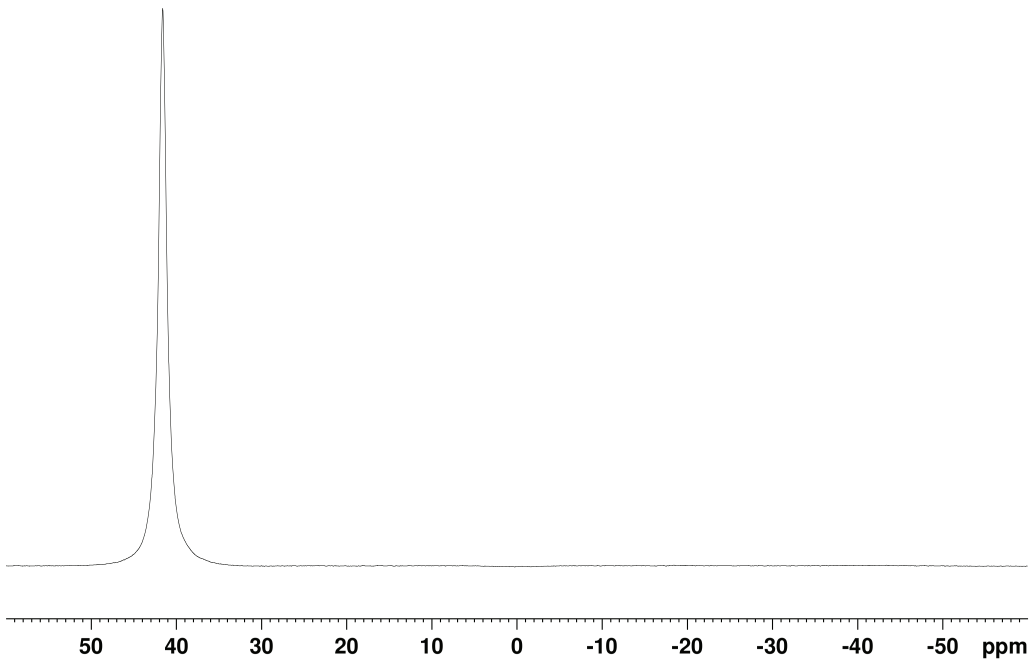

```
Current Data Parameters
NAME         Jul05-2018
EXPNO                30
PROCNO                1

F2 - Acquisition Parameters
Date_          20180705
Time              16.51
INSTRUM           av400
PROBHD   5 mm PABBO BB/
PULPROG         zgdc.js
TD                 5096
SOLVENT           CDCl3
NS                 1024
DS                    0
SWH        51020.406 Hz
FIDRES     10.011854 Hz
AQ        0.0499408 sec
RG               189.85
DW            9.800 usec
DE             6.50 usec
TE              299.1 K
D1       0.05000000 sec
D11      0.03000000 sec
TD0                   1

======== CHANNEL f1 ========
SFO1      128.3776052 MHz
NUC1                  11B
P1             10.00 usec
PLW1      52.00000000 W

======== CHANNEL f2 ========
SFO2      400.1324008 MHz
NUC2                   1H
CPDPRG[2          waltz16
PCPD2          90.00 usec
PLW2      13.00000000 W
PLW12      0.36111000 W

F2 - Processing parameters
SI                  32768
SF        128.3776389 MHz
WDW                    EM
SSB     0
LB               10.00 Hz
GB      0
PC                   1.40
```

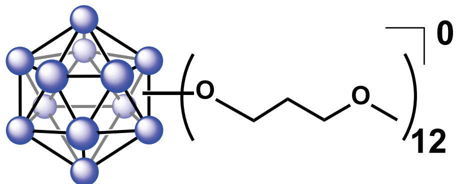

$[2]^0$

^{1}H NMR of $[2]^0$

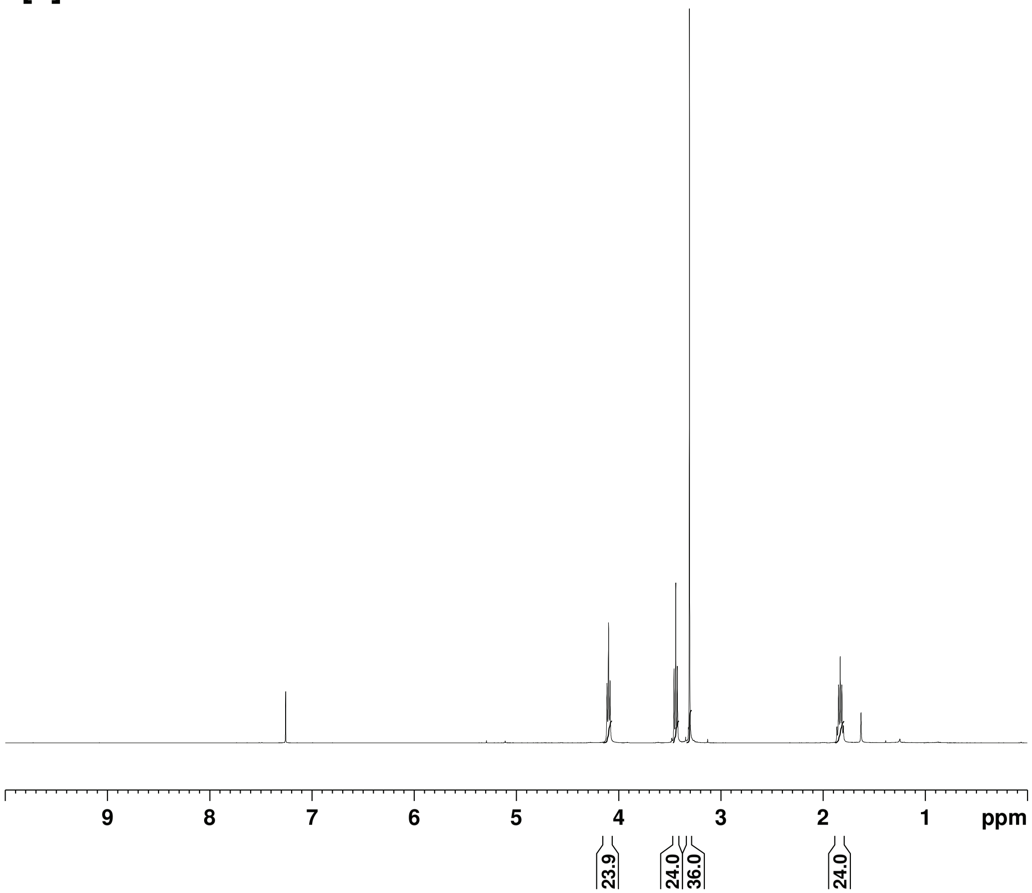

Current Data Parameters

NAME	Jul05-2018
EXPNO	31
PROCNO	1

F2 - Acquisition Parameters

Date_	20180705
Time	16.52
INSTRUM	av400
PROBHD	5 mm PABBO BB/
PULPROG	zg30
TD	52882
SOLVENT	CDCl3
NS	8
DS	0
SWH	8012.820 Hz
FIDRES	0.151523 Hz
AQ	3.2998369 sec
RG	155.85
DW	62.400 usec
DE	6.50 usec
TE	298.7 K
D1	2.00000000 sec
TD0	1

======== CHANNEL f1 ========

SFO1	400.1324008 MHz
NUC1	1H
P1	15.00 usec
PLW1	13.00000000 W

F2 - Processing parameters

SI	65536
SF	400.1300191 MHz
WDW	EM
SSB	0
LB	0.30 Hz
GB	0
PC	1.00

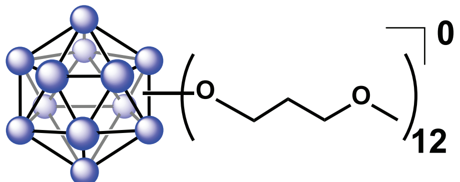

$[2]^0$

Mass Spectrum of $[2]^0$

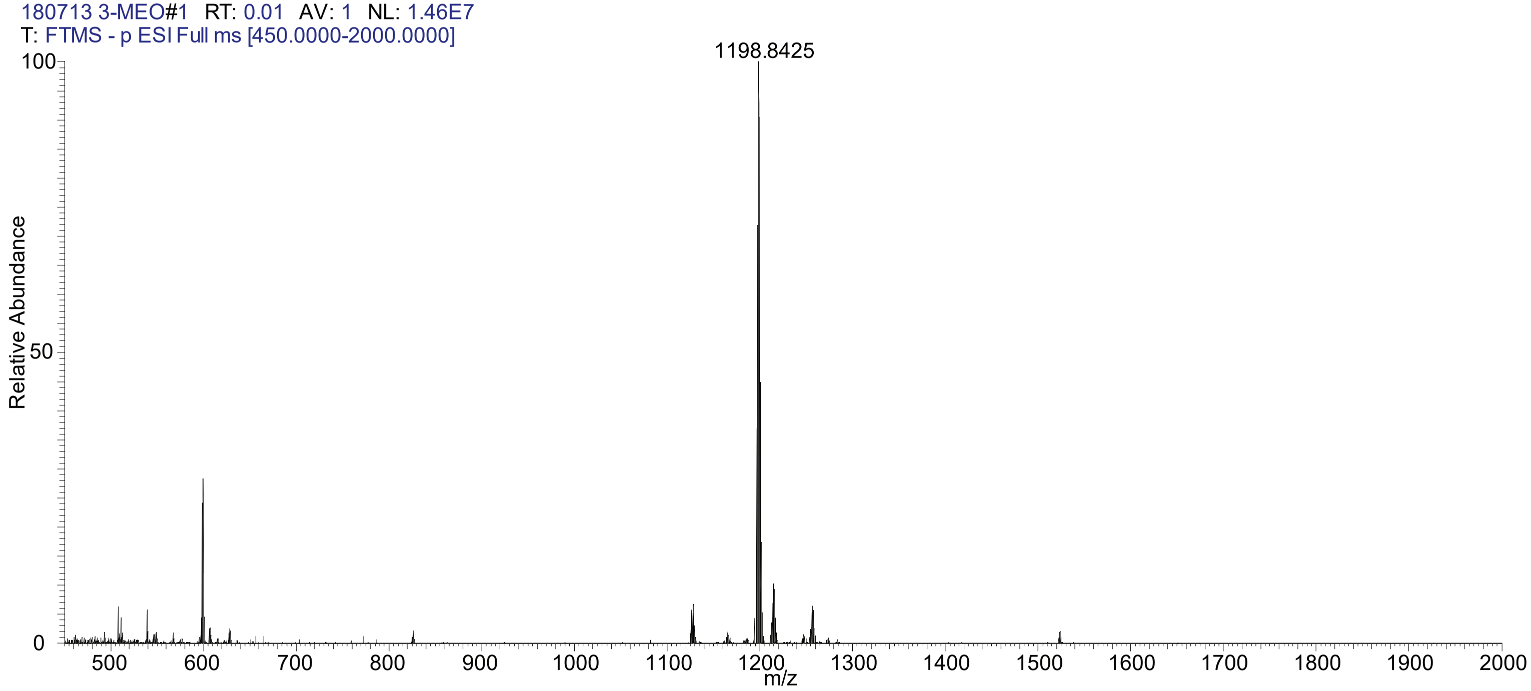

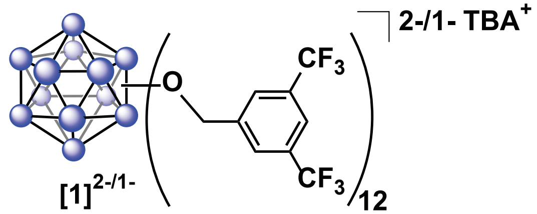

$[1]^{2-/1-}$

^{11}B {^{1}H} NMR of $[1]^{2-/1-}$ post-flow cell cycling

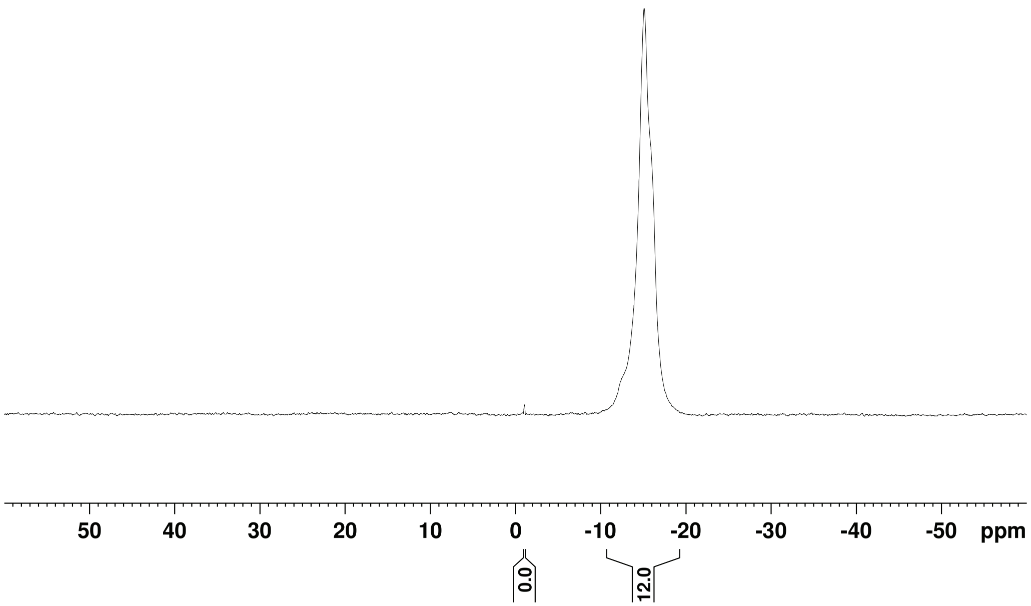

```
Current Data Parameters
NAME        Aug31-2018
EXPNO               71
PROCNO               1

F2 - Acquisition Parameters
Date_         20180831
Time             17.02
INSTRUM          av400
PROBHD   5 mm PABBO BB/
PULPROG        zgdc.js
TD                5096
SOLVENT          CDCl3
NS                1024
DS                   0
SWH         51020.406 Hz
FIDRES      10.011854 Hz
AQ          0.0499408 sec
RG              189.85
DW               9.800 usec
DE                6.50 usec
TE               299.2 K
D1          0.05000000 sec
D11         0.03000000 sec
TD0                  1

======== CHANNEL f1 ========
SFO1       128.3776052 MHz
NUC1               11B
P1               10.00 usec
PLW1       52.00000000 W

======== CHANNEL f2 ========
SFO2       400.1324008 MHz
NUC2                1H
CPDPRG[2        waltz16
PCPD2            90.00 usec
PLW2       13.00000000 W
PLW12       0.36111000 W

F2 - Processing parameters
SI               32768
SF         128.3776161 MHz
WDW                 EM
SSB     0
LB               10.00 Hz
GB      0
PC                1.40
```

^{1}H NMR of [1]$^{2-/1-}$ post-flow cell cycling

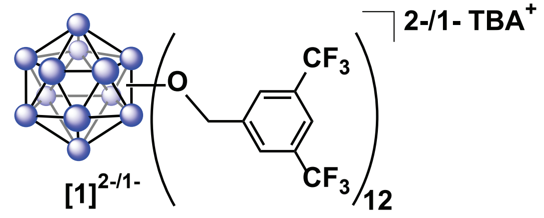

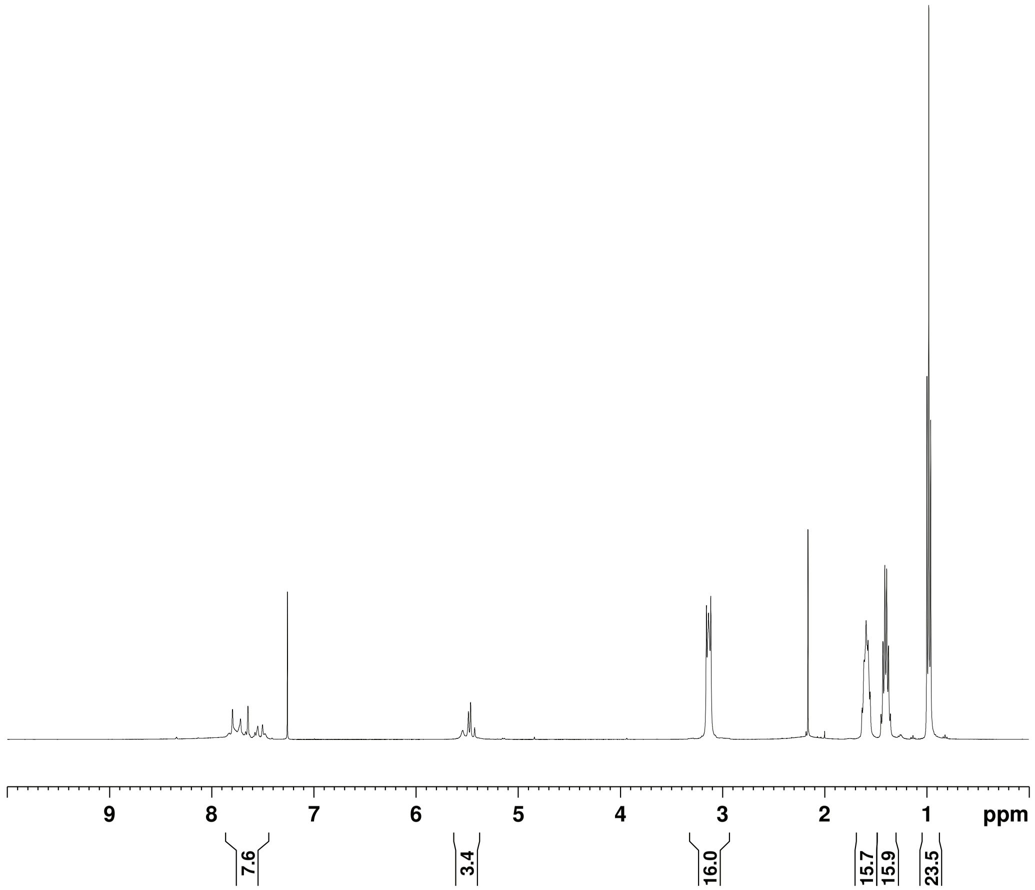

```
Current Data Parameters
NAME        Aug31-2018
EXPNO               73
PROCNO               1

F2 - Acquisition Parameters
Date_         20180831
Time             17.10
INSTRUM          av400
PROBHD   5 mm PABBO BB/
PULPROG           zg30
TD               52882
SOLVENT          CDCl3
NS                  32
DS                   0
SWH         8012.820 Hz
FIDRES      0.151523 Hz
AQ         3.2998369 sec
RG              155.85
DW          62.400 usec
DE            6.50 usec
TE             298.6 K
D1       2.00000000 sec
TD0                  1

======== CHANNEL f1 ========
SFO1     400.1324008 MHz
NUC1                 1H
P1             15.00 usec
PLW1      13.00000000 W

F2 - Processing parameters
SI               65536
SF       400.1300184 MHz
WDW                 EM
SSB      0
LB             0.30 Hz
GB       0
PC                1.00
```

^{19}F NMR of [1]$^{2-/1-}$ post-flow cell cycling

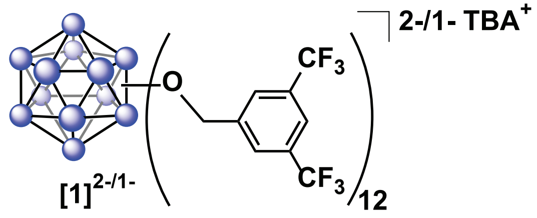

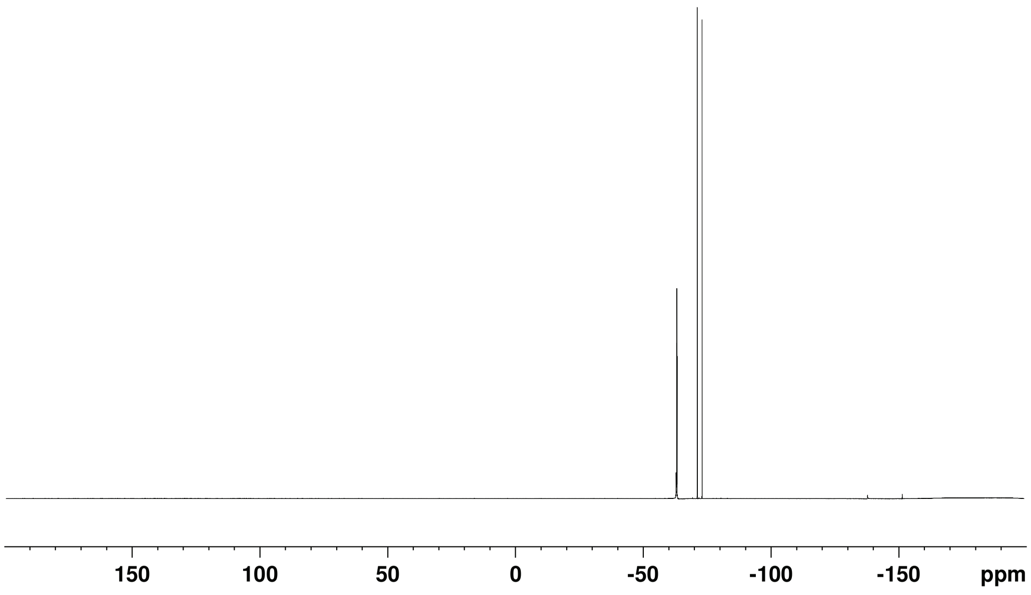

Current Data Parameters
NAME Aug31-2018
EXPNO 72
PROCNO 1

F2 - Acquisition Parameters
Date_ 20180831
Time 17.06
INSTRUM av400
PROBHD 5 mm PABBO BB/
PULPROG zgflqn30
TD 262144
SOLVENT CDCl3
NS 64
DS 0
SWH 150000.000 Hz
FIDRES 0.572205 Hz
AQ 0.8738133 sec
RG 189.85
DW 3.333 usec
DE 6.50 usec
TE 298.6 K
D1 2.00000000 sec
TD0 1

======== CHANNEL f1 ========
SFO1 376.4983660 MHz
NUC1 19F
P1 14.50 usec
PLW1 17.00000000 W

F2 - Processing parameters
SI 262144
SF 376.4983660 MHz
WDW EM
SSB 0
LB 1.00 Hz
GB 0
PC 1.00

References

(1) Stock, A. *J. Phys. Chem.* **1933**, *38* (5), 714–715.

(2) Sivaev, I. B.; Bregadze, V. I.; Sjöberg, S. *Collect. Czechoslov. Chem. Commun.* **2002**, *67* (6), 679–727.

(3) Spokoyny, A. M. *Pure Appl. Chem.* **2013**, *85* (5), 903–919.

(4) Grimes, R. *Carboranes, 2nd ed.*; Elsevier, 2011.

(5) Eberhardt, W. H.; Jr, B. C.; Lipscomb, W. N. *J. Chem. Phys.* **1954**, *22* (6), 989–1001.

(6) Longuet-Higgins, H. C.; de V. Roberts, M. *Proc. R. Soc. A Math. Phys. Eng. Sci.* **1955**, *230* (1180), 110–119.

(7) Shapiro, I.; Williams, R. E. *J. Am. Chem. Soc.* **1959**, *81* (18), 4787–4790.

(8) Pitochelli, A. R.; Hawthorne, F. M. *J. Am. Chem. Soc.* **1960**, *82* (12), 3228–3229.

(9) Moore, E. B.; Lohr, L. L.; Lipscomb, W. N. *J. Chem. Phys.* **1961**, *35* (4), 1329.

(10) Hertler, W. R.; Raasch, M. S. *J. Am. Chem. Soc.* **1964**, *86* (18), 3661–3668.

(11) Miller, H. C.; Miller, N. E.; Muetterties, E. L. *Inorg. Chem.* **1964**, *3* (10), 1456–1463.

(12) Knoth, W. H.; Miller, H. C.; Sauer, J. C.; Balthis, J. H.; Chia, Y. T.; Muetterties, E. L. *Inorg. Chem.* **1964**, *3* (2), 159–167.

(13) Wiersema, R. J.; Middaugh, R. L. *Inorg. Chem.* **1969**, *8* (10), 2074–2079.

(14) Wunderlich, J. A.; Lipscomb, W. N. *J. Am. Chem. Soc.* **1960**, *82* (16), 4427–4428.

(15) Hoffmann, R.; Lipscomb, W. N. *J. Chem. Phys.* **1962**, *36* (8), 2179.

(16) Hoffmann, R.; Lipscomb, W. N. *J. Chem. Phys.* **1962**, *37* (3), 520.

(17) Muetterties, E. L.; Merrifield, R. E.; Miller, H. C.; Knoth, W. H.; Downing, J. R. *J. Am. Chem. Soc.* **1962**, *84* (13), 2506–2508.

(18) Hoffmann, R.; Lipscomb, W. N. *J. Chem. Phys.* **1962**, *37* (12), 2872.

(19) Miller, H. C.; Miller, N. E.; Muetterties, E. L. *J. Am. Chem. Soc.* **1963**, *85* (23), 3885–3886.

(20) Ellis, I. A.; Gaines, D. F.; Schaeffer, R. *J. Am. Chem. Soc.* **1963**, *85* (23), 3885–3885.

(21) Muetterties, E. L.; Balthis, J. H.; Chia, Y. T.; Knoth, W. H.; Miller, H. C. *Inorg. Chem.* **1964**, *3* (3), 444–451.

(22) Hertler, W. R. *Inorg. Chem.* **1964**, *3* (8), 1195–1196.

(23) Grimes, R. N. *J. Chem. Ed.* **2004**, *81* (5), 657.

(24) Hawthorne, M. F. *J. Chem. Educ.* **2009**, *86* (10), 1131.

(25) Knoth, W. H.; Miller, H. C.; England, D. C.; Parshall, G. W.; Muetterties, E. L. *J. Am.*

Chem. Soc. **1962**, *84* (6), 1056–1057.

(26) Gu, W.; Ozerov, O. V. *Inorg. Chem.* **2011**, *50* (7), 2726–2728.

(27) Peryshkov, D. V; Popov, A. A.; Strauss, S. H. *J. Am. Chem. Soc.* **2009**, *131* (51), 18393–18403.

(28) Ivanov, S. V.; Miller, S. M.; Anderson, O. P.; Solntsev, K. a.; Strauss, S. H. *J. Am. Chem. Soc.* **2003**, *125* (16), 4694–4695.

(29) Hawthorne, M. F. *Pure Appl. Chem.* **2003**, *75* (9), 1157–1164.

(30) Peymann, T.; Herzog, A.; Knobler, C. B.; Hawthorne, M. F. *Angew. Chem. Int. Ed.* **1999**, *38* (8), 1061–1064.

(31) Farha, O. K.; Julius, R. L.; Lee, M. W.; Huertas, R. E.; Knobler, C. B.; Hawthorne, M. F. *J. Am. Chem. Soc.* **2005**, *127* (51), 18243–18251.

(32) Maderna, A.; Knobler, C. B.; Hawthorne, M. F. *Angew. Chem. Int. Ed.* **2001**, *40* (9), 1661–1664.

(33) Jalisatgi, S. S.; Kulkarni, V. S.; Tang, B.; Houston, Z. H.; Lee, M. W.; Hawthorne, M. F. *J. Am. Chem. Soc.* **2011**, *133* (32), 12382–12385.

(34) Welch, A. J. *Chem. Commun.* **2013**, *49* (35), 3615.

(35) Kaim, W.; Hosmane, N. S.; Záliš, S.; Maguire, J. A.; Lipscomb, W. N. *Angew. Chem. Int. Ed.* **2009**, *48* (28), 5082–5091.

(36) Rupich, M. W. *J. Electrochem. Soc.* **1985**, *132* (1), 119.

(37) Boeré, R. T.; Kacprzak, S.; Keßler, M.; Knapp, C.; Riebau, R.; Riedel, S.; Roemmele, T. L.; Rühle, M.; Scherer, H.; Weber, S. *Angew. Chem. Int. Ed.* **2011**, *50* (2), 549–552.

(38) Van, N.; Tiritiris, I.; Winter, R. F.; Sarkar, B.; Singh, P.; Duboc, C.; Muñoz-Castro, A.; Arratia-Pérez, R.; Kaim, W.; Schleid, T. *Chem. - A Eur. J.* **2010**, *16* (37), 11242–11245.

(39) Peymann, T.; Knobler, C. B.; Frederick Hawthorne, M. *Chem. Commun.* **1999**, *12* (20), 2039–2040.

(40) Peymann, T.; Knobler, C. B.; Khan, S. I.; Hawthorne, M. F. *Angew. Chem. Int. Ed.* **2001**, *40* (9), 1664–1667.

(41) Lee, M. W.; Farha, O. K.; Hawthorne, M. F.; Hansch, C. H. *Angew. Chem. Int. Ed.* **2007**, *46* (17), 3018–3022.

(42) de la Hoz, A.; Diaz-Ortiz, A.; Moreno, A. *Chem. Soc. Rev.* **2005**, *34* (2), 164.

(43) Peymann, T.; Knobler, C. B.; Khan, S. I.; Hawthorne, M. F. *J. Am. Chem. Soc.* **2001**, *123* (10), 2182–2185.

(44) Bayer, M. J.; Hawthorne, M. F. *Inorg. Chem.* **2004**, *43* (6), 2018–2020.

(45) Taft, R. W. *J. Am. Chem. Soc.* **1953**, *75* (17), 4231–4238.

(46) Hansch, C.; Leo, A.; Taft, R. W. *Chem. Rev.* **1991**, *91* (2), 165–195.

(47) Pushechnikov, A.; Jalisatgi, S. S.; Hawthorne, M. F. *Chem. Commun. (Camb).* **2013**, *49* (34), 3579–3581.

(48) Connelly, N. G.; Geiger, W. E. *Chem. Rev.* **1996**, *96* (2), 877–910.

(49) Zavarine, I. S.; Kubiak, C. P. *J. Electroanal. Chem.* **2001**, *495* (2), 106–109.

(50) Machan, C. W.; Sampson, M. D.; Chabolla, S. A.; Dang, T.; Kubiak, C. P. *Organometallics* **2014**, *33* (18), 4550–4559.

(51) Salentine, C. G. *Inorg. Chem.* **1983**, *22* (26), 3920–3924.

(52) Leites, L. A. *Chem. Rev.* **1992**, *92* (2), 279–323.

(53) Alov, N. V. *J. Anal. Chem.* **2005**, *60* (5), 431–435.

(54) Temesghen, W.; Sherwood, P. *Anal. Bioanal. Chem.* **2002**, *373* (7), 601–608.

(55) Zhu, X. P.; Yukawa, T.; Hirai, M.; Suematsu, H.; Jiang, W.; Yatsui, K.; Nishiyama, H.; Inoue, Y. *Appl. Surf. Sci.* **2006**, *252* (16), 5776–5782.

(56) Xing, M.-Y.; Li, W.-K.; Wu, Y.-M.; Zhang, J.-L.; Gong, X.-Q. *J. Phys. Chem. C* **2011**, *115* (16), 7858–7865.

(57) Goswami, L. N.; Houston, Z. H.; Sarma, S. J.; Li, H.; Jalisatgi, S. S.; Hawthorne, M. F. *J. Org. Chem.* **2012**, *77* (24), 11333–11338.

(58) Wixtrom, A. I.; Shao, Y.; Jung, D.; Machan, C. W.; Kevork, S. N.; Qian, E. A.; Axtell, J. C.; Khan, S. I.; Kubiak, C. P.; Spokoyny, A. M. *Inorg. Chem. Front.* **2016**, *3* (5), 711–717.

(59) Axtell, J. C.; Saleh, L. M. A.; Qian, E. A.; Wixtrom, A. I.; Spokoyny, A. M. *Inorg. Chem.* **2018**, *57* (5), 2333–2350.

(60) Brezesinski, T.; Wang, J.; Tolbert, S. H.; Dunn, B. *Nat. Mater.* **2010**, *9* (Copyright (C) 2014 American Chemical Society (ACS). All Rights Reserved.), 146–151.

(61) Boeré, R. T.; Kacprzak, S.; Keßler, M.; Knapp, C.; Riebau, R.; Riedel, S.; Roemmele, T. L.; Rühle, M.; Scherer, H.; Weber, S. *Angew. Chem. Int. Ed.* **2011**, *50* (2), 549–552.

(62) Boeré, R. T.; Derendorf, J.; Jenne, C.; Kacprzak, S.; Keßler, M.; Riebau, R.; Riedel, S.; Roemmele, T. L.; Rühle, M.; Scherer, H.; Vent-Schmidt, T.; Warneke, J.; Weber, S. *Chem. - A Eur. J.* **2014**, *20* (15), 4447–4459.

(63) Peymann, T.; Knobler, C. B.; Khan, S. I.; Hawthorne, M. F. *Angew. Chem. Int. Ed* **2001**, *40* (9), 1999–2002.

(64) Qian, E. A.; Wixtrom, A. I.; Axtell, J. C.; Saebi, A.; Jung, D.; Rehak, P.; Han, Y.; Moully, E. H.; Mosallaei, D.; Chow, S.; Messina, M. S.; Wang, J. Y.; Royappa, A. T.; Rheingold, A. L.; Maynard, H. D.; Král, P.; Spokoyny, A. M. *Nat. Chem.* **2017**, *9* (4), 333–340.

(65) Messina, M. S.; Axtell, J. C.; Wang, Y.; Chong, P.; Wixtrom, A. I.; Kirlikovali, K. O.;

Upton, B. M.; Hunter, B. M.; Shafaat, O. S.; Khan, S. I.; Winkler, J. R.; Gray, H. B.; Alexandrova, A. N.; Maynard, H. D.; Spokoyny, A. M. *J. Am. Chem. Soc.* **2016**, *138* (22), 6952–6955.

(66) Bondarev, O.; Khan, A. A.; Tu, X.; Sevryugina, Y. V; Jalisatgi, S. S.; Hawthorne, M. F. *J. Am. Chem. Soc.* **2013**, *135* (35), 13204–13211.

(67) Asay, M.; Kefalidis, C. E.; Estrada, J.; Weinberger, D. S.; Wright, J.; Moore, C. E.; Rheingold, A. L.; Maron, L.; Lavallo, V. *Angew. Chem. Int. Ed.* **2013**, *52* (44), 11560–11563.

(68) Lavallo, V.; Wright, J. H.; Tham, F. S.; Quinlivan, S. *Angew. Chem. Int. Ed.* **2013**, *52* (11), 3172–3176.

(69) Körbe, S.; Schreiber, P. J.; Michl, J. *Chem. Rev.* **2006**, *106* (12), 5208–5249.

(70) Gu, D.; Baumgart, H.; Abdel-Fattah, T. M.; Namkoong, G. *ACS Nano* **2010**, *4* (2), 753–758.

(71) Xie, Z.; Tsang, C.-W.; Sze, E. T.-P.; Yang, Q.; Chan, D. T. W.; Mak, T. C. W. *Inorg. Chem.* **1998**, *37* (25), 6444–6451.

(72) Duttwyler, S. *Pure Appl. Chem.* **2018**, *90* (4), 733–744.

(73) Allemann, O.; Duttwyler, S.; Romanato, P.; Baldridge, K. K.; Siegel, J. S. *Science* **2011**, *332* (6029), 574–577.

(74) Douvris, C.; Ozerov, O. V. *Science* **2008**, *321* (5893), 1188–1190.

(75) Zhang, Y.; Liu, J.; Duttwyler, S. *Eur. J. Inorg. Chem.* **2015**, *2015* (31), 5158–5162.

(76) Pluntze, A. M.; Bukovsky, E. V.; Lacroix, M. R.; Newell, B. S.; Rithner, C. D.; Strauss, S. H. *J. Fluor. Chem.* **2018**, *209*, 33–42.

(77) Bertocco, P.; Derendorf, J.; Jenne, C.; Kirsch, C. *Inorg. Chem.* **2017**, *56* (6), 3459–3466.

(78) Gu, W.; McCulloch, B. J.; Reibenspies, J. H.; Ozerov, O. V. *Chem. Commun.* **2010**, *46* (16), 2820.

(79) Ueng, S.-H.; Solovyev, A.; Yuan, X.; Geib, S. J.; Fensterbank, L.; Lacôte, E.; Malacria, M.; Newcomb, M.; Walton, J. C.; Curran, D. P. *J. Am. Chem. Soc.* **2009**, *131* (31), 11256–11262.

(80) Braunschweig, H.; Dyakonov, V.; Jimenez-Halla, J. O. C.; Kraft, K.; Krummenacher, I.; Radacki, K.; Sperlich, A.; Wahler, J. *Angew. Chem. Int. Ed.* **2012**, *51* (12), 2977–2980.

(81) Kaim, W.; Hosmane, N. S.; Záliš, S.; Maguire, J. A.; Lipscomb, W. N. *Angew. Chem. Int. Ed.* **2009**, *48* (28), 5082–5091.

(82) Thomas, J. C.; Peters, J. C. *Inorg. Chem.* **2003**, *42* (17), 5055–5073.

(83) Hudnall, T. W.; Chiu, C.-W.; Gabbaï, F. P. *Acc. Chem. Res.* **2009**, *42* (2), 388–397.

(84) Staubitz, A.; Robertson, A. P. M.; Sloan, M. E.; Manners, I. *Chem. Rev.* **2010**, *110* (7),

4023–4078.

(85) Stephan, D. W. *Angew. Chem. Int. Ed.* **2017**, *56* (22), 5984–5992.

(86) Jung, D.; Saleh, L. M. A.; Berkson, Z. J.; El-Kady, M. F.; Hwang, J. Y.; Mohamed, N.; Wixtrom, A. I.; Titarenko, E.; Shao, Y.; McCarthy, K.; Guo, J.; Martini, I. B.; Kraemer, S.; Wegener, E. C.; Saint-Cricq, P.; Ruehle, B.; Langeslay, R. R.; Delferro, M.; Brosmer, J. L.; Hendon, C. H.; Gallagher-Jones, M.; Rodriguez, J.; Chapman, K. W.; Miller, J. T.; Duan, X.; Kaner, R. B.; Zink, J. I.; Chmelka, B. F.; Spokoyny, A. M. *Nat. Mater.* **2018**, *17* (4), 341–348.

(87) Dolomanov, O. V.; Bourhis, L. J.; Gildea, R. J.; Howard, J. A. K.; Puschmann, H. *J. Appl. Crystallogr.* **2009**, *42*, 339–341.

(88) Moser, C. C.; Keske, J. M.; Warncke, K.; Farid, R. S.; Dutton, P. L. *Nature* **1992**, *355* (6363), 796–802.

(89) Gust, D.; Moore, T. A.; Moore, A. L. *Acc. Chem. Res.* **1993**, *26* (4), 198–205.

(90) Kalyanasundaram, K. *Coord. Chem. Rev.* **1998**, *177* (1), 347–414.

(91) Ji, X.; Zhang, B.; Tritt, T. M.; Kolis, J. W.; Kumbhar, A. *J. Electron. Mater.* **2007**, *36* (7), 721–726.

(92) Fukuzumi, S. *Eur. J. Inorg. Chem.* **2008**, *2008* (9), 1351–1362.

(93) Medlin, D. L.; Snyder, G. J. *Curr. Opin. Colloid Interface Sci.* **2009**, *14* (4), 226–235.

(94) Kalyanasundaram, K.; Graetzel, M. *Curr. Opin. Biotechnol.* **2010**, *21* (3), 298–310.

(95) Milshtein, J. D.; Kaur, A. P.; Casselman, M. D.; Kowalski, J. A.; Modekrutti, S.; Zhang, P. L.; Harsha Attanayake, N.; Elliott, C. F.; Parkin, S. R.; Risko, C.; Brushett, F. R.; Odom, S. A. *Energy Environ. Sci.* **2016**, *9* (11), 3531–3543.

(96) Milshtein, J. D.; Tenny, K. M.; Barton, J. L.; Drake, J.; Darling, R. M.; Brushett, F. R. *J. Electrochem. Soc.* **2017**, *164* (11), 3265–3275.

(97) Gür, T. M. *Energy Environ. Sci.* **2018**.

(98) Winsberg, J.; Hagemann, T.; Janoschka, T.; Hager, M. D.; Schubert, U. S. *Angew. Chem. Int. Ed.* **2017**, *56* (3), 686–711.

(99) Kowalski, J. A.; Su, L.; Milshtein, J. D.; Brushett, F. R. *Curr. Opin. Chem. Eng.* **2016**, *13*, 45–52.

(100) Darling, R. M.; Gallagher, K. G.; Kowalski, J. A.; Ha, S.; Brushett, F. R. *Energy Environ. Sci.* **2014**, *7* (11), 3459–3477.

(101) Chen, H.; Cong, G.; Lu, Y.-C. *J. Energy Chem.* **2018**, *0*, 1–22.

(102) Wixtrom, A. I.; Shao, Y.; Jung, D.; Machan, C. W.; Kevork, S. N.; Qian, E. A.; Axtell, J. C.; Khan, S. I.; Kubiak, C. P.; Spokoyny, A. M. *Inorg. Chem. Front.* **2016**.

(103) Majewski, M. B.; Howarth, A. J.; Farha, O. K. *Nat. Chem.* **2017**, *9* (4), 299–301.

(104) Hendriks, K. H.; Robinson, S. G.; Braten, M. N.; Sevov, C. S.; Helms, B. A.; Sigman, M. S.; Minteer, S. D.; Sanford, M. S. *ACS Cent. Sci.* **2018**, *4* (2), 189–196.

(105) Kowalski, J. A.; Casselman, M. D.; Kaur, A. P.; Milshtein, J. D.; Elliott, C. F.; Modekrutti, S.; Attanayake, N. H.; Zhang, N.; Parkin, S. R.; Risko, C.; Brushett, F. R.; Odom, S. A. *J. Mater. Chem. A* **2017**, 24371–24379.

(106) Milshtein, J. D.; Barton, J. L.; Darling, R. M.; Brushett, F. R. *J. Power Sources* **2016**, *327*, 151–159.

(107) Goulet, M.; Aziz, M. J. *J. Electrochem. Soc.* **2018**, *165* (7), 1466–1477.

(108) Milshtein, J. D.; Barton, J. L.; Darling, R. M.; Brushett, F. R. *Meet. Abstr.* **2016**, *MA2016-02* (5), 632.

(109) Huang, H.; Howland, R.; Agar, E.; Nourani, M.; Golen, J. A.; Cappillino, P. J. *J. Mater. Chem. A* **2017**, *5* (23), 11586–11591.

(110) Wei, X.; Xu, W.; Huang, J.; Zhang, L.; Walter, E.; Lawrence, C.; Vijayakumar, M.; Henderson, W. A.; Liu, T.; Cosimbescu, L.; Li, B.; Sprenkle, V.; Wang, W. *Angew. Chem. Int. Ed.* **2015**, *54* (30), 8684–8687.

(111) Wei, X.; Duan, W.; Huang, J.; Zhang, L.; Li, B.; Reed, D.; Xu, W.; Sprenkle, V.; Wang, W. *ACS Energy Lett.* **2016**, *1* (4), 705–711.

(112) Sevov, C. S.; Hickey, D. P.; Cook, M. E.; Robinson, S. G.; Barnett, S.; Minteer, S. D.; Sigman, M. S.; Sanford, M. S. *J. Am. Chem. Soc.* **2017**, *139* (8), 2924–2927.

(113) Weber, A. Z.; Mench, M. M.; Meyers, J. P.; Ross, P. N.; Gostick, J. T.; Liu, Q. *J. Appl. Electrochem.* **2011**, *41* (10), 1137–1164.

(114) Dmello, R.; Milshtein, J. D.; Brushett, F. R.; Smith, K. C. *J. Power Sources* **2016**, *330*, 261–272.

(115) Zeng, Y. K. K.; Zhou, X. L. L.; An, L.; Wei, L.; Zhao, T. S. S. *J. Power Sources* **2016**, *324*, 738–744.

(116) Duan, W.; Huang, J.; Kowalski, J. A.; Shkrob, I. A.; Vijayakumar, M.; Walter, E.; Pan, B.; Yang, Z.; Milshtein, J. D.; Li, B.; Liao, C.; Zhang, Z.; Wang, W.; Liu, J.; Moore, J. S.; Brushett, F. R.; Zhang, L.; Wei, X. *ACS Energy Lett.* **2017**, *2* (5), 1156–1161.

(117) Gong, K.; Fang, Q.; Gu, S.; Li, S. F. Y.; Yan, Y. *Energy Environ. Sci.* **2015**, *8* (12), 3515–3530.

(118) Su, L.; Darling, R. M.; Gallagher, K. G.; Xie, W.; Thelen, J. L.; Badel, A. F.; Barton, J. L.; Cheng, K. J.; Balsara, N. P.; Moore, J. S.; Brushett, F. R. *J. Electrochem. Soc.* **2016**, *163* (1), A5253–A5262.

(119) Doris, S. E.; Ward, A. L.; Baskin, A.; Frischmann, P. D.; Gavvalapalli, N.; Chénard, E.; Sevov, C. S.; Prendergast, D.; Moore, J. S.; Helms, B. A. *Angew. Chem. Int. Ed.* **2017**, *56* (6), 1595–1599.

(120) Montoto, E. C.; Nagarjuna, G.; Hui, J.; Burgess, M.; Sekerak, N. M.; Hernández-Burgos,

K.; Wei, T. S.; Kneer, M.; Grolman, J.; Cheng, K. J.; Lewis, J. A.; Moore, J. S.; Rodríguez-López, J. *J. Am. Chem. Soc.* **2016**, *138* (40), 13230–13237.

(121) Montoto, E. C.; Nagarjuna, G.; Moore, J. S.; Rodríguez-López, J. *J. Electrochem. Soc.* **2017**, *164* (7), A1688–A1694.

(122) Milshtein, J. D.; Darling, R. M.; Drake, J.; Perry, M. L.; Brushett, F. R. *J. Electrochem. Soc.* **2017**, *164* (14), A3883–A3895.

(123) VanGelder, L. E.; Kosswattaarachchi, A. M.; Forrestel, P. L.; Cook, T. R.; Matson, E. M. *Chem. Sci.* **2018**, *9* (6), 1692–1699.

(124) Chen, J.-J.; Symes, M. D.; Cronin, L. *Nat. Chem.* **2018**.

(125) Sevov, C. S.; Fisher, S. L.; Thompson, L. T.; Sanford, M. S. *J. Am. Chem. Soc.* **2016**, *138* (47), 15378–15384.

(126) Hu, B.; DeBruler, C.; Rhodes, Z.; Liu, T. L. *J. Am. Chem. Soc.* **2017**, *139* (3), 1207–1214.

(127) Friedl, J.; Lebedeva, M. A.; Porfyrakis, K.; Stimming, U.; Chamberlain, T. W. *J. Am. Chem. Soc.* **2018**, *140* (1), 401–405.

(128) Stauber, J. M.; Zhang, S.; Gvozdik, N.; Jiang, Y.; Avena, L.; Stevenson, K. J.; Cummins, C. C. *J. Am. Chem. Soc.* **2018**, *140* (2), 538–541.

(129) Milshtein, J. D.; Barton, J. L.; Carney, T. J.; Kowalski, J. A.; Darling, R. M.; Brushett, F. R. *J. Electrochem. Soc.* **2017**, *164* (12), A2487–A2499.